

https://dspace.org/

Biomimetic proteosaccharide 3d scaffold for applications in tissue engineering

Cassimjee, Henna

2022
https://hdl.handle.net/10539/34262

Downloaded from a DSpace repository. https://dspace.org/

Biomimetic Proteosaccharide 3D Scaffold for Applications in Tissue Engineering

HENNA CASSIMJEE

A dissertation submitted to the Faculty of Health Sciences, University of the Witwatersrand, in fulfilment of the requirements for the degree Master of Pharmacy.



Supervisor:

Professor Yahya Essop Choonara
University of the Witwatersrand, Department of Pharmacy and Pharmacology,
Johannesburg, South Africa

Co-supervisor:

Associate Professor Pradeep Kumar
University of the Witwatersrand, Department of Pharmacy and Pharmacology,
Johannesburg, South Africa

2022, Johannesburg, South Africa

DECLARATION

I, Henna Cassimjee, declare that this dissertation is my own, unaided work. It is being submitted for the Degree Master of Pharmacy at the University of the Witwatersrand, Johannesburg. It has not been submitted before for any degree or examination at any other University.



_____

(Signature of candidate)

_____day of_____20_____in_____

DEDICATION

This work is dedicated to my late grandmother, Fathima Cassimjee.

All that I am today, is because of you.

I miss you.

PUBLICATIONS

1. *Genipin-crosslinked proteosaccharide scaffolds for potential neural tissue engineering applications.* Henna Cassimjee, Pradeep Kumar, Philemon Ubanako and Yahya E Choonara. MDPI. Pharmaceutics 2022, 14, 441 DOI: https://doi.org/10.3390/pharmaceutics14020441 (Impact Factor: 6.321)

2. *Proteosaccharide combinations for Tissue Engineering Applications*. Henna Cassimjee, Pradeep Kumar, Yahya E Choonara and Viness Pillay. Carbohydrate Polymers. 2020, *235*, 115932 DOI: https://doi.org/10.1016/j.carbpol.2020.115932 (Impact Factor: 9.381).

Presentations

1. Biomimetic Proteosaccharide 3D scaffold for Tissue Engineering Applications. Henna Cassimjee, Pradeep Kumar and Yahya E Choonara. South Africa-Italy GYA-YSAP Mission: 17 November 2020. Oral presentation.

2. Biomimetic Proteosaccharide 3D scaffold for Tissue Engineering Applications. Henna Cassimjee, Pradeep Kumar and Yahya E Choonara. BRICS Summit 2021: 04 November 2021. Oral presentation.

ABSTRACT

Traumatic brain injuries (TBI) are considered a leading cause of morbidity and mortality all over the world particularly in adolescents and the elderly. TBI's are just the beginning of long term, secondary complications such as inflammation, neurological impairment and neureodegeneration. The lack of successful pharmacological interventions to prevent the onset and spread of secondary lesions, compromise the patient's quality of life in psychological, social, and physical aspects. Treatments to date are mainly symptomatic and focus on alleviating intracranial hypertension and convulsions. Tissue engineering aims to engender scaffolds which mimic the extracellular matrix (ECM) environment on a micro-, macro- and nano scale. Some tissue- engineered scaffolds show some experimental success, however, there remains the need for a thee-dimensional scaffold that exhibits consummate results of a clinical standard. To this end, research was conducted on protein-polysaccharide conjugates which could play a great role in neural regeneration.

This research employed two different proteosaccharide combinations, namely chitosan-gelatin and hyaluronic acid-gelatin, of which both were chemically crosslinked by the non-toxic crosslinker genipin. Various parameters, such as the temperature of crosslinking and time needed for crosslinking were troubleshooted, and two thee-dimensional scaffolds were synthesised, one being a full-IPN (Interpenetrating Polymeric Network) and the second, being a semi-IPN. Various characterization studies were employed, including Fourier Transform Infrared Spectroscopy (FTIR), Differential Scanning Calorimetry (DSC), Rheology, Scanning Electron Microscopy (SEM), X-ray Diffraction (XRD), drug release and degradation studies. *In vitro* cytotoxicity assays were also carried out using of rat pheochomocytoma (PC12) and human glioblastoma multiform (A172). The polysaccharides increased the mechanical strength of each scaffold while gelatin provided the bioactive sequence which promoted cellular interactions. The effect of crosslinking was investigated, and the crosslinked hydrogels showed higher thermal decomposition temperatures, increased resistance to degradation, and pore sizes ranging from 72.789 μm±16.85 for the full IPN and 84.289 μm±7.658 for the semi-IPN. The scaffolds were loaded with Dexamethasone-21-phosphate to investigate their efficacy as drug delivery vehicles, and the full IPN showed a 100% release in 10 days, while the semi-IPN showed a burst release in 6 hours. Both scaffolds encouraged the proliferation of rat pheochomocytoma (PC12) and human glioblastoma multiform (A172) and furthermore, provided cues for migration of A172 cells. Both scaffolds can be used as potential drug delivery vehicles and as artificial extracellular matrices for potential neural regeneration.

The last scaffold synthesised, consisted of the commercially available peptide PuraMatrix and chitosan. The composite showed in-situ gelation at a pH of 7.4. Circular dichoism was employed to evaluate the secondary structure of the blend, and the peptide, Puramatrix retained its β-sheet structure after gelation with chitosan. Other characterization methods included FTIR, DSC, SEM, textural analysis, degradation and rheology to evaluate the physicochemical and mechanical integrity of the scaffold. Chitosan increased the mechanical strength of the conjugate with the young's modulus increasing from 0.437 kPa to 0.813 kPa. Furthermore, the combination showed enhanced degradation time as compared to the PuraMatrix alone. The scaffolds formed were also tested on the A172 and the PC12 cell lines, and compared to the proteosaccharide combinations, chitosan-gelatin and hyaluronic acid-gelatin. The results showed that the CHT-PM scaffold showed higher cell viability and proliferation and a faster rate of wound closure (migration) but was closely followed by the

chitosan-gelatin and the hyaluronic acid-gelatin formulations. Overall, all thee formulations showed potential for neural regeneration, and demonstrated that protein-polysaccharide (proteosaccharide) conjugates show better regenerative potential than their individual counterparts.

ACKNOWLEDGEMENTS

In the name of the Almighty, the most Beneficent, the most Merciful

Firstly, I thank my lord and creator who has brought me so far, and listened to every prayer of mine, this journey was a difficult one and there were times when I have doubted myself enough to want to quit, however I persevered, and this could have only been from my creator. I dedicate this work to my beloved grandmother, who left me before seeing the end of this. Thank you for raising me and instilling so much of strength, courage, and ambition in me. You have been my role model in life, and all that I am is due to you. My heartfelt thanks to my two mothers, Shubnum and Shamshaad. Both of you have continuously stood by my side, even on days that were difficult. We will see a brighter future together.

I would like to thank Prof. Yahya Choonara for all his expert guidance and supervision. I would also like to thank Prof. Pradeep Kumar for always propelling me forward with his inspiring words and for giving me opportunities to present my research. I am grateful to you for your understanding nature and for making me think like a researcher. A sincere thanks to the technical staff at the Department of Pharmacy and Pharmacology, Mr Bafana Themba, Ms Tshidi Mosete, Mr. Sello Ramarumo, Ms. Nompumelelo Damane, Mr. Kleinbooi Mohlabi for their indispensable assistance.

To a special person, Zakariya, there was never a step that I took without you at my side. Thank you for support and encouragement. I am honoured to have experienced your love and companionship, even though it might have been for a brief period. To my friend, Taskeen, thank you for being my advisor, assistant, and psychologist at times. I will always treasure your advice and I will miss our times spent in the laboratory together. I would like to extend my gratitude to the friends who kept me motivated and sane during this journey. Eemaan, Abu Bakr, Shazia and Ayesha, I will miss our inside jokes and the precious shared moments.

A special thanks to the National Research Foundation (NRF), the South African Medical Research Council, and the University Research Committee (Wits) for all their financial assistance thoughout the duration of this research.

TABLE OF CONTENTS

TITLE……i
DECLARATION……ii
DEDICATION……..iii
PUBLICATIONS…….....iv
RESEARCH OUTPUT……...v
ABSTRACT……vi
AKNOWLEDGEMENTS……..…….viii
TABLE OF CONTENTS……ix
LIST OF TABLES……..……..xii
LIST OF FIGURES……..……..xiii
LIST OF EQUATIONS……..……xvi

CHAPTER.1. INTRODUCTION AND OVERVIEW OF THE STUDY 1
1.1 Tissue engineering and the extracellular matrix 1
1.2 Scaffolds in tissue engineering and polymers involved 2
1.3 Traumatic brain injuries..... 2
1.4 The use of proteins and peptides in tissue engineering..... 4
1.5 Self-assembling peptides 5
1.6 Aim and objectives:..... 7
1.7 Potential benefits of the study 7
1.8 Synopsis of dissertation 8

CHAPTER.2. REVIEW OF VARIOUS PROTEOSACCHARIDE COMBINATIONS AND THEIR TISSUE ENGINEERING APPLICATIONS 13
2.1 Introduction..... 13
2.2 Proteosaccharide interactions..... 17
2.3 Crosslinking of proteosaccharides 22
2.3.1 Physical crosslinking..... 22
2.3.2 Chemical crosslinking 23
2.3.3 Photopolymerization 26
2.3.4 Enzymatic crosslinking..... 27
2.4 Applications of proteosaccharides..... 28
2.4.1 Alginate-based proteosaccharides 28
2.4.2 Chitosan-based proteosaccharides..... 40
2.4.3 Hyaluronic acid based proteosaccharides..... 49
2.4.4 Cellulose-based proteosaccharides 55
2.4.5 Other proteosaccharides..... 60

2.5 Conclusion 63

CHAPTER.3. GENIPIN-CROSSLINKED PROTEOSACCHARIDE SCAFFOLDS FOR POTENTIAL NEURAL TISSUE ENGINEERING APPLICATIONS 65

3.1 Introduction 78

3.2 Materials and Method 83

3.2.1 Materials 83

3.2.2 Synthesis of the full interpenetrating polymer network (IPN) and semi-IPN 83

3.2.3 (ATR-FTIR) of pristine polymers and their crosslinked networks to elucidate the physicochemical transformations as a result of crosslinking 84

3.2.4 Rheological analysis of the proteosaccharide hydrogels 84

3.2.5 Analysis of crystallinity of the proteosaccharide scaffolds 85

3.2.6 Thermoanalytical analysis of the lyophilised proteosaccharide scaffolds 85

3.2.7 Swelling potential of scaffolds under physiological conditions 85

3.2.8 Morphological analysis of proteosaccharide scaffolds 86

3.2.9 Determination of bulk density of each scaffold 86

3.2.10 Degradation of proteosaccharide scaffolds 86

3.2.11 Drug release of Dexamethasone-21-Phosphate from proteosaccharide scaffolds 86

3.3 Results and Discussion 87

3.3.1 FTIR analysis of CGG and HAGG scaffolds 87

3.3.2 Rheological behaviour of proteosaccharide hydrogels 90

3.3.3 XRD analysis of amorphous proteosaccharide scaffolds 93

3.3.4 DSC analysis of lyophilised proteosaccharide scaffolds 96

3.3.5 Swelling potential of proteosaccharide scaffolds 98

3.3.6 Morphological analysis of proteosaccharide scaffolds 99

3.3.7 Bulk Density of proteosaccharide scaffolds 102

3.3.8 In vitro degradation of proteosaccharide scafffolds 102

3.3.9 Drug release of Dexamethasone-21-Phosphate from the IPN and semi-IPN hydrogel scaffolds 104

3.4 Concluding remarks 107

CHAPTER.4. IN SITU SELF-ASSEMBLING PROTEOSACCHARIDE SYSTEM FOR NEURAL TISSUE ENINEERING APPLICATIONS 111

4.1 Introduction 111

4.2 Materials 112

4.3 Methods 113

4.3.1 Synthesis of the CHT-PM scaffold for in situ gelation 113

4.3.2 Rheological analysis to determine the thermoresponsive behaviour of the proteosaccharide. 113
4.3.3 Preliminary cytotoxicity analysis of different ratios of protein:polysaccharide 113
4.3.4 Circular Dichoism (CD) spectrometry of the proteosaccharide to determine secondary structure of the peptide component..... 114
4.3.5 Attenuated total reflection Fourier transform infrared spectroscopy (ATR-FTIR) to assess physicochemical interactions between the peptide and polysaccharide..... 114
4.3.6 Differential scanning calorimetry (DSC) for determination of thermal stability..... 114
4.3.7 Morphological characterization of the proteosaccharide with SEM..... 115
4.3.8 Textural analysis of the scaffold to elucidate mechanical properties of the scaffold.. 115
4.3.9 Degradation of proteosaccharide scaffolds 115
4.4 Results and discussion 116
4.4.1 Rheological analysis to determine the thermoresponsive behaviour of the proteosaccharide. 116
4.4.2 Preliminary cytotoxicity studies to determine the most bioactive ratio 118
4.4.3 Physicochemical characterization of lyophilised proteosaccharides using FTIR spectroscopy..... 119
4.4.4 Determination of the secondary structure of the proteosaccharide..... 120
4.4.5 DSC Analysis to determine the thermal stability of the proteosaccharide 123
4.4.6 Morphological characterization of pore and fibre size..... 124
4.4.7 Textural profile analysis of lyophilised scaffold after gelation in PBS..... 128
4.4.8 Degradation of CHT-PM scaffold 130
4.5 Concluding remarks 131

CHAPTER.5. IN VITRO BIOCOMPATIBILITY ASSAYS OF PROTEOSACCHARIDES 134
5.1 Introduction..... 134
5.2 Materials 135
5.2.1 Cell lines and culture..... 135
5.3 Method..... 135
5.3.1 Aseptic technique 135
5.3.2 Seeding of PC12 and A172 cells in a 96-well plate 135
5.3.3 Migration of A172 cells..... 136
5.3.4 Image processing to determine percentage wound closure..... 137
5.3.5 Statistical analysis 137

5.4 Results and Discussion 137
5.4.1 Cytotoxicity analysis of proteosaccharide hydrogels on PC12 cells 137
5.4.2 Cytotoxicity analysis of the proteosaccharides on A172 cells 139
5.4.3 Migration of A172 cells in IPN and semi-IPN 141
5.5 Concluding remarks 146

CHAPTER.6. CONCLUSIONS, LIMITATIONS AND FUTURE PROSPECTS 148
6.1 Conclusions 148
6.2 Limitations 149
6.3 Prospects 149
Appendix A: Publications 150
Appendix B: Research outputs 152
Appendix C: Supplementary data 154

LIST OF TABLES

Table 1.1: Current therapeutic interventions for traumatic brain injuries (TBI's) and their benefits and shortcomings 3
Table 1.2: Different structures of self-assembling peptides and their characteristics 6
Table 2.1: Summary of important parameters for the development of hydrogels. Reproduced with permission from Creative Commons Attribution-Non-Commercial 4.0 License. Tiwari, S., Patil, R. and Bahadur, P. (2018) 'Polysaccharide based scaffolds for soft tissue engineering applications', Polymers. MDPI AG. doi: 10.3390/polym11010001..... 13
Table 2.2: Summary of key chemical modifications of commonly employed natural polysaccharides to better suit their tissue engineering applications..... 13
Table 0.3. A brief interpretation of the Florry Huggins Lattice model equation to determine phase separation phenomena..... 17
Table 0.4. Table showing chemical crosslinkers employed in covalently crosslinking proteosaccharides..... .23
Table 0.5. Comprehensive summary of the main proteosaccharides and salient features...54
Table 3.1: The various proteosaccharide formulations that were investigated for cross-linking effects 84
Table 3.2: Crystallinity index of each scaffold calculated from X-ray Diffraction 96
Table 3.3: Calculated density of each scaffold (n=3) 102
Table 4.1: Dimensions of each scaffold calculated from Scanning Electron Microscopic images (n=10)..... 125
Table 4.2: Processing parameters employed in calculation of the Young's modulus on the Texture Analyser..... 128

LIST OF FIGURES

Figure 2.1:Chemical reaction between a protein and polysaccharide though a Schiff base formation. Reproduced with permission from Creative Commons. Afewerki, S, Sheikhi, A, Kannan, S, Ahadian, S, Khademhosseini, A. Gelatin-polysaccharide composite s scaffolds for 3D cell culture and tissue engineering: Towards natural therapeutics. Bioengineering & Translational Medicine. 2019; 4: 96– 115. https://doi.org/10.1002/btm2.10124 20
Figure 2.2: Graphical abstract showing methods of crosslinking proteosaccharide hydrogels. Reproduced with permission from Reddy et al., 2015 © Elsevier B.V, Ltd. 28
Figure 2.3: Fluorescence microscopic images of Normal human dermal fibroblasts adhered on (a, b) alginate, (c, d) Alginate Dialdehyde (ADA)70-Gelatin (GEL)30, (e, f) ADA60-GEL40, (g, h) ADA50-GEL50, (I, j) ADA40-GEL60, and (k,, l) ADA30-GEL70 after 4 days (left column) and 7 days (right column) of incubation. The cells were stained for live cells (green) and eopei (blue). Reproduced with permission from Creative Commons Attribution-Non-Commercial 4.0 License. Sarker B, Singh R, Silva R, Roether JA, Kaschta J, Detsch R, et al. (2014) Evaluation of Fibroblasts Adhesion and Proliferation on Alginate-Gelatin Crosslinked Hydrogel. PLoS ONE 9(9): e107952. https://doi.org/10.1371/journal.pone.0107952.....31
Figure 2.4: a) Hydrogels prepared by varying the ratios of sodium alginate (SA) and collagen; b) SEM micrographs showing morphology of hydrogels; c) Live/dead staining of MSCs loaded in each hydrogel. Reproduced with permission from Creative Commons. Zhou, J., Zhang, K., Ma, S., et al. (2019). Preparing an injectable hydrogel with sodium alginate and Type I collagen to create better MSCs growth microenvironment. e-Polymers, 19(1), pp. 87-91. Retrieved 11 Nov. 2019, from doi:10.1515/epoly-2019-0011…….37
Figure 2.5: Effect of laminin and chitosan content on the viability of porcine islets embedded in matrices for 24 and 48 h (n = 3 each) (B) 10:1 matrix and (C) 20:1 matrix + LM show islets separated into fractions of non-viable and apoptotic (dead) islets, viable islets and debris. Reproduced with permission from Elsevier. B.V. Ltd © 2013…….42
Figure 2.6: Schematic showing the mechanism of cross-linking HA and gelatin in the presence of EDC/NHS. Reproduced with permission from Creative Commons Attribution-Non-Commercial 4.0 License. Khunmanee, S., Jeong, Y. and Park, H. (2016) 'Crosslinking method of hyaluronic-based hydrogel for biomedical applications', Journal of Tissue Engineering. SAGE Publications Ltd, 8. doi: 10.1177/2041731417726464…….52
Figure 2.7: a) Phase contrast image of 3D printed fibrin-factor XIII-HA strand, b) Fluorescence image of viable primary Schwann cells encapsulated in the strand. (Schwann cells-stained green using calcein-AM and their nuclei stained blue with Hoechst 33342). Reproduced with permission from Elsevier B.V, Ltd.© 2017…….54
Figure 2.8: a) Scanning Electron Microscopic images of MCT3T-E1 cells immobilised in RGD-Pectin microspheres at day 8. Reproduced with permission from F. Munarin, S. G. Guerreiro, M. A. Grellier, M. C. Tanzi, M. A. Barbosa, P. Petrini, and P. L. Granja Biomacromolecules 2011 12 (3), 568-577 DOI: 10.1021/bm101110x. Copyright © 2011 American Chemical Society…….63
Figure 3.1: Schematic illustrating the mechanism of crosslinking when genipin is used as a crosslinker. Adapted with permission from Butler et. al (2003). Mechanism and kinetics of the crosslinking reaction between biopolymers containing primary amine groups and genipin. *Journal of Polymer Science Part A: Polymer Chemistry. https://doi.org/10.1002/pola.10960* 82
Figure 3.2: Schematic showing the synthesis of each scaffold though a mixing cross-linking method with Genipin to obtain various thee-dimensional scaffolds..... 84

Figure 3.3: Fourier Transform Infrared (FTIR) spectra of A) Pristine chitosan (CHT), B) Pristine gelatin (GEL), C) chitosan-gelatin (CHTGEL), D) chitosan-genipin (CHTGEN), E) Gelatin-genipin (GELGEN), F) chitosan-gelatin-genipin (CHTGELGEN) 87
Figure 3.4: Fourier Transform Infrared spectra (FTIR) spectra of A) Pristine hyaluronic acid (HA), B) Pristine gelatin (GEL), C) hyaluronic acid-gelatin (HAGEL), D) hyaluronic acid-gelatin-genipin (HAGELGEN) 89
Figure 3.5: Storage (G') and loss (G'') modulus of: A) Chitosan, B) Gelatin, C) GELGEN, D) CHTGEN, E) CHTGELG, F) CHTGEN, G) HA, H) HAGEL, I) HAGELGEN evaluated over 24 hours Photographs alongside each graph show the tilt-bottle test results of each hydrogel at different times of crosslinking: a)0 h, b)12 h and c)24 h. .....…..93
Figure 3.6: X-ray diffractograms showing the amorphous character of: A) Chitosan, B) Gelatin, C) CHTGEL, D) CHTGEN, E) GELGEN, F) CHTGELGEN scaffolds 94
Figure 3.7: X-ray diffractograms showing the amorphous character of A) Hyaluronic acid, B) Gelatin, C) HAGEL, D) HAGELGEN scaffolds..... 95
Figure 3.8: Differential Scanning Calorimetry (DSC) thermograms of A) GEL, B) CHT, C) CHTGEN, D) GELGEN, E) CGG and F) CHTGEL scaffolds over the range 10°C to 300°C 96
Figure 3.9: Differential Scanning Calorimetry (DSC) thermograms of A) GEL, B) CHT, C) CHTGEN, D) GELGEN, E) CGG and F) CHTGEL scaffolds over the temperature range, 10 °C to 300 °C..... 97
Figure 3.10:. Swelling potential of each scaffold after immersion in PBS (n=3) (SD<4)..... 99
Figure 3.11:. Scanning Electron Microscope micrographs obtained of transverse cross-sections of a) CHTGEN, b) GELGEN, C) CHTGELGEN, d) HAGEL, e) HAGELGEN scaffolds 101
Figure 3.12: Graph depicting the degradation behaviour of each scaffold over 30 days in PBS (n=3) 104
Figure 3.13: Scanning Electron Microscope images of a) full-IPN and b) semi-IPN after 30 days…… 104
Figure 3.14: Calibration curve constructed for Dexamethasone-21-Phosphate by varying the concentration of the drug in PBS (R2=0.997) 105
Figure 3.15: Drug release behaviour of Dexamethasone-21-Phosphate from the IPN and semi-IPN in PBS at 37°C (n=3) 105
Figure 4.1: Schematic showing the synthesis of the proteosaccharide scaffold……. 113
Figure 4.2: Images showing the in-situ gelation of the proteosaccharide scaffold..... 115
Figure 4.3: Temperature sweeps of each hydrogel ratio a) PuraMatrix, b) 1:1, c) 3:1 and d) 5:1 ratios of chitosan:PuraMatrix conducted over the temperature range, 10 °C to 40 °C.. 118
Figure 4.4: Bar graph showing the cytotoxicity of each hydrogel ratio on PC12 cell lines using an XTT assay (n=3) over 48 hours (n=3) 5-FU (5-Fluorouracil, 10 µg/ml) was used as the positive control. 119
Figure 4.5: Fourier Transform Infrared (FTIR) spectra of A) PuraMatrix, B) Chitosan, C) CHT-PM (PBS), D) CHT-PM, E) CHT-PM (washed) scaffolds..... 120
Figure 4.6: CD spectra of PuraMatrix before and after self-assembling with Chitosan at 37°C. 121
Figure 4.7: Bar graph showing the secondary structure content of PuraMatrix before and after self-assembly with Chitosan using the CDtoolX software 123
Figure 4.8: Differential Scanning Calorimetry (DSC) thermograms of a) Chitosan; b) CHT-PM (gelled) and c) CHT-PM (ungelled) over temperature range 10 °C to 300 °C. 124
Figure 4.9: Scanning Electron Microscope (SEM) micrograph of PuraMatrix fibres (transverse cross section), magnification: 493x and EHT: 6.00 Kv..... 126

Figure 4.10: Scanning Electron Microscope(SEM) micrograph of chitosan scaffold (2%w/v) (transverse cross section), Magnification: 300x and EHT: 20.00kV 126
Figure 4.11: Scanning Electron Microscope(SEM) micrograph of CHT-PM (1:3) (transverse cross section), Magnification: 572 x and EHT=20.00kV 127
Figure 4.12: Scanning Electron Microscope (SEM) micrograph focusing showing varipus nanofibers and microporous structures though a large pore, Magnification: 873 X and EHT=20.00kV 127
Figure 4.13: Surface of CHT-PM scaffold showing surface porosity and roughness, Magnification=372X and EHT=20.00kV 128
Figure 4.14: Stress-strain curves of a) PuraMatrix, b) Chitosan and c) CHT-PM 129
Figure 4.15: Degradation behaviour of PuraMatrix and CHT-PM (n=3) (SD<3) 130
Figure 5.1: Bar graph showing cytotoxicity results from an XTT assay of each formulation over 72 hours on PC12 cells (n=3)..... 138
Figure 5.2: Bar graph showing cytotoxicity results from an XTT assay on the PMCHT formulation over 72 hours (n=3) 139
Figure 5.3: Bar graph showing cytotoxicity results from the XTT assay performed on A172 cells over 48 hours (n=3)..... 140
Figure 5.4: Wound closure of A172 cells following a scratch assay and treatment with PM formulation at a) 0 hours, b)8 hours, c)24 hours and d) 48 hours 142
Figure 5.5: Wound closure of A172 cells following a scratch assay and treatment with CHT-PM formulation at a) 0 hours, b)8 hours, c)24 hours and d) 48 hours..... 143
Figure 5.6: Wound closure of A172 cells following a scratch assay and treatment with CHTGELGEN full-IPN formulation at a) 0 hours, b)8 hours, c)24 hours and d) 48 hours... 143
Figure 5.7: Wound closure of A172 cells following a scratch assay and treatment with HAGELGEN semi-IPN formulation at different time intervals a) 0 hours, b) 8 hours, c) 24 hours and d) 48 hours 144
Figure 5.8: : Wound closure of A172 cells following a scratch assay and no treatment at different time intervals a) 0 hours, b) 8 hours, c) 24 hours and d) 48 hours 145
Figure 5.9: Bar graph showing the percentage wound closure at different time intervals calculated using ImageJ wound healing analysis 146

LIST OF EQUATIONS

Equation 2.1: Florry-Huggins Lattice model equation. 18
Equation 3.1: Crystallinity index of proteosaccharide scaffolds……..67
Equation 3.2: The swelling potential of each scaffold after immersion in PBS..... 68
Equation 3.3: Bulk density of proteosaccharide scaffolds……68
Equation 4.1: Cell viability of PC12 cells 114
Equation 5.1: Cell viability of PC12 and A172 cells……..117
Equation 5.2: Average wound closure calculated using ImageJ software……..132

LIST OF ABBREVIATIONS

3D	Thee-dimensional
3T3	Mouse fibroblasts
A172	Human glioblastoma cells
ADA	Alginate dialdehyde
ALG	Alginate
ATP	Adenisine triphosphate
BMSC	Bone marrow stromal cells
BSA	Bovine Serum Albumin
CD	Circular Dichoism
CGG	Chitosan-gelatin-genipin
CHT	Chitosan
CHTGEL	Chitosan-gelatin
CHTGEN	Chitosan-genipin
CHTRGD	Chitosan-RGD
CNS	Central Nervous System
CO2	Carbon dioxide
COL	Collagen
CS	Chondroitin sulfate
DEX	Dexamethasone
DMEM	Dulbecco's Modified Eagle Medium
DNA	Deoxyribonucleic acid
DSC	Differential scanning calorimetry
ECM	Extracellular Matrix
FBS	Fetal bovine serum
FTIR	Fourier transform infrared spectroscopy
GA	Glutaraldehyde
GAG	Glycosaminoglycans
GEL	Gelatin
GCHTRGD	Genipin-Chitosan-RGD
GHARGD	Genipin-Hyaluronic acid-RGD
GELGEN	Gelatin-Genipin
HAGEL	Hyaluronic Acid-Gelatin

HAGELGEN	Hyaluronic Acid-Gelatin-Genipin
HAMA	Hyaluronic acid methacrylate
HARGD	Hyaluronic acid-RGD
HDF	High density fibroblasts
HEC	Human endothelial cells
HP	Horseradish Peroxidase
HUVEC	Human umbilical vein endothelial cells
IPN	Interpenetrating polymeric network
ISO	International standards organisation
MRI	Magnetic resonance imaging
MSC	Mesenchymal stem cells
NAD	Nicotinamide-adenine dinucleotide
NHS	N-Hydroxysuccinimide
NMR	Nuclear Magnetic Resonance
PBS	Phosphate Buffered Saline
PC12	Rat adrenal medulla pheochomocytoma cells
PCL	Polycaprolactone
PEC	Polyelectrolyte complex
PEG	polyethylene glycol
PGA	polyglycolic acid
PM	PuraMatrix
PVA	Polyvinyl alcohol
RGD	Arginylglycylaspartic acid
RNA	Ribonucleic acid
ROS	Reactive Oxygen Species
SAP	Self-assembling peptide
SEM	Scanning Electron Microscopy
SF	Silk Fibroin
SMC	Smooth muscle cells
TBI	Traumatic Brain Injuries
TXA	Texture analyser
UV	Ultra-violet
VEGF	Vascular endothelial growth factor
XRD	X-ray diffraction

CHAPTER 1. INTRODUCTION AND OVERVIEW OF THE STUDY

1.1 Tissue engineering and the extracellular matrix (ECM)

Tissue engineering has significantly evolved over the past thee decades, dating from the year 1987, when the term 'tissue engineering' was first coined. However, its application had begun prior to 1987, with skin substitutes being one of the first engineered tissues by scientists in the 1970s (Berthiaume *et al.*, 2011). The terms, 'tissue engineering' and 'regenerative medicine' have often been used synonymously in literature, however each may be given a different definition. Regenerative medicine refers to the replacement or regeneration of human tissues, organs and cells with the aim of re-establishing normal function, post a traumatic injury or chonic condition (Orlando *et al.*, 2011). This regeneration or replacement may occur *in vivo,* where the body is allowed to repair itself by developing and implanting a stimulatory biomaterial which aids the body in its regeneration, or *ex vivo*, where the substitute is developed outside the body and subsequently implanted.Tissue engineering can be considered a branch of regenerative medicine which refers to the use of cells, biomaterials, biochemicals and physical factors to create a tissue like structure ex vivo, with the end goal being the implantation of these structures into the body (Berthiaume et al., 2011). Both processes involve the use of cells, natural or synthetic biomaterials or growth factors (Katari *et al.*, 2015). Some therapies may necessitate the combination of all the above

The extracellular matrix (ECM) is a complex environment consisting of biomolecules such as proteins and proteoglycans amongst others, where cells can reside, interact, and regulate their functions continuously. The ECM serves as a bioactive structural support, routinely sequestering complex biomacromolecules to induce and regulate cellular functions such as adhesion, proliferation and differentiation, which directly influences regeneration (Geckil *et al.*, 2010). Thus, regenerative medicine is predominantly focused on the development of synthetic extracellular matrices which can provide the mechanical and structural support to cells, as well as permit cellular signalling within the matrix. Key properties of the ECM which should be replicated in synthetic matrices include its elasticity, diffusivity, water holding capacity, and local degradation by cell secreted proteases to mention a few (Kyburz *et al.*, 2015). Thus, polymers recruited in tissue engineering should be adequately tuned to meet these requirements. Not only does the choice of polymer influence biomimicry, but methods employed in the development of these constructs also play a key role in the biomimicking ability of tissue engineered constructs.

1.2 Scaffolds in tissue engineering and polymers involved

Scaffolds are a necessary component in regenerative medicine as scaffolds serve as an interim synthetic ECM upon which tissue regenerates. Scaffolds have thus far been used in neural, bone, cardiac, cartilage and skin tissue engineering and have also been used in the controlled, spatial delivery of bioactive substrates such as growth factors, and drugs. Scaffolds are thee-dimensional and should ideally perform the following functions:

1. Scaffolds should be bioactive i.e., they should allow for cell-biomaterial interactions which thus influences cell adhesion on scaffolds and should regulate native ECM deposition, cellular proliferation and differentiation.
2. Scaffolds should have a porous structure, with suitable pore sizes (10-1000 μm) which allows for the diffusion of oxygen, nutrients and other growth factors.
3. Scaffolds should be biodegradable by *in vivo* enzymes at a rate which should match the rate of regeneration of native tissue.
4. Scaffolds should be biocompatible, elicit minimal immune reactions and should have negligible toxicity (Dhandayuthapani *et al.*, 2011).

Biological scaffolds refer to scaffolds prepared from human or animal tissue, while synthetic scaffolds are produced from synthetic polymers. Some natural polymers constitute part of the ECM biomacromolecules which are arranged thee dimensionally and thus influence haemostasis (Sell *et al.*, 2010). These include collagen, elastin, laminin and hyaluronic acid to mention a few (Palsson & Bhatia, 2004). It is thus advantageous to incorporate natural polymers in scaffolds due to their enhanced biocompatibility, bioactivity, and the elimination of the need for functionalization to achieve cell-scaffold interactions.

Synthetic polymers are also considered attractive candidates in tissue engineering as they can be mechanically and chemically modified with relative ease. They are readily available and may be processed under mild conditions, which do not adversely affect cells. However, synthetic polymers lack biological cues and thus need to be further modified, which can be time consuming and often affects other properties such as mechanical strength and degradation (Place *et al.*, 2009). The most commonly employed synthetic polymers include poly(ethylene glycol) (PEG), poly(vinyl alcohol) (PVA), poly(glycolic acid) (PGA), poly(caprolactone) (PCL), poly(propylene fumarate) (PPF) and poly(phosphazene) (Kunduru *et al.*, 2016).

1.3 Traumatic brain injuries

Post a traumatic brain injury, tissue loss results in the formation of fluid filled cavities which interrupt synaptic connection and leads to loss of function. The cavity formed is an inhospitable

environment which prevents neural regeneration, which is further stumped by glial scar formation. In the first thee days following traumatic brain injury, activated microglia and macrophages migrate to the cavity to remove invading pathogens and debris. On day thee to five, oligodendrocyte precursors and meningeal cells migrate to the cavity and interact with astrocytes leading to formation of the *glial limitans*, also referred to as a glial scar. The glial limitans is composed of cells which secrete inhibitory molecules which oppose regeneration. Regenerating axons are therefore not able to cross the tissue gap (Guo *et al.*, 2015). Bridging this gap is therefore the main objective for neural regeneration and this is where regenerative medicine comes into effect.

The regeneration of the central nervous system is of major interest in the field of tissue engineering. CNS injuries have long lasting and often, debilitating effects on patients. The creation of an extracellular environment that closely resembles native brain tissue is an ongoing challenge for scientists. The immunological cascade following traumatic brain injury creates a further challenge for scientists. Most researchers have tried to stabilise the affected area and prevent further damage. The peripheral nervous system (PNS) shows greater potential for neural regeneration due to the presence of Schwann cells which guide regeneration, along with secreting neurotrophins and producing ECM molecules which contribute to neural regeneration. The presence of astrocytes which form glial scars and oligodendrocytes which create an inhibitory environment surrounding the injury makes CNS regeneration much more challenging.

The current gold standard for treatment is end-to-end neurorrhaphy, however this technique can only be employed in patients where the nerve gap spans less than 1cm (Johnson *et al.*, 2005). Nerve grafts can be used for gaps that exceed 1cm, however the limited number of grafts available as well as neuroma formation and immunological responses limit this treatment option(Philips *et al.*, 2018). Other treatment options have been summarised in table 1.1.

Table 1.1: Current therapeutic interventions for TBI's and their benefits and shortcomings

Treatment option	**Benefits**	**Shortcomings**	**References**
Stem cell transplants (with/without neurotrophins)	The replacement of lost cells due to TBI's. Modification of cells to express neurotrophic factors (Brain-derived neurotrophic factor) which allows axonal regeneration.	Directed axonal growth cannot be facilitated due to the lack of a physical 3D construct. 90-99% of cells have died due to the inhibitory environment of the CNS.	(Casarosa *et al.*, 2014; Heile & Brinker, 2011; Sarnowska *et al.*, 2013)

End-to-end suturing	Gold standard for 'ideal' injuries which do not exceed 1cm gaps, and denervation over less than 6 months.	Most lesions are not ideal.	(Daly *et al.*, 2013; Liang *et al.*, 2013)
Autologous nerve transplants	Used in non-ideal lesions >1cm.	Healthy donor tissue can be sacrificed. Can lead to neural fibrosis and scar formation.	(Kuffler, 2015; Tian *et al.*, 2015)
Scaffolds	Serve as a stand in structure which guides neural regeneration across gaps. Requires no sacrifice of healthy tissue.	Polymers need to be carefully chosen and modified to closely mimic the neural environment.	(Dado & Levenberg, 2009; Yuan *et al.*, 2014)

1.4 The use of proteins and peptides in tissue engineering

Various polymers, both natural and synthetic have been employed in the creation of scaffolds and hydrogels for neural regeneration. Naturally occurring polymers possess the advantage of biocom]patibility and can easily be modified to fit the site of action. These polymers are biodegradable and yield non-toxic degradation products, thus minimising *in vivo* toxicity. Some of the polymers include proteinaceous polymers such as collagen, gelatin, elastin and keratin, and polysaccharides such as chitosan, hyaluronic acid and gelatin. A more detailed summary on the characteristics of these polymers and their applications can be found in chapter 2 of this dissertation. Proteins play an important role in physiological processes such as signal transduction, enzymatic reactions, and cell motility, thereby making proteins an attractive class of polymers to be utilised in tissue engineering. Proteins undergo fast remodelling *in vivo* favouring neovascularization and functional cells organization, elicit a negligible immune response, and are relatively cheap. Furthermore, the incorporation of proteins such as collagen and gelatin provide peptide motifs which support cell proliferation and thus render scaffolds bioactive. The incorporation of proteins into scaffolds for regenerative medicine therefore increases the biomimicking ability of scaffolds and enhance cellular interactions *in vivo* (Klimek & Ginalska, 2020). Recently, there has been a shift from using proteins to the inclusion of peptides in regenerative scaffolds. Peptide modified scaffolds show close structural and biological similarities to protein-modified scaffolds. Peptides are more beneficial than proteins due to their easier and more cost-effective modifications as compared to the fabrication of full-length macromolecular proteins. Peptides are more resistant to pH and temperature and show low immunogenicity. Some peptides which have been used to date include laminin, BMP- derived peptides, RADA-16-I and peptide QK (Klimek & Ginalska, 2020).

1.5 Self-assembling peptides

An interesting and relatively new class of peptides, known as self-assembling peptides (SAP), have also gained much attention in the field of regenerative medicine. Self-assembling peptides can be defined as peptides which spontaneously aggregate under certain conditions. They comprise of monomers of amino acids which aggregate to form a nanofibrillar structure (Ellis-Behnke *et al.*, 2006). This self-assembling mechanism can be attributed to weak non-covalent interactions such as hydrogen bonds, electrostatic interactions, hydrophobic interactions and van der waal's interactions (Kumar *et al.*, 2011). These collective interactions lead to the formation of a structurally stable, nanofibrous network which can be employed in drug delivery and tissue engineering due to their non-toxic degradation products i.e., amino acids, as well as their nanofibrous morphology which closely resembles that of the ECM. Peptides with specific sequences can be easily obtained by solid-phase synthesis; (b) the small size of peptides allows the design of appropriate sequences for assembly into supramolecular structures; and (c) new peptides can be inspired from naturally self-assembling protein motifs. Additional advantages include their multivalency, molecular specificity, and multifunctionality. When compared to other biomaterials, SAPs have numerous advantages, such as the minimal risk for biological contaminants which are present in animal-derived polymers, a thee-dimensional matrix environment which is optimal for cell growth and proliferation and no apparent immune response when introduced in vivo. SAPs are usually injectable in nature and can easily fill lesion cavities, while also having haemostatic properties (Guo *et al.*, 2009).

Many promising self-assembling peptides have been identified over the years, including RADA-16-I, PA and P11 peptides (Ravichandran *et al.*, 2014). RADA-16-I, commercialised as PuraMatrix hydrogel has found numerous applications in neural tissue engineering. This peptide undergoes self-assembly into β-sheet nanofibers under physiological conditions (pH and temperature). The 3D nanofibrous structure form has pore sizes ranging from 5-200nm and has an extensive water holding capacity (approximately 99%). Furthermore, the range of pore sizes are comparable to therapeutic moieties, thereby proposing its potential in drug delivery. Scanlon and Aggeli (2008) discovered P11, comprised of glutamine residues with alternating polar and aromatic residues, which undergo self-assembly, dependent on pH, temperature, amino acid charge and monomer concentration. These selves assemble into β-sheet monomers, tapes and fibrils and above a critical concentration, assemble into viscoelastic hydrogels (Scanlon & Aggeli, 2008). The phenomenon of self-assembly can be found in natural molecules such as ferritin, which is a hollow protein assembled from 24 block forming units, which is imperative to iron transport and storage. Furthermore, s-layer proteins self-assemble into a cell wall component for the uptake of nutrients in bacteria. Laminin also

undergoes receptor-triggered self-assembly on cell surfaces which allows for various crucial cellular activities, such as differentiation, movement, and signalling. More detail on the structures of self-assembling peptides can be found in table 1.2.

Table 1.2: Different structures of self-assembling peptides and their characteristics

Structure	Characteristics	Reference
α – helices	• Contain hydrophilic and hydrophobic amino residues. • Periodicity of 3.6 amino acids per turn. • Can self-assemble into coiled-coil confirmations. • Requires long amino acid sequences to stabilise the helical structure.	(Loo *et al.*, 2015)
β- sheet peptides	• Able to self-assemble into thee-dimensional nanofibrous structures with the involvement of ionic self-complementary peptides, • Based on the alternation of hydrophobic and hydrophilic residues into a β- sheet structure. • Can render a large variety of morphologies such as nanofibers, nanoparticles and nano-vesicles.	(Shao *et al.*, 2020)
Ionic self-complimentary peptides	• Based on the alternation of hydrophobic and hydrophilic residues. • Classified by the number of repeated ion charges: Type I has a charge pattern of "+-+-+-", Type II has "++–++– ", Type III has "+++—+++", and Type IV has "++++—". • The peptide sequences with periodically repeated positive and negative charges form the stable structure by ionic-complementary forces in a checkerboard-like pattern and then assemble typical beta-sheet structures and eventually form a hydrogel network of nanofiber	(Guo *et al.*, 2015; Yang *et al.*, 2020)
Cyclic peptides	• Constituted by alternating D and L amino acids which can form nano tubes. • Other types of cyclic peptides are characterized by amphiphilic characteristics, i.e., one side of the cycle is hydrophilic, whereas the other side contains hydrophobic and/or aggregation-prone amino acids • Composed of stacking cyclic peptide monomers with a flat conformation structure, in which the carbonyl and amino groups are pointed perpendicular to the ring and the side chains present a pseudo-equatorial outward-pointing orientation. • The nanotubes are stabilized by hydrogen bonds between amide groups in neighbouring peptide cycles	(Gelain *et al.*, 2006; Hartgerink *et al.*, 2001)
Long chain alkylated peptides	• Hydrophilic peptide sequences and hydrophobic alkyl chains. • Alkyl chain can be conjugated on both the N- and C-termini of the peptide sequences.	(Kumar *et al.*, 2011; Lee *et al.*, s.a.)

	• In the aqueous solution, individual alkylated peptides could aggregate together to form cylinder nanofibers	

1.6 Aim and objectives:

The aim of this study is to develop a biomimetic, proteosaccharide-based, 3D-bioprinted, neuro-ECM scaffold for potential neuro-regeneration after traumatic neural injuries. A cationic and anionic polysaccharide and a self-assembling peptide will be incorporated in a scaffold and tested for potential neuro-regeneration. The above aim will be achieved by carrying out the following objectives:

1. To select the most chemically and physically biocompatible polysaccharides and self-assembling peptides to form the architecture of the scaffold.
2. To carry out analytical studies to test the viscoelastic properties (storage modulus, loss modulus) on the hydrogels formed before synthesis of a scaffold.
3. To produce a scaffold by freeze-drying and carry out analytical tests such as young's modulus, compression and tensile strength, swelling ratio, porosity and scanning electron microscopy.
4. To perform *in vitro* cell studies e.g., of cell lines, on each scaffold, to assess the potential of neural regeneration and cytotoxicity of the scaffold.

1.7 Potential benefits of the study

1. The combination of a self- assembling peptide with cationic and anionic polysaccharides and subsequent 3D bioprinting, will result in the formation of a proteosaccharide scaffold with greater mechanical strength, reduced rate of degradation, and optimal drug release at the site of action, viz the CNS.
2. The scaffold may be seeded with neurotropic factors which can assist patients suffering from neurodegenerative diseases such as Parkinson's and Alzheimer's Disease.
3. Patient's quality of life will improve due to a restoration of lost function and financial strain associated with recurrent pharmacological treatments and increased hospital visits will be reduced.
4. Using MRI/CT scan data, patient-specific scaffolds can be designed, and 3D printed to meet the requirements of the defective tissue.
5. Bioactive loaded onto the scaffold would combat the challenge associated with crossing the blood-brain barrier.
6. When the scaffold is loaded with bioactive, systemic side effects will be reduced due to more precise spatial distribution of the bioactive. Due to the biodegradable nature

of the scaffold, there will be no need for surgery to remove the implanted scaffold and any degradation products yielded will be non-toxic in nature.

1.8 Synopsis of dissertation

Chapter One of this dissertation will give a brief background to the study and classes of materials to be used in the study. This chapter will also provide background information to TBI's and their current treatment options. It will also detail the aim and objectives of the study and will provide information on the novelty of the study.

Chapter Two of this dissertation will discuss the class of polymers i.e., proteosaccharide combinations that have currently been used for regenerative medicine. This chapter will provide detail on the synergism of these combinations, methods of crosslinking, molecular interactions, and the applications of each proteosaccharide thus far in tissue engineering. From this chapter, the proteosaccharide combinations and crosslinker to be utilised in this research will be selected.

Chapter Thee of this dissertation will focus on two proteosaccharide combinations employing a cationic polysaccharide (chitosan), and an anionic polysaccharide (hyaluronic acid) and crosslinking them to the anionic protein gelatin, using genipin. The physicochemical, morphological, rheological, and degradation behaviour will be discussed in this chapter. Various analytical methods such as FTIR, DSC, XRD, SEM and rheological characterisation will be applied to each proteosaccharide. Comparative drug release studies will also be discussed in this chapter, whereby the proteosaccharides will be loaded with the glucocorticoid, Dexamethasone-21-phosphate and its release at a pH of 7.4, which matches cerebrospinal fluid will be evaluated.

Chapter Four of this dissertation will focus on the final peptide-polysaccharide formulation, employing cationic chitosan with self-assembling peptide, PuraMatrix (RADA-16-I). The physicochemical, morphological, rheological, and degradation behaviour will be discussed in this chapter. This chapter will determine the effect of combining a designer peptide with a polysaccharide and discuss the proteosaccharide interaction using FTIR, XRD, DSC, SEM and textural analysis. Circular dichoism will also be used to determine the secondary structure of the peptide, before and after combining it with chitosan.

Chapter Five of this dissertation will discuss *in vitro* studies undertaken on each of the thee proteosaccharides in this dissertation. Cytotoxicity (XTT) and migration studies were performed to show the biocompatibility, toxicity, and cellular response to each biomaterial.

The *in vitro* studies will be used to establish the potential of each proteosaccharide for applications in neural regeneration by using two neural cell lines, Rat (Rattus Norvegicus) adrenal gland pheochomocytoma (PC12) and human glioblastoma multiforme (A172) cells

Chapter Six summarizes the results obtained in the previous chapters and highlights the potential of the all the proteosaccharides characterised, in neural tissue engineering. This chapter also discusses the limitations of the research conducted and further ways to optimise future research outputs.

REFERENCES

Berthiaume, F., Maguire, T.J. & Yarmush, M.L. 2011. Tissue Engineering and Regenerative Medicine: History, Progress, and Challenges. Annual Review of Chemical and Biomolecular Engineering. 2(1):403–430.

Casarosa, S., Bozzi, Y. & Conti, L. 2014. Neural stem cells: ready for therapeutic applications? Molecular and Cellular Therapies. 2(1):31.

Dado, D., & Levenberg, S. 2009. Cell-scaffold mechanical interplay within engineered tissue. Seminars in cell & developmental biology, 20(6), 656–664.

Daly, W.T., Knight, A.M., Wang, H., de Boer, R., Giusti, G., … Windebank, A.J. 2013. Comparison and characterization of multiple biomaterial conduits for peripheral nerve repair. Biomaterials. 34(34):8630–8639.

Dhandayuthapani, B., Yoshida, Y., Maekawa, T. & Sakthi Kumar, D. 2011. Polymeric Scaffolds in Tissue Engineering Application: A Review. International Journal of Polymer Science. 2011.

Ellis-Behnke, R.G., Liang, Y.X., You, S.W., Tay, D.K.C., Zhang, S., … Schneider, G.E. 2006. Nano neuro knitting: Peptide nanofiber scaffold for brain repair and axon regeneration with functional return of vision. Proceedings of the National Academy of Sciences of the United States of America. 103(13):5054–5059.

Geckil, H., Xu, F., Zhang, X., Moon, S., & Demirci, U. 2010. Engineering hydrogels as extracellular matrix mimics. Nanomedicine (London, England), 5(3), 469–484.

Gelain, F., Bottai, D., Vescovi, A. & Zhang, S. 2006. Designer Self-Assembling Peptide Nanofiber Scaffolds for Adult Mouse Neural Stem Cell 3-Dimensional Cultures. PLoS ONE. 1(1): e119.

Guo, J., Leung, K.K.G., Su, H., Yuan, Q., Wang, L., … Wu, W. 2009. Self-assembling peptide nanofiber scaffold promotes the reconstruction of acutely injured brain. Nanomedicine: Nanotechnology, Biology, and Medicine. 5(3):345–351.

Guo, J., So, K.F. & Wu, W. 2015. Self-Assembling Peptides Mediate Neural Regeneration. In: Neural Regeneration. Elsevier Inc. pp. 229–236.

Hartgerink, J.D., Beniash, E. & Stupp, S.I. 2001. Self-Assembly and Mineralization of Peptide-Amphiphile Nanofibers. Science. 294(5547):1684–1688.

Heile, A. & Brinker, T. 2011. Clinical translation of stem cell therapy in traumatic brain injury: The potential of encapsulated mesenchymal cell biodelivery of glucagon-like peptide-1. Dialogues in Clinical Neuroscience. 13(3):279–286.

Johnson, E., Zoubos, A., Injury, P.S.- & 2005, undefined. s.a. Regeneration and repair of peripheral nerves. Elsevier. https://www.sciencedirect.com/science/article/pii/S0020138305004201?casa_token=zqca94j1Wz4AAAAA:rtAz6ne3gDMqD8FMe-_8XX9PRUR0uC-iKrZU-De2clFa4yatQ9dIfH_wnhqvk7Ff2lCzxjVqozo Date of access: 08 Mar. 2021.

Katari, R., Peloso, A. & Orlando, G. 2015. Tissue Engineering and Regenerative Medicine: Semantic Considerations for an Evolving Paradigm. Frontiers in Bioengineering and Biotechnology. 2:57.

Klimek, K. & Ginalska, G. 2020. Proteins and Peptides as Important Modifiers of the Polymer Scaffolds for Tissue Engineering Applications—A Review. Polymers 2020, 12, 844

Kuffler, D. 2015. Citation: Kuffler DP (2015) Promoting Axon Regeneration and Neurological Recovery Following Traumatic Peripheral Nerve Injuries. Int J Neurorehabilitation Eng. 2(1):148.

Kumar, P., Pillay, V., Modi, G., E. Choonara, Y., C. du Toit, L. & Naidoo, D. 2011. Self-Assembling Peptides: Implications for Patenting in Drug Delivery and Tissue Engineering. Recent Patents on Drug Delivery & Formulation. 5(1):24–51.

Kunduru, K.R., Basu, A. & Domb, A.J. 2016. Biodegradable Polymers: Medical Applications. In: Encyclopedia of Polymer Science and Technology. John Wiley & Sons, Inc. pp. 1–22.

Kyburz, K.A., Anseth, K.S. & Biomed Eng, A. 2015. Synthetic Mimics of the Extracellular Matrix: How Simple is Complex Enough? HHS Public Access Author manuscript. Ann Biomed Eng. 43(3):489–500.

Lee, S., Trinh, T.H.T., Yoo, M., Shin, J., Lee, H., … Ryou, C. s.a. Molecular Sciences Self-Assembling Peptides and Their Application in the Treatment of Diseases.

Liang, Y., Walczak, P. & Bulte, J.W.M. 2013. The survival of engrafted neural stem cells within hyaluronic acid hydrogels. Biomaterials. 34(22):5521–5529.

Loo, Y., Goktas, M., Tekinay, A.B., Guler, M.O., Hauser, C.A.E. & Mitraki, A. 2015. Self-Assembled Proteins and Peptides as Scaffolds for Tissue Regeneration. Advanced Healthcare Materials. 4(16):2557–2586.

Mano, J.F., Silva, G.A., Azevedo, H.S., Malafaya, P.B., Sousa, R.A., … Reis, R.L. 2007. Natural origin biodegradable systems in tissue engineering and regenerative medicine: Present status and some moving trends. Journal of the Royal Society Interface. 4(17):999–1030.

Orlando, G., Wood, K.J., Stratta, R.J., Yoo, J.J., Atala, A. & Soker, S. 2011. Regenerative Medicine and Organ Transplantation: Past, Present, and Future. Transplantation, 91, 1310-1317.

Philips, C., Cornelissen, M., & Carriel Araya, V. S. (2018). Evaluation methods as quality control in the generation of decellularized peripheral nerve allografts. Journal Of Neural Engineering, 15(2).

Place, E.S., George, J.H., Williams, C.K. & Stevens, M.M. 2009. Synthetic polymer scaffolds for tissue engineering.

Ravichandran, R., Griffith, M. & Phopase, J. 2014. Applications of self-assembling peptide scaffolds in regenerative medicine: the way to the clinic.

Sarnowska, A., Jablonska, A., Jurga, M., Dainiak, M., Strojek, L., … Domanska-Janik, K. 2013. Encapsulation of Mesenchymal Stem Cells by Bioscaffolds Protects Cell Survival and Attenuates Neuroinflammatory Reaction in Injured Brain Tissue after Transplantation. Cell Transplantation. 22(1_suppl):67–82.

Scanlon, S. & Aggeli, A. 2008. Self-assembling peptide nanotubes. Nano Today. 3(3–4):22–30.

Sell, S.A., Wolfe, P.S., Garg, K., McCool, J.M., Rodriguez, I.A. & Bowlin, G.L. 2010. The use of natural polymers in tissue engineering: A focus on electrospun extracellular matrix analogues. Polymers. https://doi.org/10.3390/polym2040522

Shao, Q., Wong, K.M., Seroski, D.T., Wang, Y., Liu, R., … Hall, C.K. 2020. Anatomy of a selectively coassembled β-sheet peptide nanofiber. Proceedings of the National Academy of Sciences. 117(9):4710–4717.

Tian L., Prabhakaran M.P., Hu J., Chen M., Besenbacher F., Ramakrishna S. 2015. Coaxial electrospun poly (lactic acid)/silk fibroin nanofibers incorporated with nerve growth factor support the differentiation of neuronal stem cells. RSC Adv. 2; 5:49838–49848.

Yang, Z., Xu, H. & Zhao, X. 2020. Designer Self-Assembling Peptide Hydrogels to Engineer 3D Cell Microenvironments for Cell Constructs Formation and Precise Oncology Remodeling in Ovarian Cancer. Advanced Science. 7(9):1903718.

Yuan, Tian, W., Sun, L., Yuan, R., Tao, J. & Chen, D. 2014. Neural stem cell transplantation in a double-layer collagen membrane with unequal pore sizes for spinal cord injury repair. Neural Regeneration Research. 9(10):1014.

CHAPTER 2. REVIEW OF VARIOUS PROTEOSACCHARIDE COMBINATIONS AND THEIR TISSUE ENGINEERING APPLICATIONS

Carbohydrate Polymers 235 (2020) 115932

Contents lists available at ScienceDirect

Carbohydrate Polymers

journal homepage: www.elsevier.com/locate/carbpol

Proteosaccharide combinations for tissue engineering applications

Henna Cassimjee, Pradeep Kumar, Yahya E. Choonara, Viness Pillay*

Wits Advanced Drug Delivery Platform Research Unit, Department of Pharmacy and Pharmacology, School of Therapeutic Sciences, Faculty of Health Sciences, University of the Witwatersrand, Johannesburg, 7 York Road, Parktown, 2193, South Africa

ARTICLE INFO

Keywords:
Hydrogel
Biomimicry
Crosslinking
Chitosan
Alginate
Hyaluronic acid
Proteosaccharide

ABSTRACT

Biomaterials that function as tissue surrogates ought to form three dimensional structures which are conducive to cell proliferation and regeneration. Since the extracellular matrix (ECM) is composed of proteoglycans (long chain polysaccharides) and proteins, the combination of proteins and polysaccharides presents a logical strategy to mimic the ECM and guide cell growth and proliferation. Polysaccharides are distinctive scaffold materials for regeneration due to their biocompatibility, hydrophilicity, biodegradability and functional groups which may be modified to improve mechanical properties and cell signalling. However, modification of polysaccharides is often time consuming, and requires extensive chemical reactions. Therefore, to improve physiological signalling, tissue response and mechanical strength, polysaccharides are combined with proteins. This review will focus on naturally occurring proteins and polysaccharide combinations as well as draw attention to their specific use within the tissue engineering field.

2.1 Introduction

Researchers have assigned several definitions to hydrogels over the years, the most common being, “polymer networks which are extensively swollen with water” (Ahmed, 2015). According to another definition, hydrogels inherently possess the ability to swell and retain a considerable amount of water but are not water soluble (Li et al., 2013). Based on their degree of flexibility, hydrogels have been widely used in tissue engineering. The swelling ability of hydrogels is attributed to the numerous hydrophilic functional groups such as amino (-NH2,), carboxyl (−COOH), hydroxyl (−OH), amide (−CONH2,), and sulfhydryl (-SO3H) groups which may be attached to the backbone of the constituting polymers, while the resistance to dissolution is governed by the crosslinks within the network (Baham, Mohseni, & Moghtader,2016). Tissue engineering refers to the combination of polymers, engineering and cells to serve as a surrogate for damaged tissue and facilitate regeneration (Lee & Mooney, 2001). To achieve this, cells need to be cultured in a suitable scaffold. Hydrogels are attractive scaffold materials due to their excellent biocompatibility, modifiable viscoelasticity, hydrophilicity, high oxygen

and nutrient permeability, and their ability to act as bioactive conduits in a manner that is minimally invasive (Lee & Mooney, 2001; Silva et al., 2018).

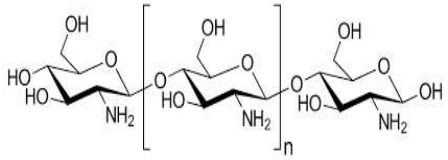
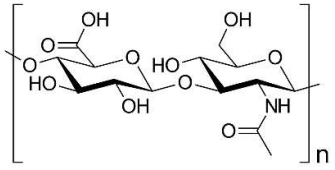
Properties of an ideal hydrogel are shown in Table 2.1. The fulfilment of all these criteria by a single biomaterial is impossible, therefore composite biomaterials are extensively used in hydrogel preparation. Hydrogels should encapsulate cells homogenously and provide a thee-dimensional microenvironment for cells which resembles the extracellular matrix (ECM). In native tissue, cell behaviour is dictated by stimuli produced by the ECM. Similarly, hydrogels should be able to provide critical cues to control cellular function and promote as well as guide tissue repair and regeneration (Li et al., 2018). Natural and synthetic polymers have been used extensively in tissue engineering, either individually or as a hybrid component. Carbohydrates are multifaceted, dynamic molecules which are well sought after for their biological capabilities. Some glyconomic researchers have also stated that capability of storing biological information of carbohydrates is significantly greater than other biological molecules, due to the presence of variable glycosidic linkages and structural conformations. Carbohydrates significantly interact with cells though glycoconjugates i.e., glycolipids, glycosaminoglycans (GAGs), glycoproteins and proteoglycans (Yanagishita, 1993). The most commonly employed carbohydrate polysaccharides are chitosan, hyaluronic acid, cellulose and alginate which account for approximately 70% of tissue engineering studies (Tchobanian, Van Oosterwyck, & Fardim, 2019). Due to the analogous function and structure of polysaccharide materials to ECM components such as glycosaminoglycans, as well as the presence of glycan moieties which provide biomolecular cues, polysaccharides are established key players in biomaterial design (Russo & Cipolla, 2016).

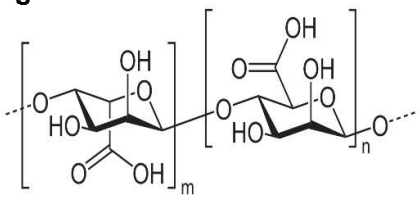
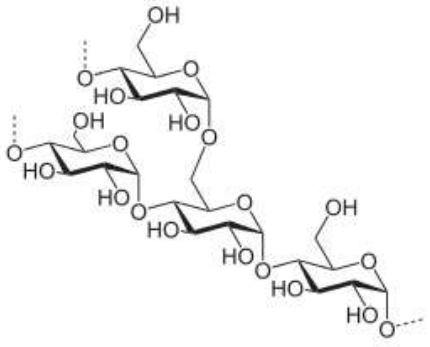
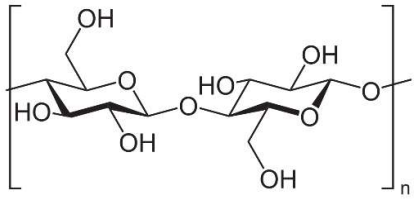
Table 2.1: Summary of important parameters for the development of hydrogels. Reproduced with permission from Creative Commons Attribution-Non-Commercial 4.0 License. Tiwari, S., Patil, R. and Bahadur, P. (2018) 'Polysaccharide based scaffolds for soft tissue engineering applications', Polymers. MDPI AG. doi: 10.3390/polym11010001.

General attributes	**Biocompatibility**	**Biological Signaling**
Composition and porosity	Predictable degradation	Biomimicry
Stiffness and elasticity	Low immunogenicity	Release of cooperative factors
Ease of administration	Non-toxic degradation products	Colonisation of host cells without inducing histological changes
		Integration with host tissues

Natural polysaccharides contain carboxyl and hydroxyl functional groups which can be modified to facilitate combination with other polymers, give specificity in function and alter biological and mechanical activity of the parent polymers. Naturally occurring polysaccharides are also able to form viscoelastic gels in aqueous media mediated by non-covalent interactions (Nishinari, Zhang, & Ikeda, 2000). Moreover, electrostatic interactions are favoured due to the high charge density present on some polysaccharides (Nishinari et al., 2000; Tiwari, Patil, & Bahadur, 2018). However, the molecular weight distribution, sequence, and branching on polysaccharides is not consistent, thus adversely affecting their rheological behaviour. Inferior mechanical strength also presents a major obstacle due to susceptibility to enzymatic hydrolysis, but this may be overcome by chemical modification of polysaccharide backbones as shown in Table 2.2, cross-linking and the incorporation of other polymers with polysaccharides in biomaterial systems (Montalbano et al., 2018).

Table 2.2: Summary of key chemical modifications of commonly employed natural polysaccharides to better suit their tissue engineering applications.

Carbohydrate	**Chemical modifications**	**Advantages**
Chitosan 	1. Carboxymethylation at amine and 6-hydroxyl sites of glucuronic units. 2. Graft co-polymerization (e.g., CS graft PCL, CS-NiPAAM, CS-graft poly (DL-Lactide). 3. Blending with other polymers such as Silk, Alginate, and Cellulose).	1. Increased water uptake capacity and solubility. 2. Increased thermoresponsiveness and pH responsiveness 3. Increased tissue regeneration ability.
Hyaluronic acid 	*-COOH modifications* 1. Amidation with carbodimides (EDC) 2. Esterification with alkyl halides (e.g., alkyl bromide, alkyl iodide). 3. Ugi condensation reaction. *-OH modifications* 1. Crosslinking with epoxides leading to ether formation.	1. Tailorable degradation kinetics. 2. Decreased aqueous solubility by increasing degree of esterification 3. Epoxides readily hydrolysed to non-toxic diols. 4. Deacetylation may destroy fragments of the polymer backbone.

	2. Esterification with alkyl succinic anhydrides. 3. Graft co-polymerization with acyl chloride. *-$NHCOCH_3$ modifications* 1. Deacetylation of N-acetyl groups.	
Alginate 	1. Graft co-polymerisation of at -OH groups (e.g., ALG-PEG, ALG-vinylsulfonic acid). 2. Oxidation of -*OH* of uronic units with sodium periodate. 3. Crosslinking with multivalent cations such as calcium and bromine. 4. Sulfation.	1. Increased pore dimensions and cell anchorage. 2. Increased swelling. 3. Sulfation results in better haemocompatibility due to its similarity to heparin.
Starch 	1. Blending with thermoplastic polymers (e.g., cellulose acetate, PCL, PVA). 2. Graft co-polymerization with acrylamide, acetonitrile or glycidyl methacrylate by radical polymerization.	1. Increased thermal and mechanical stability. 2. Improved ease of processing.
Cellulose 	1. Phosphorylation. 2. Graft copolymerization. 3. Blending with other materials to form composites.	1. Enhanced bioactivity. 2. Greater tissue engineering applications.

The use of protein-based components in hydrogels such as gelatin, collagen, silk fibroin and fibrin provide the option to insert certain peptide sequences in hydrogel systems which promote cellular adhesion and cell growth (Schloss, Williams, & Regan, 2016). Primary,

secondary and tertiary structures present on natural proteins determine their main function. Furthermore, proteins lend structural support to cells and allow for the stimulation of cell-triggered remodelling and the recognition of cell receptors in vivo (Silva et al., 2018). Cellular synthesis of proteins is considered the most precise and programmable polymer chemistry process. Protein sequences, length, and stereochemistry may be fine-tuned and varied based on genetic information, thus presenting great opportunities for engineering their function. Protein-based hydrogels are recognised widely due to their structural designability, biological functionality and stimuli-responsiveness (Wang et al., 2018).

Research on proteins and polysaccharides has mainly focused on their individual modifications and applications, however conjugation between the two classes of biomaterials for biomedical applications has seldom been mentioned due to the abundance of functional groups present which may lead to undesirable action and complicate purification and application of the composite biomaterial. Proteosaccharides refer to the glycoconjugate formed by covalent interactions of a polysaccharide and protein. The most common carbohydrate-protein interactions recognised in the body are lectin and antibodies (Y. Lee & Lee, 1995). Lectins are proteins which bind carbohydrate structures though their carbohydrate reaction domains. Antibodies which are the main components of the immune system differ in their hypervariable region referred to as the antigen binding site (Y.C. Lee & Lee, 1995). This binding site is constituted of amino acids. When an antigen presented, is a polysaccharide, a proteosaccharide interaction occurs. Proteosaccharide interactions are predominant at the glycolipid membrane (Yanagishita, 1993). These interactions can thus influence cell adhesion and recognition. Therefore, proteosaccharide combinations such as alginate-gelatin, silk-hyaluronic acid and mucin-pectin have been used by several researchers, usually with the aim of counteracting negative features associated with an individual polymer. These proteosaccharides show enhanced bioactivity and less toxicity when compared to synthetic polymers. This chapter will therefore cover different proteosaccharides and their roles in tissue engineering.

2.2 Proteosaccharide interactions

Proteosaccharide interactions have been studied extensively by researchers, however it still remains a challenging concept to understand. In any hybrid biopolymer system, the entropic and enthalpic contributions must be considered. The difference between these contributions determines if phase separation or association between the polymers will occur. Table 3 provides a brief interpretation of phase separation or association in relation to the Florry-

Huggins lattice model (de Kruif & Tuinier, 2001). When the entropic contribution exceeds the enthalpic contribution, phase separation occurs. When proteins and carbohydrates, two phase separation phenomena can be observed namely associative phase separation and segregative phase separation. When the biopolymers are oppositely charged, associative phase separation occurs, where one phase has a greater content of proteosaccharide either as a coacervate or precipitate (K. & Bandyopadhyay, 2012). Segregative phase separation is driven by strong electrostatic repulsion whereby a single phase is fomed at low concentrations, however at higher concentrations, phase separation begins to occur. Certain polysaccharides such as chitosan and cellulose undergo phase separation upon mixing with proteins such as gelatin. In order to prevent separation of the polymers, crosslinking is essential in proteosaccharide systems.

Flory-Huggins Lattice model: chemical potentials equality in each phases (subscripts 1, 2, 3: solvent, polymer 1, polymer 2)

$$\frac{\Delta\mu_1}{RT} = Ln\Phi_1 + \left(1-\frac{1}{x_2}\right)\Phi_2 + \left(1-\frac{1}{x_3}\right)\Phi_3 + \Phi_2\Phi_3(\chi_{12}+\chi_{13}-\chi_{23}) + \chi_{12}\Phi_2^2 + \chi_{13}\Phi_3^2$$

$$\frac{\Delta\mu_2}{RT} = Ln\Phi_2 + \left(1-\frac{x_2}{x_3}\right)\Phi_3 + (1-x_2)\Phi_1 + x_2\left(\chi_{23}\Phi_3^2 + \chi_{12}\Phi_1^2 + \Phi_1\Phi_3(\chi_{12}+\chi_{23}-\chi_{13})\right)$$

$$\frac{\Delta\mu_3}{RT} = Ln\Phi_3 + \left(1-\frac{x_3}{x_2}\right)\Phi_2 + (1-x_3)\Phi_1 + x_3\left(\chi_{23}\Phi_2^2 + \chi_{13}\Phi_1^2 + \Phi_1\Phi_2(\chi_{13}+\chi_{23}-\chi_{12})\right)$$

Enthalpic terms | Entropic terms

Equation 2.1.

Table 2.3. A brief interpretation of the Florry Huggins Lattice model equation to determine phase separation phenomena.

X_{23}- polymer1-polymer2 interaction	
X_{23}- (+)	Segragative phase separation between polymers
X_{23}- (-)	Associative phase separation between polymers

The formation of proteosaccharides is largely dependent on factors such as pH, temperature, choice and concentration of polymers as well as ionic strength. The formation of electrostatic complexes is dependent on the isoelectric point (p*I)* of the protein. When the pH of the medium is greater than the isoelectric point of the protein, the protein becomes anionic and is thus able to form a polyelectrolyte complex with positively charged polysaccharide and vice versa. The solution pH, however, should not be close to that of the isoelectric point of the protein as the

protein becomes neutrally charged, thus leading to weak complex formation. At high protein concentrations, thermodynamic incompatibility occurs, usually when the pH is greater than the protein pI. Therefore, variations in concentration and pH can alter proteosaccharide interactions (K. & Bandyopadhyay, 2012).

Non-covalent interactions such as H-bonding, Van der Waals forces and hydrophobic interactions are prevalent in proteosaccharide systems. Carboxylic acid groups present on polysaccharides and amino groups on proteins are associated with H-bonding, while the presence of a few non-polar segments is responsible for hydrophobic bonds. Covalent interactions between proteins and polysaccharides can be attributed to two main chemical reactions i.e. Schiff base formation and the Maillard reaction (Afewerki *et al.*, 2019). This leads to the formation of covalent bonds resembling endogenous proteogylcans.

Proteosaccharide interactions may be extensively studied though ultraviolet spectrometry, x-ray diffraction and fluorescence spectrometry (Kakehi *et al.*, 2001). FTIR analysis is the main indicator of covalent bond formation in a proteosaccharide. The most important functional groups present on polysaccharides are the hydroxyl and acetal groups, whereas proteins contain a carboxyl and defining amino group. The formation of covalent bonds between the molecules can be achieved by chemical crosslinkers which link the amino group of the protein with the hydroxyl group of the polysaccharide leading the formation of a stable amide bond. The reaction mechanism can be found in figure 2.1. Treatment of the polysaccharide with an acid or base result in ring opening of the polysaccharide, resulting in a reactive aldehyde moiety, which reacts with the primary amine group of a protein (Afewerki *et al.*, 2019). A Schiiff base adduct is formed after β-elimination leading to the formation of a proteosaccharide. The collagen-chitosan interaction was first studied by Taravel and Domard (1995) using FTIR and CD (circular dichoism) spectrometry. Their study brought to light that the primary interactions accounting for proteosaccharide formation were hydrogen and electrostatic bonds. Another group of researchers went a step further by using viscometry and wide-angle x-ray diffraction as well as FTIR and found that chitosan had disrupted the helical structure of collagen though hydrogen bond formation resulting in a more gelatin like phase, and also increased the viscosity of the network (Sionkowska *et al.*, 2004). Treesuppharat and Manuspiya (2017) confirmed the formation of an imine bond mediated by chemical crosslinker glutaraldehyde between gelatin and bacterial cellulose. Pure gelatin showed peaks at 3290cm-1 and 2960cm-1 corresponding to the N-H and C=H groups respectively. an additional peak at 3600cm-1 was

found in the composite suggesting hydrogen bond formation in the network. Imine bond formation was also reported from FTIR results of gelatin-chitosan proteosaccharides crosslinked by genipin where a C=N bond was observed at 1078cm^{-1} (Cui *et al.*, 2015). Sarker and co-workers (2014) also showed that when oxidised alginate (ADA) was crosslinked with gelatin, absorption bands found at 1621cm-1 and 1557cm-1 due to a stretch C=N vibration, indicating Schiff's base formation (Sarker *et al.*, 2014). Deepthi and Jayakumar (2018) showed the formation of an amide group in an alginate-fibrin matrix. The matrix showed a shift a peak at 1654cm-1 indicative of a -C=O stretching vibration, as well as a broadening in the peak at 3452cm-1 indicative of an interaction at the -OH group of alginates. Of main interest was the shift in the peak found at 1084cm-1 indicative of a C-N stretch (Deepthi & Jayakumar, 2018). Similarly, EDC/NHS was used to crosslink the amino and carboxyl groups of collagen, chondroitin and hyaluronic acid for cartilage regeneration(Linda, 2015) .

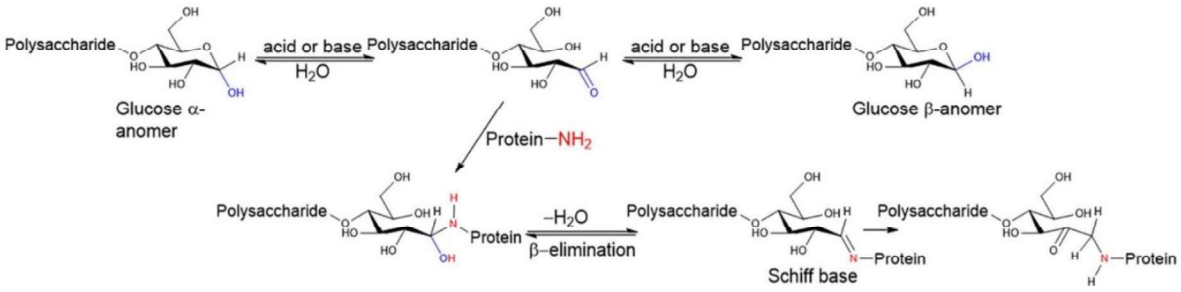


Figure 2.1:Chemical reaction between a protein and polysaccharide though a Schiff base formation. Reproduced with permission from Creative Commons. Afewerki, S, Sheikhi, A, Kannan, S, Ahadian, S, Khademhosseini, A. Gelatin-polysaccharide composite s scaffolds for 3D cell culture and tissue engineering: Towards natural therapeutics. Bioengineering & Translational Medicine. 2019; 4: 96– 115. https://doi.org/10.1002/btm2.10124

Thermal stability can be increased or reduced based on the choice of polymers. Frequently tested using thermogravimetric analysis and differential scanning calorimetry, thermal stability is an important parameter to be considered in proteosaccharides. As suggested by Rocha-Garcia (2017), thermal and kinetic behaviour of hydrogels is dependent on the thermo-responsive behaviour of the crosslinked network (Rocha-García *et al.*, 2017). Proteins are complex hierarchal structures, which are extremely sensitive to changes in temperature and pH. Gelatin is the most common temperature responsive temperature is known to renature at a temperature of 20°C. This is affected by blending with polysaccharides due to the disruption of the helical structure of gelatin, thus reducing its renaturation fraction. However, when composites are crosslinked, such as with genipin, thermal stability notably increases due to the formation of strong covalent bonds between the polymers. Additionally, certain

polysaccharides such as cellulose which have a high degradation temperature, improve the thermal stability of certain proteosaccharides. Cellulose has been proven to resist degradation up until a temperature of 295°C (Horseman *et al.*, 2017). Other polymers whose incorporation into proteosaccharide composites would result in improved thermal stability are chitosan and starch, which are thermally stable up until temperatures of 340°C and 300°C respectively (Szymańska & Winnicka, 2015; Taghizadeh & Abdollahi, 2015).

Rheological behaviour is a parameter which can be modified in proteosaccharides by varying the content of each component in the system. Rheological behaviour of hydrogels may subsequently dictate their clinical applications, therefore parameters such as gelation time and equilibrium modulus need to be considered. Certain polymers which improve the mechanical behaviour of proteosaccharides include alginate, hyaluronic acid, cellulose as well as silk. Balakrishnan and co-workers (2014) found that when alginate and gelatin were combined, the gel formation time was shortened to approximately 20 seconds as confirmed by time and frequency sweep rheology. However, the formation of a developed 3D structure cannot be established at the gelling point in any polymeric system due to the presence of some non-interacting mobile fragments. Overall, the final storage modulus of the gel was found to be greater than 1kPa, which is similar to many self-assembling peptide gels, thus allowing its application as an injectable hydrogel for cartilage regeneration (Balakrishnan *et al.*, 2014). Another group of researchers incorporated nanohydroxyapatite coatings on the ALG-GEL hydrogel which further increased the storage modulus and improved osteogenic bone differentiation (Rosellini *et al.*, 2009). The addition of alginate to collagen in a wound healing scaffold resulted in an approximate seven times increase (8.2MPa) in storage modulus as compared to pure collagen scaffolds. Another proteosaccharide which demonstrated improved rheological behaviour as compared to their parent polymers is hyaluronic acid and gelatin. Camci-unal and co-workers (2013) found that HUVEC cells did not spread in non-adhesive HAMA hydrogels, however the addition of GelMA resulted in increased cell spreading in 3D constructs. Mechanical properties were also enhanced as compared to single component hydrogels. Compressive moduli ranged from 5.0 ± 2.5 to 73.0 ± 11.1 kPa, suggesting the potential for applications in neural, cardiac, cartilage or skeletal muscle engineering (Camci-Unal *et al.*, 2013). Another group of researchers confirmed that the addition of HA resulted in an increased stiffness of the hydrogels. and 2% w/v hydrogels were more suitable for tissue engineering with a Young's modulus ranging from 4kPa for pure gelatin to 6.3kPa for pure HA (Sanmartín-Masiá *et al.*, 2017). When HA was incorporated with

collagen, the hybrid scaffold demonstrated a compressive modulus of 54.77±0.31 kPa (Mohammadi *et al.*, 2018). Kumar, Dehiya and Sindhu (2017) also reported that force bearing capacity of chitosan-gelatin scaffolds was 1.9MPa while scaffolds containing chitosan only, had a force bearing capacity of 1.4MPa, thus suggesting an improvement in mechanical strength of the proteosaccharide. It can thus be concluded that proteosaccharides have improved mechanical strength and force-bearing capacity as compared to their individual polymers.

2.3 Crosslinking of proteosaccharides

Proteosaccharides can be crosslinked in many methods to form stable hydrogels (Figure 2). Some of the reasons for crosslinking include improvement of thermal and mechanical stability, improvement of gelation behaviour, reduction in the rate of degradation and enhancement of bioactivity. Methods of crosslinking may be divided into two classes: physical and chemical crosslinking (Hennink & van Nostrum, 2012).

2.3.1 Physical crosslinking

Physical crosslinking can occur under relatively mild conditions without crosslinking agents being incorporated. This is beneficial as the incorporation of chemical crosslinkers may severely impact biocompatibility due to the possibility of cytotoxicity. Stability may also be affected due to possible interactions between the bioactive and chemical crosslinker (Hennink & van Nostrum, 2012). Ionic crosslinking is included as a method of physical crosslinking. Ionic crosslinking refers to the electrostatic interaction between a positively charged molecule and a negatively charged molecule leading to the formation of a polyelectrolyte complex (Gombotz & Wee, 2012). A common example of polymer that undergoes ionic crosslinking is alginate. Alginate may be crosslinked by the addition of divalent cations such as calcium, barium or zinc (Kong *et al.*, 2004). The gelation of alginate is usually induced prior to the addition of protein components. Montalbano and co-workers (2018) designed a collagen-alginate-fibrin hydrogel in thee sequential steps: (1) self-contained gelation of collagen, (2) gelation of alginate in a calcium chloride solution and (3) incubation of fibrinogen in thombin solution. A similar method was reported by Ma and co-workers (2012). Carboxymethylcellulose is another polysaccharide which is able to form hydrogels upon exposure to multivalent cations including iron (III) and calcium by electrostatic interactions (Arica, 2000). Alginic acid, pectin, chitosan and CMC are some of the polysaccharides which may be ionically crosslinked to proteins to form stable polyelectrolyte complexes. pH is a major parameter to be considered in the formation of polyelectrolyte complexes, due to protonation which changes the polysaccharide

charge. Charged proteins include gelatin, keratin and silk fibroin(Ma, Liu, *et al.*, 2012). Attention must be directed to the exchange of ions *in vivo,* e.g calcium ions may be exchanged with sodium ions in a saline solution, thus affecting hydrogel stability (Voron'ko *et al.*, 2016). Chitosan may also be crosslinked with transition metal ions such as Ag^{+}, Cu^{2+}, Zn^{2+}, Co^{2+}, Ni^{2+}, Cd^{2+}, and Pd^{2+}. the supramolecular structure showed a high water holding capacity, rapid gelation, and stimuli responsive ability (Sun *et al.*, 2015).

Thermogelation is another example of physical crosslinking. The most common example of a protein that undergoes thermogelation is gelatin. When the reaction temperature is lower than the upper critical solution temperature, the solution becomes a hydrogel. By initial heating, the solubility of the polymer is improved, however by further increasing the temperature, chain entanglement and hydrogen bonds are weakened (Klouda & Mikos, 2008). This phenomenon is noted for gelatin. Inverse thermogels form when heating of a solution changes water-polymer entropy or physical binding which leads to gelation or hydrogel shinkage at higher temperatures (Baham *et al.*, 2016). Polysaccharides that undergo thermogelation include chitosan, hydroxypropyl methylcellulose (HPMC), methylcellulose (MC) as well as collagen. Montalbano and co-workers(2018) designed a thermo-responsive proteosaccharide hydrogel consisting of collagen, alginate and fibrin which gelled rapidly at physiological conditions allowing material delivery in a liquid state at room temperature and crosslinking at body temperature (37°C) (Montalbano *et al.*, 2018). Stabenfeldt and co-workers (2006) functionalised methylcellulose with laminin to create a scaffold for neural tissue engineering (Stabenfeldt *et al.*, 2006). The laminin functionalised scaffold promoted neural adhesion to a greater extent than the MC scaffold, however by adjusting the concentrations, the hydrogels exhibited a lower critical solution temperature below 37°C.

2.3.2 Chemical crosslinking

Although chemical crosslinking leads to the formation of more stable hydrogels, toxicity associated with chemical crosslinkers is problematic in tissue engineering. Hydrophilic polymers containing -OH, -COOH and -NH_2 groups may be crosslinked using a water-soluble carbodiimide such as 1-ethyl-3-(3-dimethylamino) propyl carbodiimide, hydrochloride/ N-hydroxysuccinimide (EDC/NHS) (Nair & Balakrishnan, 2016; Omobono *et al.*, 2015). However, these carbodimides as well as glutaraldehyde have been shown to be cytotoxic to cells laden in hydrogels. Proteosaccharides crosslinked with EDC/NHS include collagen-hyaluronic acid, where the least amount of crosslinker (8mM) showed optimal viability of mesenchymal stem cells (MSCs). Hyaluronic acid (HA) has also been crosslinked with gelatin according to the

mechanism shown in figure 2.5, whereby EDC reacts with carboxyl groups present on hyaluronic acid leading to the formation of an intermediate acid anhydride, which undergoes further reaction with gelatin's amino group resulting in a final amide linkage (Khunmanee *et al.*, 2016) Ethylenediamine derivatives of HA have been used to produce an interpenetrating polymer network (IPN) with silk fibroin thus increasing its resistance to hydrolysis (Palumbo *et al.*, 2015). Carboxymethylcellulose was also reacted with tyramine in the presence of EDC/NHS to form a CMC-Tyramine intermediate which underwent enzymatic crosslinking with silk. The use of dual crosslinking lead to the formation of hydrogels with greater stability and a compressive modulus reaching 829kPa (Sakai *et al.*, 2009). Other proteosaccharides which may be crosslinked using EDC/NHS include HA-Gelatin and Bovine Serum Albumin (BSA)-Chitosan.

Glutaraldehyde (GA) is a commonly employed chemical crosslinker to improve mechanical strength and durability of hydrogels (Kopeček, 2007). Amine or hydroxyl groups present on the polymers are able to interact with glutaraldehyde though a Schiff base formation, resulting in an inter- and intramolecularly connected proteosaccharide. (Chajra *et al.*, 2008; Kim *et al.*, 2006). Gelatin has frequently been crosslinked with glutaraldehyde which was regarded as the gold standard chemical crosslinker, however toxicity of glutaraldehyde is a major obstacle (Treesuppharat *et al.*, 2017; Yin *et al.*, 2014). Toxicity is largely attributed to aldehyde groups present on glutaraldehyde which are toxic to cells and cause inflammation (Oryan *et al.*, 2018). Some researchers have stated that glutaraldehyde concentration should be directly influenced by the number of amine groups on the polymer while the optimal crosslinking degree should have the minimum number of aldehyde residues (Azami *et al.*, 2010; Salem *et al.*, 2010). Proteosaccharides crosslinked with glutaraldehyde include gelatin-chitosan, collagen-alginate, collagen-HA, collagen-chitosan, gelatin-cellulose, starch-gelatin and pectin-gelatin. Due to the toxicity associated with glutaraldehyde, much attention has been given to non-toxic crosslinkers such as genipin.

Due to its natural origin and low toxicity, genipin has gained significant interest in tissue engineering (Mi *et al.*, 2002). *In vitro* studies have shown that genipin is almost 10000 times less toxic and shows 5000 times greater cell proliferation than glutaraldehyde (Oryan *et al.*, 2018). Genipin reacts with polymers containing amino acids, with the reaction being macroscopically evident as a blue pigment. Both chitosan and gelatin may be crosslinked with genipin to form a blue coloured hydrogel (Cui *et al.*, 2015). Collagen may also be crosslinked

with genipin, due to the presence of lysine, hydroxylysine and arginine amino acid residues which react with genipin (Huang *et al.*, 1998). Firstly, the olefinic carbon at position 3 of genipin is attacked by primary amines which results in the opening of the dihydropyran ring and subsequent bridge formation with the participation of intermediate genipin species (Huang *et al.*, 1998). Secondly, nucleophilic substitution of genipin's ester group with an amine group leads to the formation of a secondary amide (Mi *et al.*, 2002). The second reaction takes place at a slower pace than the first (Nath *et al.*, 2015). Genipin is thus able to crosslink both chitosan and collagen to form stable hydrogels. Gilarska and co-workers (2018) identified the optimal concentration of genipin to crosslink collagen-chitosan-HA hydrogels to be 20mM (Gilarska *et al.*, 2018). Hydrogels crosslinked with a low concentration (2mM) of genipin were completely wettable with higher concentrations of genipin resulting in a more compact structure with reduced hydrophilicity (Gilarska *et al.*, 2018). Other proteosaccharides which may be crosslinked with genipin include collagen-chitosan-hyaluronic acid, silk-chitosan, BSA-Chitosan and Collagen-Cellulose. Despite the safety of genipin in tissue engineering, genipin is expensive and can bare economic implications in mass production of hydrogels (Oryan *et al.*, 2018). Table 2.2. illustrates the various chemical crosslinkers employed in covalent crosslinking of proteosaccharides along with their mechanism of action and reaction conditions.

Table 2.4. Table showing chemical crosslinkers employed in covalently crosslinking proteosaccharides.

Crosslinker	Mechanism of crosslinking	Reaction conditions
Carbodiimides (EDC, DCC)	Zero length crosslinkers which directly conjugate carboxylate to the primary amine group. Amide bonds are not formed.	• No extraneous carboxyls and amines. • pH of 4.5-5.5 or MES (4-morpholino-ethane-sulfonic acid) buffer is preferable. • PBS (pH<7.2) is also compatible. • N-hydroxysuccinimide (NHS) is added to increase reactivity of the amine intermediate.
Aldehydes (Glutaraldehyde, formaldehyde)	Amino groups of proteins e.g., lysine residues in collagen form an aminomethylol derivative upon reaction with the aldehyde e.g., formaldehyde. Crosslink formation	• Replaced by natural crosslinkers due to considerable toxicity

	occurs when the aminomethyloyl moiety is then reacted with an acid amide. Imine bonds are formed when glutaraldehyde is used to crosslink the polysaccharide due to the Schiff base reactions between the amino group of the polysaccharide (e.g., chitosan) and the aldehyde group of glutaraldehyde. Under acidic conditions, oxidation of polysaccharides occur and yields 2,3-dialdehyde polysaccharides which can crosslink the lysine or hydroxylysine residues found in proteins by C=N bonds.	
Plant phenolics (tannic acid, ferulic acid, gallic acid)	Diphenol moieties of the phenolics are oxidised under alkaline conditions leading to formation of quinone intermediates. These intermediates react with nucleophiles from amino acid groups resulting in C-N bond formation between the phenolic and amino containing polymer.	• Antioxidant properties of the plant phenolics are beneficial for biomedical applications. • A brown colour change may occur.
Genipin	Reacts with nucleophilic amino groups, resulting in an initial ring opening reaction to form an intermediate aldehyde. .	• Negligible toxicity due to natural origin. • Blue colour change may be observed associated with the generation of radicals upon exposure to oxygen or its reaction with amino groups.

2.3.3 Photopolymerization

Photopolymerisation is used in hydrogel synthesis due to its spatiotemporal controllability and biocompatibility. Polymers are modified with photoreactive methacrylate groups initially to facilitate photocrossliking (Li *et al.*, 2018). A photoinitiator is usually added, however high concentrations of photoinitiator may generate toxic radicals which may lead to cell damage. Hyaluronic acid and gelatin were photocrosslinked under UV light. The carboxylate groups on HA, and the lysine functional groups of gelatin were methacrylated to facilitate UV crosslinking

resulting in gelatin methacrylamide (GelMA) (Camci-Unal *et al.*, 2013). Methacrylate groups are reported to protect cells encapsulated in the hydrogel by quenching free radicals (Bartnikowski *et al.*, 2015). Yano and co-workers (2015) photocrosslinked fish elastin and methylcellulose by initially methacrylating fish elastin polypeptide and thereafter subjecting the composite to photoirraditation (Yano *et al.*, 2015).

2.3.4 Enzymatic crosslinking

The most commonly used enzymes in enzymatic crosslinking are transglutaminase and horseradish peroxidase(HP) (Chen *et al.*, 2003). N ǫ- (γ- glutamyl) lysine cross-links are introduced into proteins by transglutaminase though a trans-amidation reaction, while HP oxidatively couples hydroxyphenylpropionic acid moieties and leads to network formation between the polymers. Enzymatic crosslinking shows rapid gelation of hydrogels and is highly selective. Thyrosine reactive residues on silk fibroin facilitates enzymatic crosslinking with HPand H_2O_2, however the transition of random coil to β-sheet aggregates still affects mechanical stability after 4 weeks *in vitro* (Raia *et al.*, 2017). A group of researchers induced this transformation by treatment with ethanol after crosslinking by HP/H_2O_2 (Numata *et al.*, 2017; Su *et al.*, 2017). Tyramine conjugates of gelatin and hyaluronic acid were also crosslinked by HP/H_2O_2 as shown by Sanmartin-masia and co-workers (2017). Microbial transglutaminase was also used in the crosslinking of chitosan and gelatin (Sanmartín-Masiá *et al.*, 2017)

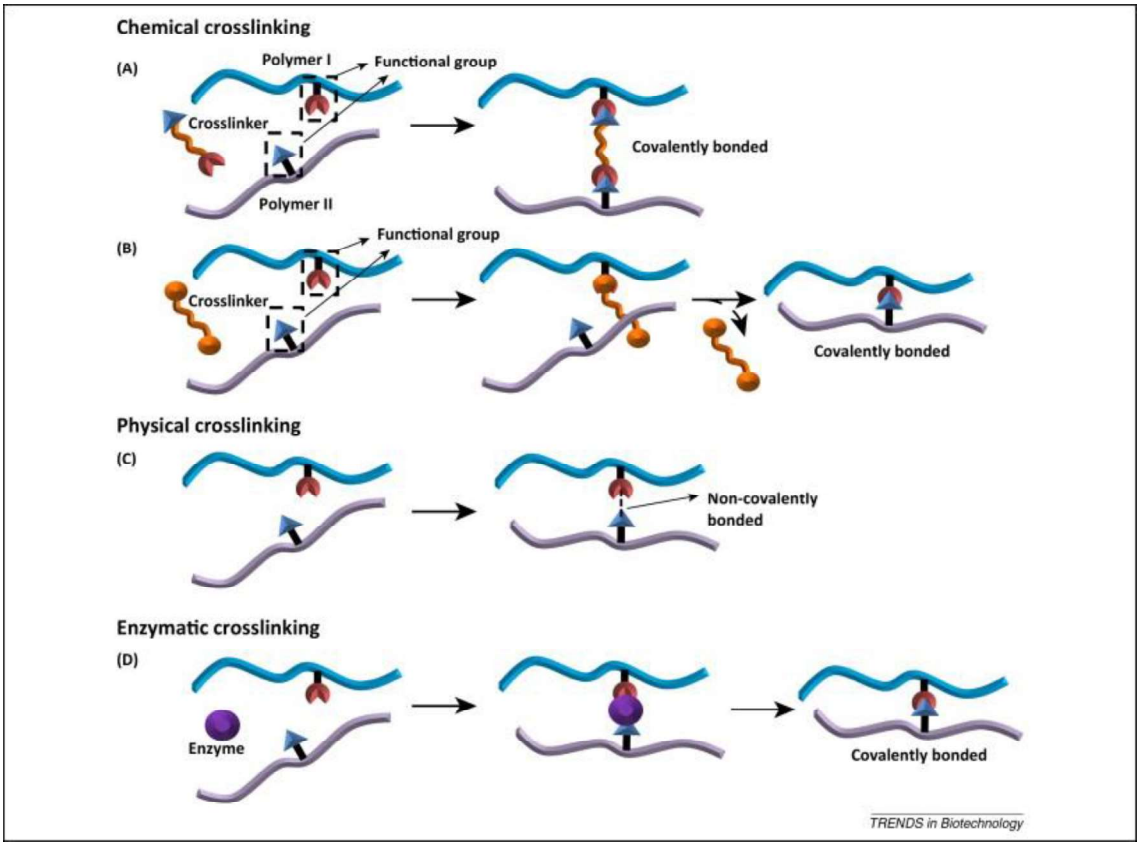


Figure 2.2. Graphical abstract showing methods of crosslinking proteosaccharide hydrogels. Reproduced with permission from Reddy et al., 2015 © Elsevier B.V, Ltd.

2.4 Applications of proteosaccharides

2.4.1 Alginate-based proteosaccharides

Alginic acid, available as an extract from brown algae, is a linear polysaccharide consisting of (1,4)-linked β-D mannuronic acid (M) linked to α-L-guluronic acid (G) residues (Smidsrod and Skjakbrk, 1990; Lee and Mooney, 2012). Despite the ease associated with ionic crosslinking of alginate, mechanical properties are inferior and uniformity of gels formed though ionic crosslinking is difficult to control, thus affecting the stability of the gel formed (Lee & Mooney, 2012). Other methods of cross-linking include covalent crosslinking which may improve the mechanical properties of the gel formed, however many crosslinking agents are toxic and need to be removed thoroughly post-formulation (Smidsrod and Skjakbrk, 1990; Kong *et al.*, 2004; Lee and Mooney, 2012). Suzuki and co-workers (1998) reported that when alginate was covalently cross-linked with ethylene diamine, a gel more biocompatible and less immunogenic than ionically cross-linked gels was formed (Suzuki *et al.*, 1998). Alginate gels can also be formed by photo-crosslinking and possess superior mechanical integrity. Such gels have been reported for use in the treatment of corneal perforation, however, the release

of acid or the light sensitizer used in the process, may be potentially toxic (Smeds & Grinstaff, 2001). Alginate hydrogels have been used as wound dressings due to their ability to maintain a moist environment and reduce bacterial infection at the site of the lesion and are capable of sustaining concentrations of biologicals such as proteinaceous bioactive agents (Aderibigbe & Buyana, 2018). Alginate gels have also demonstrated potential in the regeneration of blood vessels (neovascularization), which could be a solution to conditions such as peripheral artery disease and coronary artery disease caused by an obstruction of blood flow and subsequent ischaemia(Lee *et al.*, 2010). Alginate gels have been used as a suitable delivery vehicle of angiogenic factors such as vascular endothelial growth factor (VEGF) by Lee and researchers (2003), where a sustained release of VEGF was noted over 14 days from an alginate gel injected in ischaemic muscle tissue (Lee *et al.*, 2003). The main limitation of alginate as a biomaterial include its poor cell attachment, and lack of cell-biomaterial interactions as well as poorly controllable degradation kinetics (Lee & Mooney, 2012). Therefore, alginate has been combined with proteins such as collagen, elastin, fibrin and gelatin.

Gelatin, typically of fish, bovine or porcine origin is obtained though the hydrolysis of collagen (Elzoghby, 2013). Gelatin possesses lower antigenicity than collagen, yet upon hydrolysis, still maintains information signals i.e. Arginine-Glycine-Aspartate (RGD) sequence which promotes cell-biomaterial interactions (Elzoghby, 2013). Due to the similarity of gelatin to proteins in the ECM, biocompatibility, biodegradability and low, gelatin has been exploited in regenerative immunogenicity medicine and other biomedical applications (Ghasemi-Mobarakeh *et al.*, 2008). Additionally, the low cost of procurement, abundance and the presence functional groups which allow for facile chemical modifications favours the use of gelatin as a biomaterial (Ghasemi-Mobarakeh *et al.*, 2008). The main challenges associated with gelatin as a biomaterial include its high viscosity, sensitivity to enzymatic degradation, low solubility in aqueous media and inferior mechanical properties (Elzoghby, 2013). Due to the sol-gel transition properties of gelatin at 30°C, gelatin must be cross-linked to avoid dissolution when introduced in the body (Ghasemi-Mobarakeh *et al.*, 2008). Gelatin consists of various amino acids such as glycine, hydroxyproline, arginine, cysteine and tyramine. However, the glycine and hydroxyproline residues are thought to be the most important. hydroxyproline contains a hydroxyl group, endowing the molecule with its ability to interact with water, while glycine plays an important role in specific linkages with polysaccharides due to its optimal orientation of polar or charged lateral groups of amino acids.

Gelatin and alginate have been used synergistically in biomaterial systems in an attempt to counteract the shortcomings of the individual polymers. When gelatin and alginate are combined, usually by covalent crosslinking, alginate benefits from the cell binding motif present on gelatin, allowing for better cellular interactions and gelatin benefits from the mechanical strength provided by alginate (Balakrishnan *et al.*, 2014). To facilitate covalent crosslinking, alginate may be partially oxidised to form alginate dialdehyde (ADA), which then reacts with gelatin though a Schiff's base formation (Sarker *et al.*, 2014). Free amino groups present on lysine or the hydroxylysine amino acid residues of gelatin react with aldehyde groups present on ADA to form a crosslinked ADA-GEL hydrogel microcapsules (Sarker *et al.*, 2014). Sarker and co-workers (2014) found that by decreasing gelatin content, the degree of crosslinking was increased due to greater availability of reactive aldehyde groups of ADA to react with gelatin (Sarker *et al.*, 2014). When gelatin content was increased, available reactive aldehyde groups are consumed resulting in some uncrosslinked amino groups on gelatin. In increase in gelatin content resulted in reduced gelation times and increased adherence of fibroblasts as shown in figure 2.3, indicating the significant effect of gelatin on bioactivity and gel behaviour.

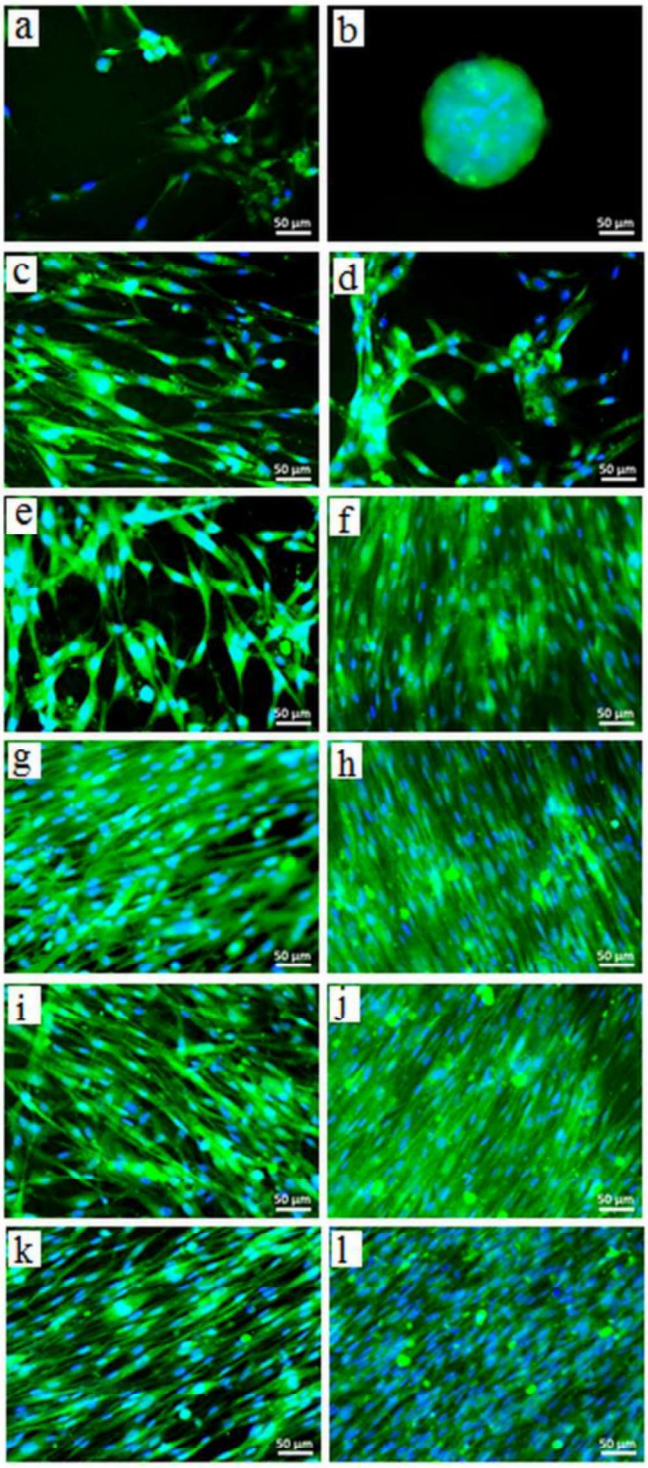


Figure 2.3. FM images of Normal human dermal fibroblasts adhered on (a, b) alginate, (c, d) ADA70-GEL30, (e, f) ADA60-GEL40, (g, h) ADA50-GEL50, (I, j) ADA40-GEL60, and (k,, l) ADA30-GEL70 after 4 days (left column) and 7 days (right column) of incubation. The cells were stained for live cells (green) and dead (blue). Reproduced with permission from Creative

Commons Attribution-Non-Commercial 4.0 License. Sarker B, Singh R, Silva R, Roether JA, Kaschta J, Detsch R, et al. (2014) Evaluation of Fibroblasts Adhesion and Proliferation on Alginate-Gelatin Crosslinked Hydrogel. PLoS ONE 9(9): e107952. https://doi.org/10.1371/journal.pone.0107952
.

Self-crosslinking is another mechanism in which hydrogels are prepared without non-toxic crosslinkers. Self-cross-linked oxidised alginate-gelatin hydrogels have been used in the treatment of osteoarthitis (Balakrishnan *et al.*, 2014). Self-crosslinking of periodate oxidised alginate and gelatin in the presence of borax, without the use of toxic crosslinking agents yielded biodegradable, injectable hydrogels with minimal gelation time (within 20 seconds) (Balakrishnan *et al.*, 2014). The presence of Borax results in an increase in pH thus reducing gelation time. The hydrogel showed good integration with cartilage tissue and showed a burst pressure of 70 ± 3 mmHg indicative of its adhesive nature (Balakrishnan *et al.*, 2014). Primary murine chondrocytes maintained their phenotype indicated by aggrecan and collagen type II expression (Balakrishnan *et al.*, 2014). It is however not possible to synthesise ADA-GEL microcapsules in the presence of borax as an increase in pH may result in reduced cell viability, therefore microcapsules can be fabricated in PBS which also increases pH and reduces gelation time. (Sarker *et al.*, 2014)

ALG-GEL has also been used in cardiac tissue engineering. Films composed of the alginate-gelatin blend were synthesised, with Ca^{2+} ions used to crosslink alginate, and glutaraldehyde to crosslink gelatin for cardiac tissue engineering (Rosellini *et al.*, 2009). As proven by FTIR analysis, both polymers showed good molecular compatibility. Typical adsorption bands of alginate at 1587.6cm^{-1} (C=O) and 1025.6cm^{-1} (C-O-C) shifted to higher wavelengths when gelatin content was increased whereas when the alginate content was increased, the amide II adsorption band at to a higher wavelength, evident of strong intermolecular interactions (Rosellini *et al.*, 2009). *In vitro* tests performed using C2C12 myoblasts demonstrated good proliferation for blends with gelatin content greater than 60%. The best blend to be used in the production of scaffolds was the 20:80 alginate-gelatin blend which allowed for cell differentiation.

By varying the ratios of gelatin and alginate, suitable bioinks can be designed for 3D printing. As the concentrations of gelatin and alginate increased, thinner strands with a minimum width of 0.31mm were printed (Giuseppe *et al.*, 2018). As the concentration of alginate increased, printing accuracy was increased, whereas when gelatin concentrations exceeded 10%, a reduction in printing accuracy was observed. By increasing the concentration of both

polymers, compressive modulus was found to increase. Hydrogels with a 5%Alg-6% Gel mixture showing a compressive modulus of 29.8kP. Blends of 5%Alg-6%Gel, 5%Alg-8%Gel and 7%Alg-8%Gel showed intact plasma membranes after bioprinting (Giuseppe *et al.*, 2018). Soni and co-workers(2018) incorporated silica nanoparticles in the proteosaccharide hydrogel and found that the incorporation of 5% of Sio_2 which interacts with the -COO- and -OH group on gelatin resulted in the formation of new hydrogen bonds which increased viscosity and reduced degradation, thus enhancing the stability of 3D proteosaccharide constructs (Soni *et al.*, 2018).

Luo and co-workers (2018) 3D printed alginate-gelatin scaffolds with homogenous nano apatite coatings for bone tissue engineering (Luo *et al.*, 2018). The young's modulus for scaffolds with nano apatite coating was found to be 2-fold higher than scaffolds without apatite coatings showing that alginate-gelatin scaffolds may be further functionalised for bone tissue regeneration by inclusion of nano apatite coatings (Luo *et al.*, 2018). The nano apatite coating also significantly enhanced the proliferation of rat bone marrow stem cells as well as their osteogenic differentiation (Luo *et al.*, 2018). The proteosaccharide was also applied in cardiac tissue engineering where heterogenous aortic valve conduits were 3D bioprinted using gelatin-alginate hydrogels. The study showed good viability of aortic root sinus muscle cells and aortic valve leaflet interstitial cells for a period of 7 days in culture (Duan *et al.*, 2013). Tensile biomechanics of the cell-laden hydrogel remained constant while acellularized hydrogels exhibited reduced modulus and strength over 7 days. SMCs also expressed increased levels of alpha smooth muscle actin while VICs showed elevated vimentin levels thus demonstrating the potential of aortic gelatin-alginate hydrogel conduits in valvular heart disease (Duan *et al.*, 2013). Therefore, the proteosaccacharide hydrogel possesses desirable characteristics for 3D printing applications which can be further tuned to enhance its *in vivo* applications (Giuseppe *et al.*, 2018).

Wang and co-workers (2016) additionally incorporated nanocrystalline cellulose (NCC) to ALG-GEL blends. The synthesis involved ionic crosslinking of alginate with zinc ions, formation of an ALG-GEL IPN and supramolecular interactions with NCC (Wang *et al.*, 2016). The incorporation of NCC increased mechanical properties of the hydrogel and the hydrogel showed desirable porosity and swelling behaviour. Even though, NCC incorporation increased the mechanical integrity and crystallinity of the hydrogel, hydrophilicity was compromised when excessive NCC was used. The hydrogels could be used to incorporate osteoblasts and

BMP-2, therefore NC-GEL-ALG hydrogels could be used for cell delivery and the delivery of growth factors in bone healing (Wang *et al.*, 2016). The combination of gelatin and alginate has proven to be very beneficial in tissue engineering, however mechanical strength can further be enhanced by substituting gelatin with collagen.

Collagen, a long fibrous protein containing thee peptide chains in a triple helical structure, is the main protein found in the mammalian and animal connective tissue. Collagen compromises 20-30% of the whole body-protein content and upon hydrolysis yields gelatin, another biomaterial widely utilised in regenerative medicine (Baniasadi & Minary-Jolandan, 2015; Wang *et al.*, 2009). Properties favouring the use of collagen include its great tensile strength, bioabsorbability, biocompatibility and negligible antigenicity (Wang *et al.*, 2009).In a study conducted by Thumann and co-workers (2009), it was found that a collagen membrane implanted into the subconjunctival place for 24 weeks elicited no inflammatory response and was successfully absorbed into the subconjunctival space in a time period of 17 weeks (Thumann *et al.*, 2009). Collagen has also been successfully used in skin substitutes for burn management. Commercialised burn management products include collapat II® (Biomet Inc.), Healos® (Depoy Spine, Inc.), and Biostite® (Vebas S.r.l.) (Wang *et al.*, 2009).

The addition of collagen enables many different cell types to recognise the matrix though integrins such as α1β1, α2β1, α10β1 and α11β1, while the interaction of the amine groups of collagen with the carboxyl groups of alginate confers greater stability to the hydrogel (Loeser, 2014). Additionally, collagen adds fibrous structure to the alginate hydrogel thus allowing further resemblance to native tissue. The interaction between collagen and alginate has not been extensively investigated, however alginate can be oxidised by periodate to form aldehyde groups which may react with the amino groups of collagen, though a mechanism similar to glutaraldehyde (Hu *et al.*, 2014). Hu and co-workers (2014) investigated the crosslinking reaction between ADA and collagen and reported that ADA functions as a crosslinker which firms the triple helical structure of collagen without destroying the backbone of collagen (Hu *et al.*, 2014). Collagen-ADA membranes showed a homogenous macrostructure characterised by surface roughness with no phase separation indicating good miscibility of the polymers (Hu *et al.*, 2014). Microroughness was increased when the crosslinker concentration was increased to 20%, suggesting stronger interactions in the proteosaccharide. The water contact angle was increased by the incorporation of ADA which increases the hydrophilicity of the collagen-ADA membranes, due to hydroxyl groups of ADA

being brought into collagen side chains. Cytotoxicity studies using L929 fibroblasts showed no toxicity of the collagen-ADA membrane to the cells. Furthermore, optical density of pure collagen was greater than in control groups suggesting its excellent bioactivity. ADA can support cell proliferation at concentrations not exceeding 10% due to the possible reaction of aldehyde groups on excessive ADA with proteins and polysaccharides within the cells.

Alginate and collagen fibrils were also ionically crosslinked using calcium carbonate to form an alginate- type 1 collagen fibril hydrogel (Baniasadi & Minary-Jolandan, 2015). Rheological characterisation of the hydrogels showed that the addition of collagen fibrils increased the elastic and loss moduli of the hydrogels and had a pronounced effect on the nanoindentation properties which improved by 2-fold, as compared to alginate without collagen fibrils. Rheological properties showed the most improvement for hydrogels with 4x collagen concentrations (Baniasadi & Minary-Jolandan, 2015). Yang and co-workers (2018) further reported that the addition of collagen, increased the expression of chondrogenic genes such as ACAN, COL2AL and SOX9 and improved the mechanical strength of the SA/COL bioink, thus supporting the use of the proteosaccharide in the repair of articular cartilage (Yang *et al.*, 2018). Microscale hydroxyapatite particles were incorporated in a collagen-alginate film to explore its potential in cartilage tissue engineering. Collagen-alginate-hydroxyapatite (CAHA) films showed good cytocompatibility and cytoviability of rabbit chondrocytes with rapid proliferation observed in 4-6 days (Sun *et al.*, 2008). Cartilage ECM was secreted from chondrocytes on the CAHA film, whereas collagen-alginate (CO-AL) showed a loss of chondrogenic phenotype evident by poor staining of pericellular collagen type II (Sun *et al.*, 2008). A novel stem cell delivery system comprising of collagen as the core and alginate as the shell was also tested for the delivery of mesenchymal stem cells to a rat calvarium bone defect (Perez *et al.*, 2014). The hydrogel carriers showed a high swelling capacity (98%) and continuous fibre diameter of 700-100 μm and 200-500μm for the core and shell respectively (Perez *et al.*, 2014). The 3D printed scaffold showed a 22% degradation rate at 7 days and 43% at 14 days, with MSC proliferation up to 21 days, with expression of high levels of osteocalcin, bone sialoprotein, and osteopontin thus suggesting the potential of the 3D matrix in bone tissue engineering (Perez *et al.*, 2014). Zhou and co-workers (2019) reported that by increasing the sodium alginate content (2:1 ALG: COL), hydrogels had a shorter gelation time and exhibited stable rheological behaviour. The hydrogel showed a pore size of 50-100μm allowing better protection of MSCs as MSCs maintain their sizes in dozens of microns as shown in figure 2.4. The pore diameter of SA ranged from 300 to a 1000 μm, while the

hydrogels with a 4:1 ratio showed diameters ranging from 200 to 500 μm. The same hydrogel showed higher MSC viability and proliferation (Zhou *et al.*, 2019). Sobhanian and co-workers (2019) grafted collagen extracted from rat tail onto a nanofibrous scaffold containing polyvinyl alcohol/alginate/gelatin. The addition of collagen increased the hydrophilicity of the scaffold and improved adhesion and proliferation of fibroblasts as shown in figure 2.4 (Sobhanian *et al.*, 2019).

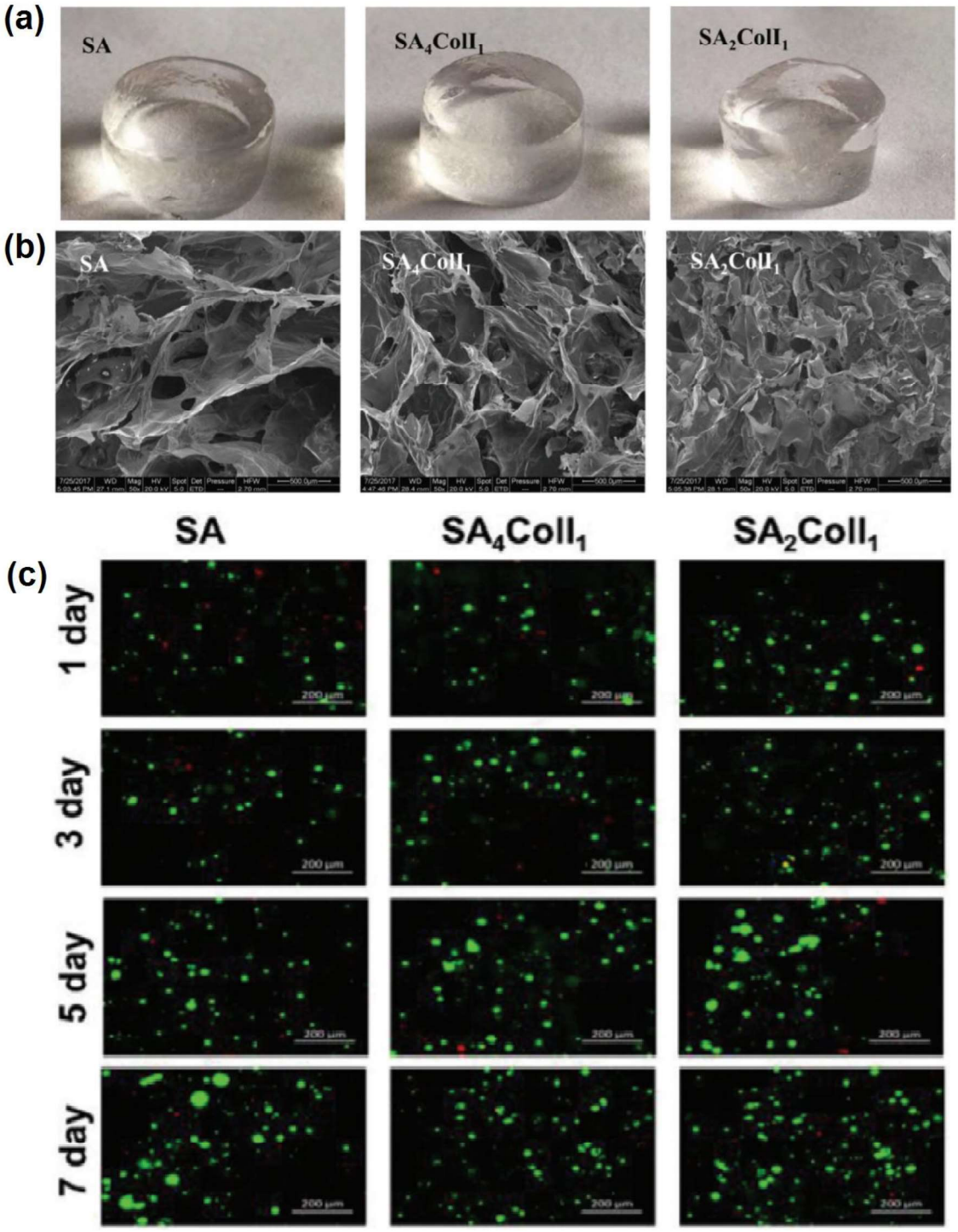


Figure 2.4. a) Hydrogels prepared by varying the ratios of sodium alginate (SA) and collagen; b) SEM micrographs showing morphology of hydrogels; c) Live/dead staining of MSCs loaded in each hydrogel. Reproduced with permission from Creative Commons. Zhou, J., Zhang, K., Ma, S., et al. (2019). Preparing an injectable hydrogel with sodium alginate and Type I collagen

to create better MSCs growth microenvironment. e-Polymers, 19(1), pp. 87-91. Retrieved 11 Nov. 2019, from doi:10.1515/epoly-2019-0011

The first scaffold encountered by a cell in wound healing, is a fibrin network. Extracellular matrices formed by collagen, laminin and proteoglycans assemble in a slow, ordered manner as dictated by their secretory cells, however fibrin gels undergo rapid assembly by a polycondensation reaction from fibrinogen when thombin is activated leading to a formation of a 3D fibre network which at relatively low concentrations lead to hydrogel formation (Ahmed *et al.*, 2008; Neumann *et al.*, 2013; Wang *et al.*, 2009). Its abundance, ease of purification, ability to control gelation behaviour by alteration of thombin concentration, high seeding efficiency, adhesion capabilities and viscoelastic behaviour make fibrin an attractive candidate in wound healing and tissue engineering (Weijers, 2011). Fibrin hydrogels have been used in adipose, cardiovascular, ocular, liver, skin, cartilage and bone regeneration(Noori *et al.*, 2017). The most common disadvantages associated with fibrin hydrogels include gel shinkage which occurs during flat sheet formation, inferior mechanical properties and rapid degradation prior to tissue regeneration (Snyder *et al.*, 2014)(Arulmoli *et al.*, 2016). These disadvantages necessitate the combination of fibrin with alginate.

Chitosan-alginate-fibrin hydrogels have been used as wound dressings (Devi *et al.*, 2012). Chitosan does not possess enough mechanical strength to be used individually as a wound dressing, however chitosan does possess wound healing capacity. Alginate and fibrin were added to improve the tensile strength of the composite while polyethylene glycol (PEG) was added to improve flexibility of the matrix. The matrix formed was porous, with a pore size ranging between 100-400µm. The porous nature of the matrix would facilitate quick absorbance of wound fluids and reduce the chances of bacterial infection thus accelerating healing (Devi *et al.*, 2012).

Ma and co-workers (2012) investigated the effects of changing the protein to polysaccharide ratio and observed that when the fibrin-to-alginate ratio was reduced, fibrin architecture transitioned from uniform to an interconnected fibrous structure and ultimately disconnected islands within the hydrogel (Ma et al., 2012). (Ma, Titan, *et al.*, 2012). The opposite trend was observed in alginate architecture. Alginate improved the biostability of the gel and supported GAG and collagen II production and chondrogenic expression while fibrin promoted cell proliferation and maintained the gel's extensibility (Ma *et al.*, 2012). Montalbano and co-workers(2018) further incorporated collagen to form a tripolymer hydrogel (Montalbano *et al.*,

2018). This hydrogel showed thermoresponsive behaviour at physiological conditions and mechanical properties similar to native tissue. A larger collagen content enhanced the osteogenic potential of hMSCs. Large MIN6-B cell aggregates approximately 50-150 um in size were observed indicating the formation of pseudo-islets. Therefore, CAF hydrogels may be applied in pancreatic tissue engineering (Montalbano *et al.*, 2018).

The main function of elastin in the ECM is to provide elasticity to tissues and organs where elasticity dictates their functions, such as blood vessels, lungs and skin (Coenen *et al.*, 2018). Due to its highly crosslinked nature and hydrophobicity, elastin is poorly soluble thus limiting its processing into new biomaterials. Therefore elastin derivatives including treoplastin and α-elastin are used to produce hydrogels due to their better solubility(Tsai *et al.*, 2017). Alginate lacks cell adhesion domains and undergoes slow and unfavourable degradation kinetics; therefore, the combination of alginate and elastin would prove to be beneficial. Silva and co-workers (2018) combined bovine elastin which is known for its excellent bioactivity with self-crosslinked alginate (Silva *et al.*, 2018). Fibroblasts were able to attach and proliferate on alginate-elastin hydrogels better than on alginate only hydrogels showing that elastin incorporation improved cell-material interactions. The hybrid hydrogel showed a greater degree of crosslinking resulting in a more robust matrix suitable for soft tissue regeneration. In their previous work, keratin was successfully combined with alginate to form a stable hydrogel with good mechanical strength (Silva *et al.*, 2014). Human umbilical vein cells were used to assess cell-biomaterial interactions and it was found that the proteosaccharide composite was able to support cell adhesion, spreading and proliferation. These results proved that such proteosaccharide hydrogels have exploitable potential in soft tissue regeneration (Silva *et al.*, 2014).

Due to the lack of bioactive ligands which are necessary for cellular interactions, the strategy of cell-crosslinking, which is the introduction of bioactive ligands e.g., RGD onto alginate hydrogels has been utilised. The RGD peptide is an oligopeptide derived from proteins such as fibronectin, laminin, or collagen, whose attachment to polymers have significantly improved cell adhesion and proliferation. Carbodiimide chemistry has been used in the chemical coupling and mammalian cell receptors may bind to the ligand when introduced into alginate hydrogels (Sun & Tan, 2013). However, despite the excellent bioactivity displayed by cell-crosslinked hydrogels, the resulting network shows poor mechanical strength thus limiting its applications. RGD modified alginate gels may be modified with growth factors e.g. Bone

Morphogenic Protein (BMP) as shown by Park and co-workers (2009) where a low dose of BMP allowed for complete regeneration in rodents with femoral defects (Park *et al.*, 2009). Additionally, RGD modified alginate gels seeded with primary rabbit chondrocytes and injected into mice were found to be effective in the regeneration of cartilage. These gels formed were shear-reversibly cross-linked, i.e. the gels could recover their primary structure post shear-induced breakdown (Park *et al.*, 2009). Alginate has also been combined with collagen type I and β-tricalcium phosphate and compared to pure alginate gels. Bone marrow stromal cells did not readily attach nor proliferate on pure alginate hydrogels; however, they were observed to attach and proliferate on the composite hydrogels suggesting the synergistic effect of the polymers (Lawson *et al.*, 2004).

2.4.2 Chitosan-based proteosaccharides

Chitosan, a linear semi-crystalline polysaccharide consisting of D-glucosamine and N-acetyl-D-glucosamine residues, is obtained though the deacetylation of chitin (Croisier & Jérôme, 2013). Although chitin, which is obtained after deproteinisation, demineralisation and depigmentation of the shells of crustaceans and arthopods, has been used as a biomaterial; chitosan which is formed by the deacetylation of chitin is considered a more attractive biomaterial (Younes & Rinaudo, 2015). Chitin deacetylation yields chitosan with many beneficial physicochemical and biological properties such as biocompatibility, biodegradability, cell adhesivity and antibacterial activity (Sivashankari & Prabaharan, 2016). To be named ‘chitosan’, the degree of deacetylation [DD] which can be calculated as the ratio of D-glucosamine to the sum of D-glucosamine and N-acetyl-D-glucosamine units, must be greater than 50% (Sivashankari & Prabaharan, 2016). Biocompatibility is reported to be directly proportional to DD with an increase in DD improving biocompatibility(Sivashankari & Prabaharan, 2016). Chitosan has been used as a scaffolding component in bone, vasculature, skin, cartilage and liver tissue engineering due to its excellent mechanical strength, biocompatibility, and biodegradability. (Hozumi & Nomizu, 2018; McEwan *et al.*, 2016; Tiwari *et al.*, 2018).

The hydroxyl groups of hydroxyproline in collagen, play a significant role in hydrogen bonding between collagen chains whereas the side groups such as the -COOH and -NH2 are able to interact with other molecules. These side chains are especially important in the reaction with the polysaccharide chitosan. The -COOH and -NH2 groups of collagen can form hydrogen bonds with the -OH and NH2 groups of chitosan. Additionally, chain entanglement between

the triple helix of collagen and chitosan can lead to a more viscous complex. PEC may also form between the cationic chitosan and -COOH of collagen (Sionkowska et al., 2004).

McEwan and co-workers (2016) incorporated collagen, chitosan and laminin into a hydrogel which acted as a conduit for insulin producing tissue in the treatment of type 1 Diabetes. By increasing chitosan content, stiffness and time to gelation was increased, however porosity was reduced from 22% to 16%. Embedded circulatory angiogenic cells (CACs) and porcine cells were more viable in hydrogels with a greater collagen content i.e., collagen: chitosan content of 20:1, and glucose stimulation indices were more favourable for 20:1 hydrogel when compared to values in the literature. The incorporation of laminin did improve short-term viability of circulatory angiogenic cells (CACs) and improved islet cell viability as shown in figure 2.5 (McEwan *et al.*, 2016). Chitosan also shows good cytocompatibility for neural growth, specifically for peripheral nerve regeneration. However, chitosan does not possess specific bioactivity to interact with neurons and guide axons in nerve regeneration. This was addressed by Zhu and co-workers (2010) who blended laminin, an extracellular matrix protein and putative axon adhesion and guidance molecule with chitosan to support and guide neurite development (Zhu *et al.*, 2010). A dispensing-based rapid prototyping (DBRP) technique was used to create two-dimensional grid patterns by dispensing the proteosaccharide in orthogonal directions. Adult dorsal root ganglion neurites grew preferentially upon and followed the orthogonal direction of the laminin-chitosan pathways. Laminin thus enhanced the scaffold's bioactivity which manifested though the growth of viable neurons, whose length was directly proportional to the laminin concentration. (Zhu *et al.*, 2010).

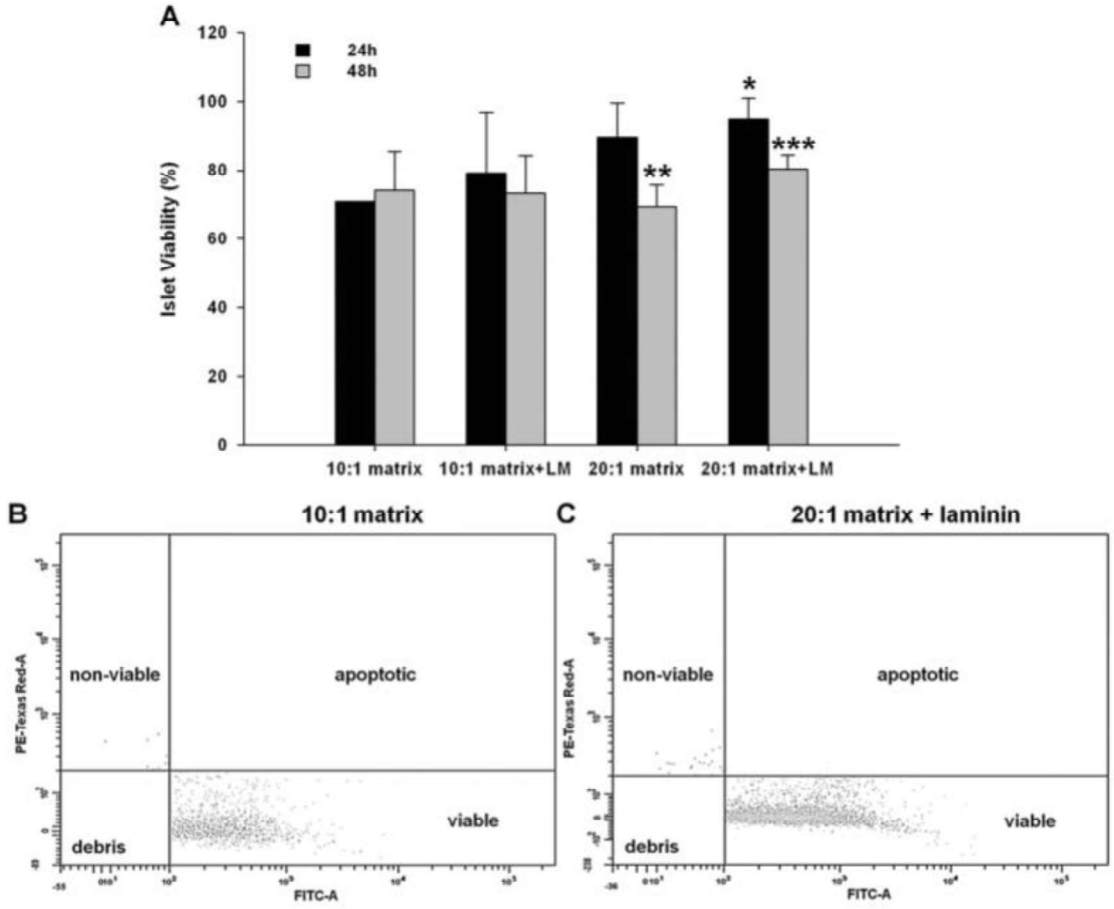


Figure 2.5. Effect of laminin and chitosan content on the viability of porcine islets embedded in matrices for 24 and 48 h (n = 3 each) (B) 10:1 matrix and (C) 20:1 matrix + LM show islets separated into fractions of non-viable and apoptotic (dead) islets, viable islets and debris. Reproduced with permission from Elsevier. B.V. Ltd © 2013

Another area of interest is the incorporation of peptides with chitosan to form a matrix, capable of complex cell interactions. Peptide-chitosan matrices specifically interact with cellular receptors and by using receptor-specific peptides such as SIKVAV, RGD, and AG73, the peptide-chitosan matrix may reproduce multi-receptor interactions and enhance biological activity (Hozumi & Nomizu, 2018). A biomimetic fragment of the laminin –Ser-Ile-Lys-Val-Ala-Val (SIKVAV) conjugated with chitosan was investigated by Chen and co-workers (2015) for wound healing and tissue regeneration(Chen *et al*., 2015). The peptide conjugated hydrogel significantly supported the adhesion and proliferation of BMSCs, and *in vivo* tests showed that the hydrogel accelerated wound contraction and led to the formation of new blood vessels as confirmed by H&E staining. Masson staining showed the formation of many new collagen fibrils in the conjugated peptide hydrogel when compared to the chitosan hydrogel. The

hydrogel also showed quick reepithelialisation, thus proving that the peptide can significantly enhance the function of chitosan in wound healing and skin regeneration(Chen *et al.*, 2015). RGD-containing peptides immobilised to chitosan also significantly improve cell attachment and proliferation (Ho *et al.*, 2005). RGD-chitosan matrices have been used in bone regeneration where rat osteosarcoma cells, bone marrow stromal cells and chondrocytes were found to attach well and promote mineralization of bone (Masuko *et al.*, 2005). Lv and co-workers (2019) further reported that that calcitonin gene-related peptide/chitosan containing cement promoted VEGF and mRNA expression while promoting the proliferation of HUVEC (human umbilical vein endothelial cell) cells (Lv *et al.*, 2019).

Chitosan has been frequently combined with gelatin for tissue engineering applications due to many reasons: the RGD peptide sequence found in gelatin promotes the adhesion and proliferation of cells thus leading to enhanced biological activity and biocompatibility, the cationic nature of chitosan promotes electrostatic interactions with anionic GAGs, both biomaterials are miscible at the molecular level, and gelatin is quickly degraded due to its weak mechanical strength which can be overcome by combining gelatin with other stronger polymers i.e. chitosan (Kumar *et al.*, 2017; Mao *et al.*, 2003). This combination has been investigated in bone defects where glutaraldehyde was employed as a crosslinker, and a micro- and macro-porous structure was observed using SEM. The scaffold produced also had a force bearing capacity of approximately 1.9 mPa with high tensile strength (Kumar *et al.*, 2017). Peter and co-workers (2010), further enhanced the biological activity of their proteosaccharide scaffold for bone tissue by incorporating nanohydroxyapatite crystals and observed a pore size of 150-300 um on the scaffold (Peter *et al.*, 2010). A pore size of less than 300μm is adequate for osteoblast activity and *de novo* bone formation, thus MG63 cells were able to adhere and proliferate on the proteosaccharide scaffold. Chitosan-gelatin has also been used as a scaffold for skin tissue engineering. Liu and co-workers(2014) also employed glutaraldehyde as a crosslinker and reported that the optimum ratio of C/G was 1:1 with a 6-8% Vr of 0.25 wt% of GA (Liu *et al.*, 2014).The scaffold formed was propitious to cultivate human keratinocyte cells (HaCaT) which grew uniformly across the scaffold with round and triangular morphology (Liu *et al.*, 2014). The proteosaccharide hydrogel showed a sufficiently high viscosity suitable for 3D printing and printed constructs (~400 μm for 3 layers) were representative of the epidermal and part of the dermal region of skin. Seeded HFF-1 cells were round and evenly distributed on the hydrogel surface and were able to attach and proliferate due to the incorporation of gelatin which shielded excessive positive charge on

chitosan, thereby enabling better attachment and proliferation as opposed to pure chitosan (Liu *et al.*, 2014). Apart from chemical crosslinking with glutaraldehyde, enzymatic crosslinking can also yield a proteosaccharide with good mechanical strength. Studies show that the use of both physical and chemical crosslinking mechanisms may synergistically enhance the bioactivity of the proteosaccharide.

Silva and co-workers (2014) used both physical and chemical crosslinking mechanisms to crosslink the proteosaccharide (Da Silva *et al.*, 2014). Selected amounts of tranglutaminase were added to the proteosaccharide and the solution was quickly cooled to 21^{o}C which is below the gelation temperature of gelatin. Thereafter, mTGase was removed by thermal deactivation at 70^{o}C (Da Silva *et al.*, 2014). Microbial transglutaminase catalyses the reaction between the glucosamine amine of chitosan and the glutamine residue of gelatin in a calcium-independent manner (Da Silva *et al.*, 2014). In chemically cross-linked hydrogels, gelatin and chitosan present as single strands whereas in the dual physical-chemical (PC) crosslinked gel, the transient physical gelatin gel is filled with chitosan strands. The PC gel showed a higher shear modulus than the chemically crosslinked gel and were found to be less turbid (Da Silva *et al.*, 2014). The presence of chitosan enhanced the shear modulus of all gels and MC3T3 cells proliferated better in the PC gels than in the chemically-crosslinked gel (Da Silva *et al.*, 2014).

Re and co-workers (2019) prepared a thee-dimensional gelatin-chitosan hybrid hydrogel which was combined with human platelet lysate (Re *et al.*, 2019). Bone marrow and adipose tissue mesenchymal cells were seeded on the hydrogels with varying chitosan content. Hydrogels with chitosan content of 8.1% and 14.9% showed up to a level of 90% cell viability (Re *et al.*, 2019). Mineralisation was also detected 21 days after culture and 59 proteins involved in cellular adhesion, differentiation and repair were highlighted though proteomic characterisation of HPL, and thus reinforcing that the combination of the gelatin-chitosan hybrid gels may present a promising strategy for bone regeneration (Re *et al.*, 2019). Chitosan-gelatin scaffolds with chitosan nanoparticles containing fibroblast growth factor and bovine serum albumin (BSA) were synthesised by Azizian and co-workers (2018). The scaffolds showed a good swelling ratio and water uptake capacity due to the presence of chitosan nanoparticles. Enhanced proliferation of human dermal fibroblasts and increased cell viability was also observed in scaffolds containing BSA and fibroblast growth factor. These

scaffolds could be particularly useful in tissue engineering where angiogenesis is required, particularly bone regeneration (Azizian *et al.*, 2018).

The combination of collagen and chitosan has been widely used in skin tissue engineering (Ma *et al.*, 2003). Collagen has been exploited due to its excellent biocompatibility for skin applications, however the main challenge faced with collagen as a biomaterial is its poor mechanical strength and quick degradation rate. Therefore, collagen must be cross-linked with GA, EDC polyglycidyl ether and polyepoxidic resins (Ahmad *et al.*, 2015). Gilarska and co-workers (2018) investigated a collagen-chitosan-hyaluronic acid hydrogel using genipin as a crosslinker (Gilarska *et al.*, 2018). By varying the concentration of crosslinker, various mechanical properties of the hydrogel could be tuned with the optimal concentration of genipin being 20mM (Gilarska *et al.*, 2018). The hydrogel was found to be suitable for bone engineering. An interpenetrating polymer network (IPN) was created due to electrostatic interactions between cationic chitosan and anionic HA, thus ensuring the incorporation of HA in the hydrogel. Swelling ratio of the hydrogel was reduced with an increase in genipin content (Gilarska *et al.*, 2018). Hydrogels crosslinked with a low concentration (2mm) of genipin were completely wettable with higher concentrations of genipin resulting in a more compact structure with reduced hydrophilicity (Gilarska *et al.*, 2018). However, hydrogels with a chitosan:HA ratio of 30:20 were not affected by genipin concentration and were completely wettable, soft and susceptible to disintegration (Gilarska *et al.*, 2018). Hydrogels with a 40:10 chitosan:HA ratio were the most compact and uniform, independent of the concentration of genipin. MG63 cells cultured in collagen-chitosan (ColCh) hydrogels were spherical and had the lowest spread area (Gilarska *et al.*, 2018). However, cells cultured in collagen-chitosan-hyaluronic acid (ColChHA) hydrogels were more flattened with a greater spread area. Cells occupied a greater area with hydrogels crosslinked with 20mM genipin than 10mM due to cells being able to spread and extend easier on rigid substrates with a more diversified morphology (Gilarska *et al.*, 2018).

Shagiera and co-workers (2018) synthesised an injectable hydrogel consisting of collagen, chitosan and bioactive molecule, thymosin β4 (Tβ4) which is used in the treatment of myocardial infarctions (Shaghiera *et al.*, 2018). The hydrogels lacked interconnecting pores and were non-toxic proven by cell viability being greater than 50% (Shaghiera *et al.*, 2018). As confirmed by histopathological anatomy, the hydrogels could stimulate angiogenesis and migration of epithelial heart cells. The addition of chitosan resulted in greater angiogenesis

compared to collagen only hydrogels (Shaghiera *et al.*, 2018). The release of Tβ4 was slow compared to collagen only hydrogels which released Tβ4 within 3 days. This is explained by the fact that collagen is easily degraded by collagenases which accelerates the release of Tβ4 (Shaghiera *et al.*, 2018). Chitosan increases the hydrogel's ability to retain Tβ4 *in vivo,* however when the collagen: chitosan ratio was 1:1, a decline was observed in the proangiogenic trend, due to the matrix becoming denser with an increase in chitosan composition resulting in a decline in Tβ4 release

In a study conducted by Wu and co-workers (2006), preadipocytes were cultured on a collagen-chitosan hydrogel chemically cross-linked by glutaraldehyde and demonstrated potential in adipose tissue engineering (Wu *et al.*, 2007). The scaffold was implanted in a rat subcutaneous pocket and showed that the resulting scaffolds were biocompatible and could induce vascularisation and the formation of adipose tissue (Wu *et al.*, 2007). A thermoresponsive hydrogel prepared with chitosan/β-glycerophosphate and collagen was investigated for its ability to support adipogenesis. The hydrogel was seeded with human adipose tissue-derived stem cells which showed high viability and an expansion of 30% over 7 days. *In vivo* studies involving the subcutaneous injection of the hydrogel into nude mice, and subsequent histological analysis revealed that the hydrogel was able to persist for 4 weeks post implantation and was biocompatible with a great number of adipocy tes and vascularised adipose tissue in induced ADSC-C/GP/Co hydrogels thus pointing to the favourability of the hybrid hydrogel for adipogenesis. A hybrid chitosan/gelatin/ polyvinyl alcohol hydrogel has also demonstrated potential in wound healing (Fan *et al.*, 2016). The hydrogel was prepared by gamma irradiation of 40kGy and was characterised for blood clotting activity. Results revealed that the hydrogels demonstrated good coagulation and took only 5 minutes for the BCI (Blood clotting index) to reach 0.032 (Fan *et al.*, 2016). The gel also showed good tensile strength, pH sensitivity and swelling ability thus showing a promising potential for application as a wound dressing (Fan *et al.*, 2016).

In a study conducted by Silva and co-workers (2008), a porous sponge was prepared using a hydrogel composed of silk-fibroin and chitosan, using genipin as a cross linker for the purpose of cartilage tissue engineering. Hydrogels formed where dark blue in colour due to oxygen-radical-induced polymerization of genipin as well as its reaction with amino groups/amino acids(Silva *et al.*, 2008). The sponges also exhibited pH dependent swelling behaviour with the most swelling occurring at pH=3 and reducing with an increase in pH. Higher swelling

degrees were presented in an acidic pH due to the protonation of amino groups of chitosan which promoted solubility and interaction with water (Silva *et al.*, 2008). The sponges favoured adhesion and proliferation of chondrocytes especially when 50/50 wt % CS was cross-linked with genipin thus demonstrating the potential of the proteoaccharide for cartilage tissue engineering (Silva *et al.*, 2008). Zhang and co-workers (2018) introduced milled silk particles into a natural chitosan hydrogel for 3D printing and found that the addition of silk particles resulted in a 5-fold increase in the compressive modulus as compared to pure chitosan scaffolds, and also offered increased stability and printing accuracy (Zhang *et al.*, 2018). The inks exhibited good flowability during printing and loading of 300% (w/w) silk resulted in only minor rheological changes. Loading of silk particles also improved biodegradability and surface roughness. The scaffolds showed no cytotoxicity and supported the growth of human dermal fibroblasts (Zhang *et al.*, 2018).

Another protein which is less frequently combined with chitosan is albumin, most commonly bovine serum albumin. Serum albumin is the most abundant plasma protein with a concentration of 35 to 50 mg.ml−1 in human serum. Its abundance and ease of isolation makes serum albumin one of the least expensive commercially available proteins (Amdursky *et al.*, 2018). Albumin tissue scaffolds possess mechanical properties similar to collagen. Both albumin and collagen have excellent resilience, high water binding capacity (>1:40), good tensile strength and high porosities (>97%). Albumin also possessed good cell-binding characteristics and supports cell growth. (Li et al., 2014) Serum albumin has also been applied in cardiac tissue engineering, lung tissue engineering, and in drug delivery of chemotherapeutics such as doxorubicin and paclitaxel due to preferential accumulation in tumor and inflamed tissues (Zhang, Sun and Jiang, 2018). He and co-workers (2012) fabricated a chitosan-BSA hydrogel using the coupling reagent, EDC(He *et al.*, 2012). FTIR spectrum revealed the formation of an amide bond between BSA's carboxyl group and chitosan's amino group. Further investigation revealed that the maximum number of chitosan chains which are able to bind to BSA were 6, with the optimal number being 2. When the molar ratio of chitosan to BSA was increased, the anionic surface charge of BSA was decreased and the secondary structure was damaged. Native BSA has an α-helix content of 55.2%, however when chitosan concentration was increased, the α-helix content decreased to 36.0%.

BSA-chitosan hybrids may also be prepared without EDC/NHS due to their polyelectrolyte nature. BSA is cationic at a pH less than 4.7 and anionic at a pH greater than 4.7. Chitosan is

also cationic in solutions of pH less than 6.0. Therefore, at a pH greater than 6, a polyelectrolyte complex may be formed between chitosan and BSA. (Roy *et al.*, 2017). A novel pH-sensitive drug delivery system was developed by Guo and co-workers (2011) using a chitosan-albumin conjugate hydrogel (Guo and Huang, 2011). Two types of hydrogels, namely a comb type and reticular type were prepared by changing the feeding modes of the reactants. The hydrogels were synthesised by an amidation reaction between 6-O-succinoylated N-phthaloyl chitosan and albumin. Due to the numerous carboxyl groups present on modified chitosan and the steric configuration of BSA varying with a change in pH, the gels were expected to possess pH sensitivity (Guo and Huang, 2011). Albumin was introduced to endow the hydrogel with a greater water-holding capacity and was successful in doing so. Self-crosslinked BSA possessed a water holding capacity of 63%, whereas the comb-type copolymer hydrogel reached 400% while the reticular type of copolymer hydrogel reached 180%. This was attributed to the difference in content in the hydrophilic constituent. In the comb-type copolymer hydrogel, many albumin molecules existed on the side chain of chitosan molecules, whereas in the reticular-type, albumin was used as a crosslinking agent, with limited concentrations. The comb-type copolymer also had a looser packing due to physical entanglement allowing for water to penetrate, whereas covalent crosslinking in the reticular-type copolymer hydrogel resulted in a tightly packed structure, which limited chain movement of the hydrogel system and shielded the hydrophilic property of the hydrogel. *In vitro* release of rifampicin showed that both hydrogels could provide controlled release for more than 50 hours, with a greater release rate under basic conditions. The comb type copolymer hydrogel showed a faster release rate than the reticular hydrogel (Guo and Huang, 2011).

Butler and co-workers (2006) reported that genipin-crosslinking BSA-chitosan hydrogels are suitable for the controlled release of drug in the stomach and in the enhancement of gastric retention. BSA primarily dictated the swelling behaviour of the composite due to acid-induced denaturation at a pH of 3 leading to a sharp increase in swelling ratio. (Butler *et al.*, 2006). Hydrogels underwent partial dissolution in gastric media over long periods of time. The mechanical properties of the hydrogel were governed by chitosan, which endowed the hydrogel with a compressive modulus of 10kPa, thus making the hydrogel resistant to the 7kPa pressure associated with the grinding action of the stomach. The use of BSA-Chitosan is particularly beneficial in controlling drug release, however more research needs to be undertaken on the use of the proteosaccharide in tissue engineering.

2.4.3 Hyaluronic acid based proteosaccharides

Hyaluronic acid (HA), a linear polysaccharide comprising of repeating disaccharide units of β-1,4-D-glucuronic acid - β-1,3-N-acetyl-D-glucosamine, is ubiquitously found thoughout the human body and is critical for cellular and tissue function (Menaa et al., 2013). Due to its high water holding capacity, HA can be transformed into soft or stiff hydrogels, nanoparticulate fluids and porous nanofibrillar sponges(Menaa et al., 2013). Hyaluronic acid has been applied in wound healing, ophthalmic and orthopaedic surgeries due to its non-immunogenicity and viscoelastic properties, however HA is quickly degraded *in vivo* by hyaluronidases and free radicals (Gin, Luttseva and Voronkina, 2016). HA is also soluble in water, thus limiting the biomedical applications of HA (Gin, Luttseva and Voronkina, 2016). Gin and co-workers (2016) proved this by synthesising gels devoid of chemical crosslinkers and evaluated their stability in buffer solutions. Fibronectin and human dermal fibroblasts (HDFs) were used as biological linkages in the gels. Results showed that HA diffused out of the proteosacccharide gel within 3 days and the biological linkages did not prevent the diffusion of HA in the buffer solutions thus necessitating a chemical crosslinker.

Hydroxyl and carboxyl groups of HA play the most important role in crosslinking of HA. Ether linkages are formed when hydroxyl groups are involved while ester linkages are formed when carboxyl groups are involved (Collins & Birkinshaw, 2008). Imino linkages are formed when glutaraldehyde is used as a crosslinker, ether linkages in the presence of formaldehyde or divinylsulfone, and ester linkages when carbodimides or polyhydric alcohols are used (Collins & Birkinshaw, 2008). As explained preciously, the addition of collagen to HA would enhance the adhesion and proliferation of cells, while HA enhances the strength of collagen gels thereby inhibiting cell-induced contraction (Huang-Lee & Nimni, 1994; Park *et al.*, 2003; Tang & Spector, 2007). HA-Collagen hydrogels have demonstrated great potential in bone and cartilage regeneration (Chajra *et al.*, 2008; Mohammadi *et al.*, 2018). A possible explanation of the reaction between HA and collagen is ring opening oxidation resulting in the availability of aldehyde groups on HA which can subsequently be covalently crosslinked with collagen without organic reagents. Physical properties can be tuned by varying the polymer ratios. By increasing collagen content, a more porous sponge-like matrix was created, whereas by increasing the HA content, a viscous gel-like structure is created. Type I collagen is preferred for bone engineering while type II is preferred for cartilage regeneration. Greater bone healing was observed with HA/COL implants than with collagen alone, indicating that HA enhanced bioactivity of the implant (Lin-Shu *et al.*, 1999).

In a study conducted by Mohammadi and co-workers (2018), hybrid scaffolds comprising of collagen and HA were investigated for the treatment of osteoarthitis. To enhance the therapeutic potential of the scaffold, prednisolone, an anti-inflammatory agent was incorporated (Mohammadi *et al.*, 2018). Polyethylene glycol diglycidyl ether was used as a chemical crosslinker in this study. The hybrid scaffold demonstrated better mechanical and chemical characteristics with a compressive modulus of 54.77±0.31 kPa, a water uptake of greater than 1200% and pore size of 20-200 µm. Gelation time was approximately 2.4 minutes under a temperature of 32^{o}C. Controlled release of prednisolone over 5 days was also shown by the Higuchi release kinetic model. This study showed that the scaffold could be used in cartilage regeneration as well as a controlled release system in the treatment of osteoarthitis (Mohammadi *et al.*, 2018). Several growth factors such as the recombinant human growth and differentiation factor-5 (rhGDF-5) and bone morphogenetic protein (BMP) may be incorporated in the proteosaccharide matrix to improve bioactivity (Kadler *et al.*, 2000). GDF-5 loaded matrices induced the formation of chondrogenic nodules in fetal rat calvarial cells, while rhGDF-5 loaded matrices induced osseous tissue formation The RGD peptide may also be immobilised on HA chains and thereafter frozen and lyophilised to produce a 3D sponge like structure. These sponges demonstrated potential in wound healing by providing a matrix for skin regeneration(Liu *et al.*, 2012).In a study conducted by Konturri and co-workers(2014), a hydrogel comprising of type II collagen, hyaluronic acid and 4SPEG (poly(ethylene glycol) ether tetrasuccinimidyl glutarate) further loaded with transforming growth factor β1 (TGFβ1), a growth factor abundant in native cartilage was tested as a potential chondrocyte carrier (Kontturi *et al.*, 2014). Encapsulated chondrocytes within the hydrogel were observed to be viable with increased expression of aggrecan and type I collagen (Kontturi *et al.*, 2014). The injectable hydrogel is thus a potential chondrocyte carrier in cartilage tissue engineering (Kontturi *et al.*, 2014). EDC/NHS cross-linked collagen-HA hydrogels have also demonstrated potential in the regeneration of the nucleus polposus of degenerated IVDs (Calderon *et al.*, 2010). Collagen and hyaluronic acid have furthermore been combined with chondroitin sulfate for cartilage tissue engineering(Guo *et al.*, 2012). The IPN hydrogels were prepared by collagen crosslinking cross linking polymerization of chondroitin sulfate-methacrylate (CSMA) and hyaluronic acid-methacrylate simultaneously and was found to upregulate the expression of cartilage specific genes, and the secretion of glycosaminoglycan and collagen II from chondrocytes (Guo *et al.*, 2012).

Collagen and HA have also been used in the preparation of aortic valve ECM mimicking scaffolds with EDC as a crosslinker (Nazir *et al.*, 2019). The scaffolds showed a pore size of 66-126 μm, appropriate for valvular tissue engineering. The proteosaccharide showed a high bending modulus of up to 1660 kPa, spanning the range of native aortic valves (Nazir *et al.*, 2019). Cardio sphere-derived cells from rat hearts were cultured on the hybrid scaffold and showed that crosslinking density increased the *in vitro* bending moduli up to 2 fold and also prevented *in vitro* disintegration (Nazir *et al.*, 2019). The combination of gelatin and hyaluronic acid is also beneficial in promoting cell attachment. HA does not promote cell attachment individually due to the glucoronic, carboxyl group of hyaluronic acid being anionic at physiological pH, which hinders cell attachment (Fallacara *et al.*, 2018). Crosslinking of the proteosaccharide is often achieved with a water-soluble carbodimide (EDC) which reacts with carboxyl groups on gelatin or HA to form an intermediate acid anhydride, which further reacts with the amino group of gelatin to form an amide linkage (Khunmanee *et al.*, 2016).

HA may also be photocrosslinked upon exposure to UV light (Camci-Unal *et al.*, 2013). The carboxylate groups on HA may undergo chemical modification or methacrylation to facilitate crosslinking upon UV exposure (Camci-Unal *et al.*, 2013). Hyaluronic acid methacrylamide (HAMA) of different degrees of methacrylation may be synthesised to produce hydrogels with tunable degradation kinetics, stiffness and porosity (Camci-Unal *et al.*, 2013). Despite HAMA being a promising hydrogel candidate, its non-adhesive nature prevents cell spreading, thus the addition of gelatin would improve cell adhesion. By increasing the concentrations of methacrylated hyaluronic acid (HAMA) added, degradation rate was slowed, and the compressive modulus of GelMA-HAMA hydrogels ranged from 5.0 ± 2.5 to 73.0 ± 11.1 kPa, suggesting the potential of the hydrogel in tissue engineering applications. Hydrogels composed of only HAMA did not support HUVEC cells adhesion, and this was improved by the addition of GelMA (Camci-Unal *et al.*, 2013). A novel treatment for early stage intervertebral disc generation proposed was an *in situ* forming injectable oxidized hyaluronic acid–gelatin–adipic acid dihydrazide (oxi-HAG–ADH) hydrogel seeded with nucleus polposus (NP) cells (Chen *et al.*, 2013). Key advantages of the hydrogel included sterilisability, viscoelastic properties similar to that of native tissue i.e. shear modulus of ∼11–14 kPa for hydrogels, 11.3 kPa for native NP and increased NP expression of ECM related genes (COL2A1, AGN, SOX-9, and HIF-1A) indicating that the oxi-HAG2–ADH hydrogel is a potential solution to early stage intervertebral disc degeneration (Chen *et al.*, 2013). The steps followed in the reaction can be seen in figure 2.6.

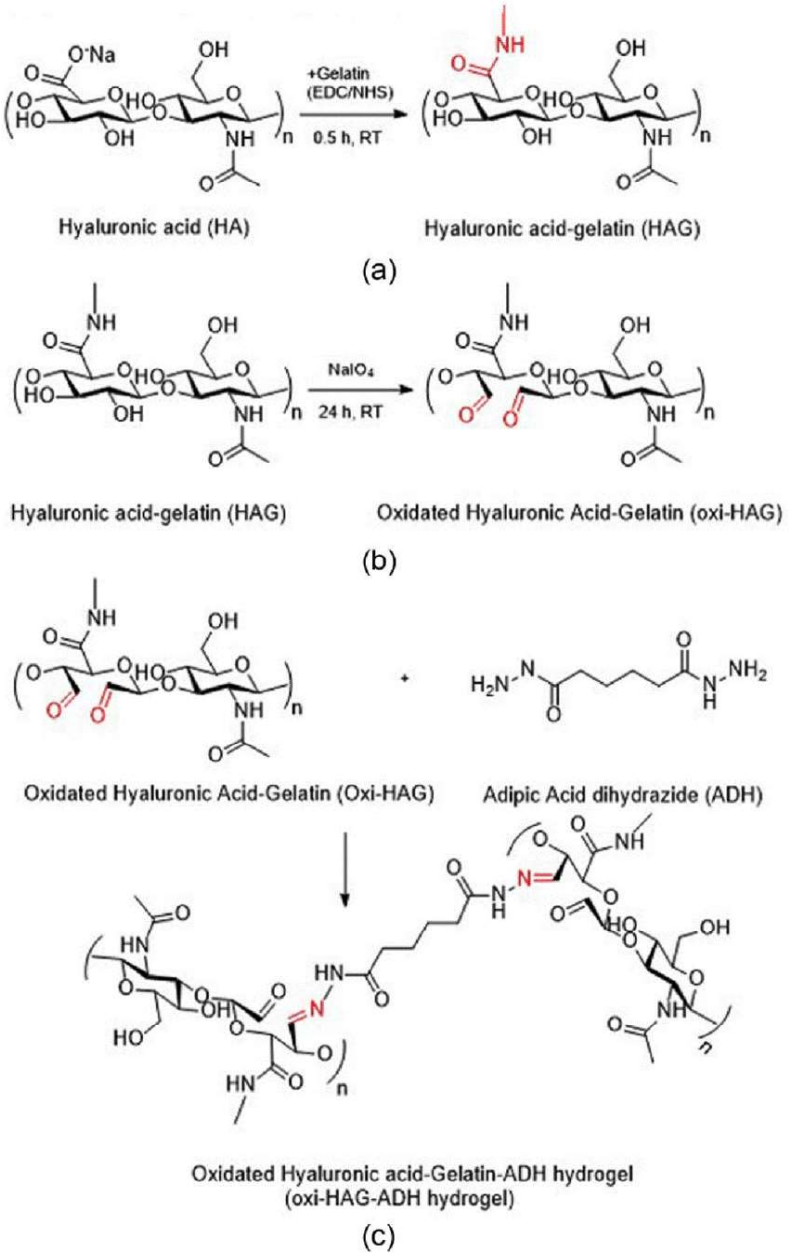


Figure 2.6. Schematic showing the mechanism of cross-linking HA and gelatin in the presence of EDC/NHS. Reproduced with permission from Creative Commons Attribution-Non-Commercial 4.0 License. Khunmanee, S., Jeong, Y. and Park, H. (2016) 'Crosslinking method of hyaluronic-based hydrogel for biomedical applications', *Journal of Tissue Engineering*. SAGE Publications Ltd, 8. doi: 10.1177/2041731417726464.

In a study conducted by Levett and co-workers (2014), a hydrogel composed of photocurable gelatin, hyaluronic acid and chondroitin sullfate (CS) was synthesised to serve as a synthetic extracellular matrix for cartilage tissue engineering (Levett *et al.*, 2014). Hyaluronic acid and

CS were incorporated due to their abundance in the cartilage ECM as glycosaminoglycans (Levett *et al.*, 2014). This study showed that when gel-MA was used alone, gel-MA did not sufficiently support the proliferation of chondrocytes *in vitro*, however the addition of the GAG molecules created an environment that was conducive to the deposition of cartilage-like matrix (Levett *et al.*, 2014). *In vitro* cell studies proved that chondrocytes remained viable for a period of 8 weeks with a significant production of ECM observed and an improvement in mechanical properties. MAHA was found to be a more potent modulator of chondrocyte adhesion and differentiation due its greater participation in cell-matrix interactions than CS-MA. When both GAGs were included, stiffness of the resulting hydrogel was increased thus suggesting potential benefit in the incorporation of both GAGs (Levett *et al.*, 2014).

Lee and Kurisawa (2013) produced an IPN consisting of hyaluronic acid-tyramine and fibrin to improve the mechanical properties of fibrin gels. Fibrinogen was first cleaved with thombin to produce fibrin monomers which rapidly polymerized (Lee & Kurisawa, 2013). HA-tyr was formed by coupling tyramine moieties using horseradish peroxidase and hydrogen peroxide. The IPN gels completely degraded in the presence of plasmin, however the shape of the gels was maintained due to HA-tyr which provided structural support. The proteosaccharide hydrogel furthermore showed potential in the delivery of mesenchymal stem cells and cartilage repair in osteoarthitis. The reinforcement of the hydrogel with hyaluronic acid-methacrylamide significantly increased the mechanical strength of the *in situ* forming hydrogel. The crosslinked fibrin-HAMA hydrogels also provided a conducive environment for the proliferation of BMSCs (Snyder *et al.*, 2014). However, for the purposes of cartilage tissue engineering, the rate of ECM synthesis and degradation must be at equilibrium, therefore silk was incorporated into the fibrin-HA hydrogel due to its excellent mechanical properties (Park *et al.*, 2011). Hydrophobic β-sheets formed by silk decreased gel shinkage during cell culture. Mechanical strength benefits from the β-sheet conformation in silk. Chondrogenesis was found to be superior in gels with lower silk concentrations, however a low silk concentration resulted in volume shinkage. Type II collagen, Sox-9 and aggrecan expression was improved in gels with a lower silk concentration. Therefore, a balance between mechanical strength and chondrogenesis must be achieved when silk is added (Park et al., 2011). The proteosaccharide has been used by Kang and co-workers (2011) as a scaffold surface coating for the delivery of BMP-2 and adipose-derived stromal cells (ASCs). The coating significantly enhanced cell attachment while allowing the sustained release of BMP-2 over 3 days. Alkaline phosphatase activity was stimulated in the ASCs. The coated scaffold improved bone

formation and mineralisation as compared to the uncoated scaffold thus showing that the mere incorporation of the proteosaccharide as a coating can have pronounced effects on bone regeneration (Kang *et al.*, 2011; Snyder *et al.*, 2014)

Arulmoli and co-workers (2016) showed that laminin may also be incorporated with HA and silk fibroin to form IPNs which match the physical properties of brain tissue (Arulmoli *et al.*, 2016). The proteosaccharide scaffolds promoted the differentiation of human neural stem/progenitor cells (HNSPCs) while combating degradation associated with fibrin hydrogels. Fibrinogen and laminin-binding integrins mediate cellular interactions by HNSPCs. The proteosaccahide and HNSPCs act synergistically to encourage neovascularisation which is an important step in neural tissue engineering. England and co-workers (2017) went a step further by extruding fibrinogen into thombin solution and incorporating HA and polyvinylalcohol (PVA) to improve the viscosity of fibrinogen and thombin, thus making the hydrogel more conducive to 3D bioprinting. Additionally, clotting factor XIII was added to crosslink fibrin. The scaffold was seeded with Schwann cells which were observed to be viable. Longitudinally aligned fibrin fibers provided hapotactic cues which directed the alignment and elongation of DRG neurites as shown in figure 2.7 (England *et al.*, 2017).

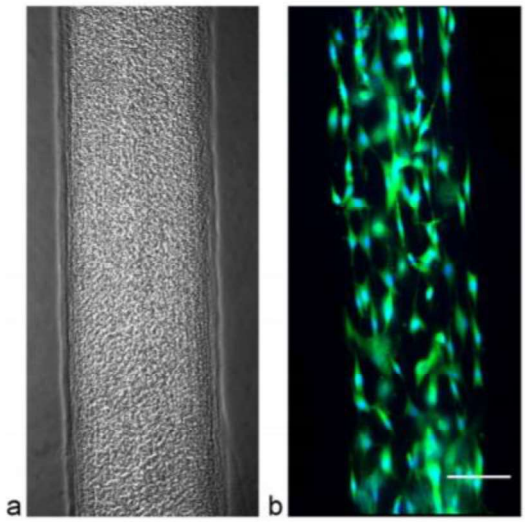


Figure 2.7. a) Phase contrast image of 3D printed fibrin-factor XIII-HA strand, b) Fluorescence image of viable primary Schwann cells encapsulated in the strand. (Schwann cells-stained green using calcein-AM and their nuclei stained blue with Hoechst 33342). Reproduced with permission from Elsevier B.V, Ltd.© 2017

HA-based hydrogels were also modified with a series of peptides including RGD, YISGR, IKVAV and RGD. A storage modulus of 337Pa was the most optimal hydrogel for the

attachment and spreading of hiPS-NPCs (human induced pluripotent stem cell-derived neural progenitor cells) (Lam *et al.*, 2015). Wei and co-workers (2007) also investigated the *in vivo* biocompatibility of IKVAV-modified EDC-crosslinked HA hydrogels. After implantation in the hydrogel in a unilateral cortex lesion site in rats, the hydrogel showed no evidence of cavities and scarring 6 weeks after implantation. The hydrogel showed good biocompatibility and integrated well with host tissue (Wei *et al.*, 2007).

2.4.4 Cellulose-based proteosaccharides

Cellulose is a linear polysaccharide consisting of a hundred to over ten thousand β (1 - 4) linked D-glucose units (Hickey & Pelling, 2019). Cellulose can be isolated from green or woody plants, bacteria and fungi. Although bacterial cellulose is structurally similar to plant cellulose, bacterial cellulose does not require intensive purification due to the absence of contaminant molecules such as lignin and hemicellulose(Hickey & Pelling, 2019). Cellulose fibers possess a unique structural hierarchy as nanofiber assemblies. The diameter of a single cellulose nanofiber ranges from 3-5nm (Ramos *et al.*, 2016). Gelation of cellulose occurs upon heating. Two main derivatives of cellulose include Methylcellulose and Hydroypropylmethylcellulose with lowest critical solution temperature values of 40-50°C and 75-90°C respectively (Van Vlierberghe *et al.*, 2011). Gelation is induced by intermolecular hydrophobic interactions of methoxy side chains. Upon heating, dehydration of the fully hydrated macromolecule occurs resulting in an increase in viscosity. At the transition temperature, a polymer network is formed. Methylcellulose has been applied in the treatment on multiple-site brain injuries (Tate *et al.*, 2001).

The major drawback of using unmodified bacterial cellulose in tissue engineering is that the β (1 - 4) linked D-glucose units cannot be enzymatically metabolised in the human body as opposed to fungi and bacteria (Domingues, Gomes, & Reis, 2014; Mohite & Patil, 2014). Cellulose can therefore effectively fill a gap for damaged tissue but will not degrade as damaged tissue regenerates (Domingues *et al.*, 2014). However, this can be combated by the oxidation of cellulose i.e. the conversion of glucose residues to glucoronic acid residues, using oxidising agents such as $NaClO_2$ and CCl_4 (Courtenay *et al.*, 2018). Physical and chemical cross-linking methods can be used in the synthesis of irreversible cellulose networks. Examples of chemical crosslinkers include aldehydes and carbodimides, however toxicity associated with aldehyde usage must be considered (Sannino *et al.*, 2009). The cellulose backbone may also be modified by the addition of acrylate moieties prior to cross-linking to circumvent the use of toxic chemical cross-linkers and provide better control over the cross-

linking process (Pal *et al.*, 2006). 2,3-dialdehyde cellulose (DAC) may also be used to crosslink cellulose with collagen. DAC can be prepared by regioselective oxidation of cellulose with periodate(Pietrucha & Safandowska, 2015). The reaction is accomplished between collagen's amino group and the aldehyde group of DAC without affecting the triple helix structure of collagen to a large extent. The proteosaccharide shows greater thermal stability, reduced susceptibility to degradation and a high crosslinking density. The incorporation of DAC however increases the hydrophobicity of the composite which can be adjusted by increasing the collagen content (Pietrucha & Safandowska, 2015). Cellulose nanowhiskers, which may be obtained by acid hydrolysis of cellulose fibres have gained interest for its biomedical applications. The rod like polysaccharide nanoparticles show excellent mechanical properties, large surface area, good hydrophilicity as compared to native cellulose and are biocompatible and biodegradable (Eichhorn, 2011). In the presence of periodic acid, the nanowhiskers undergo oxidative cleavage at the C2-C3 glycol bond resulting in dialdehyde groups at the carbon atoms. The aldehyde groups function as crosslinkers which react with amino groups of proteins such as gelatin though Schiff's base formation (Dash *et al.*, 2013). Rheological studies showed a 150% storage modulus improvement compared to gelatin. Resistance to thermal degradation was also increased with the degradation temperature of the proteosaccharide at 50°C (Dash *et al.*, 2013).

The poor mechanical property of gelatin limits its application as a bioink for printing of 3D scaffolds. The incorporation of cellulose nanofibers increases the tensile strength of the hydrogel thus making it more suitable for 3D printing with the optimal concentrations of cellulose (5%) and gelatin (10%). This composite showed good biocompatibility using CCK-8 and Hoechst 33342/PI double staining assays (Jiang *et al.*, 2018). Lu and co-workers (2018) used a one pot method for the construction of cellulose-gelatin hydrogels. Briefly, cellulose was dissolved in an ethylene diamine/potassium thiocyanate (EDA/KSCN) system by heating and thereafter cyclic freezing and thawing was used to accelerate hydrogen bonding between cellulose and gelatin. Intermolecular hydrogen bonds are easily formed and are more stable at lower temperatures, therefore the process of cyclic freezing and thawing led to the formation of stable, supramolecular hydrogel. The hydrogel showed a high breaking strength of 2.4MPa and were pH sensitive, which was attributed to gelatin incorporation (Lu et al., 2018). Bacterial cellulose nanofibers were also incorporated into silk/gelatin bioinks to enhance mechanical properties and for the improvement of shape fidelity of 3D scaffolds. The scaffolds were conducive to L929 cell proliferation and tissue ingrowth and were mechanically robust and

showed good shape fidelity after 3D printing (Huang et al., 2019). Kim and co-workers (2017) adopted a new method for the preparation of cellulose-silk hydrogels. This method entailed dissolution of silk fibroin and cellulose in lithium bromide and subsequent treatment with methanol resulting in the regeneration of silk fibroin (Kim *et al.*, 2017). The gels were highly porous, thee-dimensional networks composed of long interconnected fibrils. The dissolution-regeneration process of silk and cellulose induced a change in the crystalline structure of cellulose II and silk II. A larger concentration of silk fibroin resulted in reduced porosity and swelling ratio, however when compared to films prepared from -butyl-3-methylimidazolium chloride, the hydrogels showed a 25-30 times greater swelling ratio (Shang *et al.*, 2011). However, water uptake exceeded 90% independent of silk content which could have been attributed to the 3D porous structure formed. hASCs adhered to and showed better growth on hydrogels with greater silk content, thus showing that silk incorporation largely impacts bioactivity (Shang *et al.*, 2011).

Cellulose-silk composites may also be applied in wound healing. Ju and co-workers (2011) designed a novel wound dressing hydrogel composed of alginate, carboxymethyl cellulose and silk fibroin. The hydrogel was compared to commercially available Purilon Gel® and medical gauze. The composite hydrogel showed excellent cell adhesion and biocompatibility for the healing of second-degree burns(Ju *et al.*, 2014). NIH 3T3 fibroblasts showed a higher cell growth than Purilon Gel® and faster healing was observed with the proteosaccharide hydrogel. The formation of collagen arrays also took place faster in the proteosaccharide hydrogel. This study showed that the proteosaccharide hydrogel which is cheaper and readily available has the ability to replace the commercialised Purilon Gel® (Ju et al., 2014). Collagen-cellulose hydrogels have also shown potential in wound healing. The incorporation of collagen allows for tissue repair due to its excellent biological properties. Collagen provides strength, structure and integrity to tissues. De Sousa Moraes and co-workers (2016) observed a porous structure in collagen-cellulose hydrogels with irregularly arranged fibres and interconnected pores. The addition of collagen did however reduce the thermal stability of the hydrogel due to a decrease in bacterial cellulose crystallinity after the addition of collagen, however the hydrogel still showed good thermal stability. The BC-COL hydrogel showed quick re-epithelialisation within 7-15 days of the postoperative period and no inflammation at the wound site in Rattus norvegicus rats (De Sousa Moraes et al., 2016).

Collagen-cellulose composites have also been used as tendon or ligament replacements and tested in simulated physiological conditions. Collagen-cellulose composites showed strength and elongation of 37-57 MPa and 15-17% respectively, similar to native tissue. The proteosaccharide composite was crosslinked with genipin and a 75% w/w concentration of cellulose showed a strength of 55MPa at strain of 0.5% which reduced to 16 MPa post-sterilisation. The composite showed good biocompatibility and supported HLC and HEC cell adhesion and phenotype expression. The composite can be considered ideal in ligament repair and connective tissue regeneration (Mathew et al., 2013). Table 2.3 provides a brief summary of the salient features and applications inherent to various proteosaccharides combinations discussed in this review.

Table 2.5. Comprehensive summary of the main proteosaccharides and salient features.

Proteosaccharide	Salient features	References
ALG-GEL	Improved mechanical strength and thermal stability compared to gelatin hydrogels. Improved cell adhesion and protein adsorption compared to alginate hydrogels. Attachment and proliferation of chondrocytes, C2C12 myoblasts, smooth muscle cells (SMC). Alginate improves 3D printing accuracy. **Applications:** valvular, cardiac, bone and cartilage regeneration. Incorporation of cellulose further increases mechanical strength of the composite.	(Balakrishnan *et al.*, 2014; Duan *et al.*, 2013; Luo *et al.*, 2018; Rosellini *et al.*, 2009; Wang *et al.*, 2016)
ALG-COL	Improved mechanical integrity and thermal stability due to collagen addition. Fibrous structure provided by collagen. Increased hydrophilicity due to collagen addition. Attachment and proliferation of L929 fibroblasts, MSCs, keratinocytes and chondrocytes. **Applications:** bone, cartilage, skin regeneration and wound healing.	(Hu *et al.*, 2014; Kim *et al.*, 2011; Perez *et al.*, 2014; Yang *et al.*, 2018)
ALG-FIBRIN	Improved tensile strength and extensibility due to incorporation of fibrin. Improved cell adhesion and proliferation compared to alginate hydrogels. Attachment and proliferation of MSCs and fibroblasts. **Applications:** wound healing, cartilage regeneration. Incorporation of chitosan improves wound healing properties.	(Devi *et al.*, 2012; Ma, Titan, *et al.*, 2012)

CHT-LAM	Improved mechanical strength, stiffness and stability provided by chitosan. Improved cell adhesion and bioactivity due to incorporation of laminin. Axon guidance and proliferation of circulatory angiogenic cells when collagen was also included. **Applications:** neural tissue engineering and pancreatic tissue engineering (Treatment of type I Diabetes).	(McEwan *et al.*, 2016; Zhu *et al.*, 2010)
CHT-GEL	Improved mechanical strength, force bearing capacity and reduced degradation. Improved cell adhesion, hydrophilicity and bioactivity due to incorporation of gelatin. Attachment and proliferation of HFF1 cells MG63, thyroid cartilage and HaCT cells. **Applications:** bone, skin, cartilage regeneration.	(Kumar *et al.*, 2017; Levett *et al.*, 2014; Liu *et al.*, 2014; Shen *et al.*, 2015)
CHT-COL	Improved mechanical strength, rigidity, tensile strength and swellability. Improved bioactivity and cell adhesion due to incorporation of collagen. Attachment and proliferation of MG63, fibroblasts and keratinocytes. **Applications**: neural, skin, cardiac, adipose and wound healing.	(Berthod *et al.*, 2001; Gilarska *et al.*, 2018; Gingras *et al.*, 2003; Shaghiera *et al.*, 2018)
CHT-SILK	Improved mechanical strength, reduced degradation and compressive modulus due to silk incorporation. Improved cell adhesion and biocompatibility. Silk improved the stability of the hydrogel for 3D printing. Attachment and proliferation of MC3T3-E1 cells, HDF and rabbit articular chondrocytes. **Application:** cartilage, bone.	(Li *et al.*, 2019; Samal *et al.*, 2014; Silva *et al.*, 2008)
HA-COL	Increased mechanical strength (compressive modulus =54.77±0.31 kPa). Increased hydrophilicity and biocompatibility. Attachment and proliferation of chondrocytes and cardio sphere derived rat cells. **Applications:** treatment of osteoarthitis, cartilage, bone and aortic valve regeneration.	(Guo *et al.*, 2012; Kontturi *et al.*, 2014; Mohammadi *et al.*, 2018; Nazir *et al.*, 2019)
HA-GEL	Improved mechanical strength, compressive modulus, stiffness and reduced degradation due to hyaluronic acid incorporation. Increased cell adhesion and hydrophilicity due to gelatin. Attachment and proliferation of HUVEC cells and chondrocytes. **Applications:** neural, cardiac, cartilage or skeletal muscle engineering.	(Camci-Unal *et al.*, 2013; Levett *et al.*, 2014; Sanmartín-Masiá *et al.*, 2017)

CELL-COL	Improved mechanical strength, reduced degradation. (Collagen may reduce thermal stability). Improved fidelity of biological constructs due to cellulose incorporation. Attachment and proliferation of L929 fibroblasts, HLC and HEC cells. **Applications:** cartilage (tendon or ligament repair), wound healing.	(Mathew *et al.*, 2013; De Sousa Moraes *et al.*, 2016)
CELL-GEL	Improved mechanical strength, thermal stability and storage modulus due to incorporation of cellulose. Reduced degradation due to cellulose incorporation. Increased stability for 3D printing due to cellulose addition. Adhesion and proliferation of CCK8 cells. **Applications**: wound healing, skin regeneration, bone.	(Huang *et al.*, 2019; Vatankhah *et al.*, 2014)

2.4.5 Other proteosaccharides

Besides chitosan, hyaluronic acid and alginate, there exist many other polysaccharides which have not been used as extensively yet possess some beneficial characteristics for tissue engineering. One such polysaccharide is starch. Starch is a plant polysaccharide composed of anhydrous glucose units.Starch has been gaining interest for due to its abundance, affordability and complete biodegradability into water and carbon dioxide. In order to meet the requirements for tissue engineering, starch must be destructured by heating in water (Carvalho *et al.*, 2016). This leads to swelling and the formation of a viscous paste which destroys most of the hydrogen links thus leading to irreversible loss of structural organisation and crystallinity (Carvalho *et al.*, 2016).

Van Nieuwenhove and co-workers (2015) produced an IPN comprising of photocrosslinked starch and gelatin. Gelatin was modified with methacrylic anhydride and starch was modified with pentenoic anhydride. ADSCs were able to adhere to the hydrogels however phase separation between the gelatin and starch led to areas of local cell detachment. When the separated phases were compared, it was concluded that gelatin promoted cell attachment to a greater extent, thus endowing the hydrogel with its bioactivity (Van Nieuwenhove *et al.*, 2015). Due to the available aldehyde groups on starch ε-amino groups of the lysine or hydroxylysine side groups of gelatin, a Schiff base formation may also occur (Dai *et al.*, 2017). Meskinfam and co-workers (2011) additionally reported the synthesis of nanohydroxyapatite in a starch-gelatin matrix (Meskinfam, 2011). Due to the hydrophilicity of gelatin, hydroxyapatite could be homogenised well in an aqueous solution, while the polar nature of

starch allows for strong adhesion between hydroxyapatite and starch. Gelatin-starch blends may also be used for the controlled release of hydrophilic drugs. As reported by Phomsopha and Baimark (2014), blends crosslinked by glutaraldehyde showed controlled release of a model drug (methylene blue) over 24 hours. An decrease in the amount of drug released over 24 hours was observed as the content of gelatin in the blends was increased. This is attributed to glutaraldehyde crosslinking which inhibits drug release. Drug released ranged from 78% for gels comprising of 100% gelatin to 97% for blends with a 50:50 starch: gelatin ratio. Therefore, it can be concluded that the protein-polysaccharide ratio must be appropriately adjusted to achieve the desirable release profile (Phomsopha & Baimark, 2014).

Chondroitin sulfate has been used as a scaffold material in bone, cartilage and skin regeneration. Wang and co-workers (2006) developed a bilayer scaffold consisting of CS, Gelatin and HA. After culturing in an air-liquid interface, embedded keratinocytes differentiated into stratified squamous epithelium. The scaffold also showed positive effects on promoting the wound healing process on full thickness wounds in mice(Wang *et al.*, 2006). Wang and co-workers (2010) further substituted gelatin for collagen and also observed successful repair of full thickness defects *in vivo* (Wang *et al.*, 2010). The tripolymer system has also been useful in cartilage tissue engineering, as chondroitin provided protection against collagenase-induced degradation, and preserved the porosity of gelatin while hyaluronic acid allowed better host tissue integration (Quan *et al.*, 2014). By excluding gelatin, silk fibroin-chondroitin-hyaluronic acid has also demonstrated potential in dermal tissue engineering where SF provides mechanical support and acts as a template for new tissue formation, and HA increases the hydrophilicity and promotes binding of vascular endothelial cells thereby promoting vascularisation. The SF/CS/HA 3-D scaffolds stimulated the secretion of growth factors PDGF, VEGF and bFGF and induced neodermis synthesis (Yan *et al.*, 2013). When compared to another tripolymer graft comprising of collagen, chondroitin and HA, it was found that the SF/CS/HA artificial dermal tissue showed a higher speed of dermal reconstruction. The application of CS in neural tissue engineering is problematic, as chondroitin sulfate proteoglycan plays a significant role in the activation of microglia and macrophages following a spinal cord injury. This leads to scar formation, which is a major obstacle encountered in neural regeneration. chemical modification of CS with methacrylate or aldehyde groups facilitate its crosslinking to proteins.

Gelatin cannot be used alone due to its rapidly dissolving nature at body temperature. Researchers have therefore looked at silk-gelatin composites. This can be supported by the fact that β-sheet-rich silk domains can stabilise the network and lead to a hydrogel with better solid-like characteristics (Gil *et al.*, 2005). Methacrylated gelatin has furthermore been photocrosslinked with silk for cellular encapsulation and photolithography by Sawatjui and co-workers (2015). The 3D scaffold was evaluated for its ability to support BM-MSCs and displayed significantly better cell proliferation and differentiation than SF scaffolds. Sulphated GAG production was also increased along with increased expression of as COL II, AGC, SOX-9 and COL X(Sawatjui *et al.*, 2015).

Pectin is a is a linear polysaccharide composed of (1,4)-α-D-galacturonic acid units randomly interrupted by (1,2)-linked L-rhamnoside-chains and other neutral sugars (Wenpo *et al.*, 2015). Pectin is chemically modified with acrylamide groups via grafting and crosslinked by glutaraldehyde (J. Chen et al., 2015). Modified pectin showed better gelation than the parent polymer with pH dependant swelling behaviour (Lara-Espinoza *et al.*, 2018). Pectin has been used as a potential drug carrier in colon-specific therapy, however pectin alone shows poor mechanical properties and bioactivity, this it is combined with proteins including gelatin and collagen (Lara-Espinoza *et al.*, 2018). Another protein which may be incorporated with pectin is mucin. By combining pectin with mucin, is a major glycosylated protein of the mucus gel found lining human body cavities, an IPN with enhanced physicomechanical properties was formed due to the multiple hydroxyl and carboxyl functional groups present on the multi-oligosaccharide branches of mucin which reacted with pectin. Interactions at the mucosal surface included hydrogen bonding, electrostatic interactions and Van de waal's forces. Electrostatic interactions were strengthened when crosslinked with calcium ions. Mashingaidze and co-workers (2013) proved that the enhanced physicomechanical properties of the proteosaccharide can be useful in modified drug release (Mashingaidze *et al.*, 2013).

Misha and co-workers (2011) investigated the pectin-gelatin combination crosslinked by glutaraldehyde in wound healing. FTIR studies showed strong hydrogen bonds formed between the polymers. Tensile strength and elongation break increased with an increase in gelatin content up to a certain point. The proteosaccharide was cytocompatible with B16 melanoma cells and the addition of glycine improved the wound healing properties of the proteosaccharide (Misha *et al.*, 2011). Collagen is commonly applied in wound healing, however its susceptibility to degradation necessitates its combination with other polymers. The

addition of pectin to collagen scaffolds may be applied in diabetic wound dressings as demonstrated by Wenpo and co-workers (2015). The rationale behind this combination is that the incorporation of pectin improves the thermal stability of the hydrogel by 14°C and additionally inhibits the degradation of collagen by collagenases, thereby increasing the structural stability of collagen (Jayakumar *et al.*, 2014).

By modifying pectin with an RGD-containing oligopeptide, pectin can serve as a cell vehicle for bone regeneration (Munarin *et al.*, 2011). The modification occurs though carbodiimide chemistry. Proteoblasts immobilised in the hydrogel microspheres maintained constant viability for 29 days. Cells grew not only inside but were able to spread outside the microscpheres and organise themselves into 3D structures producing a mineralised ECM as shown in figure 2.8 thus showing that pectin may serve as an injectable cell carrier for bone engineering (Munarin *et al.*, 2011).

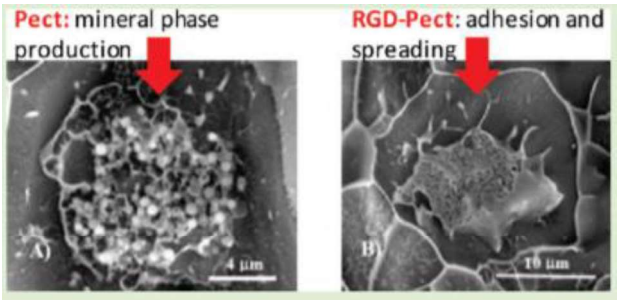


Figure 2.8. a) SEM images of MCT3T-E1 cells immobilised in RGD-Pectin microspheres at day 8. Reproduced with permission from F. Munarin, S. G. Guerreiro, M. A. Grellier, M. C. Tanzi, M. A. Barbosa, P. Petrini, and P. L. Granja Biomacromolecules 2011 12 (3), 568-577 DOI: 10.1021/bm101110x. Copyright © 2011 American Chemical Society.

2.5 Conclusion

The use of naturally occurring proteosaccharides have contributed to the advancement of regenerative strategies for tissue engineering applications. Several proteosaccharides which can overcome the limitations of synthetic polymers and better resemble the ECM have been reviewed. It can be concluded that certain polysaccharides are able to complement protein function and thus provide key therapeutic cues which could not be seen with the individual components. Despite the superiority of proteosaccharide materials in terms of mechanical strength, biomimicry and bioactivity, attention must be directed to the degradation pathways and products of polysaccharides in the composite, such as the production of immunogenic

substances associated with cellulose degradation. Apart from the polysaccharides and proteins discussed, there exists many other natural proteosaccharides whose potential has not been exploited to the fullest.

REFERENCES

Aderibigbe, B.A. & Buyana, B. 2018. Alginate in Wound Dressings. Pharmaceutics.10(2) 42.

Afewerki, S., Sheikhi, A., Kannan, S., Ahadian, S. & Khademhosseini, A. 2019. Gelatin-polysaccharide composite scaffolds for 3D cell culture and tissue engineering: Towards natural therapeutics. Bioengineering & Translational Medicine. 4(1):96–115.

Ahmad, Z., Shepherd, J.H., Shepherd, D. V., Ghose, S., Kew, S.J., … Rushton, N. 2015. Effect of 1-ethyl-3-(3-dimethylaminopropyl) carbodiimide and N-hydroxysuccinimide concentrations on the mechanical and biological characteristics of cross-linked collagen fibres for tendon repair. Regenerative Biomaterials. 2(2):77–85.

Ahmed, T.A.E., Dare, E. V. & Hincke, M. 2008. Fibrin: a versatile scaffold for tissue engineering applications. Tissue engineering. Part B, Reviews. 14(2), 199–215. https://doi.org/10.1089/ten.teb.2007.0435

Amdursky, N., Mazo, M.M., Thomas, M.R., Humphey, E.J., Puetzer, J.L., … Stevens, M.M. 2018. Elastic serum-albumin based hydrogels: Mechanism of formation and application in cardiac tissue engineering. Journal of Materials Chemistry B. 6(35):5604–5612.

Arica, M.Y. 2000. Immobilization of polyphenol oxidase on carboxymethylcellulose hydrogel beads: Preparation and characterization. Polymer International. 49(7):775–781.

Arulmoli, J., Wright, H.J., Phan, D.T.T., Sheth, U., Que, R.A., … Flanagan, L.A. 2016. Combination scaffolds of salmon fibrin, hyaluronic acid, and laminin for human neural stem cell and vascular tissue engineering. Acta Biomaterialia. 43:122–138.

Azami, M., Rabiee, M. & Moztarzadeh, F. 2010. Glutaraldehyde crosslinked gelatin/hydroxyapatite nanocomposite scaffold, engineered via compound techniques. Polymer Composites. 31(12):2112–2120.

Azizian, S., Hadjizadeh, A. & Niknejad, H. 2018. Chitosan-gelatin porous scaffold incorporated with Chitosan nanoparticles for growth factor delivery in tissue engineering. Carbohydrate polymers. 202:315–322.

Baham, M., Mohseni, N. & Moghtader, M. 2016. An Introduction to Hydrogels and Some Recent Applications. In: Emerging Concepts in Analysis and Applications of Hydrogels. InTech.

Balakrishnan, B., Joshi, N., Jayakrishnan, A. & Banerjee, R. 2014. Self-crosslinked oxidized alginate/gelatin hydrogel as injectable, adhesive biomimetic scaffolds for cartilage regeneration. Acta Biomaterialia. 10(8):3650–3663.

Baniasadi, M. & Minary-Jolandan, M. 2015. Alginate-Collagen Fibril Composite Hydrogel. Materials (Basel, Switzerland). 8(2):799–814.

Bartnikowski, M., Bartnikowski, N.J., Woodruff, M.A., Schobback, K. & Klein, T.J. 2015. Protective effects of reactive functional groups on chondrocytes in photocrosslinkable hydrogel systems. Acta biomaterialia. 27:66–76.

Berthod, F., Germain, L., Li, H., Xu, W., Damour, O. & Auger, F.A. 2001. Collagen fibril network and elastic system remodeling in a reconstructed skin transplanted on nude mice. Matrix Biology. 20(7):463–473.

Butler, M.F., Clark, A.H. & Adams, S. 2006. Swelling and Mechanical Properties of Biopolymer Hydrogels Containing Chitosan and Bovine Serum Albumin.

Calderon, L., Collin, E., Velasco-Bayon, D., Murphy, M., O'Halloran, D. & Pandit, A. 2010. Type II collagen-hyaluronan hydrogel--a step towards a scaffold for intervertebral disc tissue engineering. European cells & materials. 20:134–48. http://www.ncbi.nlm.nih.gov/pubmed/20821371 Date of access: 01 Sep. 2019.

Camci-Unal, G., Cuttica, D., Annabi, N., Demarchi, D. & Khademhosseini, A. 2013. Synthesis and characterization of hybrid hyaluronic acid-gelatin hydrogels. Biomacromolecules. 14(4):1085–1092.

Carvalho, P.P., Rodrigues, M.T., Reis, R.L. & Gomes, M.E. 2016. Starch-Based Blends in Tissue Engineering. In: Biomaterials from Nature for Advanced Devices and Therapies. Wiley Blackwell. pp. 244–257.

Chajra, H., Rousseau, C.F., Cortial, D., Ronzière, M.C., Herbage, D., … Freyria, A.M. 2008. Collagen-based biomaterials and cartilage engineering. Application to osteochondral defects. Bio-medical materials and engineering. 18(1 Suppl):S33-45. http://www.ncbi.nlm.nih.gov/pubmed/18334722 Date of access: 28 Oct. 2019.

Chen, S., Zhang, M., Shao, X., Wang, X., Zhang, L., … Zhang, L. 2015. A laminin mimetic peptide SIKVAV-conjugated chitosan hydrogel promoting wound healing by enhancing angiogenesis, re-epithelialization and collagen deposition. Journal of Materials Chemistry B. 3(33):6798–6804.

Chen, T., Small, D.A., McDermott, M.K., Bentley, W.E. & Payne, G.F. 2003. Enzymatic methods for in situ cell entrapment and cell release. Biomacromolecules. 4(6):1558–1563.

Chen, Y.C., Su, W.Y., Yang, S.H., Gefen, A. & Lin, F.H. 2013. In situ forming hydrogels composed of oxidized high molecular weight hyaluronic acid and gelatin for nucleus pulposus regeneration. Acta Biomaterialia. 9(2):5181–5193.

Coenen, A. M. J., Bernaerts, K. V., Harings, J. A. W., Jockenhoevel, S., & Ghazanfari, S. 2018. Elastic materials for tissue engineering applications: Natural, synthetic, and hybrid polymers. Acta Biomaterialia, 79, 60–82.

Collins, M.N. & Birkinshaw, C. 2008. Physical properties of crosslinked hyaluronic acid hydrogels. Journal of Materials Science: Materials in Medicine. 19(11):3335–3343.

Courtenay, J.C., Sharma, R.I. & Scott, J.L. 2018. Recent Advances in Modified Cellulose for Tissue Culture Applications. Molecules (Basel, Switzerland). 23(3).

Croisier, F., & Jérôme, C. 2013. Chitosan-based biomaterials for tissue engineering. European Polymer Journal, 49, 780–792.

Cui, L., Xiong, Z., Guo, Y., Liu, Y., Zhao, J., … Zhu, P. 2015. Fabrication of interpenetrating polymer network chitosan/gelatin porous materials and study on dye adsorption properties. Carbohydrate Polymers. 132:330–337.

Dai, R., Woo, M.W., Chen, H., Dang, X., Mansouri, S. & Shan, Z. 2017. Hydrogel beads based on oxidized corn starch cross-linked with gelatin for tartrazine adsorption from aqueous environments. Polymer Journal. 49(7):549–555.

Dash, R., Foston, M. & Ragauskas, A.J. 2013. Improving the mechanical and thermal properties of gelatin hydrogels cross-linked by cellulose nanowhiskers. Carbohydrate Polymers. 91(2):638–645.

Deepthi, S. & Jayakumar, R. 2018. Alginate nanobeads interspersed fibrin network as in situ forming hydrogel for soft tissue engineering. Bioactive Materials. 3(2):194–200.

Devi, M.P., Sekar, M., Chamundeswari, M., Moorthy, A., Krithiga, G., … Sastry, T.P. 2012. A novel wound dressing material- Fibrin-chitosan-sodium alginate composite sheet. Bulletin of Materials Science. 35(7):1157–1163.

Domingues, R.M.A., Gomes, M.E. & Reis, R.L. 2014. The potential of cellulose nanocrystals in tissue engineering strategies. Biomacromolecules, 15(7), 2327–2346. https://doi.org/10.1021/bm500524s

Duan, B., Hockaday, L.A., Kang, K.H. & Butcher, J.T. 2013. 3D Bioprinting of heterogeneous aortic valve conduits with alginate/gelatin hydrogels. Journal of Biomedical Materials Research - Part A. 101 A(5):1255–1264.

Eichhorn, S.J. 2011. Cellulose nanowhiskers: promising materials for advanced applications. Soft matter 2(7). 303-315

Elzoghby, A.O. 2013. Gelatin-based nanoparticles as drug and gene delivery systems: reviewing thee decades of research. Journal of controlled release : official journal of the Controlled Release Society, 172(3), 1075–1091.

England, S., Rajaram, A., Scheyer, D.J. & Chen, X. 2017. Bioprinted fibrin-factor XIII-hyaluronate hydrogel scaffolds with encapsulated Schwann cells and their in vitro characterization for use in nerve regeneration. Bioprinting. 5:1–9.

Fallacara, A., Baldini, E., Manfredini, S. & Vertuani, S. 2018. Hyaluronic Acid in the Third Millennium. Polymers, 10(7), 701. https://doi.org/10.3390/polym10070701

Fan, L., Yang, H., Yang, J., Peng, M. & Hu, J. 2016. Preparation and characterization of chitosan/gelatin/PVA hydrogel for wound dressings. Carbohydrate Polymers. 146:427–434.

Farid, M. 2013. Hyaluronic Acid and Derivatives for Tissue Engineering. Journal of Biotechnology & Biomaterials. s3.

Ghasemi-Mobarakeh, L., Prabhakaran, M.P., Morshed, M., Nasr-Esfahani, M.-H. & Ramakrishna, S. 2008. Electrospun poly(epsilon-caprolactone)/gelatin nanofibrous scaffolds for nerve tissue engineering. Biomaterials. 29(34):4532–9.

Gil, E.S., Frankowski, D.J., Spontak, R.J. & Hudson, S.M. 2005. Swelling behavior and morphological evolution of mixed gelatin/silk fibroin hydrogels. Biomacromolecules. 6(6):3079–3087.

Gilarska, A., Lewandowska-Łańcucka, J., Horak, W. & Nowakowska, M. 2018. Collagen/chitosan/hyaluronic acid – based injectable hydrogels for tissue engineering applications – design, physicochemical and biological characterization. Colloids and Surfaces B: Biointerfaces. 170:152–162.

Gin (Ermakova), I.I., Luttseva (Vershevskaya), E.A. & Voronkina, I. V. s.a. STABILITY OF THE GELS BASED ON TYPE I COLLAGEN AND HYALURONIC ACID. Tsitologiia. 58(6):467–75. http://www.ncbi.nlm.nih.gov/pubmed/30192118 Date of access: 01 Sep. 2019.

Gingras, M., Paradis, I. & Berthod, F. 2003. Nerve regeneration in a collagen-chitosan tissue-engineered skin transplanted on nude mice. Biomaterials. 24(9):1653–1661.

Giuseppe, M. Di, Law, N., Webb, B., A. Macrae, R., Liew, L.J., … Doyle, B.J. 2018. Mechanical behaviour of alginate-gelatin hydrogels for 3D bioprinting. Journal of the Mechanical Behavior of Biomedical Materials. 79:150–157.

Gombotz, W.R. & Wee, S.F. 2012. Protein release from alginate matrices. Adv. Drug Deliv. Rev. 64, 194–205.

Guo, J. & Huang, Y. s.a. Synthesis and Characterization of Chitosan-Albumin Conjugates as pH-Sensitive Bioactive Hydrogels Drug delivery View project Bioengineering View project. https://www.researchgate.net/publication/233387136 Date of access: 28 Oct. 2019.

Guo, Y., Yuan, T., Xiao, Z., Tang, P., Xiao, Y., … Zhang, X. 2012. Hydrogels of collagen/chondroitin sulfate/hyaluronan interpenetrating polymer network for cartilage tissue engineering. Journal of Materials Science: Materials in Medicine. 23(9):2267–2279.

He, N., Wang, R., He, Y. & Dang, X. 2012. Fabrication, structure and surface charges of albumin-chitosan hybrids. Science China Chemistry. 55(9):1788–1795.

Hennink, W.E. & van Nostrum, C.F. 2012. Novel crosslinking methods to design hydrogels. Advance Drug Delivery. Rev. 64. 223-236.

Hickey, R.J. & Pelling, A.E. 2019. Cellulose Biomaterials for Tissue Engineering. Frontiers in bioengineering and biotechnology, 7, 45. https://doi.org/10.3389/fbioe.2019.00045

Ho, M.H., Wang, D.M., Hsieh, H.J., Liu, H.C., Hsien, T.Y., … Hou, L.T. 2005. Preparation and characterization of RGD-immobilized chitosan scaffolds. Biomaterials. 26(16):3197–3206.

Horseman, T., Tajvidi, M., Diop, C.I.K. & Gardner, D.J. 2017. Preparation and property assessment of neat lignocellulose nanofibrils (LCNF) and their composite films. Cellulose. 24(6):2455–2468.

Hozumi, K. & Nomizu, M. 2018. Mixed peptide-conjugated chitosan matrices as multi-receptor targeted cell-adhesive scaffolds. International Journal of Molecular Sciences. 19(9).

Hu, Y., Liu, L., Gu, Z., Dan, W., Dan, N. & Yu, X. 2014. Modification of collagen with a natural derived cross-linker, alginate dialdehyde. Carbohydrate Polymers. 102(1):324–332.

Huang-Lee, L.L.H. & Nimni, M.E. 1994. Crosslinked CNBr-activated hyaluronan-collagen matrices: Effects on fibroblast contraction. Matrix Biology. 14(2):147–157.

Huang, L., Du, X., Fan, S., Yang, G., Shao, H., … Zhang, Y. 2019. Bacterial cellulose nanofibers promote stress and fidelity of 3D-printed silk based hydrogel scaffold with hierarchical pores. Carbohydrate Polymers. 221:146–156.

Huang, L.L., Sung, H.W., Tsai, C.C. & Huang, D.M. 1998. Biocompatibility study of a biological tissue fixed with a naturally occurring crosslinking reagent. Journal of biomedical materials research. 42(4):568–76. http://www.ncbi.nlm.nih.gov/pubmed/9827681 Date of access: 01 Sep. 2019.

Jayakumar, G.C., Usharani, N., Kawakami, K., Rao, J.R. & Nair, B.U. 2014. Studies on the physico-chemical characteristics of collagen-pectin composites. RSC Advances. 4(109):63840–63849.

Jiang, Y., Zhou, J., Yang, Z., Liu, D., Xv, X., … Zhang, Q. 2018. Dialdehyde cellulose nanocrystal/gelatin hydrogel optimized for 3D printing applications. Journal of Materials Science. 53(16):11883–11900.

Ju, H.W., Lee, O.J., Moon, B.M., Sheikh, F.A., Lee, J.M., … Lee, H.R. 2014. Silk fibroin based hydrogel for regeneration of burn induced wounds. Tissue Engineering and Regenerative Medicine. 11(3):203–210.

K., A. & Bandyopadhyay, P. 2012. Polysaccharide-Protein Interactions and Their Relevance in Food Colloids. In: The Complex World of Polysaccharides. InTech.

Kakehi, K., Oda, Y., & Kinoshita, M. 2001. Fluorescence polarization: Analysis of carbohydrate-protein interaction. Analytical Biochemistry, 297, 111–116.

Kang, S.W., Kim, J.S., Park, K.S., Cha, B.H., Shim, J.H., … Lee, S.H. 2011. Surface modification with fibrin/hyaluronic acid hydrogel on solid-free form-based scaffolds followed by BMP-2 loading to enhance bone regeneration. Bone. 48(2):298–306.

Khunmanee, S., Jeong, Y. & Park, H. 2016. Crosslinking method of hyaluronic-based hydrogel for biomedical applications. Journal of Tissue Engineering. 8.

Kim, G., Ahn, S., Kim, Y., Cho, Y. & Chun, W. 2011. Coaxial structured collagen-alginate scaffolds: Fabrication, physical properties, and biomedical application for skin tissue regeneration. Journal of Materials Chemistry. 21(17):6165–6172.

Kim, H.J., Yang, Y.J., Oh, H.J., Kimura, S., Wada, M. & Kim, U.J. 2017. Cellulose–silk fibroin hydrogels prepared in a lithium bromide aqueous solution. Cellulose. 24(11):5079–5088.

Kim, S.S., Lim, S.H., Cho, S.W., Gwak, S.J., Hong, Y.S., … Kim, B.S. 2006. Tissue engineering of heart valves by recellularization of glutaraldehyde-fixed porcine valves using bone marrow-derived cells. Experimental & molecular medicine. 38(3):273–83.

Klouda, L. & Mikos, A.G. 2008. Thermoresponsive hydrogels in biomedical applications. European journal of pharmaceutics and biopharmaceutics : official journal of Arbeitsgemeinschaft fur Pharmazeutische Verfahenstechnik e.V, 68(1), 34–45.

Kong, H.J., Kaigler, D., Kim, K. & Mooney, D.J. 2004. Controlling Rigidity and DegradatioKong, H. J., Kaigler, D., Kim, K., & Mooney, D. J. (2004). Controlling Rigidity and Degradation of Alginate Hydrogels via Molecular Weight Distribution. Biomacromolecules, 5(5), 1720–1727. https://doi.org/10.1021/bm04987. Biomacromolecules. 5(5):1720–1727.

Kontturi, L.S., Järvinen, E., Muhonen, V., Collin, E.C., Pandit, A.S., … Urtti, A. 2014. An injectable, in situ forming type II collagen/hyaluronic acid hydrogel vehicle for chondrocyte delivery in cartilage tissue engineering. Drug Delivery and Translational Research. 4(2):149–158.

Kopeček, J. 2007. Hydrogel biomaterials: A smart future? Biomaterials. 28(34):5185–5192.

de Kruif, C.. & Tuinier, R. 2001. Polysaccharide protein interactions. Food Hydrocolloids. 15(4–6):555–563.

Kumar, P., Dehiya, B.S. & Sindhu, A. 2017. Comparative study of chitosan and chitosan–gelatin scaffold for tissue engineering. International Nano Letters. 7(4):285–290.

Lam, J., Carmichael, S.T., Lowry, W.E. & Segura, T. 2015. Hydrogel design of experiments methodology to optimize hydrogel for iPSC-NPC culture. Advanced Healthcare Materials. 4(4):534–539.

Lara-Espinoza, C., Carvajal-Millán, E., Balandrán-Quintana, R., López-Franco, Y. & Rascón-Chu, A. 2018.

Lawson, M.A., Barralet, J.E., Wang, L., Shelton, R.M. & Triffitt, J.T. 2004. Adhesion and growth of bone marrow stromal cells on modified alginate hydrogels. Tissue Engineering. 10(9–10):1480–1491.

Lee, F. & Kurisawa, M. 2013. Formation and stability of interpenetrating polymer network hydrogels consisting of fibrin and hyaluronic acid for tissue engineering. Acta Biomaterialia. 9(2):5143–5152.

Lee, J., Bhang, S.H., Park, H., Kim, B.-S. & Lee, K.Y. 2010. Active blood vessel formation in the ischemic hindlimb mouse model using a microsphere/hydrogel combination system. Pharmaceutical research. 27(5):767–74.

Lee, K.Y., Peters, M.C. & Mooney, D.J. 2003. Comparison of vascular endothelial growth factor and basic fibroblast growth factor on angiogenesis in SCID mice. Journal of controlled release : official journal of the Controlled Release Society. 87(1–3):49–56.

Levett, P.A., Melchels, F.P.W., Schobback, K., Hutmacher, D.W., Malda, J. & Klein, T.J. 2014. A biomimetic extracellular matrix for cartilage tissue engineering centered on photocurable gelatin, hyaluronic acid and chondroitin sulfate. Acta Biomaterialia. 10(1):214–223.

Li, T., Song, X., Weng, C., Wang, X., Gu, L., … Chen, C. 2019. Silk fibroin/carboxymethyl chitosan hydrogel with tunable biomechanical properties has application potential as cartilage scaffold. International Journal of Biological Macromolecules. 137:382–391.

Li, X., Sun, Q., Li, Q., Kawazoe, N. & Chen, G. 2018. Functional Hydrogels With Tunable Structures and Properties for Tissue Engineering Applications. Frontiers in chemistry, 6, 499.

Lin-Shu, L., Thompson, A.Y., Heidaran, M.A., Poser, J.W. & Spiro, R.C. 1999. An osteoconductive collagen/hyaluronate matrix for bone regeneration. Biomaterials. 20(12):1097–1108.

Liu, L. S., Kost, J., Yan, F., & Spiro, R. C. 2012. Hydrogels from biopolymer hybrid for biomedical, food, and functional food applications. Polymers, 4, 997–1011.

Liu, Y., An, M., Wang, L. & Qiu, H. 2014. Preparation and characterization of chitosan-gelatin/glutaraldehyde scaffolds. Journal of Macromolecular Science, Part B: Physics. 53(2):309–325.

Loeser, R. F. (2014, October 1). Integrins and chondrocyte-matrix interactions in articular cartilage. Matrix Biology, 39, 11–16. https://doi.org/10.1016/j.matbio.2014.08.007

Luo, Y., Li, Y., Qin, X. & Wa, Q. 2018. 3D printing of concentrated alginate/gelatin scaffolds with homogeneous nano apatite coating for bone tissue engineering. Materials and Design. 146:12–19.

Lv, T., Liang, W., Li, L., Cui, X., Wei, X., … Li, B. 2019. Novel calcitonin gene-related peptide/chitosan-strontium-calcium phosphate cement: Enhanced proliferation of human umbilical vein endothelial cells in vitro. Journal of Biomedical Materials Research - Part B Applied Biomaterials. 107(1):19–28.

Ma, G., Liu, Y., Fang, D., Chen, J., Peng, C., … Nie, J. 2012. Hyaluronic acid/chitosan polyelectrolyte complexes nanofibers prepared by electrospinning. Materials Letters. 74:78–80.

Ma, K., Titan, A.L., Stafford, M., Zheng, C.H. & Levenston, M.E. 2012. Variations in chondrogenesis of human bone marrow-derived mesenchymal stem cells in fibrin/alginate blended hydrogels. Acta Biomaterialia. 8(10):3754–3764.

Ma, L., Gao, C., Mao, Z., Zhou, J., Shen, J., … Han, C. 2003. Collagen/chitosan porous scaffolds with improved biostability for skin tissue engineering. Biomaterials. 24(26):4833–4841.

Mao, J.S., Zhao, L.G., Yin, Y.J. & Yao, K. De. 2003. Structure and properties of bilayer chitosan-gelatin scaffolds. Biomaterials. 24(6):1067–1074.

Mashingaidze, F., Choonara, Y.E., Kumar, P., Du Toit, L.C., Maharaj, V., … Pillay, V. 2013. Exploration of the biomacromolecular interactions of an interpenetrating proteo-saccharide hydrogel network at the mucosal interface. Journal of Biomedical Materials Research - Part A. 101(12):3616–3629.

Masuko, T., Iwasaki, N., Yamane, S., Funakoshi, T., Majima, T., … Nishimura, S.I. 2005. Chitosan-RGDSGGC conjugate as a scaffold material for musculoskeletal tissue engineering. Biomaterials. 26(26):5339–5347.

Mathew, A.P., Oksman, K., Pierron, D. & Harmand, M.F. 2013. Biocompatible Fibrous Networks of Cellulose Nanofibres and Collagen Crosslinked Using Genipin: Potential as Artificial Ligament/Tendons. Macromolecular Bioscience. 13(3):289–298.

McEwan, K., Padavan, D.T., Ellis, C., McBane, J.E., Vulesevic, B., … Suuronen, E.J. 2016. Collagen–chitosan–laminin hydrogels for the delivery of insulin-producing tissue. Journal of Tissue Engineering and Regenerative Medicine. 10(10):E397–E408.

Meskinfam, M. 2011. Biomimetic Preparation of Nano Hydroxyapatite in Gelatin-Starch Matrix. https://www.researchgate.net/publication/272178387 Date of access: 31 Oct. 2019.

Mi, F.L., Sung, H.W. & Shyu, S.S. 2002. Drug release from chitosan-alginate complex beads reinforced by a naturally occurring cross-linking agent. Carbohydrate Polymers. 48(1):61–72.

Misha, R.K., Majeed, A.B.A. & Banthia, A.K. 2011. Development and characterization of pectin/gelatin hydrogel membranes for wound dressing. International Journal of Plastics Technology. 15(1):82–95.

Mohammadi, F., Mohammadi Samani, S., Tanideh, N. & Ahmadi, F. 2018. Hybrid Scaffolds of Hyaluronic Acid and Collagen Loaded with Prednisolone: an Interesting System for Osteoarthitis. Advanced pharmaceutical bulletin. 8(1):11–19.

Mohite, B. V & Patil, S. V. s.a. A novel biomaterial: bacterial cellulose and its new era applications. Biotechnology and applied biochemistry. 61(2):101–10.

Montalbano, G., Toumpaniari, S., Popov, A., Duan, P., Chen, J., … Ferreira, A.M. 2018. Synthesis of bioinspired collagen/alginate/fibrin based hydrogels for soft tissue engineering. Materials Science and Engineering C. 91:236–246.

Munarin, F., Guerreiro, S.G., Grellier, M.A., Tanzi, || M C, Barbosa, M.A., … Granja, P.L. 2011. Pectin-Based Injectable Biomaterials for Bone Tissue Engineering. Biomacromolecules. 12:568–577.

Nair, L.S. & Balakrishnan, B. 2016. Injectable Hydrogels by Chemical Crosslinking. In: Injectable Hydrogels for Regenerative Engineering. IMPERIAL COLLEGE PRESS. pp. 155–200.

Nath, S.D., Abueva, C., Kim, B. & Lee, B.T. 2015. Chitosan-hyaluronic acid polyelectrolyte complex scaffold crosslinked with genipin for immobilization and controlled release of BMP-2. Carbohydrate polymers. 115:160–9.

Nazir, R., Bruyneel, A., Carr, C. & Czernuszka, J. 2019. Collagen type I and hyaluronic acid based hybrid scaffolds for heart valve tissue engineering. Biopolymers. (April, 8):e23278.

Neumann, A.J., Schoeder, J., Alini, M., Archer, C.W. & Stoddart, M.J. 2013. Enhanced adenovirus transduction of hMSCs using 3D hydrogel cell carriers. Molecular Biotechnology. 53(2):207–216.

Van Nieuwenhove, I., Van Vlierberghe, S., Salamon, A., Peters, K., Thienpont, H. & Dubruel, P. 2015. Photo-crosslinkable biopolymers targeting stem cell adhesion and proliferation: the case study of gelatin and starch-based IPNs. Journal of Materials Science: Materials in Medicine. 26(2).

Noori, A., Ashafi, S.J., Vaez-Ghaemi, R., Hatamian-Zaremi, A. & Webster, T.J. 2017. A review of fibrin and fibrin composites for bone tissue engineering. International journal of nanomedicine. 12:4937–4961.

Numata, K., Ifuku, N., Masunaga, H., Hikima, T. & Sakai, T. 2017. Silk Resin with Hydrated Dual Chemical-Physical Cross-Links Achieves High Strength and Toughness. Biomacromolecules. 18(6):1937–1946.

Omobono, M.A., Zhao, X., Furlong, M.A., Kwon, C.H., Gill, T.J., … Redmond, R.W. 2015. Enhancing the stiffness of collagen hydrogels for delivery of encapsulated chondrocytes to articular lesions for cartilage regeneration. Journal of Biomedical Materials Research - Part A. 103(4):1332–1338.

Oryan, A., Kamali, A., Moshiri, A., Baharvand, H., & Daemi, H. 2018. Chemical crosslinking of biopolymeric scaffolds: Current knowledge and future directions of crosslinked engineered bone scaffolds. International Journal of Biological Macromolecules, 107, 678–688.

Pal, K., Banthia, A.K. & Majumdar, D.K. 2006. Development of carboxymethyl cellulose acrylate for various biomedical applications. Biomedical materials (Bristol, England). 1(2):85–91.

Palumbo, F.S., Fiorica, C., Pitarresi, G., Agnello, S. & Giammona, G. 2015. Interpenetrated 3D porous scaffolds of silk fibroin with an amino and octadecyl functionalized hyaluronic acid.

Park, H., Kang, S.W., Kim, B.S., Mooney, D.J. & Lee, K.Y. 2009. Shear-reversibly crosslinked alginate hydrogels for tissue engineering. Macromolecular Bioscience. 9(9):895–901.

Park, S.-H., Cho, H., Gil, E.S., Mandal, B.B., Min, B.-H. & Kaplan, D.L. s.a. Silk-Fibrin/Hyaluronic Acid Composite Gels for Nucleus Pulposus Tissue Regeneration.

Park, S.-N., Lee, H.-J., Lee, K.-H. & Suh, H. 2003. Biological characterization of EDC-crosslinked collagen-hyaluronic acid matrix in dermal tissue restoration. Biomaterials. 24(9):1631–41.

Perez, R.A., Kim, M., Kim, T.H., Kim, J.H., Lee, J.H., … Kim, H.W. 2014. Utilizing core-shell fibrous collagen-alginate hydrogel cell delivery system for bone tissue engineering. Tissue Engineering - Part A. 20(1–2):103–114.

Peter, M., Ganesh, N., Selvamurugan, N., Nair, S. V., Furuike, T., … Jayakumar, R. 2010. Preparation and characterization of chitosan-gelatin/nanohydroxyapatite composite scaffolds for tissue engineering applications. Carbohydrate Polymers. 80(3):687–694.

Phomsopha, T. & Baimark, Y. 2014. Preparation of Starch/Gelatin Blend Microparticles by a Water-in-Oil Emulsion Method for Controlled Release Drug Delivery.

Pietrucha, K. & Safandowska, M. 2015. Dialdehyde cellulose-crosslinked collagen and its physicochemical properties. Process Biochemistry. 50(12):2105–2111.

Quan, R., Zheng, X., Xu, S., Zhang, L. & Yang, D. 2014. Gelatin-chondroitin-6-sulfate-hyaluronic acid scaffold seeded with vascular endothelial growth factor 165 modified hair follicle stem cells as a thee-dimensional skin substitute. Stem Cell Research & Therapy. 5(5):118.

Raia, N.R., Partlow, B.P., McGill, M., Kimmerling, E.P., Ghezzi, C.E. & Kaplan, D.L. 2017. Enzymatically crosslinked silk-hyaluronic acid hydrogels. Biomaterials. 131:58–67.

Ramos, M., Valdés, A. & Garrigós, M.C. 2016. Multifunctional Applications of Nanocellulose-Based Nanocomposites. In: Multifunctional Polymeric Nanocomposites Based on Cellulosic Reinforcements. Elsevier Inc. pp. 177–204.

Re, F., Sartore, L., Moulisova, V., Cantini, M., Almici, C., … Russo, D. 2019. 3D gelatin-chitosan hybrid hydrogels combined with human platelet lysate highly support human mesenchymal stem cell proliferation and osteogenic differentiation. Journal of Tissue Engineering. 10.

Rocha-García, D., Guerra-Contreras, A., Reyes-Hernández, J. & Palestino, G. 2017. Thermal and kinetic evaluation of biodegradable thermo-sensitive gelatin/poly(ethylene glycol) diamine crosslinked citric acid hydrogels for controlled release of tramadol. European Polymer Journal. 89:42–56.

Rosellini, E., Cristallini, C., Barbani, N., Vozzi, G. & Giusti, P. 2009. Preparation and characterization of alginate/gelatin blend films for cardiac tissue engineering. Journal of Biomedical Materials Research - Part A. 91(2):447–453.

Roy, J.C., Salaün, F., Giraud, S., Ferri, A., Chen, G. & Guan, J. 2017. Solubility of Chitin: Solvents, Solution Behaviors and Their Related Mechanisms. In: Solubility of Polysaccharides. InTech. 7:109-128

Sakai, S., Ogushi, Y. & Kawakami, K. 2009. Enzymatically crosslinked carboxymethylcellulose-tyramine conjugate hydrogel: Cellular adhesiveness and feasibility for cell sheet technology. Acta Biomaterialia. 5(2):554–559.

Salem, M., Mauguen, Y. & Prangé, T. 2010. Revisiting glutaraldehyde cross-linking: The case of the Arg-Lys intermolecular doublet. Acta Crystallographica Section F: Structural Biology and Crystallization Communications. 66(3):225–228.

Samal, S.K., Dash, M., Chiellini, F., Wang, X., Chiellini, E., … Kaplan, D.L. 2014. Silk/chitosan biohybrid hydrogels and scaffolds via green technology. RSC Advances. 4(96):53547–53556.

Sanmartín-Masiá, E., Poveda-Reyes, S. & Gallego Ferrer, G. 2017. Extracellular matrix–inspired gelatin/hyaluronic acid injectable hydrogels. International Journal of Polymeric Materials and Polymeric Biomaterials. 66(6):280–288.

Sannino, A., Demitri, C., & Madaghiele, M. 2009. Biodegradable cellulose-based hydrogels: Design and applications. Materials, 2, 353–373. https://doi.org/10.3390/ma2020353

Sarker, B., Papageorgiou, D.G., Silva, R., Zehnder, T., Gul-E-Noor, F., … Boccaccini, A.R. 2014. Fabrication of alginate-gelatin crosslinked hydrogel microcapsules and evaluation of the microstructure and physico-chemical properties. Journal of Materials Chemistry B. 2(11):1470–1482.

Sawatjui, N., Damrongrungruang, T., Leeanansaksiri, W., Jearanaikoon, P., Hongeng, S. & Limpaiboon, T. 2015. Silk fibroin/gelatin-chondroitin sulfate-hyaluronic acid effectively

enhances in vitro chondrogenesis of bone marrow mesenchymal stem cells. Materials science & engineering. C, Materials for biological applications. 52:90–6.

Shaghiera, A., Widiyanti, P. & Yusuf, H. 2018. Synthesis and Characterization of Injectable Hydrogels with Varying Collagen–Chitosan–Thymosin β4 Composition for Myocardial Infarction Therapy. Journal of Functional Biomaterials. 9(2):33.

Shang, S., Zhu, L. & Fan, J. 2011. Physical properties of silk fibroin/cellulose blend films regenerated from the hydrophilic ionic liquid. Carbohydrate Polymers. 86(2):462–468.

Shen, Z. Sen, Cui, X., Hou, R.X., Li, Q., Deng, H.X. & Fu, J. 2015. Tough biodegradable chitosan-gelatin hydrogels via in situ precipitation for potential cartilage tissue engineering. RSC Advances. 5(69):55640–55647.

Silva, R., Singh, R.S.J., Sarker, B., Papageorgiou, D.G., Juhasz, J.A., … Boccaccini, A.R. 2014. Hybrid hydrogels based on keratin and alginate for tissue engineering. Journal of Materials Chemistry B. 2(33):5441–5451.

Silva, R., Singh, R., Sarker, B., Papageorgiou, D.G., Juhasz-Bortuzzo, J.A., … Boccaccini, A.R. 2018. Hydrogel matrices based on elastin and alginate for tissue engineering applications. International Journal of Biological Macromolecules. 114:614–625.

Silva, S.S., Motta, A., Rodrigues, M.T., Pinheiro, A.F.M., Gomes, M.E., … Migliaresi, C. 2008. Novel genipin-cross-linked chitosan/silk fibroin sponges for cartilage engineering strategies. Biomacromolecules. 9(10):2764–74.

Da Silva, M.A., Bode, F., Drake, A.F., Goldoni, S., Stevens, M.M. & Dreiss, C.A. 2014. Enzymatically cross-linked gelatin/chitosan hydrogels: Tuning gel properties and cellular response. Macromolecular Bioscience. 14(6):817–830.

Sionkowska, A., Wisniewski, M., Biomaterials, J.S.- & 2004, undefined. s.a. Molecular interactions in collagen and chitosan blends. Elsevier. https://www.sciencedirect.com/science/article/pii/S0142961203005957 Date of access: 02 Jan. 2020.

Sivashankari, P.R. & Prabaharan, M. 2016. Deacetylation modification techniques of chitin and chitosan. In: Vol. 1. Chitosan Based Biomaterials. Elsevier Inc. pp. 117–133.

Smeds, K.A. & Grinstaff, M.W. 2001. Photocrosslinkable polysaccharides for in situ hydrogel formation. Journal of Biomedical Materials Research. 54(1):115–121.

SMIDSROD, O. & SKJAKBRK, G. 1990. Alginate as immobilization matrix for cells. Trends in Biotechnology. 8:71–78.

Snyder, T.N., Madhavan, K., Intrator, M., Dregalla, R.C. & Park, D. 2014. A fibrin/hyaluronic acid hydrogel for the delivery of mesenchymal stem cells and potential for articular cartilage repair. Journal of biological engineering, 8, 10. https://doi.org/10.1186/1754-1611-8-10

Sobhanian, P., Khorram, M., Hashemi, S.S. & Mohammadi, A. 2019. Development of nanofibrous collagen-grafted poly (vinyl alcohol)/gelatin/alginate scaffolds as potential skin substitute. International Journal of Biological Macromolecules. 130:977–987.

Soni, R., Roopavath, U.K., Mahanta, U., Deshpande, A.S. & Rath, S.N. 2018. Sodium alginate/gelatin with silica nanoparticles a novel hydrogel for 3D printing. In: Vol. 1966. AIP Conference Proceedings. American Institute of Physics Inc.

De Sousa Moraes, P.R.F., Saska, S., Barud, H., De Lima, L.R., Da Conceicao Amaro Martins, V., … Gaspar, A.M.M. 2016. Bacterial cellulose/collagen hydrogel for wound healing. Materials Research. 19(1):106–116.

Stabenfeldt, S.E., Garcia, A.J. & LaPlaca, M.C. 2006. Thermoreversible laminin-functionalized hydrogel for neural tissue engineering. Journal of Biomedical Materials Research - Part A. 77(4):718–725.

Su, D., Yao, M., Liu, J., Zhong, Y., Chen, X. & Shao, Z. 2017. Enhancing Mechanical Properties of Silk Fibroin Hydrogel though Restricting the Growth of β-Sheet Domains. ACS Applied Materials and Interfaces. 9(20):17489–17498.

Sun, Jinchen, & Tan, H. 2013. Alginate-based biomaterials for regenerative medicine applications. Materials, 6, 1285–1309.

Sun, J., Wang, R., Zheng, L., Tan, Y.F., Xiao, Y.M., … Zhang, X.D. 2008. Improvement of Bioactivity of Collagen/Alginate Scaffolds by Hydroxyapatite for Tissue Engineering Cartilage. Key Engineering Materials. 396–398:445–448.

Sun, Z., Lv, F., Cao, L., Liu, L., Zhang, Y. & Lu, Z. 2015. Multistimuli-Responsive, Moldable Supramolecular Hydrogels Cross-Linked by Ultrafast Complexation of Metal Ions and Biopolymers. Angewandte Chemie (International ed. in English). 54(27):7944–8.

Suzuki, Y., Nishimura, Y., Tanihara, M., Suzuki, K., Nakamura, T., … Kakimaru, Y. 1998. Evaluation of a novel alginate gel dressing: Cytotoxicity to fibroblasts in vitro and foreign-body reaction in pig skin in vivo. Journal of Biomedical Materials Research. 39(2):317–322.

Szymańska, E., & Winnicka, K. 2015. Stability of chitosan - A challenge for pharmaceutical and biomedical applications. Marine Drugs, 13, 1819–1846. h

Taghizadeh, M.T. & Abdollahi, R. 2015. A Kinetics Study on the Thermal Degradation of Starch/Poly (Vinyl Alcohol) Blend. Chemical and Materials Engineering. 3(4):73–78.

Tang, S. & Spector, M. 2007. Incorporation of hyaluronic acid into collagen scaffolds for the control of chondrocyte-mediated contraction and chondrogenesis. In: Vol. 2. Biomedical Materials.

Tate, M.C., Shear, D.A., Hoffman, S.W., Stein, D.G. & LaPlaca, M.C. 2001. Biocompatibility of methylcellulose-based constructs designed for intracerebral gelation following experimental traumatic brain injury. Biomaterials. 22(10):1113–1123.

Thumann, G., Viethen, A., Gaebler, A., Walter, P., Kaempf, S., … Salz, A.K. 2009. The in vitro and in vivo behaviour of retinal pigment epithelial cells cultured on ultrathin collagen membranes. Biomaterials. 30(3):287–94.

Tiwari, S., Patil, R., & Bahadur, P. 2018. Polysaccharide based scaffolds for soft tissue engineering applications. Polymers, 11.

Treesuppharat, W., Rojanapanthu, P., Siangsanoh, C., Manuspiya, H. & Ummartyotin, S. 2017. Synthesis and characterization of bacterial cellulose and gelatin-based hydrogel composites for drug-delivery systems. Biotechnology Reports. 15:84–91.

Tsai, K.J., Dixon, S., Hale, L.R., Darbyshire, A., Martin, D. & de Mel, A. 2017. Biomimetic heterogenous elastic tissue development. npj Regenerative Medicine. 2(1).

Vatankhah, E., Prabhakaran, M.P., Jin, G., Mobarakeh, L.G. & Ramakrishna, S. 2014. Development of nanofibrous cellulose acetate/gelatin skin substitutes for variety wound treatment applications. Journal of Biomaterials Applications. 28(6):909–921.

Van Vlierberghe, S., Dubruel, P. & Schacht, E. 2011. Biopolymer-Based Hydrogels As Scaffolds for Tissue Engineering Applications: A Review. Biomacromolecules. 12:1387–1408.

Voron'ko, N.G., Derkach, S.R., Kuchina, Y.A. & Sokolan, N.I. 2016. The chitosan-gelatin (bio)polyelectrolyte complexes formation in an acidic medium. Carbohydrate polymers. 138:265–72.

Wang, H. J., Di, L., Ren, Q. S., & Wang, J. Y. 2009. Applications and degradation of proteins used as tissue engineering materials. Materials, 2, 613–635.

Wang, K., Nune, K.C. & Misra, R.D.K. 2016. The functional response of alginate-gelatin-nanocrystalline cellulose injectable hydrogels toward delivery of cells and bioactive molecules. Acta Biomaterialia. 36:143–151.

Wang, T.-W., Wu, H.-C., Huang, Y.-C., Sun, J.-S. & Lin, F.-H. 2006. Biomimetic bilayered gelatin-chondroitin 6 sulfate-hyaluronic acid biopolymer as a scaffold for skin equivalent tissue engineering. Artificial organs. 30(3):141–9.

Wang, W., Zhang, M., Lu, W., Zhang, X., Ma, D., … Jin, Y. 2010. Cross-linked collagen-chondroitin sulfate-hyaluronic acid imitating extracellular matrix as scaffold for dermal tissue engineering. Tissue Engineering - Part C: Methods. 16(2):269–279.

Wei, Y.T., Tian, W.M., Yu, X., Cui, F.Z., Hou, S.P., … Lee, I.S. 2007. Hyaluronic acid hydrogels with IKVAV peptides for tissue repair and axonal regeneration in an injured rat brain. In: Vol. 2. Biomedical Materials.

Weijers, E.M. 2011. The Influence of Hypoxia and Fibrinogen Variants on the Expansion and Differentiation of Adipose Tissue-Derived Mesenchymal Stem Cells Tissue Engineering Part A.Nov 2011.2675-2685.

Wenpo, F., Gaofeng, L., Shuying, F., Yuanming, Q. & Keyong, T. 2015. Preparation and characterization of collagen-hydroxyapatite/pectin composite. International Journal of Biological Macromolecules. 74:218–223.

Wu, X., Black, L., Santacana-Laffitte, G. & Patrick, C.W. 2007. Preparation and assessment of glutaraldehyde-crosslinked collagen-chitosan hydrogels for adipose tissue engineering. Journal of Biomedical Materials Research - Part A. 81(1):59–65.

Yan, S., Zhang, Q., Wang, J., Liu, Y., Lu, S., … Kaplan, D.L. 2013. Silk fibroin/chondroitin sulfate/hyaluronic acid ternary scaffolds for dermal tissue reconstruction. Acta biomaterialia. 9(6):6771–82.

Yang, X., Lu, Z., Wu, H., Li, W., Zheng, L. & Zhao, J. 2018. Collagen-alginate as bioink for thee-dimensional (3D) cell printing based cartilage tissue engineering. Materials Science and Engineering C. 83:195–201.

Yano, S., Mori, M., Teramoto, N., Iisaka, M., Suzuki, N., … Shibata, M. 2015. Preparation of photocrosslinked fish elastin polypeptide/microfibrillated cellulose composite gels with elastic properties for biomaterial applications. Marine Drugs. 13(1):338–353.

Yin, O.S., Ahmad, I., Cairul, M. & Amin, I.M. 2014. Synthesis of chemical cross-linked gelatin hydrogel reinforced with cellulose nanocrystals (CNC) ARTICLES YOU MAY BE INTERESTED IN. 1614:375.

Younes, I. & Rinaudo, M. 2015. Chitin and chitosan preparation from marine sources. Structure, properties and applications. Marine drugs, 13(3), 1133–1174.

Zhang, J., Allardyce, B.J., Rajkhowa, R., Zhao, Y., Dilley, R.J., … Liu, X. 2018. 3D Printing of Silk Particle-Reinforced Chitosan Hydrogel Structures and Their Properties. ACS Biomaterials Science and Engineering. 4(8):3036–3046.

Zhou, J., Zhang, K., Ma, S., Liu, T., Yao, M., … Guan, F. 2019. Preparing an injectable hydrogel with sodium alginate and Type i collagen to create better MSCs growth microenvironment. E-Polymers. 19(1):87–91.

Zhu, N., Li, M.G., Guan, Y.J., Scheyer, D.J. & Chen, X.B. 2010. Effects of laminin blended with chitosan on axon guidance on patterned substrates. Biofabrication. 2(4).

CHAPTER 3. GENIPIN-CROSSLINKED PROTEOSACCHARIDE SCAFFOLDS FOR POTENTIAL NEURAL TISSUE ENGINEERING APPLICATIONS

pharmaceutics

MDPI

Article

Genipin-Crosslinked, Proteosaccharide Scaffolds for Potential Neural Tissue Engineering Applications

Henna Cassimjee, Pradeep Kumar, Philemon Ubanako and Yahya E. Choonara *

Wits Advanced Drug Delivery Platform Research Unit, Department of Pharmacy and Pharmacology, School of Therapeutic Sciences, Faculty of Health Sciences, University of the Witwatersrand, Johannesburg 2193, South Africa; 1054426@students.wits.ac.za (H.C.); pradeep.kumar@wits.ac.za (P.K.); philemon.ubanako@wits.ac.za (P.U.)
* Correspondence: yahya.choonara@wits.ac.za

Abstract: Traumatic brain injuries (TBIs) are still a challenge for the field of modern medicine. Many treatment options such as autologous grafts and stem cells show limited promise for the treatment and the reversibility of damage caused by TBIs. Injury beyond the critical size necessitates the implementation of scaffolds that function as surrogate extracellular matrices. Two scaffolds were synthesised utilising polysaccharides, chitosan and hyaluronic acid in conjunction with gelatin. Both scaffolds were chemically crosslinked using a naturally derived crosslinker, Genipin. The polysaccharides increased the mechanical strength of each scaffold, while gelatin provided the bioactive sequence, which promoted cellular interactions. The effect of crosslinking was investigated, and the crosslinked hydrogels showed higher thermal decomposition temperatures, increased resistance to degradation, and pore sizes ranging from 72.789 ± 16.85 μm for the full interpenetrating polymer networks (IPNs) and 84.289 ± 7.658 μm for the semi-IPN. The scaffolds were loaded with Dexamethasone-21-phosphate to investigate their efficacy as a drug delivery vehicle, and the full IPN showed a 100% release in 10 days, while the semi-IPN showed a burst release in 6 h. Both scaffolds stimulated the proliferation of rat pheochromocytoma (PC12) and human glioblastoma multiforme (A172) cell cultures and also provided signals for A172 cell migration. Both scaffolds can be used as potential drug delivery vehicles and as artificial extracellular matrices for potential neural regeneration.

Keywords: chitosan; hyaluronic acid; neural; extracellular matrix; proteosaccharide; gelatin; crosslinking; genipin; dexamethasone; drug release; scaffold

Citation: Cassimjee, H.; Kumar, P.; Ubanako, P.; Choonara, Y.E. Genipin-Crosslinked, Proteosaccharide Scaffolds for Potential Neural Tissue Engineering Applications. *Pharmaceutics* 2022, *14*, 441. https://doi.org/10.3390/pharmaceutics14020441

3.1 Introduction

Tissue engineering aims to address the continuous rise in the need for organ transplants by providing a suitable surrogate matrix which promotes the regeneration of damaged tissues. Research in this field is aimed at the use of naturally occurring polymers which are bioactive, biocompatible and non-toxic. The ultimate objective of tissue engineering is to create duplicates of native tissue, which can function as substitutes and promote regeneration. The creation of thee-dimensional (3D) scaffolds is crucial in the field of tissue engineering. These scaffolds not only function as templates upon which new tissue can be produced, but also need to be porous to ensure adequate transport of oxygen and nutrients. Mechanical

properties such as compressive strength and stiffness also dictate the success of a scaffold at its sight of action, specifically in the regeneration of soft tissue such as cartilage. The scaffolds can be produced from natural or synthetic polymers, with the former being favoured for its low toxicity.

The use of polysaccharides such as chitosan and hyaluronic acid in regenerative medicine has become increasingly popular. Chitosan is a semi-crystalline polysaccharide obtained by the deacetylation of chitin and is a co-polymer of d-glucosamine and N-acetyl d- glucosamine Chitosan is insoluble in solutions above pH of 7 however in weakly acidic solutions (pH 6), the free amine groups of chitosan are protonated which allows the molecule to be solubilised. Chitosan has been used extensively due to its biocompatibility, hydrophilicity, biodegradability, and structural similarity to GAGs found in the ECM. However, chitosan does not possess significant mechanical strength. This can be overcome by diverse methods of crosslinking such as photo-crosslinking and chemical crosslinking. Its cationic nature allows for electrostatic interactions with other polymers. previous studies have shown that chitosan supports the attachment and proliferation of fibroblasts, chondrocytes, neurites and hepatocytes, thus making it a promising candidate for tissue engineering applications. An additional advantage is that it is haemostatic and therefore, can be exploited in healing (Okamoto et al., 2003) (Chandrashekar 2006; Roeder et al, 2002). Chitosan has been employed in the field of neural tissue engineering due to it being an effective neuroprotector following spinal cord injuries (Chedly *et al.*, 2017). Mo and researchers (2010) observed migration of cells and axonal stimulation when a chitosan scaffold was implanted into the rat hippocampus. This led to re-established continuity of the neural circuit, with improved cognitive capacity (Mo *et al.*, 2010). Other advantages include its biocompatibility, biodegradability, antibacterial activity and low toxicity (Chandy et al, 1990; Roy *et al.*, 2017; Tiwari, Patil and Bahadur, 2018)

Gelatin which is obtained by the hydrolysis of collagen and is a main component of the ECM has also been widely used due to its antigenicity and biocompatibility (Sionkowska *et al.*, 2004). Hydrolysis is of collagen results in the breakage of its triple helical structure which yields gelatin (Levenberg & Langer, 2004). Gelatin is an anionic protein thus favouring the formation of a polyelectrolyte complex with chitosan (Voron'ko *et al.*, 2016). The blending of gelatin with chitosan furthermore improves the biological activity of the resulting scaffold as gelatin confers its Arg–Gly–Asp (RGD)-like sequence to the product, thus improving cell

adhesion and proliferation (Re *et al.*, 2019). Gelatin has been used in this study to reduce the stiffness of the hydrogel to match the mechanical strength of brain tissue. Furthermore, gelatin rich constructs support the prolonged proliferation of stem cells and multiple neurons along with their plasticity. Gelatin however dissolves rapidly in an aqueous environment thus necessitating crosslinking. Physical crosslinking of these polymers is advantageous as they do not cause potential harm, however the desired degree of crosslinking can be difficult to obtain. Thus, chemical crosslinkers such as glutaraldehyde, carbodimides and genipin can be used (Maitra & Shukla, 2014).

Until today, chitosan-gelatin composites have been used extensively in tissue engineering, notably in hepatic, skin and cartilage regeneration (Georgopoulou *et al.*, 2018; Liu *et al.*, 2014). The blends are beneficial due to their porosity, biocompatibility, and mechanical properties. The blend is, however, unstable in aqueous solutions and readily undergoes dissolution without the presence of crosslinkers.

Hyaluronic acid is an anionic polysaccharide which can be found in the ECM of brain, cartilage and epithelial tissue (England *et al.*, 2017; Guo *et al.*, 2012; Tiwari *et al.*, 2018). Hyaluronic acid functions though various receptors in the brain, mainly CD44 and the hyaluronan associated mobility receptor (RHAMM), and plays an extensive role in cellular interactions such as migration and proliferation, which impact haemostasis in the brain (Wolf & Kumar, 2019). The molecular weight of hyaluronic acid influences cellular responses, with low molecular weight HA (80-800kDa) inducing the production of pro-inflammatory markers, while high Mw (>1600kDa) inhibiting these mediators (JE *et al.*, 2015). Other researchers have shown that low Mw HA enhanced the proliferation of astrocytes in rat spinal cord injuries and high molecular weight reduced the proliferation of astrocytes (Khaing *et al.*, 2011). Hyaluronic acid can easily be modified though its thee different functional groups, the glucuronic acid carboxylic acid, the primary and secondary hydroxyl groups, and the N-acetyl group (Burdick & Prestwich, 2011). These modifications influence the mechanical properties and biological properties of HA; however, modification must be carried out carefully as a high degree of modification can impair its biological activity.

A main disadvantage of hyaluronic acid is the lack of cell adherence to its surface. This can be overcome by combining HA with other biologically active molecules. Spector and co-worker showed that the addition of collagen favoured neuronal differentiation. (K *et al.*, 2007; Tang &

Spector, 2007). The combination of gelatin and hyaluronic acid is not new to regenerative medicine and has been applied in cardiac, adipose and epithelial cell regeneration. in this study, a semi-IPN will be prepared by crosslinking gelatin with genipin and blending with hyaluronic acid to form a proteosaccharide scaffold. This will be evaluated for its applications in TBI's and neural tissue engineering. High Mw HA will be used in this study due to its stiffness and astrocyte inhibition activity.

Over the years, Genipin which is derived from *Gardenia Jasminoides* has replaced glutaraldehyde and other carbodimide crosslinkers due to the expanded biochemical significance of genipin-crosslinked hydrogels but also due to its stability, biocompatibility, and predictable chemistry. Cytotoxicity studies of genipin against fibroblasts showed that genipin was 10 000-fold less toxic than glutaraledehyde, and fibroblasts proliferated 5000-fold more as compared to when treated with glutaraldehyde (ME *et al.*, 2012). Furthermore, genipin can be utilized in penetrating TBI's due to its antimicrobial properties and ability to reduce sepsis, this reducing the risk of nosocomial infections (Kim *et al.*, 2012). Da Silva and co-workers (2021) showed that the genipin component of the IPNs researched exhibited antimicrobial properties against nine bacterial pathogens associat-ed with postsurgical brain infections, which justifies the use of genipin in neural scaffolds (Silva *et al.*, 2021). The mechanism of crosslinking of amino-containing polymers such as chitosan and gelatin, by genipin can be

shown in figure 3.1.

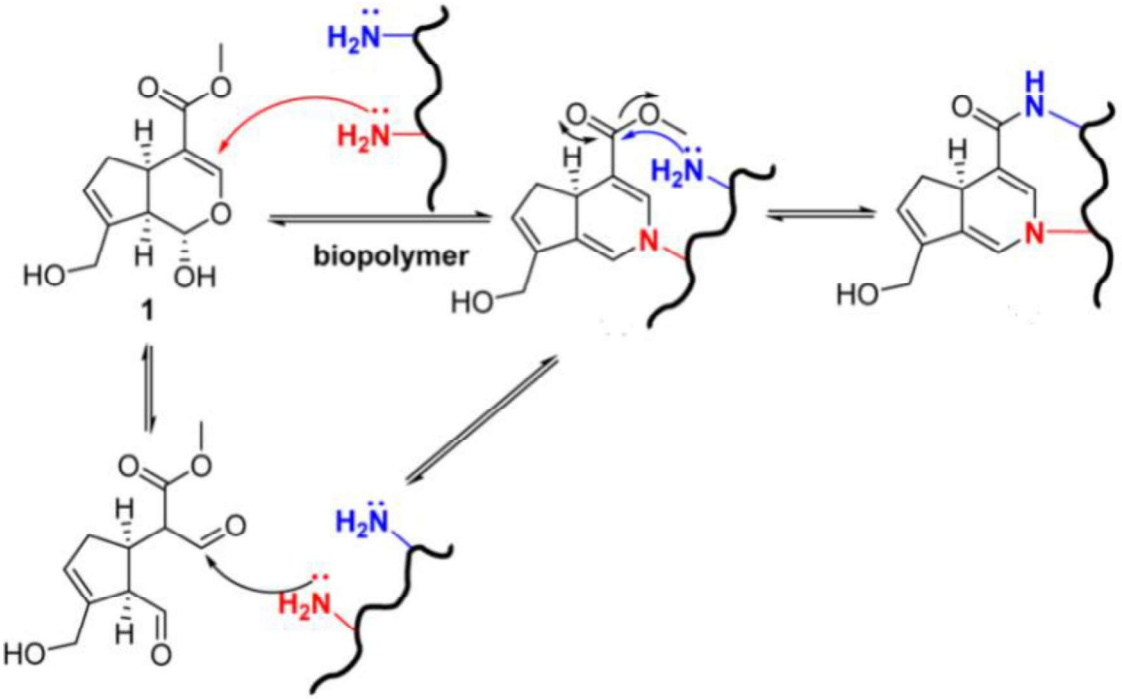


Figure 3.1. Schematic illustrating the mechanism of crosslinking when genipin is used as a crosslinker. Adapted with permission from Butler et. al (2003). Mechanism and kinetics of the crosslinking reaction between biopolymers containing primary amine groups and genipin. *Journal of Polymer Science Part A: Polymer Chemistry.* https://doi.org/10.1002/pola.10960 (Appendix C)

A ring opening reaction is initiated under basic conditions, by nm attack of genipin by hydroxyl ions in an aqueous solution. Thereafter schiff's base formation occurs between the aldehyde present on genipin and amine of the chitosan or gelatin. in an acidic or neutral medium. The amino group of the polymer attacks the olefinic carbon (C3) of genipin, leading to dihydropyran ring opening and subsequent attack on the aldehyde group of genipin by the secondary amino group of the polymer. Genipin crosslinked biomaterials are more stable than glutaraldehyde crosslinked counterparts due to the condensation reaction. Furthermore, a blue-violet pigment is formed upon reaction of genipin with amino groups, which can be used to determine if crosslinking has taken place (JS *et al.*, 2011; Oryan *et al.*, 2018). Hyaluronic acid does not contain free primary amino groups which can react with genipin; however, its hydroxyl groups are able to form glycosidic bonds with genipin, resulting in a stable hydrogel which swells instead of readily dissolving without crosslinking.

In this research, genipin crosslinked chitosan-gelatin and hyaluronic acid-gelatin scaffolds will be prepared and evaluated for their application in neural tissue engineering, an area of regenerative medicine that it has not previously been applied in. These proteosaccharides will overcome the limitations associated with the use of their pristine forms. Due to gelatin possessing weak mechanical strength, it will be used in combination with hyaluronic acid which, due to its stiffness in a hydrated form, will impart mechnanical integrity to the scaffolds. In addition, hyaluronic acid will provide good hydration and diffusivity of nutrients and waste compounds in vivo. Gelatin will provide a peptide sequence to each proteosaccharide which would be recognised by cell integrins and equip the proteosaccharides with bioactivity.

3.2 Materials and Method

3.2.1 Materials

Low molecular weight chitosan, Gelatin (Type B) and glacial acetic acid were purchased from Sigma-Aldrich (St. Louis, Missouri, USA). Genipin was purchased from Challenge Bioproducts Co., Ltd. (Yun-Lin Hsien, Taiwan). HA from Streptococcus Equi was purchased from Sigma-Aldrich (MO, USA). Dulbecco's Modified Eagles Medium-high glucose, Roche Cell Proliferation Kit I (MTT), dimethyl sulfoxide (DMSO) and trypsin–EDTA solution were obtained from Sigma Aldrich (Steinheim, Germany). Donor Equine Serum (DES) was purchased from Hyclone (Logan, Utah, USA). Ethanol (99% absolute) was purchased from LabChem, (Johannesburg, South Africa). Fetal Bo-vine Serum and Ham's F-12 Nutrient Mix (F12) were purchased from (PAN Biotech, Aidenbach, Germany). Rat (Rattus Norvegicus) adrenal gland pheochomocytoma (PC12) and human glioblastoma multiforme (A172) cells were purchased from Cel-Ionex (Separations, South Africa). Penicillin/Streptomycin/Amphotericin B (P/S/AB) solution was purchased from Lonza (Bend, Oregon, USA).

3.2.2 Synthesis of the full IPN and semi-IPN

A 2% solution of Chitosan was prepared by dissolving 2 g in 100 mL of 0.5 M glacial acetic acid. A 2% solution of Gelatin was prepared by dissolving 2 g in 100 mL of distilled water over a magnetic stirrer at 50°C. These solutions were blended and subsequently crosslinked with a 0.01% w/v solution of genipin, obtained by dissolving 100 mg in a 1:4 ethanol: distilled water solution. A mixing crosslinking method was used to prepare the hydrogels. A semi-IPN was prepared similarly by substituting chitosan with HA dissolved in cold distilled water. An optimised 50:50 volumetric ratio of protein to polysaccharide was used in the preparation of the semi-IPN and full-IPN. Genipin was added dropwise to each blend at a concentration of 1% v/v. The blends were allowed to crosslink for a period of 24 h until a blue pigment had

appeared and the gel showed an increased viscosity which indicated the reaction of genipin with amino groups present in each blend. e formation of amide bonds. A volume of 250µl of each hydrogel was cast into each well of a 24-well plate and was subsequently frozen at -80°C and freeze-dried in a lyophiliser for 14 h. Porous scaffolds were obtained and subsequently washed with ethanol to remove excess crosslinker (Figure 3.2). The scaffolds synthesised are stated in table 3.1.

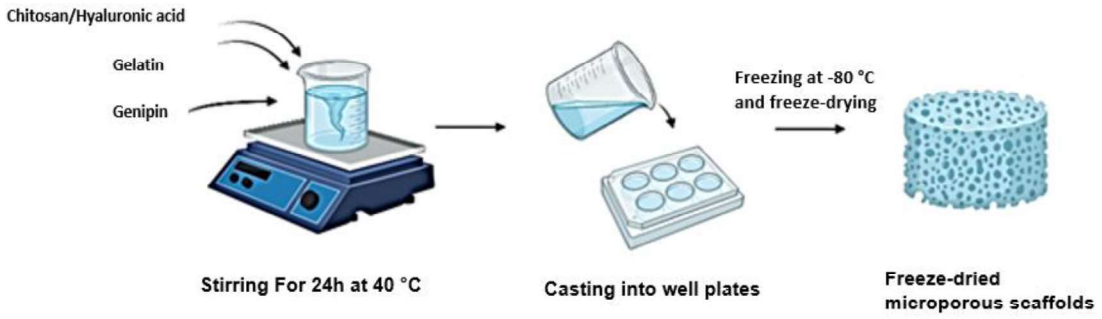


Figure 3.2. Schematic showing the synthesis of each scaffold though a mixing cross-linking method with Genipin to obtain various thee-dimensional scaffolds

Table 3.1. The various proteosaccharide formulations that were investigated for cross-linking effects

Chitosan+ Gelatin (50:50) (CHTGEL)	Chitosan+ Gelatin+ Genipin (50:50) (CGG)
Gelatin+ Genipin (GELGEN)	Chitosan+ Genipin- (CHTGEN)
Hyaluronic acid +Gelatin (HAGEL)	Hyaluronic acid+Gelatin+Genipin (HAGG)

3.2.3 (ATR-FTIR) of pristine polymers and their crosslinked networks to elucidate the physicochemical transformations as a result of crosslinking

Scaffolds were analysed with a Spectrum 2000 FTIR Spectrometer (PerkinElmer, MA, USA) at wave numbers of 4000-650cm-1 at 10 scans/second under a constant pressure of 120 psi and a single-reflection diamond MIRTGS detector. The stage for the sample was cleaned with methanol prior to analysis and a background spectrum was obtained. The spectra obtained were plotted on OriginPro and the formation of amide bonds was confirmed in the region 1600-1700$cm^{-1.}$

3.2.4 Rheological analysis of the proteosaccharide hydrogels

The Elastosens BIO2 (Rheolution Instruments, Montreal, Canada) was used to analyse the viscoelastic behaviour of the resulting networks. A laser was used to measure the displacement of the polymers to minimum amplitude vibration. A volume of 2 mL of each

proteosaccharide hydrogel was be added to a sample receptacle which encapsulated an elastic membrane. This was done immediately after the addition of genipin to determine the time taken for crosslinking to take place by monitoring the change in storage (G') and loss modulus (G''). Viscoelastic behaviour of each hydrogel was observed by tilting each bottle containing the hydrogels. The formation of a meniscus indicated the absence of gelation, while the absence of a meniscus upon tilting indicated hydrogel formation. A tilt bottle test was used for visual confirmation of crosslinking. The gels were photographed after 24 h and 48 h of crosslinking to show the flow and crosslinking intensity of each hydrogel prior to lyophilisation.

3.2.5 Analysis of crystallinity of the proteosaccharide scaffolds

X-Ray Diffraction using the Rigaku Miniflex 60 (Rigaku Corporation, Tokyo, Japan) was used to determine the degree of crystallinity of the scaffold matrix. Each scaffold was mounted using carbon tape and flattened with a glass slip. The proteosaccharide matrix was scanned at a start angle of 5° and a stop angle of 60° at 10° /minute over a 2θ range. This was conducted at room temperature. The crystallinity index was calculated using the following equation:

$$Crystallinity\ Index\ (Ci) = \frac{Sum\ of\ areas\ under\ crystalline\ peaks}{Total\ area\ under\ crystalline\ and\ amorphous\ peaks}$$

Equation 3.1.

3.2.6 Thermoanalytical analysis of the lyophilised proteosaccharide scaffolds

Proteosaccharide-based scaffolds were analysed using the Mettler Toledo, DSC1, STARe System (Schwerzenback, Switzerland). The scaffolds weighing 5-10 mg were heated at a temperature range of 10-350 °C at 10 °C /minute to identify degradation, melting point, and the glass transition temperature (Tg) in an aluminium pan (40DL) and sealed with a 0.2mm opening in the lid for heat flow. This range was used to establish the temperature at which the proteosaccharides will degrade. The test was run under constant N2 gas. The resulting thermogram was compared to a reference ther-mogram run with an empty sample holder.

3.2.7 Swelling potential of scaffolds under physiological conditions

Swelling potential of the scaffolds was measured after immersing the scaffolds into PBS (pH=7.4) until they had reached their equilibrium swelling after 2 h at 37 °C. Thereafter, the surface water was removed using filter paper and samples were weighed (Wet weight). Experiments were done in triplicate. The swelling ratio was calculated using the following formula:

Swelling ratio= (Wet Weight−Dry weight) / Dry weight

Equation 3.2.

3.2.8 Morphological analysis of proteosaccharide scaffolds

The morphological structure of a scaffold is critical to its function in tissue engineering. The scaffolds were observed under a Scanning Electron Microscope (SEM) (FEI Nova NanoLab SEM, FEI Co., Hillsboro, OR USA). Each scaffold was mounted on a stub using carbon tape and coated with carbon and a mixture of gold and palladium (Au/Pd). The structure and porosity were observed.

3.2.9 Determination of bulk density of each scaffold

The bulk density of each scaffold was determined using the following equation:

$$\rho\text{bulk} = \frac{mass}{volume} = \frac{4m}{\pi d^2 h}$$

Equation 3.3

where ρ is the Apparent density of porous material (g/mm^2), m is Mass of scaffold formulations after saturation with water (gm), d is Diameter of scaffold formulations after saturation with water (cm), and h is Height of scaffold formulations after saturation with water (mm).

3.2.10 Degradation of proteosaccharide scaffolds

The rate of degradation of the scaffolds was measured by placing each scaffold into polytops consisting of phosphate-buffered saline and lysozyme (10 000IU/ml) into an orbital shaker at 37 °C and 25rpm. The degradation medium was changed every second day to mimic physiological sink conditions. Scaffolds were removed on days 0, 3, 7, 14, 21 and 28 and weighed after drying. The weight at each time interval was compared to the initial weight of the scaffolds and the rate of degradation was determined. The degradation behaviour of a scaffold is crucial in preventing a premature collapse of the scaffold and the accumulation of potentially toxic by-products.

3.2.11 Drug release of Dexamethasone-21-Phosphate from proteosaccharide scaffolds

Dexamethasone-21-phosphate (DEX) was loaded into hydrogels at a concentration of 0.25 mg/mL to compare drug release kinetics from the full IPN and semi-IPN hydrogel. Each scaffold of the same weight was immersed in 3mL PBS (pH=7.4) in an orbital shaker maintained at 37.5°C. A volume of 2 mL was withdrawn from each sample and replaced with 2 mL of fresh PBS at different time intervals (t=0.5 h, 1 h, 2 h, 4 h, 6 h, 8 h, 10 h, 12 h, 24 h and every 24 h thereafter). The absorbance was read at 242 nm. These were plotted and compared to a standard curve of DEX and cumulative drug release was measured.

3.3 Results and Discussion

3.3.1 FTIR analysis of CGG and HAGG scaffolds

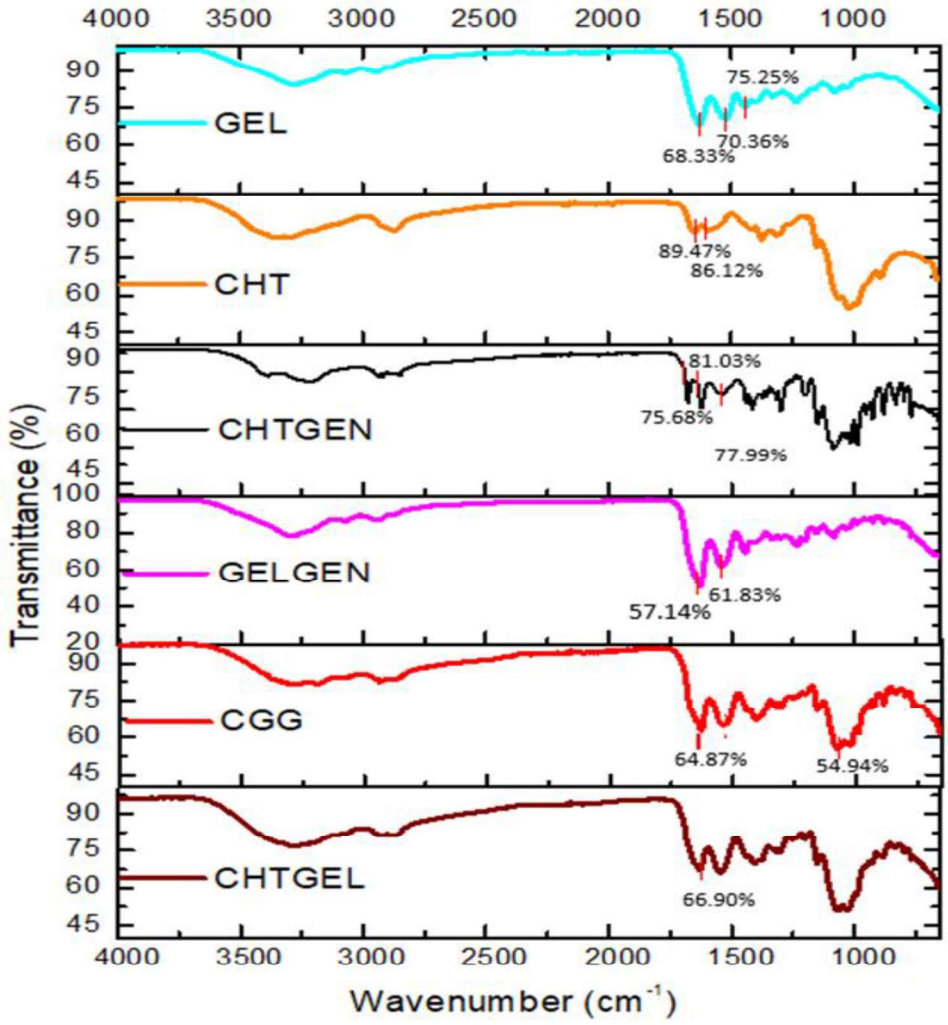


Figure 3.3. FTIR spectra of A) Pristine chitosan (CHT), B) Pristine gelatin (GEL), C) chitosan-gelatin (CHTGEL), D) chitosan-genipin (CHTGEN), E) Gelatin-genipin (GELGEN), F) chitosan-gelatin-genipin (CHTGELGEN). The decreased transmittance values imply an increase in the concentration of certain chemical bonds.

The FTIR spectrum of gelatin shows the typical N-H and O-H overlap at 3284.10 cm^{-1} while bands at 1627 cm^{-1},1520 cm^{-1} and 1443 cm^{-1} are representative of the C=O stretching vibration of amide I, N-H bending vibration of amide II and carbonyl group respectively (Figure 3.3A). In the FTIR spectrum of chitosan, the adsorption band at 3356.08 cm- 1 indicates partially overlapping hydroxyl and amino groups (Figure 3.3B). Peaks between 2800cm^{-1}

represent C-H stretch vibrations. Peaks found at 1648.84 cm^{-1} and 1591.61 cm^{-1} represent the N-H bending vibrations of primary amine groups. Bands found at 1374 cm^{-1} are indicative of a C-O-H primary alcoholic group, while bands at 1023 cm^{-1} and 1149 cm^{-1} indicate C-O and C-N vibrations respectively. FTIR of crosslinked chitosan shows the typical OH stretch at 3210.45 cm^{-1}, with C-H vibrations at 2935.55 cm^{-1}. The band found at 1535 cm^{-1} is indicative of the N-H deformation leading to the formation of a secondary amide, due to the reaction of ester and O-H groups of genipin with the amino group of chitosan. The band found at 1623 cm^{-1} represents the C=O vibration of secondary amides. An increase in the number of bands between 1400 and 1000 cm^{-1} indicate C-N stretch and C-O-H vibrations is observed after genipin crosslinking (Figure 3.3C). Characteristic peaks of gelatin are found at 3289.65 cm^{-1} and 2936.28 cm^{-1}, however, due to the reaction of gelatin with genipin, the band at 1538.19 cm^{-1} is of greater intensity than in uncrosslinked gelatin, due to the formation of C-N bonds, indicating amide bond formation (Figure 3.3D). FTIR spectrum of the CGG IPN network shows an increase in the intensity of band rations between 1629 $cm^{-1}$and 1538 $cm^{-1.}$ The band at 1538 cm^{-1} indicates the formation of C-N bonds, due to the formation of a secondary amide as a result of the reaction between primary amino groups of chitosan and gelatin with the ester group of genipin. The band at 1064 cm^{-1} shows increased adsorption at the expense of the band at 1023 cm^{-1} of chitosan (Figure 3.3E). FTIR of the proteosaccharide hydrogel devoid of crosslinker shows the typical N-H and O-H stretch vibration at 3279.38 cm^{-1} and CH stretch at 2875 cm^{-1} the spectrum shows no new bands, however, the increase in the intensity of the carbonyl band at 1629.13 cm^{-1} is indicative of proteosaccharide interaction (Figure 3.3F).

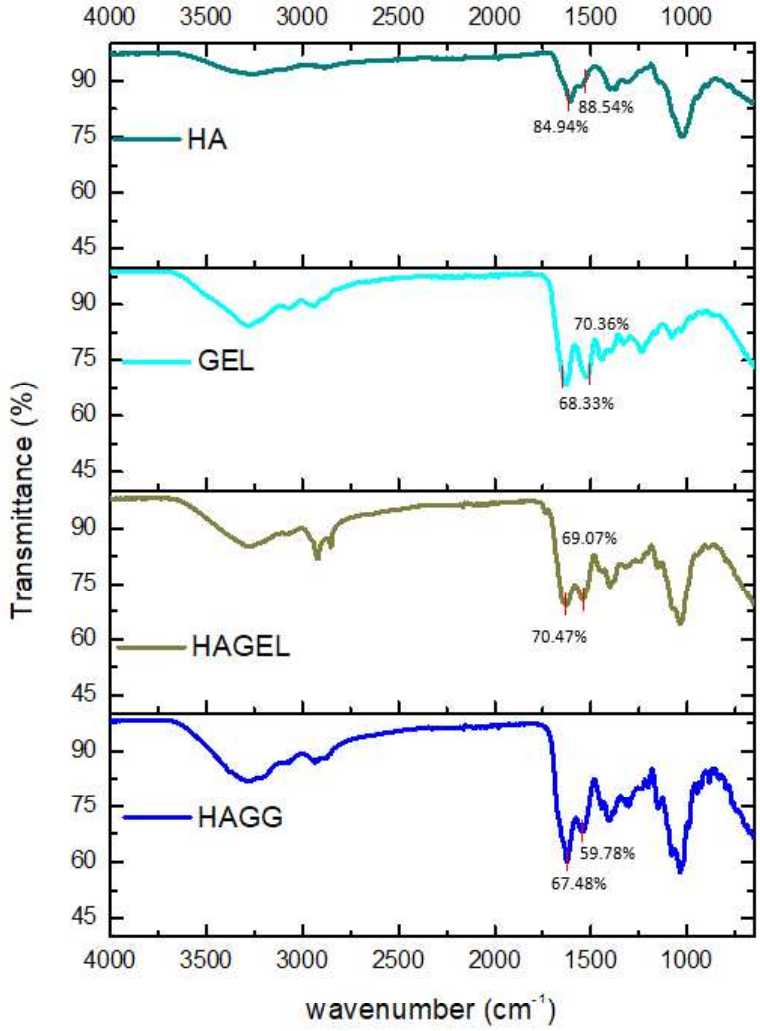


Figure 3.4. FTIR spectra of A) Pristine hyaluronic acid (HA), B) Pristine gelatin (GEL), C) hyaluronic acid-gelatin (HAGEL), D) hyaluronic acid-gelatin-genipin (HAGELGEN)

The FTIR spectrum of HA shows a vibration at 3254.81 cm^{-1} which is indicative of intra- and intermolecular OH stretch vibrations. The band found at 2872 cm^{-1} represents the CH_2 group of HA. Bands at 1606.57 cm^{-1} and 1375.18 cm^{-1} are indicative of symmetrical and asymmetrical COO vibrations while the peak at 1020.07 cm^{-1}represents the C-O-C hemiacetal saccharide units (Figure 3.4A). No new peaks were found in the FTIR spectrum of the HA-gelatin proteosaccharide, however, an increase in the intensity of the amide II peak was observed at 1542.01 cm-1 indicating a molecular interaction in the proteosaccharide (Figure 3.4C). From the FTIR spectrum of the HA-GEL-GEN, it can be concluded that a semi-IPN is formed in this proteosaccharide combination, due to the presence of an amide bond at 1539.72 cm^{-1}, indicating the crosslinking of gelatin with genipin while the characteristic bands

of HA at 3285.46 cm^{-1} and 2936.83 cm^{-1}, indicative of the carboxylic O-H stretch vibration and CH_2 groups respectively, remain (Figure 3.4D).

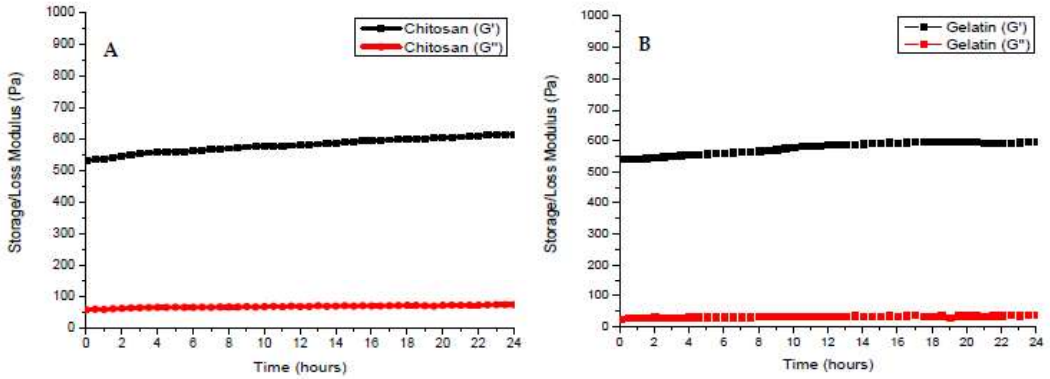
3.3.2 Rheological behaviour of proteosaccharide hydrogels

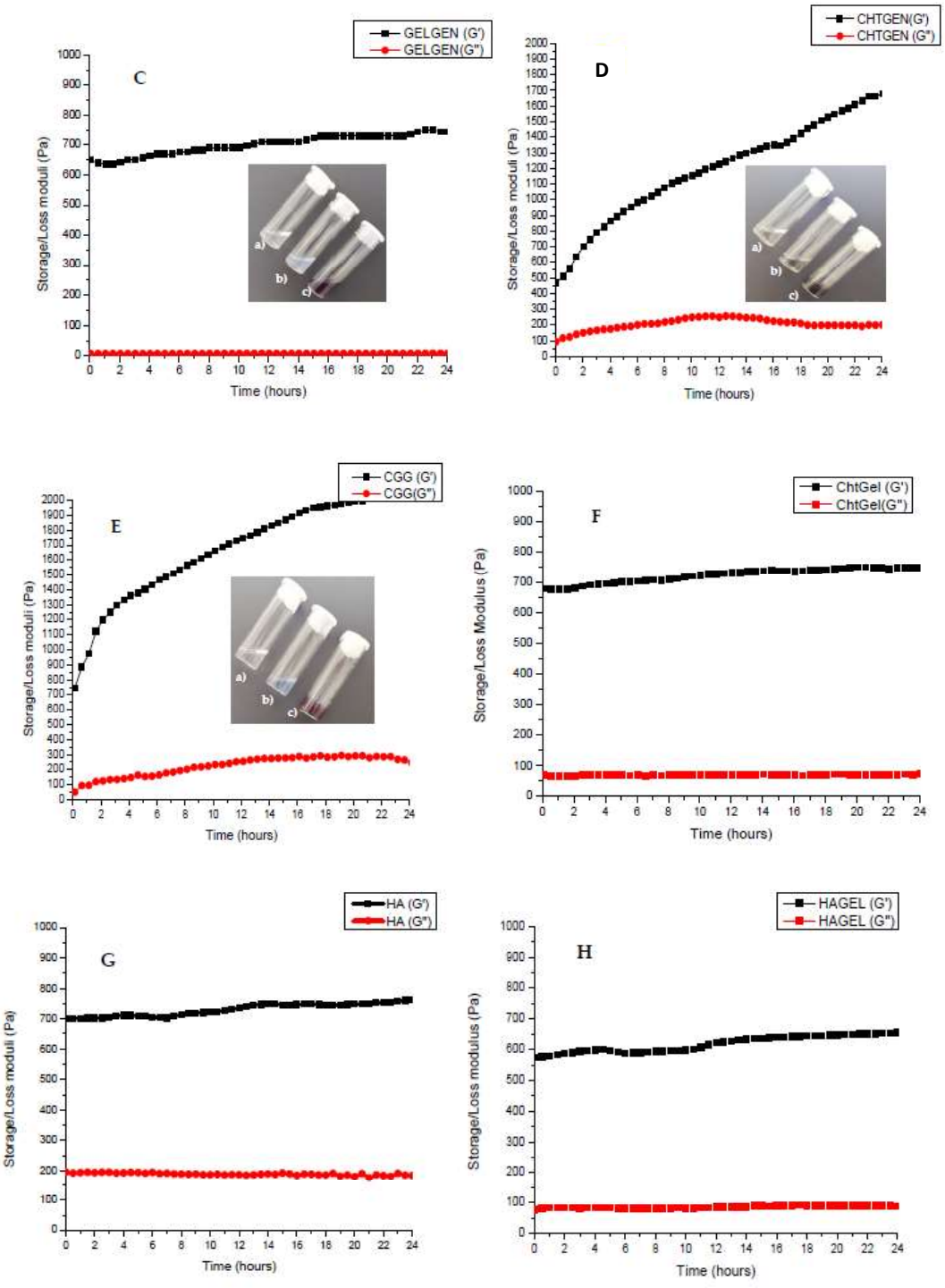
It has been observed that neurons are more prone to thive when the elastic modulus of a hydrogel is similar to the soft ECM of the brain whereas astrocytes behave better on stiff substrates (Madhusudanan *et al.*, 2020). Softer hydrogels induce increased neuronal sprouting as compared to harder hydrogels. Axonal tips also advance faster on softer hydrogels and appear to retreat from harder areas on a scaffold. Therefore, the elastic modulus required for optimal neuronal growth is <1kPa (Georges *et al.*, 2006).

The rheological behaviour of each polymer and their crosslinked composites were studied over a period of 24 h. Viscoelastic studies of all polymeric composites showed a G'>G'' which indicated a more solid viscoelastic behaviour. The storage modulus of chitosan had plateaued at 626.2 Pa while the storage modulus of gelatin had plateaued at 593 .8Pa (Figure 3.5A, B). This is expected as chitosan is known to exhibit a greater storage modulus than gelatin at a concentration of 2% w/v. Crosslinking of gelatin with genipin resulted in an increased storage modulus of 743.33Pa indicating the formation of amide bonds and greater viscoelastic behaviour (Figure 3.5C). Crosslinking of chitosan with genipin showed the same effect, with the storage modulus rising to 1678.0 Pa from 465.2 Pa (Figure 3.5D). The polyelectrolyte complex showed a final G' of 735 Pa. This is greater than the storage modulus of the pristine polymers, thus indicating a strong electrostatic interaction. The CHTGELGEN IPN showed the largest storage modulus of 2030.6 Pa due to the formation of amide bonds between the carboxyl group of gelatin and the amino group of chitosan. The final storage modulus of the IPN can be attributed more to the crosslinking of chitosan with genipin resulting in a rigid structural support (Figure 3.5E, F). The crosslinking of chitosan with genipin occurs at a faster rate than the crosslinking of gelatin which can be deduced from the slope of the graph.

The rheological profile HAGEL network devoid of crosslinker, shows an initial storage modulus of 574.2Pa, less than that of HA due to the incorporation of gelatin at a low concentration and a final storage modulus of 654 Pa (Figure 3.5G, H). The rheological profile of pristine HA plateaued at 761.67. The water content in the network was increased by combining two aqueous polymers. Both polymers are anionic in nature, therefore, electrostatic interactions are not favourable, thus the incorporation of gelatin weakened the network. The rheological curve of the HAGG gel followed the same trend as the full-IPN curve, however, the inclusion

of HA resulted in a larger G' after 24 h. The initial G' was found to be 526 Pa, and the final G' was 1868.47 Pa (Figure 3.5l). All of the rheological profiles indicate that crosslinking with genipin, is a timely process and the inclusion of genipin increases the mechanical rigidity of the hydrogels. It can be seen that the effects of crosslinking in each hydrogel can clearly be seen after 4 h. Temperature is also an important factor to consider in crosslinking with genipin, as the reaction proceeds at a faster rate at 40 °C than at room temperature (±25 °C). All of the resulting hydrogels were blue in colour which was macroscopic confirmation that crosslinking had taken place.




C
GELGEN (G')
GELGEN(G")
Storage/Loss moduli (Pa)
Time (hours)
a)
b)
c)
D
CHTGEN(G')
CHTGEN (G")
Storage/Loss moduli (Pa)
Time (hours)
E
CGG (G')
CGG(G")
Storage/Loss moduli (Pa)
Time (hours)
F
ChtGel (G')
ChtGel(G")
Storage/Loss Modulus (Pa)
Time (hours)
G
HA (G')
HA (G")
Storage/Loss moduli (Pa)
Time (hours)
H
HAGEL (G')
HAGEL (G")
Storage/Loss modulus (Pa)
Time (hours)

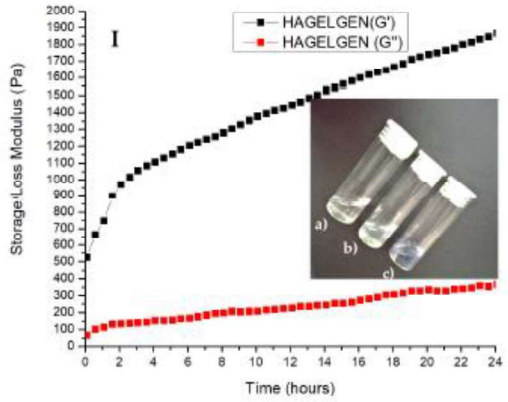


Figure 3.5. Storage (G') and loss (G'') modulus of: A) Chitosan, B) Gelatin, C) GELGEN, D) CHTGEN, E) CHTGELG, F) CHTGEN, G) HA, H) HAGEL, I) HAGELGEN evaluated over 24 hours Photographs alongside each graph show the tilt-bottle test results of each hydrogel at different times of crosslinking: a)0 h, b)12 h and c)24 h.

3.3.3 XRD analysis of amorphous proteosaccharide scaffolds

Gelatin and chitosan are both amorphous biopolymers as shown by the absence of sharp crystalline peaks and peaks of low intensity (Figure 3.6 A, B). Gelatin typically possesses two peaks at 2θ=20° and 2θ=8. The latter is related to the triple helix content of gelatin. Peaks at 2θ=10° and 2θ=20° are typical fingerprints of chitosan powder. When chitosan and gelatin are combined, the peak at 2θ=8° become flatter, thus indicating that the incorporation of chitosan results in a decreased crystallinity of gelatin (Figure 3.6 C). This can be attributed to hydrogen bonding between the two biopolymers which hinders the triple helix formation of gelatin. When chitosan was crosslinked with genipin, depression of the chitosan peak occurred at 2θ=20° as genipin reduced the crystallinity of chitosan resulting in an amorphous network (Figure 3.6 D). When gelatin was crosslinked with genipin, gelatin retained its peak at 2θ=8° with the peak found at 2θ=25° decreasing in intensity and becoming broader (Figure 3.6 E). The diffractogram of the IPN formed, is amorphous in nature and shows a similar pattern to the CHTGEL scaffold, however the formation of intermolecular crosslinks with genipin resulted in a decrease in crystallinity.

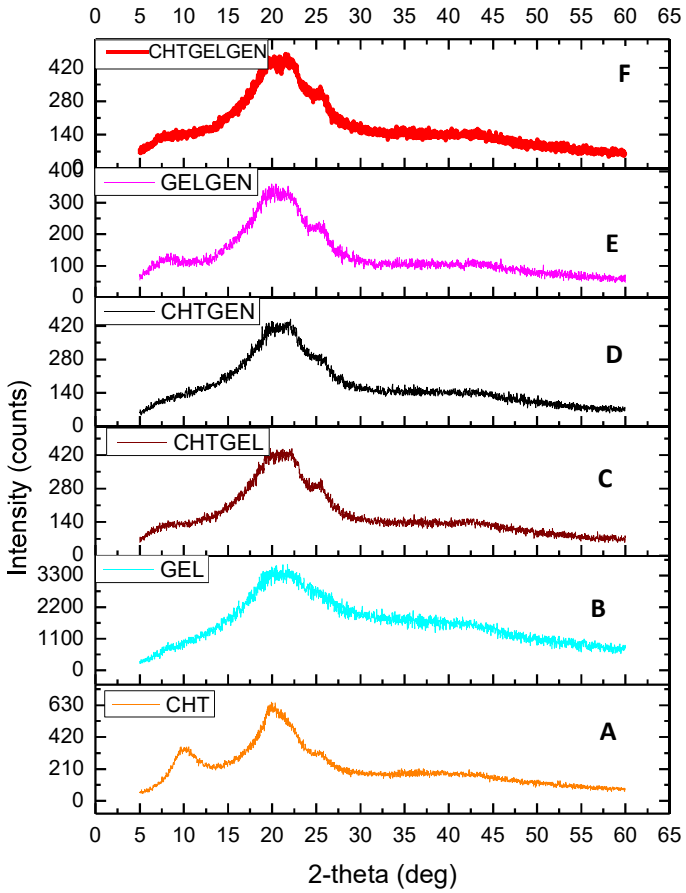


Figure 3.6. X-ray diffractograms showing the amorphous character of: A) Chitosan, B) Gelatin, C) CHTGEL, D) CHTGEN, E) GELGEN, F) CHTGELGEN scaffolds

The XRD of HA shows two peaks, at 2θ=20° and a flatter peak at 2θ=24° (Figure 3.7A). When gelatin is combined with HA, the same two peaks can be found indicating that the polymers are miscible and show increased crystallinity due to gelatin incorporation (Figure 3.7C). The latter peak is flattened when the semi-IPN is formed upon crosslinking with genipin (Figure 3.7D). Thus, the semi-IPN shows a lower crystallinity index than the uncrosslinked network, however, crystallinity is enhanced by incorporating gelatin alone. Crosslinking introduces a defect in the crystalline structure of polymers and thus crosslinking results in a reduced crystallinity. The increased density of crosslinking results in a slower crystallization process and a reduction in the final crystallinity of the networks and rejection of crosslinks into the amorphous phase.

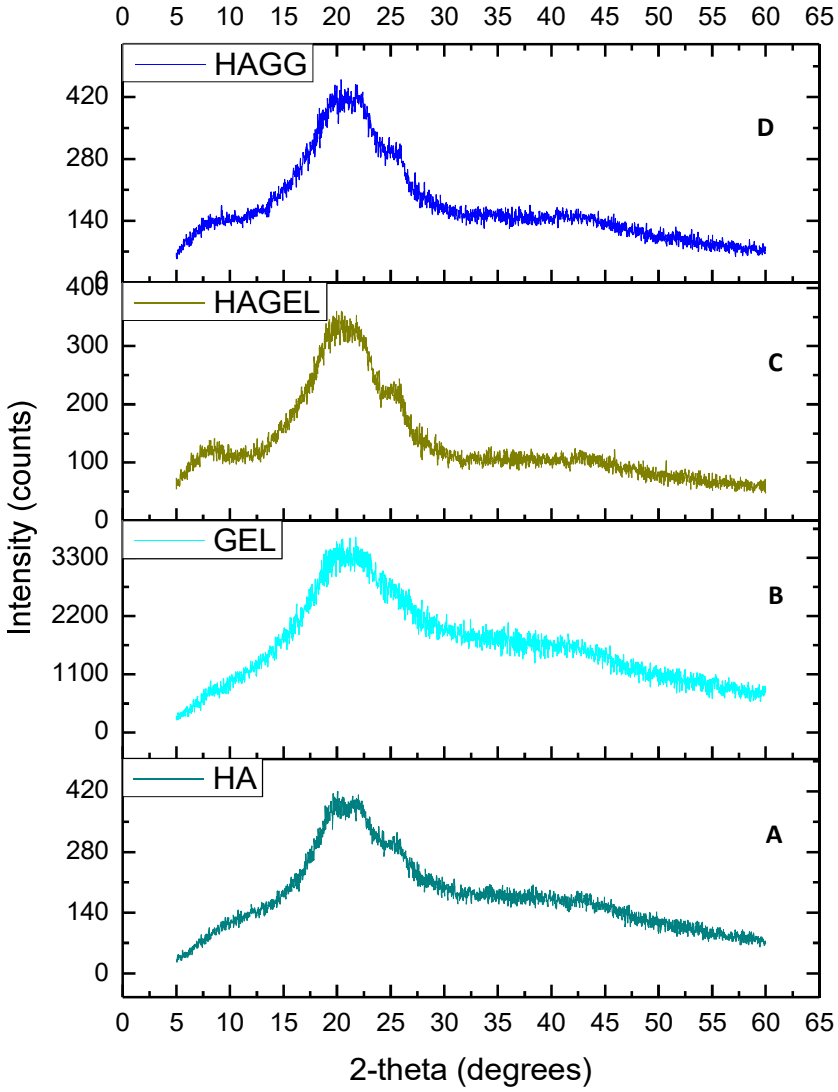


Figure 3.7. X-ray diffractograms showing the amorphous character of A) Hyaluronic acid, B) Gelatin, C) HAGEL, D) HAGELGEN scaffolds

It can therefore be concluded that both the full IPN and semi-IPN were amorphous and crosslinking with genipin resulted in an increase in the amorphousness of the networks despite the addition of gelatin, which should have resulted in increased crystallinity. The crystallinity index of each scaffold was calculated and has been shown in table 3.2.

Table 3.2. Crystallinity index of each scaffold calculated from XRD using equation 3.1.

Scaffold	Ci	Scaffold	Ci
Chitosan	0.61821 ±0.0599	Hyaluronic acid	0.43432 ±0.0152
Gelatin	0.51431 ±0.0212	Hyaluronic acid-Gelatin	0.51289 ±0.0178
Chitosan-Gelatin	0.62533 ±0.0374	Hyaluronic acid Gelatin-Genipin	0.49226 ±0.0210
Chitosan-Genipin	0.46459 ±0.0165	Chitosan-Gelatin-Genipin	0.50380 ±0.0410
Gelatin-Genipin	0.52687 ±0.0138		

3.3.4 DSC analysis of lyophilised proteosaccharide scaffolds

The DSC thermogram of gelatin shows thee endothermic peaks at 95.04 °C, 226.07 °C, and 280.54°C. the endothermic peak found at 95.04 °C can be attributed to the denaturation of gelatin i.e., the helix-coil transition of gelatin (Figure 3.8A). The DSC thermogram of pristine chitosan shows a broad endothermic peak at 99.20 °C which can be attributed to the loss of water from the sample which is a non-equilibrium process, and a second thermal event showed by a broad exothermic peak which can be found at 291.80 °C attributed to the decomposition of glucosamine units in chitosan. (Figure 3.8B). All polymers showed a single endothermic peak between 0-125 °C, corresponding to the release of molecular water. When chitosan is crosslinked with genipin, the endothermic peak shifts to 98.31 °C and the exothermic peak shifts to 290.26 °C. Crosslinking results in an increase in thermal stability, however other researchers agree that the incorporation of genipin leads to an increase in hydrophilicity of the network and therefore results in a lower decomposition temperature due to a lower degree of crosslinking (Figure 3.8C). When gelatin was crosslinked with genipin, each endothermic peak shifted to higher values i.e., 86.71 °C, 228.41 °C, and 283.19 °C. This can be explained by the reaction of gelatin with genipin, wherein an amide linkage is formed (Figure 3.8D). The full IPN showed a broad endothermic peak at 87.93 °C and an exothermic peak at 293.03°C which suggests greater thermal stability than the proteosaccharide blend as more energy was required to break the bonds formed due to covalent crosslinking. This, therefore, confirms the formation of a full IPN (Figure 3.8E). The CHT-GEL blend showed a broad endothermic peak at 85.15 °C which can be said to be an intermediate of the Tg of the pristine polymers with a similar peak width to the pristine polymers, thus indicating a single-phase behaviour of the composite and an exothermic peak at 262.47 °C (Figure 3.8F).

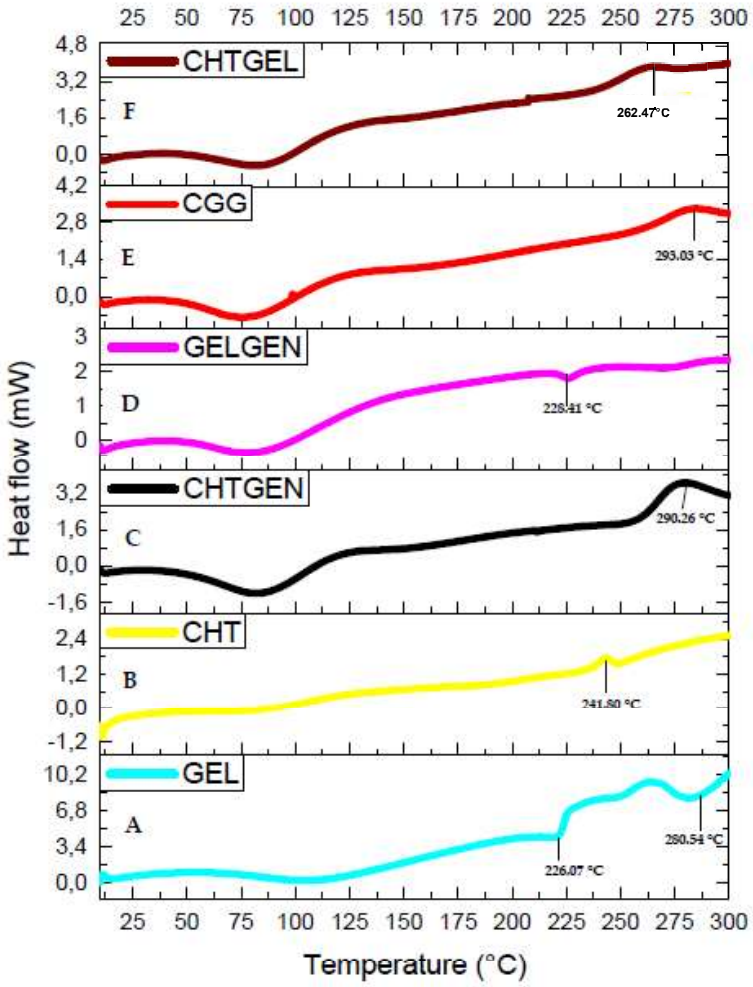


Figure 3.8. DSC thermograms of A) GEL, B) CHT, C) CHTGEN, D) GELGEN, E) CGG and F) CHTGEL scaffolds over the range 10 °C to 300 °C

The thermogram of HA shows two peaks, an endothermic peak at 80.13 °C corresponding to dehydration of HA and an exothermic peak at 275.17 °C corresponding to the decomposition of the glycosidic bonds between glucosamine and glucuronic acid residues (Figure 3.9A). The incorporation of gelatin results in an increase in hydrophilicity of the network and a lower decomposition temperature of 236.92 °C (Figure 3.9C). The semi-IPN is more thermally stable than the HAGEL blend and exhibits a higher decomposition temperature at 240.54 °C due to the formation of amide bonds in gelatin after reacting with genipin (Figure 3.9D). Therefore, it can be concluded that the combination of the two hydrophilic polymers, results in lower thermal stability, which is slightly improved by crosslinking one of the polymers, that being gelatin in

this study. Thermal stability would be significantly improved by modifying HA, using thiolation or methacrylation (Snyder *et al.*, 2014; Rodrigues *et al.*, 2021)

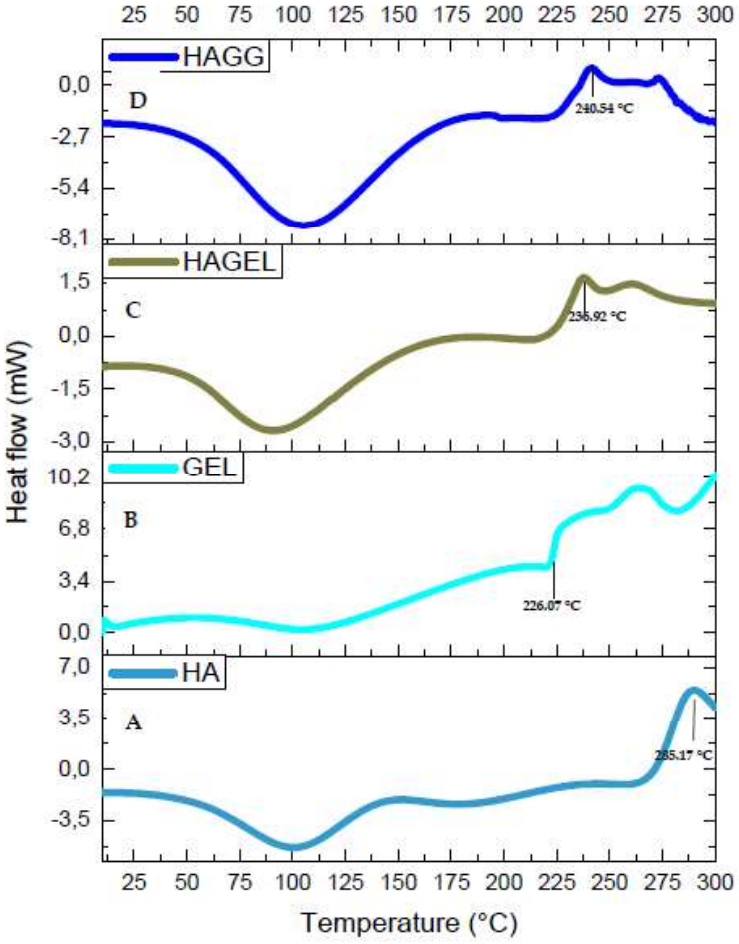


Figure 3.9. DSC thermograms of A) GEL, B) CHT, C) CHTGEN, D) GELGEN, E) CGG and F) CHTGEL scaffolds over the temperature range, 10 °C to 300 °C

3.3.5 Swelling potential of proteosaccharide scaffolds

Hydrogel scaffolds are preferred due to their ability to swell and retain water. Many factors such as crosslinking density, crystallinity and porosity influence the swelling of a hydrogel scaffold. This has implications on degradation and permeability. Swelling enhances biomimicry in the context of the CNS due to the increased mobility of metabolites and nutrients in the scaffold. The brain is composed of ~80% of water, therefore the scaffold must be able to swell and retain its architectural morphology, instead of dissolving in the fluid rich environment. Gelatin and HA undergo dissolution in the absence of a crosslinker. Chitosan undergoes a certain level of swelling in the absence of genipin, before undergoing dissolution due to the greater mechanical strength of the polymer which supports the reason for its

employment in this study. Swelling is inversely proportional to the degree of crosslinking, which explains why crosslinked networks swell less than their uncrosslinked counterparts The swelling ratio of CHTGEN is increased by the incorporation of genipin, due to Chitosan alone containing hydrophobic residues and genipin increasing the hydrophilicity of the network. The full IPN showed a higher swelling ratio than GELGEN, but a lower swelling ratio than CHTGEL and CHTGEN, thus proving the effects of crosslinking. The HAGEL network dissolved in less than 1 hour, while the HAGG network showed a swelling ratio of 8.31, which is close to that of GELGEN, indicating that the semi-IPN was able to retain its architecture, instead of dissolving due to the crosslinking of the gelatin component. High swelling ratios of scaffolds can lead to tissue compression and subsequent damage; therefore, crosslinking was employed to reduce the swelling ratio and to increase the mechanical strength of the scaffold (Figure 3.10).

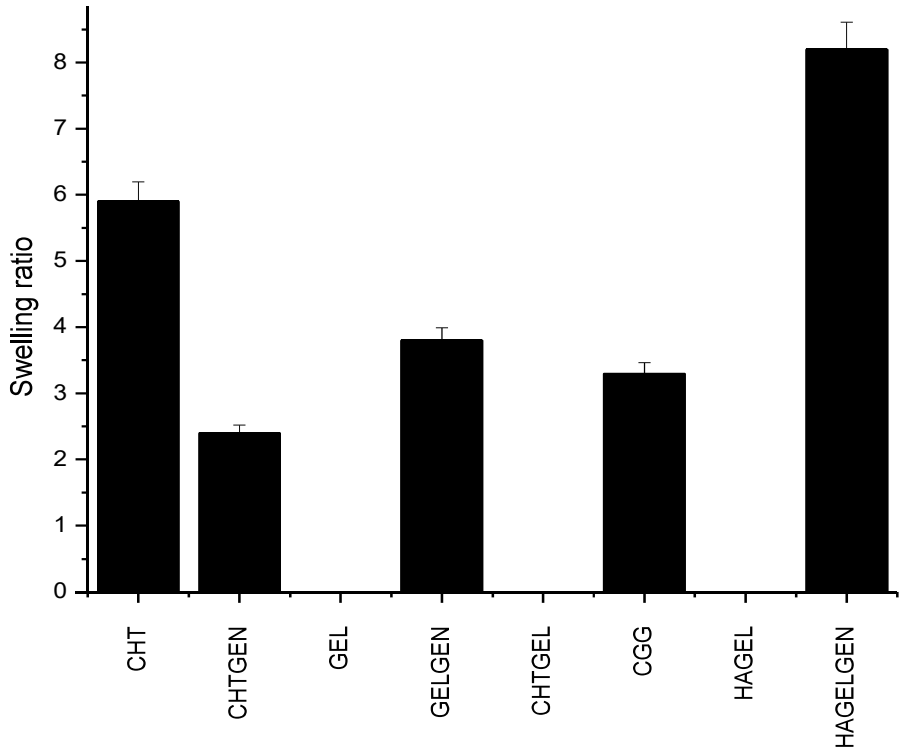


Figure 3.10. Swelling potential of each scaffold after immersion in PBS (n=3) (SD<4)

3.3.6 Morphological analysis of proteosaccharide scaffolds

Transverse cross-sections of each hydrogel scaffold were used to calculate the average diameter of each pore and porosity as shown in table 3.3. The SEM micrograph of CHTGEN showed a micro-porous structure with well-defined and carefully delineated pores. The pores

were geometrically round with an average diameter of the pores being 148.920μm±6.335 (Figure 3.11 A). The SEM micrograph of GELGEN revealed very thin walls with weakly interconnected pores. This can be attributed to the low concentration of gelatin used in this study, therefore resulting in low mechanical integrity (Figure 3.11 B). The average pore size was calculated to be 65.298±9.936μm, which was much smaller than the CHTGEN scaffold. The CHTGELGEN network showed a tissue-paper like structure but showed better defined pore walls, which was sourced from CHTGEN crosslinking, with an average pore size of 72.789±16.85μm. Pores were more closely packed, with smaller pore diameters and thicker walls than the GELGEN scaffold (Figure 3.11 C). The HAGELGEN scaffold showed a microporous structure, which was difficult to observe on a transverse cross-section due to the linear arrangement of hyaluronic acid fibres. The average diameter of the pores was calculated at 84.289±7.65μm, which is smaller than that of the uncrosslinked blend (Figure 3.11 D, E). The presence of pores is imperative to the architecture of the scaffold. Both scaffolds showed the presence of multiple pores. The porosity was calculated using the SEM images and the CGG scaffold was less porous (71.335%) than the GELGEN scaffold (76.985%) but was more porous than the CHTGEN scaffold (52.791%). The HAGELGEN scaffold showed a porosity of 73.614%. A porous scaffold is crucial for the diffusion of oxygen and nutrients in the scaffold. The CHTGEN scaffold was the least porous due to the higher crosslinking density of the scaffold. Genipin was able to crosslink chitosan to a greater effect than it was able to crosslink gelatin. The GELGEN scaffold showed a high porosity due to the low concentration of gelatin employed, as well as the low crosslinking density. The HAGELGEN scaffold also showed a high porosity due to the network being largely hydrophilic, and the freeze-drying process resulting in the removal of molecular water. Other researchers have used scaffolds with an 85% porosity for neural tissue engineering. Both the IPN and semi-IPN showed comparable porosities and would be compatible for the migration of cells in vitro while maintaining their structural integrity.

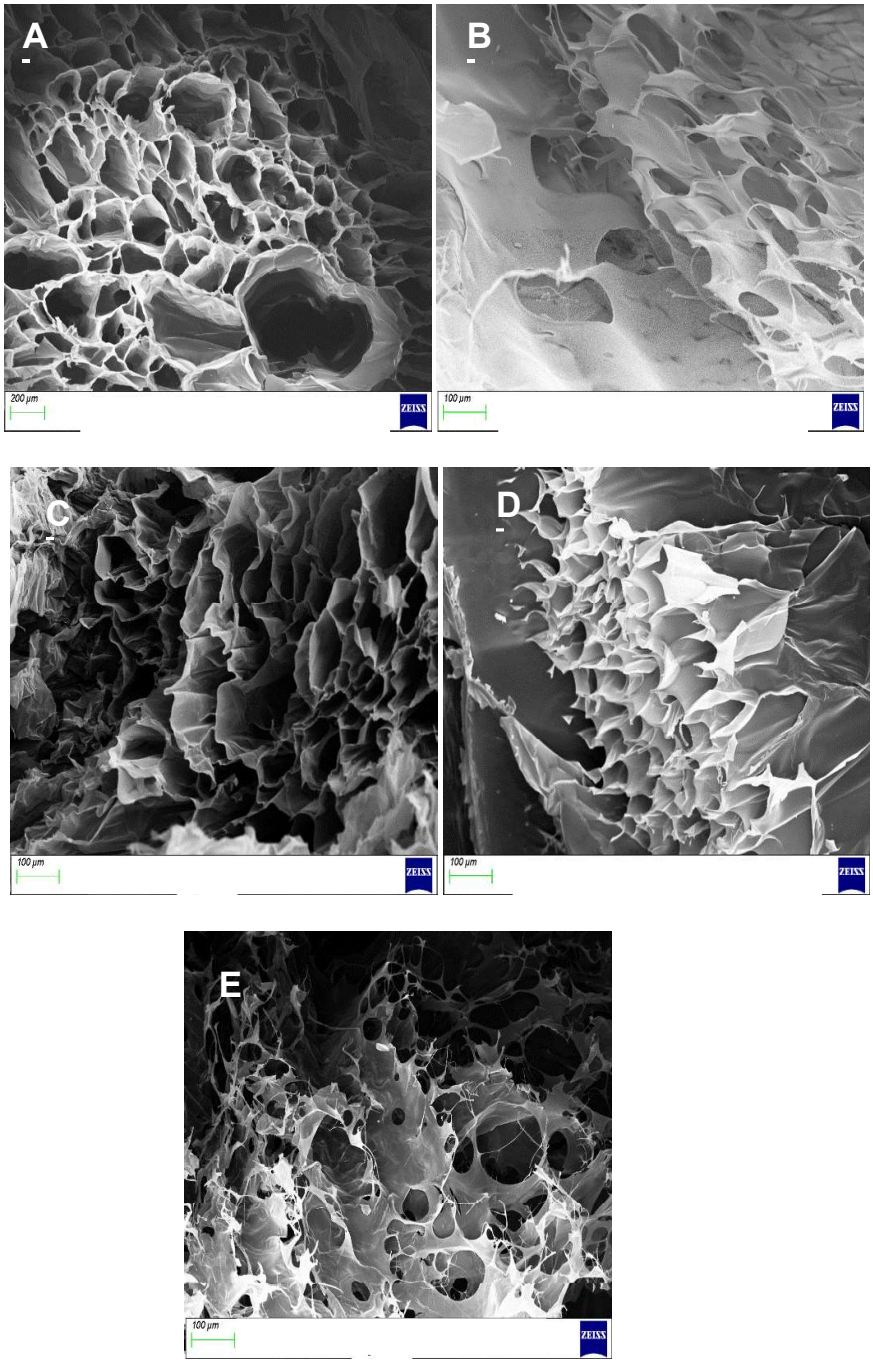


Figure 3.11. SEM micrographs obtained of transverse cross-sections of a) CHTGEN, b) GELGEN, C) CHTGELGEN, d) HAGEL, e) HAGELGEN scaffolds

Table 3.3. Average pore diameter and porosity of each scaffold (n=6)

Scaffold	Average Pore diameter (µm)	Porosity (%)	Scaffold	Average Pore diameter (µm)	Porosity (%)
CHTGEN	148.920 µm±6.335µm	52.791%	**HAGEL**	107.54 µm±13.52µm	73.614%
GELGEN	65.298µm ±9.936µm	76.985%	**HAGELGEN**	84.289 µm±7.658µm	46.257%
CHTGELGEN	72.789 µm±16.85µm	71.335%			

3.3.7 Bulk Density of proteosaccharide scaffolds

Density has a direct implication on the swelling potential and can be directly related to the crosslinking density of the polymeric networks. The semi-IPN was surprisingly the densest network. This could be due to the high molecular weight of HA which resulted in a heavier scaffold, as compared to the full-IPN. The full IPN was denser than the CHTGEN and GELGEN scaffolds, therefore proving that crosslinking of both polymers results in a dense hybrid scaffold, which swells less and should be more resistant to degradation. There were more amide bonds formed in the full IPN encompassing both chitosan and gelatin.

Table 3.4: Calculated density of each scaffold (n=3)

Combination	Density (mg/mm^3)	Combination	Density (mg/mm^3)
CHT	0.048±0.002	CHTGEN	0.1345±0.037
GEL	0.0323±0.016	GELGEN	0.0572±0.028
HA	0.0457±0.021	HAGELGEN	0.1967±0.059
CHTGEL	0.0573±0.013	CHTGELGEN	0.1476±0.065
HAGEL	0.0276±0.008		

3.3.8 *In vitro* degradation of proteosaccharide scafffolds

A scaffold must be mechanically robust and degrade constantly into non-toxic by products. Biodegradability prevents the unnecessary process of removal of the scaffold which could cause secondary injury. Surface erosion is favoured over bulk erosion to allow the scaffold to maintain its stable architecture and not collapse in *vivo.* Ideally, a scaffold should degrade at a rate that matches that of neogeneration (Mahumane *et al.*, 2018).

A scaffold that degrades too rapidly results in the accumulation of degradation components, resulting in a hypertonic and stressful environment for cells. Furthermore, cells are not given enough time to establish a niche within the scaffold to drive neural regeneration. The hydrophilicity and hydrophobicity of the system are also pertinent to its degradation behaviour. A largely hydrophilic system will absorb more water and undergo rapid bulk degradation; therefore, polymer ratios must be carefully selected. The gelatin-genipin scaffold degraded too rapidly, with greater than 78% of its weight lost on day 3 only. This can be explained by the hydrophilic nature of gelatin and the low degree of crosslinking. For this reason, gelatin needed to be combined with other components i.e., chitosan and HA. The semi-IPN showed a faster degradation rate than the full-IPN. This is due to the presence of HA which is a hydrophilic polymer. HA encouraged swelling and subsequent degradation; however, the scaffold was able to retain its shape for the full 28 days. The full IPN showed a slower degradation rate, with only 47% degraded at day 28. This was due to the formation of amide bonds between the amine of chitosan and the carboxyl group of gelatin. This led to greater stability and resistance to enzymatic degradation (Figure 3.12). The degradation behaviour can be further tuned by adjusting the ratio of polysaccharide to gelatin, which would greatly improve the rigidity of the scaffold, however careful consideration must be given to the mechanical strain that a hard scaffold can exert on neural tissue which could lead to secondary damage. Furthermore, the use of more crosslinkers can prove to be toxic to cells. SEM images in figure 3.13 show the morphology of the degraded IPN and semi-IPN after 30 days. As can be seen, the pore walls appear to be thinner and more fragile. Pores are distended and there is no distinct circular morphology of pores. The CGG network shows the presence of a few rounded pores, ranging from 43.73μm to 61.76μm, which were still densely packed while the semi-IPN shows the presence of oval shaped pores ranging 18.36μm to 26.74μm. These images show that the scaffold's architecture was still maintained over 30 days and did not collapse.

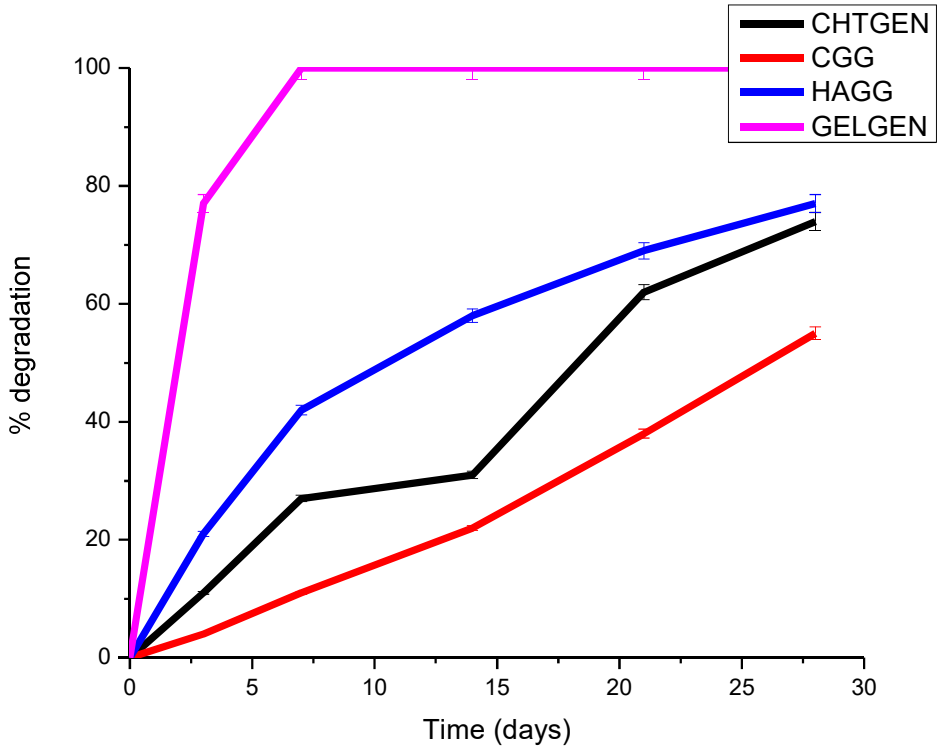


Figure 3.12. Graph depicting the degradation behaviour of each scaffold over 30 days in PBS (n=3)

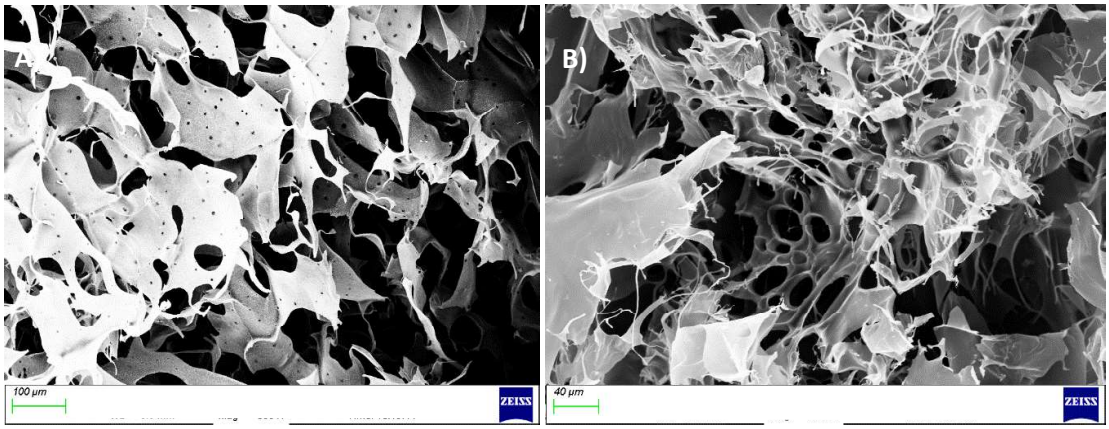


Figure 3.13. SEM images of the full-IPN (A) and semi- IPN at day 30 following degradation

3.3.9 Drug release of Dexamethasone-21-Phosphate from the IPN and semi-IPN hydrogel scaffolds

Dexamethasone-21-phosphate is a synthetic glucocorticoid steroid with anti-inflammatory activity. DEX can therefore play an important role in TBI'S, due to its ability to bind to astrocyte

glucocorticoid receptors and prevent the proliferation of astrocytes (Sirivisoot *et al.*, 2011). Furthermore, DEX can lower the production of cytokines such as IL-1β, INF-γ, and TNF-α (Sirivisoot *et al.*, 2011). The use of other corticosteroids such as high dose methylprednisolone is not permitted for use in patients with TBI's to improve their therapeutic outcomes according to the Brain Trauma Foundation, however a study conducted by Moll et al. showed the beneficial effect of DEX in patients with brain contusions (Moll *et al.*, 2020). Another double-blinded study showed that DEX administered in high doses reduced mortality and improved neurological outcomes in patients with head injuries (Faupel *et al.*, 1979). Therefore, the release of DEX from hydrogel scaffolds was tested. A calibration curve was constructed, using concentrations ranging from 5µg/mL to 25µg/ mL and the linear regression coefficient (R^2) was determined to be 0.998. The equation of the graph was used to calculate the concentration of drug released at each interval (Figure 3.14).

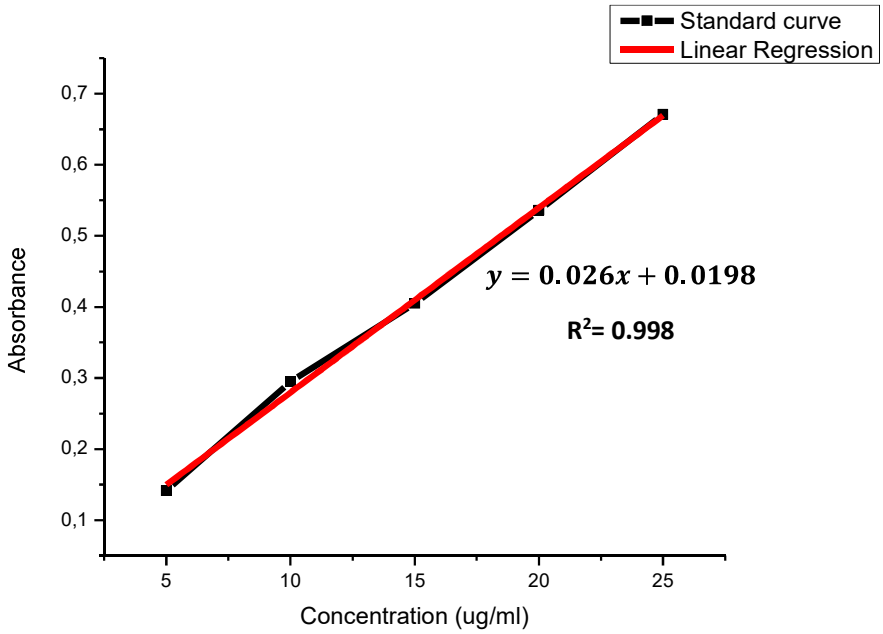


Figure 3.14. Calibration curve constructed for Dexamethasone-21-Phosphate by varying the concentration of the drug in PBS (R^2=0.998)

Dex-21-Phosphate is a highly soluble phosphate salt of DEX, a systemic glucocorticoid. Due to its high-water solubility, the delivery system needs to be densely crosslinked to prolong its release. From the drug release profiles, the semi-IPN does not support the sustained release of DEX-21-Phosphate, due to the low crosslinking density of gelatin by genipin, and the low concentration of gelatin used, which does not allow for the formation of a strong hydrogel

network. A burst release of DEX-21-phosphate was seen in both the IPN and semi-IPN, however the semi-IPN showed a 100% release in 6 h.

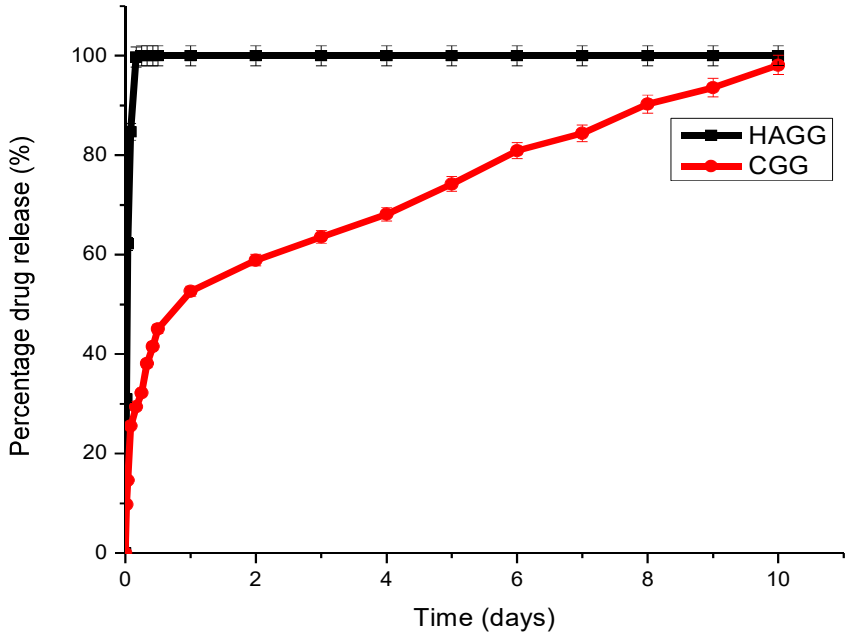


Figure 3.15. Drug release behaviour of Dexamethasone-21-Phosphate from the IPN and semi-IPN in PBS at 37°C (n=3)

Under clinical circumstances, the fast release of DEX-21-phosphate could be beneficial in reducing local inflammation post traumatic brain injury and in the prevention of inflammatory cells such as astrocytes and macrophages, thus preventing glial scar formation The full IPN showed two phases of drug release. A burst release was seen in the first 24 h with 52.61% of the drug being released. A second phase observed from day 2 to day 7 was due to the decay of the polymeric matrix and the release of entrapped drug according to linear kinetics. This would be beneficial in the clinical setting by preventing local oedema surrounding the lesion and allowing the scaffold to swell and serve as a surrogate for tissue repair. Burst releases occur due to drug molecules that are trapped on the surface of the scaffold being released and the sustained release can be attributed to drug molecules entrapped within the core of the matrix. Drug release kinetics can be interpreted according to different mathematical models. The release of DEX from the CGG scaffold showed a linear pattern post the burst release in the first 24 h. This linear pattern is characteristic of zero-order kinetics, where drug

release is time dependent. The half-life ($t_{1/2}$) of DEX in the full IPN was 23 h, while the half-life in the semi-IPN was calculated to be 1.3 h.

3.4 Concluding remarks

The IPN and semi-IPN characterised in this chapter showed promise for neural tissue regenerative applications as well as for drug delivery of a corticosteroid. An increase in the concentration of gelatin would result in a stronger hydrogel and would further prolong the release of the drug *in vivo.* The hydrogel scaffolds showed a porous structure with rounded morphology and high porosity. The hydrogels also displayed time-dependent crosslinking behaviour and shear thinning behaviour which supports its use for neural regeneration. Temperature ramps were also conducted which justified the temperature used for crosslinking and can be found in the appendices. NMR results can also be found in the appendices which demonstrate that crosslinking had occurred largely on the lysine residues of gelatin and carbonyl group of chitosan. *In vitro* cell viability and migration assays can be found in chapter 5.

REFERENCES

Burdick, J.A. & Prestwich, G.D. 2011. Hyaluronic acid hydrogels for biomedical applications. Advanced Materials (Deerfield Beach, Fla.). 23(12):H41.

Brännvall, K., Bergman, K., Wallenquist, U., Svahn, S., Bowden, T., Hilborn, J., & Forsberg-Nilsson, K. 2007. Enhanced neuronal differentiation in a thee-dimensional collagen-hyaluronan matrix. Journal of neuroscience research. 85(10):2138–2146.

Chandy, T., & Sharma, C. P. 1990. Chitosan--as a biomaterial. Biomaterials, Artificial Cells, and Artificial Organs. 18(1):1–24.

Chedly, J., Soares, S., Montembault, A., von Boxberg, Y., Veron-Ravaille, M., Mouffle, C., Benassy, M. N., Taxi, J., David, L., & Nothias, F. 2017. Physical chitosan microhydrogels as scaffolds for spinal cord injury restoration and axon regeneration. Biomaterials. 138:91–107.

England, S., Rajaram, A., Scheyer, D.J. & Chen, X. 2017. Bioprinted fibrin-factor XIII-hyaluronate hydrogel scaffolds with encapsulated Schwann cells and their in vitro characterization for use in nerve regeneration. Bioprinting. 5:1–9.

Faupel, G., Reulen, H.J., Müller, D. & Schürmann, K. 1979. Dexamethasone in severe head injuries. Neurosurgical Review 1978 2:3. 2(3):105–111.

Frohbergh, M. E., Katsman, A., Botta, G. P., Lazarovici, P., Schauer, C. L., Wegst, U. G., & Lelkes, P. I. 2012. Electrospun hydroxyapatite-containing chitosan nanofibers crosslinked with genipin for bone tissue engineering. Biomaterials. 33(36):9167–9178.

Georges, P.C., Miller, W.J., Meaney, D.F., Sawyer, E.S. & Janmey, P.A. 2006. Matrices with Compliance Comparable to that of Brain Tissue Select Neuronal Over Glial Growth in Mixed Cortical Cultures. Biophysical Journal. 90(8):3012–3018.

Georgopoulou, A., Papadogiannis, F., Batsali, A., Marakis, J., Alpantaki, K., … Chatzinikolaidou, M. 2018. Chitosan/gelatin scaffolds support bone regeneration. Journal of Materials Science: Materials in Medicine. 29(5):1–13.

Guo, Y., Yuan, T., Xiao, Z., Tang, P., Xiao, Y., … Zhang, X. 2012. Hydrogels of collagen/chondroitin sulfate/hyaluronan interpenetrating polymer network for cartilage tissue engineering. Journal of Materials Science: Materials in Medicine. 23(9):2267–2279.

Khaing, Z. Z., Milman, B. D., Vanscoy, J. E., Seidlits, S. K., Grill, R. J., & Schmidt, C. E. 2011. High molecular weight hyaluronic acid limits astrocyte activation and scar formation after spinal cord injury. Journal of Neural Engineering. 8(4).

Kim, T.-H., Yoon, S.-J. & Lee, S.-M. 2012. Genipin Attenuates Sepsis by Inhibiting Toll-Like Receptor Signaling. Molecular Medicine 2012 18:3. 18(3):455–465.

Levenberg, S. & Langer, R. 2004. Advances in Tissue Engineering. Current Topics in Developmental Biology. 61:113–134.

Liu, Y., An, M., Wang, L. & Qiu, H. 2014. Preparation and characterization of chitosan-gelatin/glutaraldehyde scaffolds. Journal of Macromolecular Science, Part B: Physics. 53(2):309–325.

Madhusudanan, P., Raju, G. & Shankarappa, S. 2020. Hydrogel systems and their role in neural tissue engineering. Journal of the Royal Society, Interface, 17(162),

Maitra, J. & Shukla, V.K. 2014. Cross-linking in Hydrogels - A Review. American Journal of Polymer Science. 4(2):25–31.

Mo, L., Yang, Z., Zhang, A., & Li, X. 2010. The repair of the injured adult rat hippocampus with NT-3-chitosan carriers. Biomaterials. 31(8):2184–2192.

Mohite, B. V & Patil, S. V. 2014. A novel biomaterial: bacterial cellulose and its new era applications. Biotechnology and Applied Biochemistry. 61(2):101–10.

Moll, A., Lara, M., Pomar, J., Orozco, M., Frontera, G., … Pérez-Bárcena, J. 2020. Effects of dexamethasone in traumatic brain injury patients with pericontusional vasogenic edema: A prospective-observational DTI-MRI study. Medicine. 99(43): e22879.

Oryan, A., Kamali, A., Moshiri, A., Baharvand, H. & Daemi, H. 2018. Chemical crosslinking of biopolymeric scaffolds: Current knowledge and future directions of crosslinked engineered bone scaffolds. International Journal of Biological Macromolecules, 107(Pt A), 678–688.

Rayahin, J. E., Buhman, J. S., Zhang, Y., Koh, T. J., & Gemeinhart, R. A. 2015. High and low molecular weight hyaluronic acid differentially influence macrophage activation. ACS Biomaterials Science & Engineering. 1(7):481–493.

Re, F., Sartore, L., Moulisova, V., Cantini, M., Almici, C., … Russo, D. 2019. 3D gelatin-chitosan hybrid hydrogels combined with human platelet lysate highly support human mesenchymal stem cell proliferation and osteogenic differentiation. Journal of Tissue Engineering. 10: 1-16

Roy, J.C., Salaün, F., Giraud, S., Ferri, A., Chen, G. & Guan, J. 2017. Solubility of Chitin: Solvents, Solution Behaviors and Their Related Mechanisms. In: Solubility of Polysaccharides. InTech. 7:109-128

Silva, K. Da, Kumar, P., Vuuren, S.F. van, Pillay, V. & Choonara, Y.E. 2021. Thee-Dimensional Printability of an ECM-Based Gelatin Methacryloyl (GelMA) Biomaterial for Potential Neuroregeneration. ACS Omega. 6 (33), 21368-21383

Sionkowska, A., Wisniewski, M., Skopinska, J., Kennedy, C.J. & Wess, T.J. 2004. Molecular interactions in collagen and chitosan blends. Biomaterials. 25(5):795–801.

Sirivisoot, S., Pareta, R. & Webster, T.J. 2011. Electrically controlled drug release from nanostructured polypyrrole coated on titanium. Nanotechnology. 22(8).

Snyder, T.N., Madhavan, K., Intrator, M., Dregalla, R.C. & Park, D. 2014. A fibrin/hyaluronic acid hydrogel for the delivery of mesenchymal stem cells and potential for articular cartilage repair. Journal of Biological Engineering, 8(27):8-10

Tang, S. & Spector, M. 2007. Incorporation of hyaluronic acid into collagen scaffolds for the control of chondrocyte-mediated contraction and chondrogenesis. Biomedical materials (Bristol, England). 2(3):S135–S141.

Velasco-Rodriguez, B.; Diaz-Vidal, T.; Rosales-Rivera, L.C.; García-González, C.A.; Alvarez-Lorenzo, C.; Al-Modlej, A.; Domínguez-Arca, V.; Prieto, G.; Barbosa, S.; Soltero Martínez, J.F.A.; Taboada, P. 2021. Hybrid methacrylated gelatin and hyaluronic acid hydrogel scaffolds. preparation and systematic characterization for prospective tissue engineering applications. International journal of molecular sciences. 22(13).

Voron'ko, N.G., Derkach, S.R., Kuchina, Y.A. & Sokolan, N.I. 2016. The chitosan-gelatin (bio)polyelectrolyte complexes formation in an acidic medium. Carbohydrate polymers. 138:265–72.

Wolf, K.J. & Kumar, S. 2019. Hyaluronic acid: incorporating the bio into the material. ACS Biomaterials Science & Engineering. 5(8):3753–3765.

Yoo, J. S., Kim, Y. J., Kim, S. H., & Choi, S. H. 2011. Study on genipin: a new alternative natural crosslinking agent for fixing heterograft tissue. The Korean Journal of Thoracic and Cardiovascular Surgery. 44(3):197–207.

CHAPTER 4. IN SITU SELF-ASSEMBLING PROTEOSACCHARIDE SYSTEM FOR NEURAL TISSUE ENGINEERING APPLICATIONS

4.1 Introduction

As discussed in previous chapters, the production of an artificial extracellular matrix is crucial for neural tissue regeneration. Neuronal regeneration is challenging due the slow growth rate, difficulty in differentiation and complexity of the neuronal environment in vivo. The only part of the brain that is capable of regeneration is the subventricular zone and dentate gyrus, therefore regeneration in other areas affected by traumatic brain injuries, as well neuronal degeneration due to Parkinson's and Alzheimer's remains a challenge (Pettikiriarachchi *et al.*, 2010). Various polymers have been explored in this field over the past decades. These can be divided into two groups, based on their origin; natural polymers such as collagen, silk, chitosan and synthetic polymers such as polyglycolic acid, polylactic acid, poly(lactic-co-glycolic acid and polyvinyl alcohol (Chen & Liu, 2016). These polymers can be further optimised to suit their area of employment by chemical modification, crosslinking or the production of co-polymeric blends. Each class has their own drawbacks, such as synthetic polymers lacking bioactivity, and natural polymers varying in structural characteristics due to their origin (Mano *et al.*, 2007). Self-assembling peptides are an interesting class of smart biopolymers which can form highly organised nanoscale structures, which enable greater cellular interactions. The self-assembling phenomena has been employed in regenerative medicine, drug delivery, tissue engineering and the creation of thee-dimensional cell culture substrates. Basic examples of self-assembled structures in the human body, are DNA and RNA which spontaneously aggregate under thermodynamically favourable conditions to form well defined complex gene encoding molecules (Sharma *et al.*, 2018). These molecules are held together by non-covalent forces such as van der waal's, electrostatic, hydrophobic and hydrogen bonds. Self-assembling materials are advantageous due to their ease of design and ability to upscale via solid peptide synthesis (Loo *et al.*, 2015). Their nanofibrous architecture mimics the ECM to a greater extent than other naturally occurring polymers such as collagen, and they undergo degradation into non-toxic amino acids. Additional advantages include their multifunctionality, multivalency and molecular specificity (Kumar *et al.*, 2011).

The specific peptide which will be explored in this research is the commercialised Corning PuraMatrix hydrogel, derived from RADA-16. PuraMatrix is a type I self-assembling peptide, also referred to as molecular lego forming hydrogels due to the complementary ionic bonds with regular repeats on the hydrophilic surface. An important factor to be considered is the pH of the peptide at the site of its employment. These untreated peptides can cause damage to the spinal cord at a low pH of 3-4, and therefore must be slowly brought up to neutrality for

their tissue engineering application (Moradi *et al.*, 2012). At a pH of 4, the peptide loses its helical structure, and a stable solution can only be established at a pH of 5 upwards.

The self-assembling peptide, RADA-16-I (Ac $(RADA)_4CONH_2$) is composed of repeating units of positively charged arginine, hydrophobic alanine and negatively charged aspartic acid residues, thus making it an amphiphilic peptide with a high-water retention capacity of >90%. RADA-16-I undergoes spontaneous self-assembly into a nanofibrous scaffold in response to physiological pH (7.4). In a study undertaken by Ellis-Benhke and co-workers (2006), the optic tract in the midbrain of hamsters was severed resulting in a loss of vision. RADA-16-I promoted the regeneration of axons across the lesion and restoration of vision (Ellis-Behnke *et al.*, 2006). In another study, cyst formation was eliminated by RADA-16-I following injury to the sensory motor cortex of the rat brain. Reduced astrocytic and macrophage infiltration in the lesion area was also observed (Guo *et al.*, 2009).

Scientists have shown successful neuronal outgrowth in RADA-16-I and RADA-16-II scaffolds. These scaffolds were tested in mouse cerebellum and rat hippocampus cells and showed sustained growth for 4 weeks resulting in active synaptic formation(Silva *et al.*, 2004). The addition of SKPPGTSS, -PFSSTKT-, and RGD motifs to RADA-16-I peptides increased the levels of neuronal markers such as β-tubulin and nestin (Cunha *et al.*, 2011; Gelain *et al.*, 2006). RADA-16 employed alone in the form of a hydrogel scaffold was able to reconnect injured rat spinal cord and facilitate axonal regeneration. This further led to the recovery of locomotor function and promoted the reconstruction of acutely injured rat brain (Guo *et al.*, 2009).

In this paper, a co-polymeric network will be synthesised using the PuraMatrix and Chitosan for the purposes of neural tissue regeneration. The combination of PuraMatrix with a polysaccharide could prove to be advantageous in many ways. The incorporation of Puramatrix would add cell-adhesive properties to chitosan which can in return, strengthen the Puramatrix hydrogel. Chitosan is known to precipitate at a pH greater than its pKa (6.5), where the positively charged amino groups of chitosan, will interact ionically with the negatively charged base and cause the long chains of chitosan to wrap around the negatively charged base and result in precipitation. For this reason, this research is focused on the synthesis and characterisation of an *in situ* self-assembling scaffold.

4.2 Materials

Low molecular weight chitosan was purchased from Sigma-Aldrich (MO, USA). PuraMatrix (1%w/v) hydrogel was purchased from BD Biosciences. Dulbecco's Modified Eagles Medium-

high glucose, Roche Cell Proliferation Kit I (MTT), dimethyl sulfoxide (DMSO), and trypsin–EDTA solution were obtained from Sigma Aldrich (Steinheim, Germany). Donor Equine Serum (DES) was purchased from Hyclone (UT, USA). Ethanol (99% absolute) was purchased from LabChem, Johannesburg, South Africa. Fetal Bovine Serum and Ham's F-12 Nutrient Mix (F12) were purchased from (PAN Biotech, Aidenbach, Germany). Rat (Rattus Norvegicus) adrenal gland pheochomocytoma (PC12) cells were purchased from Cellonex (Separations, South Africa). Penicillin/Streptomycin/Amphotericin B (P/S/AB) solution was purchased from Lonza (OR, USA).

4.3 Methods

4.3.1 Synthesis of the CHT-PM scaffold for in situ gelation

Chitosan (2%) was prepared by dissolving 2g in a 0.5M acetic acid solution, PuraMatrix was diluted to a 0.5% concentration using a 20% sucrose solution. The 0.5% v/v solution of PuraMatrix was slowly added to the 2% chitosan solution in thee different ratios namely, 1: 1, 1:3 and 1:5 and allowed to stir overnight. The pH of the solution was measured, and the gels were frozen overnight (-80°C) and lyophilised for a period of 12 h as shown in figure 4.1.

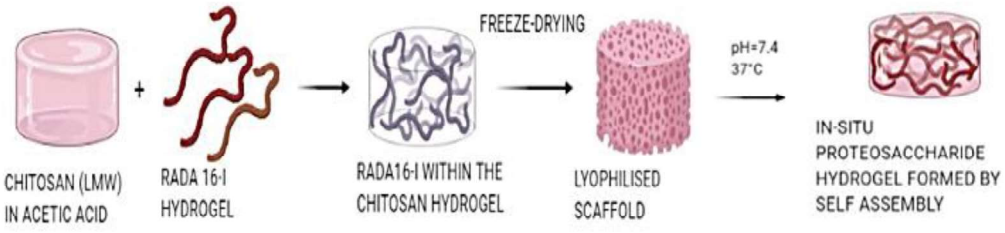


Figure 4.1. Schematic showing the synthesis of the proteosaccharide scaffold

4.3.2 Rheological analysis to determine the thermoresponsive behaviour of the proteosaccharide

To determine the thermoresponsiveness of the system, a temperature sweep was carried out on the PuraMatrix alone and on the proteosaccharide. A volume of 2mL was added to the stage of a Haake Modular Advanced Rheometer System (ThermoFisher Scientific, Germany) and run over a temperature range of 10 °C to 40 °C at a heating rate of 1 °C/min with the use of a C35/1° Titanium rotor, using parallel plate geometry, at a constant strain of 1% and frequency of 6 rad/s. The storage and loss moduli after gelation with PBS was observed in the temperature range of 33 °C to 40 °C.

4.3.3 Preliminary cytotoxicity analysis of different ratios of protein to polysaccharide

An XTT assay was performed to determine the cytotoxicity of different ratios of formulations on rat pheochomocytoma cells isolated from rat adrenal medulla (PC12). The PC12 cells were

cultured to 80% confluence in Ham's F12 growth medium, supplemented with 2.5% Fetal Bovine Serum (FBS), 15% Donor Equine Serum (DES) and 1%(v/v) Penicillin/Streptomycin. The medium was replaced after washing with phosphate-buffered saline (PBS) every second day to remove cellular debris. The cells were incubated overnight, and different ratios of each treatment were added to each well. Post-treatment, further cell incubation was done for 48h at 37 °C. Thereafter, 50 µl of the XTT mixture (0.5 mL electron coupling reagent and 5 mL of XTT reagent) were added to each well and the plates were incubated for 4 h at 37 °C. Absorbances were read on a Victor X3 microplate reader (Perkin Elmer, MA, USA) at 540 nm and 690 nm. The average absorbances were compared to that of the untreated and the positive control (10 µg/ml of 5-fluorouracil (5-FU)). The %cell viability was calculated as follows:

$$\%\ cell\ viability = \frac{Average\ absorbance\ of\ treated\ wells - blank}{Average\ absorbance\ of\ untreated\ wells}\ x\ 100$$

Equation 4.1.

4.3.4 Circular Dichoism (CD) spectrometry of the proteosaccharide to determine secondary structure of the peptide component

CD spectrometry was used to investigate the secondary structure of the proteosaccharide hydrogel. A Jasco-1500 spectrometer was used over wavelengths, 190nm-250nm, with a band width of 5nm, scan speed of 200nm/min and 7 accumulations/cycle at a temperature of 37 °C. The proteosaccharide and peptide were diluted in Phosphate Buffered Saline (pH=7.4). The data was buffer corrected and plotted on OriginPro. CDtoolX was used to calculate the content of each secondary structure.

4.3.5 Attenuated total reflection Fourier transform infrared spectroscopy (ATR-FTIR) to assess physicochemical interactions between the peptide and polysaccharide

Scaffolds were analysed with a Spectrum 2000 FTIR Spectrometer (PerkinElmer, MA, USA) at wave numbers of 4000-650cm^{-1} at 10 scans/second under a constant pressure of 120 psi and a single-reflection diamond MIRTGS detector. The stage for the sample was cleaned with methanol prior to analysis and a background spectrum was obtained. The spectra obtained were plotted on OriginPro.

4.3.6 Differential scanning calorimetry (DSC) for determination of thermal stability

Proteosaccharide-based scaffolds were analysed using the Mettler Toledo, DSC1, STARe System (Schwerzenback, Switzerland). The scaffolds weighing 5-10mg were heated at a temperature range of 10-300 °C at 5°/minute to identify degradation, melting point and the glass transition temperature (Tg) in an aluminium pan (40DL) and sealed with a 0.2mm

opening in the lid for heat flow. This range was used to establish the temperature at which the proteosaccharides will degrade. The test was run under constant N_2 gas. The resulting thermogram was then compared to a reference thermogram run with an empty sample holder.

4.3.7 Morphological characterization of the proteosaccharide with SEM

The morphology of each scaffold was determined using a Scanning Electron Microscope (Zeiss, Oberkochen, Germany) equipped with an accelerating voltage of 0.02−30.00 kV. Cross sections of scaffolds were mounted on aluminium stubs and subsequently coated with one coat of carbon and two coats of gold palladium (AuPd). Pore sizes were calculated from SEM micrographs and analysed on ImageJ.

4.3.8 Textural analysis of the scaffold to elucidate mechanical properties of the scaffold

The biomimetic mechanical properties of the proteosaccharide scaffold were evaluated using a TA. XTplus Texture Analyzer (Stable MicroSystems, Surrey, UK). For compression testing, scaffolds were soaked in PBS (pH=7.4) at 37 °C overnight and thereafter mounted onto a stage. Thereafter, a compression test was performed using a radius cylindrical probe (P/0.5R). A 90% strain was applied using a 50kg load cell and the young's modulus was calculated from the slope of the graph. The scaffolds after incubation in PBS are shown in figure 4.2.

a) Scaffold formed by freeze-drying b) Gelation of the scaffold in PBS (pH=7,4



Figure 4.2. Images showing the in-situ gelation of the proteosaccharide scaffold

4.3.9 Degradation of proteosaccharide scaffolds

The rate of degradation of scaffolds were measured by placing each scaffold into polytops consisting of phosphate buffered saline, into an orbital shaker at 37 °C and 25rpm. The degradation medium was changed every second day to mimic physiological sink conditions. Scaffolds were removed on day 0, 3, 7, 14, 21 and 28 and weighed after drying. The weight at each time interval was compared to the initial weight of the scaffolds and the rate of

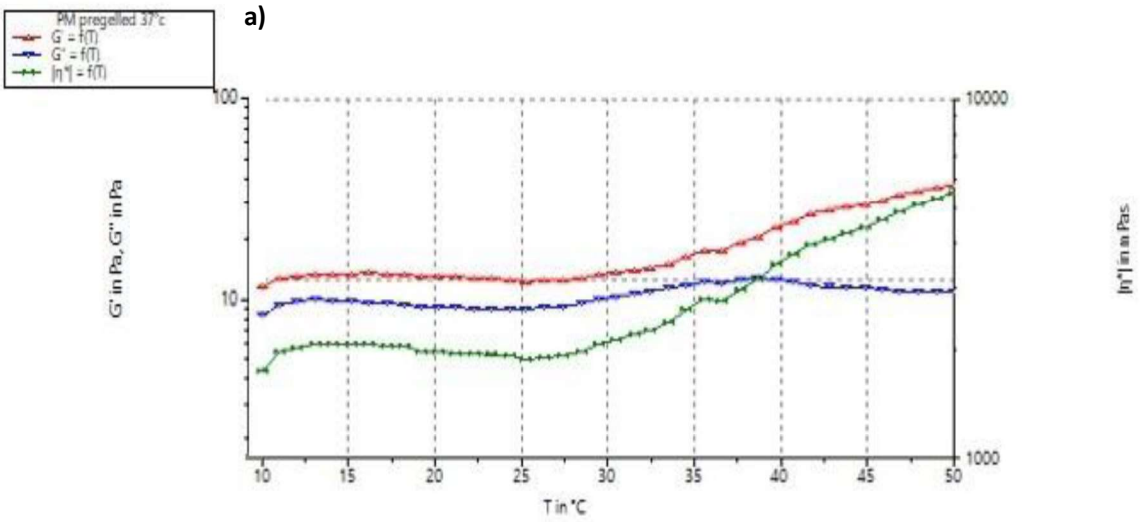
degradation was determined. The degradation behaviour of a scaffold is crucial in order to prevent premature collapse of the scaffold and to prevent the accumulation of potentially toxic by-products.

4.4 Results and discussion

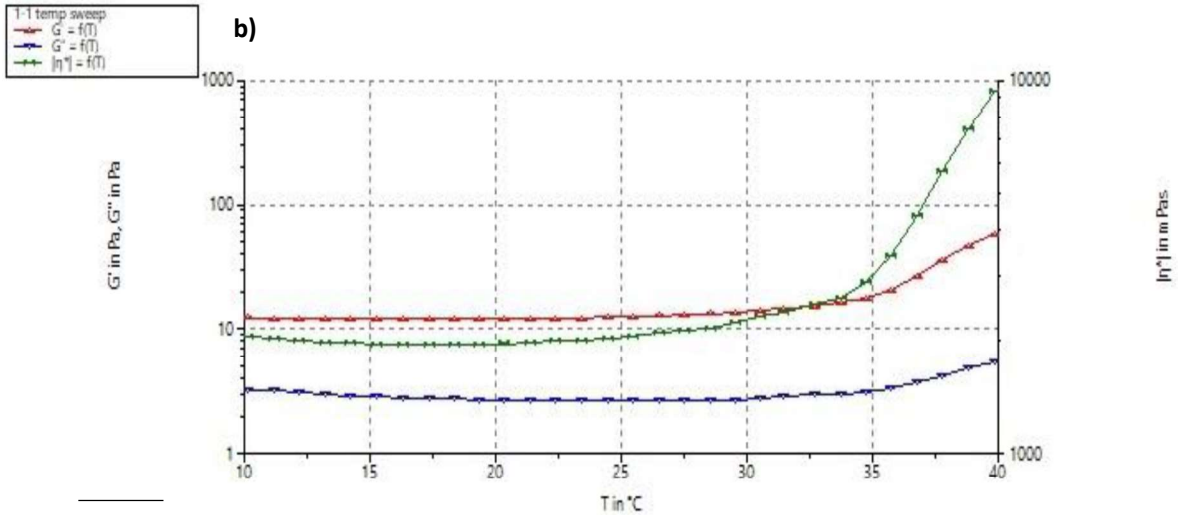
4.4.1 Rheological analysis to determine the thermoresponsive behaviour of the proteosaccharide.

Temperature sweeps were carried on each ratio of CHT-PM gels (1:1, 1:3, and 1:5) to determine which gel was most temperature responsive in the 10 °C to 50 °C. This was necessary to determine the behaviour of the proteosaccharide *in vivo,* at physiological temperature. The storage modulus (G') refers to the solid-like character of the gel, while the loss modulus (G'') refers to the liquid-like character of the gel. As can be seen in figure 4.3, all thee parameters (G', G'' and dynamic viscosity) remain relatively constant, until a temperature of 35 °C, when a slow increase in each of these parameters, most importantly G' can be seen. G' remains greater than G'' implying that the solution is more viscoelastic than fluid in nature. At physiological temperature, the G' value of PuraMatrix was 15.854 Pa and the G'' was 9.7744 Pa (Figure 4.3A). The incorporation of chitosan, resulted in higher G', G'' and n* from the beginning of the temperature sweep. The incorporation of chitosan thus leading to a more viscous polymeric network with G' beginning to rise from 32 °C. The incorporation of chitosan thus reduced the temperature at which gelation may occur. This could be overcome by modifying chitosan with dendritic oligoethylene glycols (OEGs) which would afford better thermoresponsive behaviour to the system, however this was not investigated in this study. As shown in figure 4.3 B, the 1:1 ratio showed an increase in G' and G'' at 35 °C and thereafter. The human brain has a G' value of 140- 620 Pa and the 1:1 ratio showed a G' of 35.711Pa at 37 °C. Therefore, this ratio was not ideal for applications in the human brain. The 1:3 ratio showed a G' of 125.057 Pa at 37 °C while the 1:5 ratio showed a G' of 83.748 Pa (Figure 4.3 C, D). Therefore, based on the G' values, the 1:3 ratio was deemed most appropriate for *in situ* application. All ratios showed G'>G" which showed that each hydrogel was more viscoelastic in nature. Viscosity curves (η*) closely followed the trend of the G' curve with the 3:1 ratio attaining the highest dynamic viscosity at 37 °C.

a)


PM pregelled 37°c
G' = f(T)
G'' = f(T)
|η*| = f(T)
G' in Pa, G'' in Pa
|η*| in m Pas
T in °C
100
10
10000
1000
10
15
20
25
30
35
40
45
50

b)


1-1 temp sweep
G' = f(T)
G'' = f(T)
|η*| = f(T)
G' in Pa, G'' in Pa
|η*| in m Pas
T in °C
1000
100
10
1
10000
1000
10
15
20
25
30
35
40

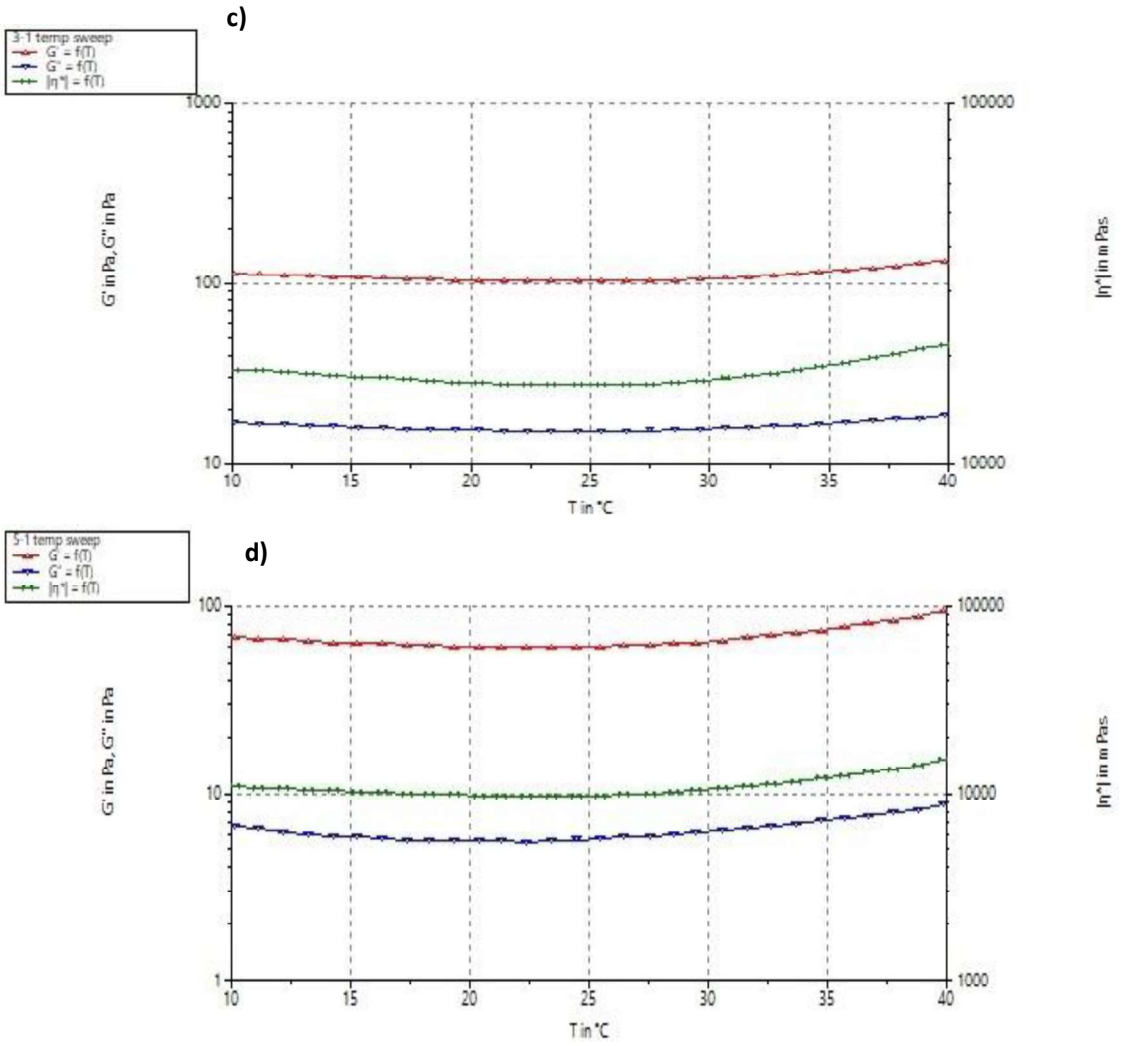


Figure 4.3. Temperature sweeps of each hydrogel ratio a) PuraMatrix, b) 1:1, c) 3:1 and d) 5:1 ratios of chitosan:PuraMatrix conducted over the temperature range, 10 °C to 40 °C.

4.4.2 Preliminary cytotoxicity studies to determine the most bioactive ratio

To determine the most appropriate ratio of protein to polysaccharide, a cytotoxicity assay was conducted using PC12 cells. As shown in figure 4.4, the 1:3 ratio was the least cytotoxic and supported cell proliferation the most, with a cell viability of 118.08%. It is necessary for the chitosan to be completely blended with the self-assembling peptide for an increase in mechanical strength, and for the self-assembly process to not be interrupted by the cationic polymer. The 1:1 ratio showed a cell viability of 92.02%, while the 1:5 ratio showed a cell viability of 90.436%. The PuraMatrix alone, showed a cell viability of 119.87%. It can be argued that the addition of chitosan, reduced the cell viability, however it must be noted, that by combining chitosan with PuraMatrix, the quantity of PuraMatrix employed was drastically reduced, and the bioactivity was made up for, by addition of chitosan. When a 1:1 ratio was used, the electrostatic interactions between the positively charged amino side chain of

chitosan and the negatively charged aspartic acid residues were too strong to form a hydrogel network. When the 5:1 ratio was used, the cell viability dropped, but it was still not cytotoxic. The electrostatic interactions could not hold the hydrogel together, and the self-assembly process was interrupted. The 3: 1 ratio was therefore chosen to characterise further, as self-assembly and bioactivity was maintained.

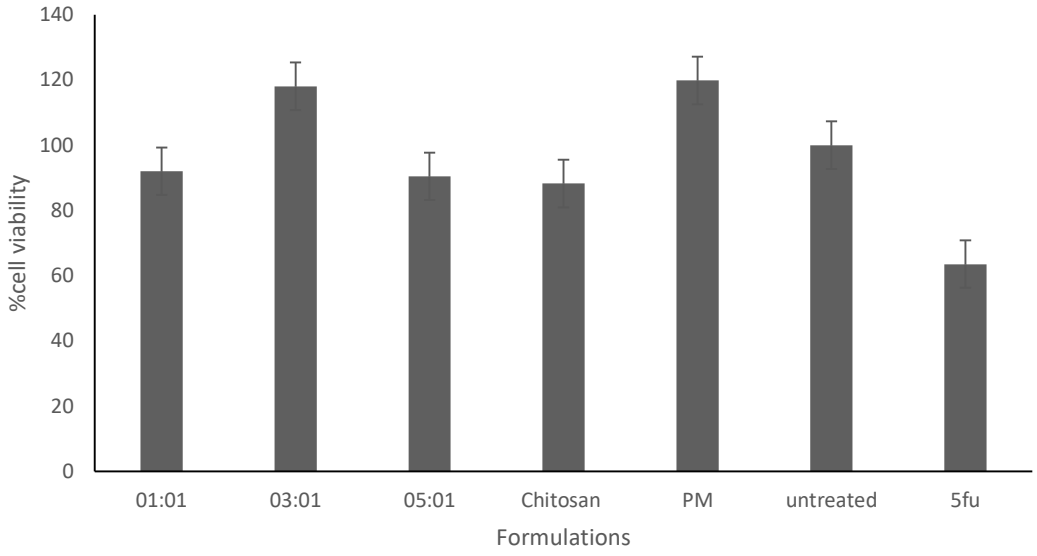


Figure 4.4. Bar graph showing the cytotoxicity of each hydrogel ratio on PC12 cell lines using an XTT assay (n=3) over 48 hours (n=3). 5-FU (5-Fluorouracil, 10 µg/ml) was used as the positive control.

4.4.3 Physicochemical characterization of lyophilised proteosaccharides using FTIR spectroscopy

The region of interest lies between 1800cm-^{1} and 1400cm^{-1}, where amino acids such as aspartate and arginine are known to give off peaks. The β-sheet can be monitored by noting the changes in the wavenumbers in the region of 1600-1700cm$^{-1.}$ As noted in the previous chapter employing chitosan, chitosan contains a C=O bond at 1629.15cm^{-1} and the same can be found in the PM at 1624.42cm^{-1} (Fig.4.5). By combining chitosan with PM, minimal difference is noted in the wavenumber (1629.15cm^{-1}). This can be explained by no self-assembly taking place merely by the interaction of chitosan and PuraMatrix as chitosan is a cationic polymer which carries a positive charge of approximately 5.7. To observe gelation of the PuraMatrix, the pH of the system must be brought to physiological pH (7.4), whereby chitosan would become protonated and interact with the negatively charged residues of PuraMatrix,

When the system is exposed to a physiological pH, the shift in wavenumber of the amide I bond is distinctly noticeable. This shift in wavenumber to 1635.08cm^{-1} is attributed to gelling

of PuraMatrix around chitosan. When washed with distilled water, the band remains at 1635.08cm^{-1}, showing that the β-sheet structure formed, remains and is irreversible after exposure to physiological pH. Another band of interest is in the region of 1530-1540cm^{-1}. This region correlates to N-H bonds of amide I. These bonds can be formed in both chitosan (1535.60cm^{-1}) and PuraMatrix (1530.16 cm^{-1}). These bonds are found at a higher wavenumber of 1546.07cm^{-1}) upon gelation and shifts to a lower wavenumber of 1541.76cm^{-1} when the scaffolds were washed with distilled water. This suggests an electrostatic interaction between both components of the system.

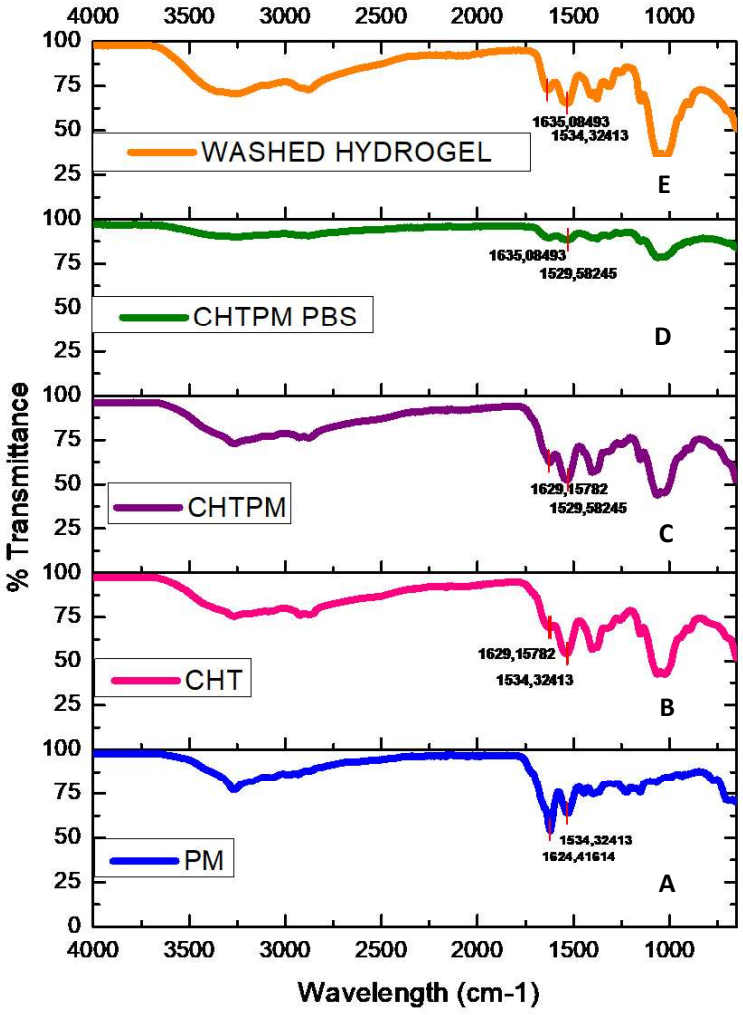


Figure 4.5. FTIR spectra of A) PuraMatrix, B) Chitosan, C) CHT-PM (PBS), D) CHT-PM, E) CHT-PM (washed) scaffolds

4.4.4 Determination of the secondary structure of the proteosaccharide

Circular dichoism (CD) can be applied to peptides and proteins due to their optical activity. The principle of CD is the differential absorption of left and right circularly polarized light by the chiral peptide. The process of self-assembly is driven by the transition of peptide

secondary structure and can be used to identify the location of alpha helices or beta-sheets. The process of self-assembly has been described by Mu et. al in thee steps, firstly the interaction of monomers via antiparallel pairing, followed by the transition to α-helices; secondly, the assembly of peptide pairs to form fibres and finally the formation of fibrils via nucleation-dependent polymerization (Mu & He, 2011).

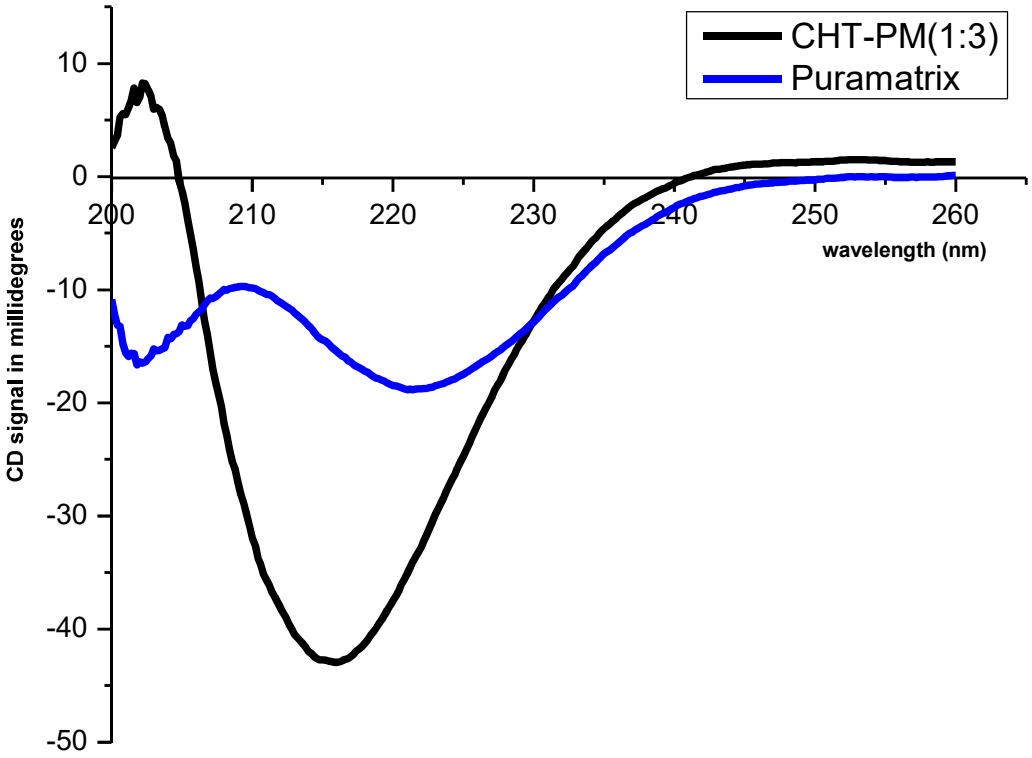


Figure 4.6. CD spectra of PuraMatrix before and after self-assembling with Chitosan at 37 °C.

It has already been shown in previous studies that RADA-16 I has the propensity to form stable β-sheet structures which leads to nanofibrillar morphology (Chen *et al.*, 2017). This can be further categorised into parallel and anti-parallel β-sheets. Parallel β-sheets consist of strands which run unidirectionally with hydrophobic residues on both sides of the sheet, whereas anti-parallel β-sheets have strands which run in different direction and have hydrophobic residues on only one side of the sheet (Crichton, 2008). The co-existence of parallel and anti-parallel β-sheets can be seen in the CD spectrum of both PuraMatrix and the proteosaccharide, (Figure 4.6). The CD spectrum of PuraMatrix showed a maximum ellipticity at 221.0 nm and minimum ellipticity at 202.2nm. The spectrum shows a mix of β-sheets and α-helices with a

greater β-sheet content. The α-helix structure is expected due to the pH of the solution, not being appropriate to self-assembly. The peptide was dissolved in distilled water at a concentration of 0.02%w/v. Incorporation of chitosan, resulted in a shift in pH to approximately 5.7 and therefore allowed for some self-assembly to take place. This led to increased amplitude of the β-sheet. Furthermore, the anti-parallel β-sheet structure was more prevalent than the parallel β-sheet structure. This can be explained by interaction of the carboxyl groups of chitosan with the -NH groups present on PuraMatrix, resulting in a more stable β-sheet structure. This thereby improves mechanical properties of the proteosaccharide. This shows that the PuraMatrix maintained its β-sheet conformation when co-existing with chitosan. Furthermore, the α-helical content was found to be lower than the β-sheet content (both parallel and anti-parallel), indicating the formation of fibrils in the proteosaccharide, indicative of the *in situ* self-assembly process. Alpha-helix structures are stabilised by the hydrogen bonds of a carbonyl oxygen of one amino acid to the amino group of a second amino acid. The alpha helical content had increased from 1.4% to 5.7%, which would indicate the interaction of the amino group of aspartic acid residues of PuraMatrix to the carbonyl oxygen of chitosan. Glycine is known to be an alpha helix destabiliser and aspartate has a greater alpha-helix inducing ability than alanine, therefore the interaction was largely induced by aspartate (Farood et al., 1993). The random coil content was largely reduced upon the incorporation of chitosan, leading to the conclusion that less amino acid residues were left exposed, and more were involved in the formation of more stable secondary structures such as α-helices and β-sheets.

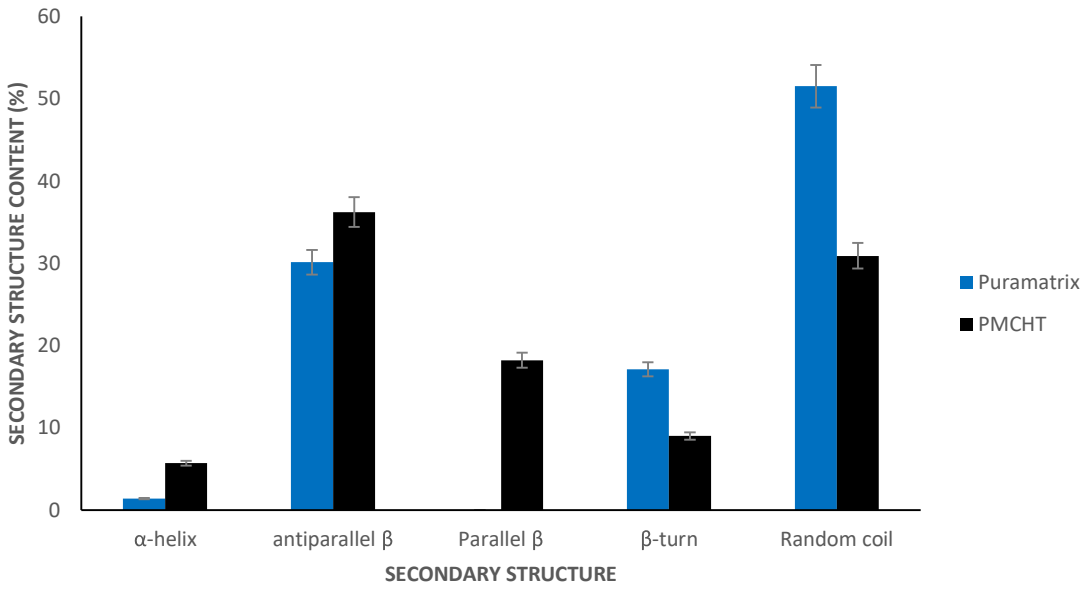


Figure 4.7. Bar graph showing the secondary structure content of PuraMatrix before and after self-assembly with Chitosan using the CDtoolX software

4.4.5 DSC Analysis to determine the thermal stability of the proteosaccharide

DSC thermograms of chitosan reveal an endothermic peak at 99.20 °C and an exothermic peak at 291.80°C. The first peak can be associated with dehydration of the polymer and the second can be attributed to the decomposition of the glucosamine units in chitosan. The addition of PuraMatrix resulted in a reduced thermal stability of the co-polymer, with the dehydration temperature shifting to 82.65 °C and the decomposition temperature shifted to 276.54 °C. It has been reported by other researchers that the peptide loses its β-sheet structure at 80°C (Taraballi *et al.*, 2010). A possible explanation for this, is the absence of chemical crosslinkers to strengthen the thermal stability of chitosan. Furthermore, PuraMatrix is an amphiphilic peptide comprising of both hydrophilic and hydrophobic residues. The hydrophilic residues contribute to a lower temperature associated with dehydration of the sample. An increase in the decomposition temperature can be explained by the electrostatic interactions with positively charged chitosan and the negatively charged terminals of PuraMatrix. The incorporation of PuraMatrix resulted in an increased organisation and closer packing in the proteosaccharide, thus resulting in a greater temperature needed to rupture glucosamine residues in chitosan. The first endothermic peak seen in chitosan, appears to be flatter in comparison to the endothermic peak in the proteosaccharide. This peak can be associated with the release of bound water within the self-assembled peptide. An endothermic peak at 169.10 °C (circled) appears more prominently in the thermogram of the gelled proteosaccharide, which corresponds to the melting of the β-sheet of PuraMatrix, which is absent in the thermogram of the proteosaccharide blend. Other researchers have reported the melting point of RADA-16 at 127.6 °C, therefore it can be argued that the incorporation of chitosan and the in situ gelation resulted in an increased thermal stability of the proteosaccharide (Aramvash *et al.*, 2019).

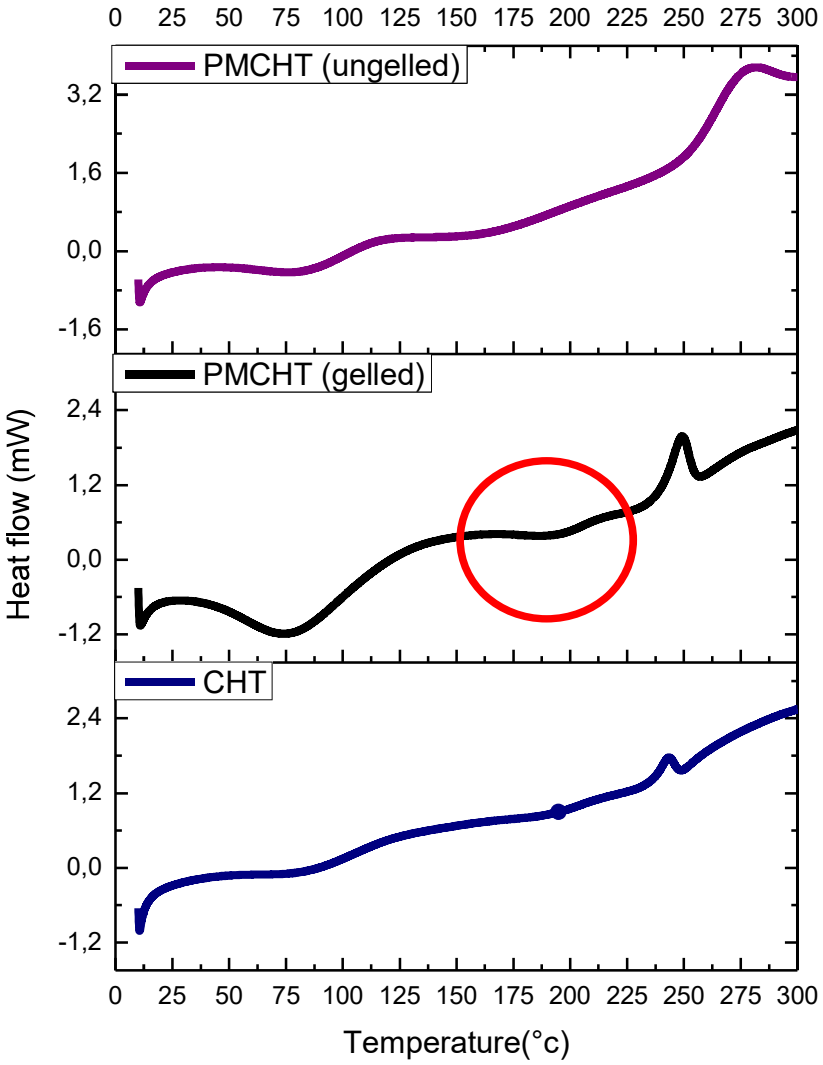


Figure 4.8. DSC thermograms of a) Chitosan; b) CHT-PM (gelled) and c) CHT-PM (blend) over temperature range 10 °C to 300°C.

4.4.6 Morphological characterization of pore and fibre size

SEM images of a cross-section of a PuraMatrix (0.5%w/v) scaffold revealed the presence of abundant nanofibrous structures and nano-sized pores ranging from 5 to 200nm. The SEM of pristine chitosan showed a disorganised microporous structure with loosely connected pores and thicker walls as compared to the PuraMatrix scaffold the final composite showed both properties of chitosan and PuraMatrix. PuraMatrix maintained its nanofibrous structure and was found to assemble around micro- scaled pores which can be ascribed to chitosan. The average pore size was determined for each cross-section using the scale bar below each image and is shown in table 4.1. The average pore diameter of a 0.5%w/v concentration of PuraMatrix was calculated to be 13.130µm, while pores found in chitosan showed a much

larger average diameter of 132.678μm (Figure 4.9; 4.10). The introduction of PuraMatrix resulted in a drastic reduction in pore size, due to the self-assembly process within the scaffold and the presence of multiple fibrous channels which would guide neuron repair. The pore size was reduced to 14.938μm, which is slightly bigger than the diameter of a pristine PuraMatrix scaffold i.e., 13.130μm, however is still conducive to neuronal guidance and diffusivity of nutrients within the scaffold (Figure 4.11). Furthermore, fibres were present in the CHT-PM scaffold, however these were larger and not of a nanoscale (Figure 4.12). The addition of chitosan thickened the diameters of the fibres from 0.565μm to 16.641μm, which made the scaffold more mechanically robust and less susceptible to collapse in vivo. The ideal pore size for cellular interactions is dependent on the type of cell, scaffold material and processing parameters employed, such as lyophilization. There were various micro scaled pores ranging from 6-10μm on the slightly rough surface of the composite scaffold as shown in figure 4.13. The size of PC12 cells vary from 10 to 12μm. It is generally agreed upon by researchers that larger pore sizes result in an increased nutrient and oxygen supply, resulting in faster and more efficient migration (Mandal & Kundu, 2009; Nunes-Pereira *et al.*, 2015). When pore sizes are smaller than the cell size, cells favour cell bridging across the fibres which results in lengthier migration times. Larger pores stimulate alignment along a single fibre which supports directional growth, faster attachment and faster migration (Mandal & Kundu, 2009). Porosity is also an important factor to be considered in the preparation of scaffolds for the CNS. The chitosan scaffold showed a porosity of 49.456% which was less than the porosity of PuraMatrix (60.749%). Porosity was increased to 66.329% by combining the peptide with the polysaccharide. A porous scaffold is necessary for the diffusion of nutrients, as well as for the scaffold to retain its structural integrity after swelling *in vivo.*

Table 0.1. Dimensions of each scaffold calculated from SEM images (n=10)

	Chitosan	**PuraMatrix**	**CHT-PM**
Average Pore diameter (μm)	132.678±17.681μm	13.130μm ±8.874μm	14.938±2.587μm
Fibre diameter	Absent	0.565±0.277μm	1.641±5.616μm
Porosity (%)	49.456%	60.749%	66.329%

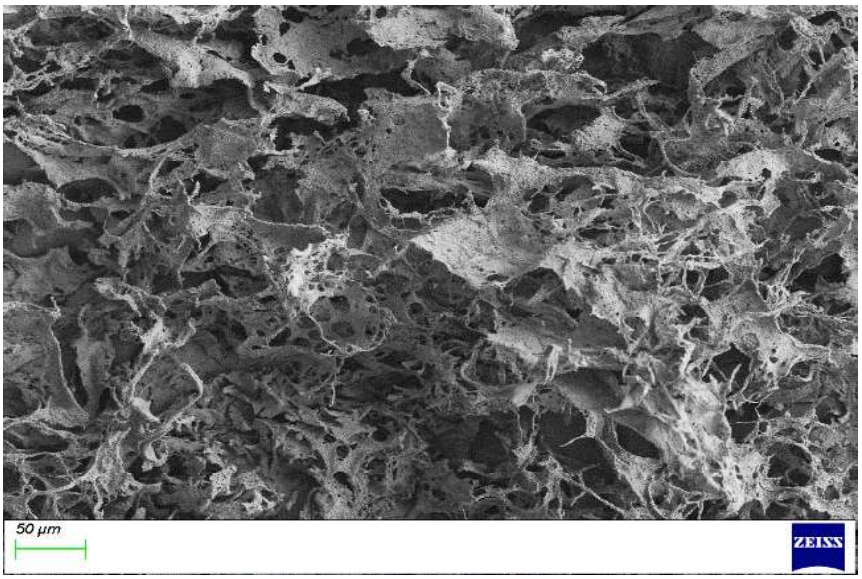


Figure 4.9. SEM micrograph of PuraMatrix fibres (transverse cross section), magnification: 493x and EHT: 6.00 Kv.

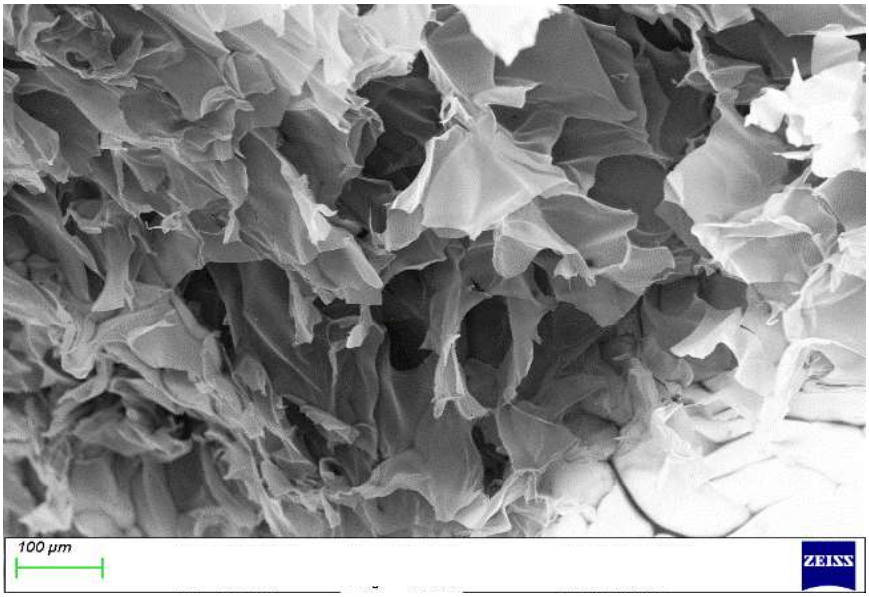


Figure 4.10. SEM micrograph of chitosan scaffold (2%w/v) (transverse cross section), Magnification: 300x and EHT: 20.00kV

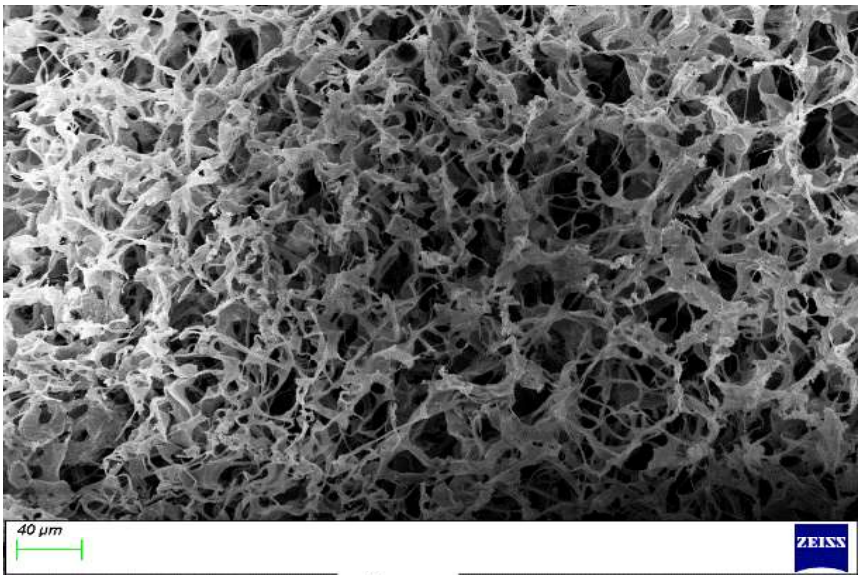


Figure 4.11. SEM micrograph of CHT-PM (1:3) (transverse cross section), Magnification: 572 x and EHT=20.00kV

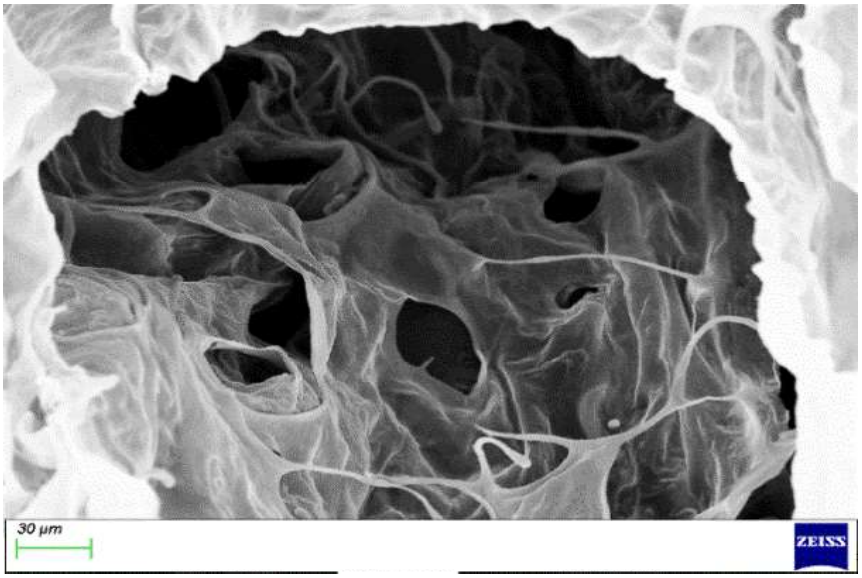


Figure 4.12. SEM micrograph focusing showing various nanofibers and microporous structures though a large pore, Magnification: 873 X and EHT=20.00kV

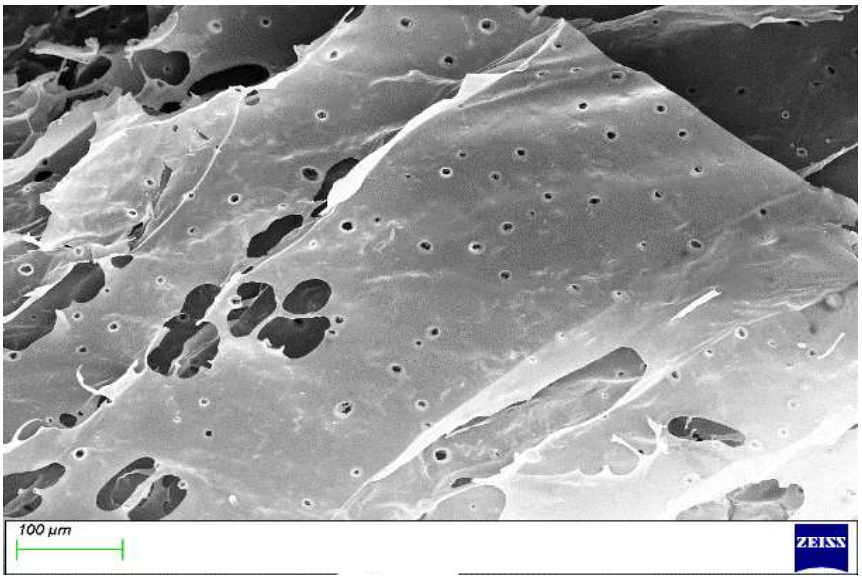


Figure 4.13 Surface of CHT-PM scaffold showing surface porosity and roughness, Magnification=372X and EHT=20.00kV

4.4.7 Textural profile analysis of lyophilised scaffold after gelation in PBS

The Young's modulus (E') of a scaffold is a quantitative measure of its stiffness, which is the scaffold's resistance to force applied. The TXA was used to determine the young's modulus of the scaffold, which was immersed in PBS for 24 hours until swelling had reached an equilibrium. The TXA was equipped with a cylindrical stainless-steel probe and samples with the diameter of 10mm were compressed until 90% strain was reached.

Table 4.2: Processing parameters employed in calculation of the Young's modulus on the TXA

Test parameter	Test settings
Pre-test speed	0.5mm/sec
Post-test speed	0.5mm/sec
Test speed	0.1mm/sec
Maximum strain	90%
Trigger force	Button
Dimensions of scaffold	Cylindrical

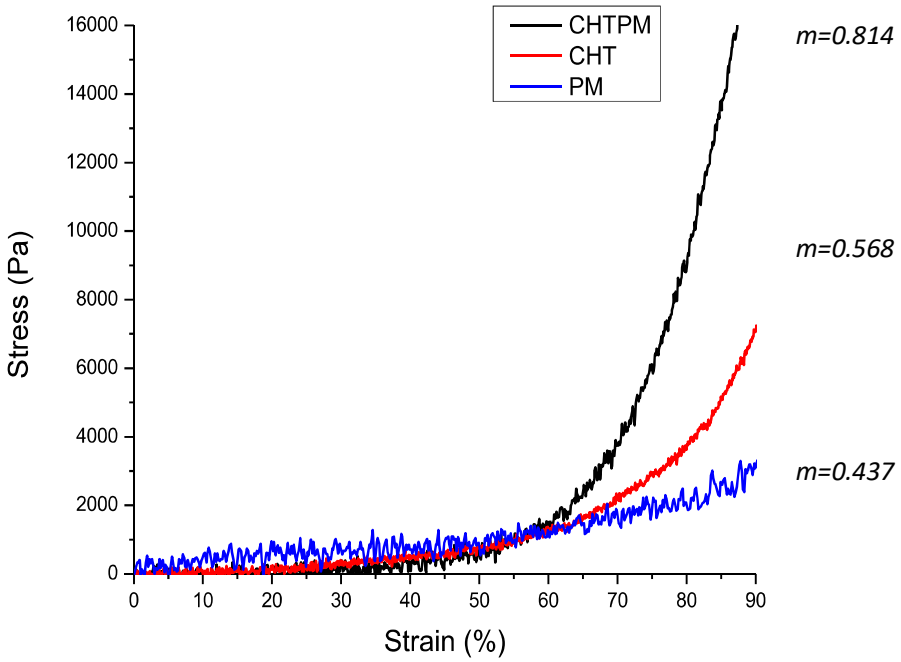


Figure 4.14. Stress-strain curves of a) PuraMatrix, b) Chitosan and c) CHT-PM

The slope of each graph in figure 4.14 was calculated to determine the young's modulus of the sample. The stiffness of a scaffold is an important parameter in determining if the scaffold is suitable for cell attachment and proliferation. Cells are bathed in a fluid filled biological system and experience shear stress applied by the fluid. The brain is composed of 75% of water, thus scaffolds implanted must be able to resist deformation. Several researchers have concluded that brain scaffolds should ideally possess an elastic modulus of less than 1kPa. Neuronal Stem Cells (NSC) were able to grow on scaffolds with a young's modulus of ~500Pa. After addition of serum proteins, scaffolds were able to promote neurogenesis, however harder hydrogel scaffolds (1kPa-10kPa) supported differentiation into glial cells (Saha *et al.*, 2008). Mixed differentiation was induced, and it was found that the fraction of astrocytes decreased, and neurons increased with increasing softness of the IPNs tested. The elastic modulus of the PuraMatrix scaffold (unmodified) was calculated to be 0.437kPa. The scaffold was not able to withstand a strain greater than 70%. The elastic modulus of the CHT-PM scaffold was measured to be 0.814 kPa and was able to withstand a strain of 82%. The chitosan scaffold had a young's modulus of 0.568kPa, which was stronger than the PuraMatrix scaffold, therefore it can be concluded that the addition of chitosan resulted in a scaffold with greater mechanical behaviour and resistance to deformation, as compared to the pristine PuraMatrix scaffold. Furthermore, scaffolds that are too stiff may not be ideal for mimicking the neural environment *in vivo* and for the promotion of neuronal differentiation. However, other factors such as ease of handling, the rate of degradation and vulnerability to pores collapsing need

to be carefully considered in deciding on the ideal scaffold composition. Furthermore, the scaffold was able to return to its original shape after deformation.

4.4.8 Degradation of CHT-PM scaffold

Ideally, the degradation rate of a scaffold should match the rate of regeneration of the tissue at the injury site. Scaffolds that degrade too quickly do not allow sufficient time for the establishment of an extracellular niche by cells which have started residing on the scaffold, and a fast rate of degradation would result in a hypertonic environment within the neural cavity, raising intracerebral pressure and exerting mechanical stress on other areas of the brain (Lins *et al.*, 2016; Mahumane *et al.*, 2018; Pettikiriarachchi *et al.*, 2010).

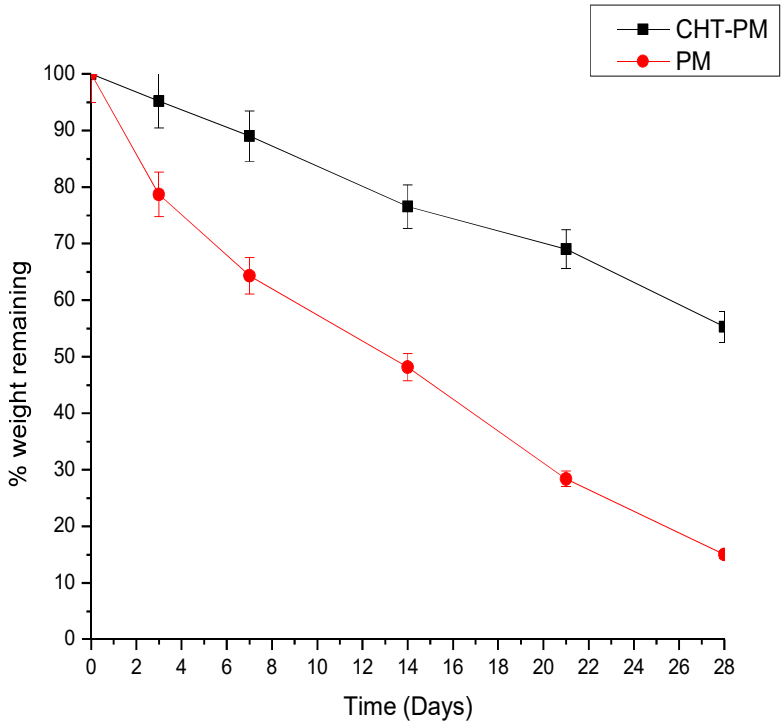


Figure 4.15. Degradation behaviour of PuraMatrix and CHT-PM (n=3) (SD<3)

An advantage of the PuraMatrix scaffold is its degradation into non-toxic amino acids. The degradation behaviour of PuraMatrix alone has not yet been reported in literature. However, it is known that the 3D structure of PuraMatrix is more loosely composed after 10 days with culture of neural progenitor cells (Ortinau *et al.*, 2010). When the gel is degraded over time by physical stimuli, such as shaking in the orbital shaker, the fibres formed by the ionic bonds between the adjacent peptide molecules, arginine- aspartate (R-D) and hydrophobic bonds between aspartate-aspartate (A-A), collapse and result in the degradation of the hydrogel. In this research, PuraMatrix was gelled and left in an orbital shaker to degrade. The PuraMatrix scaffold degraded by 85% by day 28. The incorporation and *in situ* gelation of PuraMatrix

within the chitosan shell resulted in a reduced molecular mobility, which limits the extension of chitosan under loading and reduced its rate of degradation. The scaffold showed an almost linear rate of degradation with a much slower rate of degradation as compared to PuraMatrix, with 55.287% remaining at day 28 (Figure 4.15). The first stage of degradation is referred to as surface erosion, while the second stage is related to the degradation of the polymeric backbone. Surface erosion occurs due to the availability of hydrophilic groups on the surface of the co-polymer, followed by the polymeric degradation. It can be proposed that the interaction of the amino acids on the PuraMatrix backbone with the carbonyl group on chitosan, resulted in stabilisation of the co-polymer and slowed the rate of degradation of PuraMatrix. Furthermore, the thicker fibres found in the proteosaccharide scaffold increased the rigidity of the scaffold and resulted in a greater resistance to mechanical degradation. The incorporation of chitosan resulted in an increased hydrophobicity of the proteosaccharide, which made the proteosaccharide more resistant to hydrolytic degradation.

4.5 Concluding remarks

The proteosaccharide scaffold showed improved thermal stability, slowed degradation, preserved biological activity and a microporous architecture which supported cellular proliferation. This research thus shows that the addition of chitosan was synergistic and resulted in a reduction of cost of synthesis due to the low ratio of PuraMatrix employed, which would result in a higher yield of scaffolds. Comparative biocompatibility assays will be discussed in chapter 5, and the system will be compared with the systems discussed in chapter 3.

REFERENCES

Aramvash, A., Zarei, H., Azizi, A. & Seyedkarimi, M.S. 2019. Investigating the Structural Stability of RADA16-I Peptide Conjugated to Gold Nanoparticles. International Journal of Peptide Research and Therapeutics. 25(2):753–760.

Chen, S., Zhang, M., Shao, X., Wang, X., Zhang, L., … Zhang, L. 2015. A laminin mimetic peptide SIKVAV-conjugated chitosan hydrogel promoting wound healing by enhancing angiogenesis, re-epithelialization and collagen deposition. Journal of Materials Chemistry B. 3(33):6798–6804.

Chen, S., Zhou, A., He, B., Zhao, W., Chen, X. & Jiang, D. 2017. Designer D-form self-assembling peptide scaffolds promote the proliferation and migration of rat bone marrow-derived mesenchymal stem cells. International Journal of Molecular Medicine. 40(3):679–688.

Crichton, R.R. 2008. Structural and Molecular Biology for Chemists. Biological Inorganic Chemistry. (January, 1):43–76.

Cunha, Villa, Silva, Gelain & Panseri, S. 2011. 3D culture of adult mouse neural stem cells within functionalized self-assembling peptide scaffolds. International Journal of Nanomedicine. 6:943.

Ellis-Behnke, R.G., Liang, Y.X., You, S.W., Tay, D.K.C., Zhang, S., … Schneider, G.E. 2006. Nano neuro knitting: Peptide nanofiber scaffold for brain repair and axon regeneration with functional return of vision. Proceedings of the National Academy of Sciences of the United States of America. 103(13):5054–5059.

Gelain, F., Bottai, D., Vescovi, A. & Zhang, S. 2006. Designer Self-Assembling Peptide Nanofiber Scaffolds for Adult Mouse Neural Stem Cell 3-Dimensional Cultures. PLoS ONE. 1(1):e119.

Guo, J., Leung, K.K.G., Su, H., Yuan, Q., Wang, L., … Wu, W. 2009. Self-assembling peptide nanofiber scaffold promotes the reconstruction of acutely injured brain. Nanomedicine: Nanotechnology, Biology, and Medicine. 5(3):345–351.

Kumar, P., Pillay, V., Modi, G., E. Choonara, Y., C. du Toit, L. & Naidoo, D. 2011. Self-Assembling Peptides: Implications for Patenting in Drug Delivery and Tissue Engineering. Recent Patents on Drug Delivery & Formulation. 5(1):24–51.

Lins, L.C., Wianny, F., Livi, S., Hidalgo, I.A., Dehay, C., … Gérard, J.F. 2016. Development of Bioresorbable Hydrophilic-Hydrophobic Electrospun Scaffolds for Neural Tissue Engineering. Biomacromolecules. 17(10):3172–3187.

Loo, Y., Goktas, M., Tekinay, A.B., Guler, M.O., Hauser, C.A.E. & Mitraki, A. 2015. Self-Assembled Proteins and Peptides as Scaffolds for Tissue Regeneration. Advanced Healthcare Materials. 4(16):2557–2586.

Mahumane, G.D., Kumar, P., Du Toit, L.C., Choonara, Y.E. & Pillay, V. 2018. 3D scaffolds for Brain Tissue Regeneration: architectural challenges. Biomaterials Science. 6 (11): 2812-2837

Mandal, B.B. & Kundu, S.C. 2009. Cell proliferation and migration in silk fibroin 3D scaffolds. Biomaterials. 30(15):2956–2965.

Mano, J.F., Silva, G.A., Azevedo, H.S., Malafaya, P.B., Sousa, R.A., … Reis, R.L. 2007. Natural origin biodegradable systems in tissue engineering and regenerative medicine: Present status and some moving trends. Journal of the Royal Society Interface. 4(17):999–1030.

Moradi, F., Bahktiari, M., Joghataei, M. T., Nobakht, M., Soleimani, M., Hasanzadeh, G., Fallah, A., Zarbakhsh, S., Hejazian, L. B., Shirmohammadi, M., & Maleki, F. 2012. BD PuraMatrix peptide hydrogel as a culture system for human fetal Schwann cells in spinal cord regeneration. Journal of neuroscience research. 90(12):2335–2348.

Mu, C. & He, J. 2011. Confined conversion of CuS nanowires to CuO nanotubes by annealing-induced diffusion in nanochannels. Nanoscale Research Letters. 6(1).

Nunes-Pereira, J., Ribeiro, S., Ribeiro, C., Gombek, C.J., Gama, F.M., … Lanceros-Méndez, S. 2015. Poly(vinylidene fluoride) and copolymers as porous membranes for tissue engineering applications. Polymer Testing. 44:234–241.

Ortinau, S., Schmich, J., Block, S., Liedmann, A., Jonas, L., … Frech, M.J. 2010. Effect of 3D-scaffold formation on differentiation and survival in human neural progenitor cells. BioMedical Engineering Online. 9.

Pettikiriarachchi, J.T.S., Parish, C.L., Shoichet, M.S., Forsythe, J.S. & Nisbet, D.R. 2010. Biomaterials for brain tissue engineering. In: Vol. 63. Australian Journal of Chemistry. CSIRO Publishing. pp. 1143–1154.

Saha, K., Keung, A.J., Irwin, E.F., Li, Y., Little, L., … Healy, K.E. 2008. Substrate Modulus Directs Neural Stem Cell Behavior. Biophysical Journal. 95(9):4426–4438.

Sharma, A., Vaghasiya, K., Verma, R.K. & Yadav, A.B. 2018. DNA nanostructures: chemistry, self-assembly, and applications. Emerging Applications of Nanoparticles and Architectural Nanostructures: Current Prospects and Future Trends. (January, 1):71–94.

Silva, G.A., Czeisler, C., Niece, K.L., Beniash, E., Harrington, D.A., … Stupp, S.I. 2004. Selective Differentiation of Neural Progenitor Cells by High-Epitope Density Nanofibers. Science. 303(5662):1352–1355.

Taraballi, F., Natalello, A., Campione, M., Villa, O., Doglia, S.M., … Gelain, F. 2010. Glycine-spacers influence functional motifs exposure and self-assembling propensity of functionalized substrates tailored for neural stem cell cultures. Frontiers in Neuroengineering. 3(FEB).

Yang, Z., Xu, H. & Zhao, X. 2020. Designer Self-Assembling Peptide Hydrogels to Engineer 3D Cell Microenvironments for Cell Constructs Formation and Precise Oncology Remodeling in Ovarian Cancer. Advanced Science. 7(9):1903718.

CHAPTER 5. IN VITRO BIOCOMPATIBILITY ASSAYS OF PROTEOSACCHARIDES

5.1 Introduction

The use of reliable, preclinical assays is mandatory for the understanding of drug systems in vitro. The interplay of ECM components with cells and the surrounding bloody supply is crucial to maintaining a haemostatic balance which ensures optimal tissue functioning. An important feedback loop exists between the ECM and cells residing in the native tissue. The ECM is secreted by resident cells and the ECM influences various cellular interactions such as migration and proliferation (Bonnans *et al.*, 2014; Humphey *et al.*, 2014). *In vitro* tests are imperative to gauge further insight on the behaviour of native cells in response to delivery systems. Cytotoxicity can be ascertained by multiple assays, such as an MTT (3-(4,5-dimethylthiazol-2-yl)-2,5-diphenyltetrazolium bromide) tetrazolium reduction assay, Alamar Blue and an XTT assay (2,3-bis(2-methoxy-4-nitro-5-sulfophenyl)-5-carboxanilide-2H-tetrazolium). These assays are interchangeable and can be used for the determination of cell viability at different time points, post exposure to the drug delivery system. The XTT assay, which will be used in this research to determine cell viability, is based on the extracellular reduction of XTT, by NADH (which is a form of nicotinamide adenine dinucleotide (NAD)) found in the mitochondria (Munarin *et al.*, 2011).

In the early stages of brain development, cell death is an inevitable occurrence which allows for excess cells to be eliminated. However, during adulthood cell death is usually attributed to neurological disorders or neurotoxic materials (Arulmoli *et al.*, 2016). During *in vitro* cytotoxicity assays, only living cells possess metabolic activities which cause a colour change in the viability reagents. For XTT assays, the colour change observed is from a yellow to an orange-red colour based on the quantity of living cells. In order to close the lesion site, it is necessary for cells to react to certain biological cues in the therapeutic platform, and to migrate across the lesion to re-establish continuity. The scratch assay is considered a standard in vitro technique to measure co-ordinated cell movement in a 2D model. Cells such as A172 and PC12's undergo sheet migration. Sheet migration refers to the migration exhibited by cell monolayers which move in two dimensions in response to a gap created in the assay. This is influenced by various mechanical forces and biological cascades which induce migration to close the exposed gap. In this research, a gap will be created using a pipette tip to scratch the monolayer once cells are confluent to track migration.

In this chapter, the proteosaccharide systems listed in chapter 3 and 4 will be assessed for their cytotoxicity and migration potential using an XTT and wound healing assay. These results

will be used to elucidate the biocompatibility of each system and their potential for application in TBI's.

5.2 Materials

5.2.1 Cell lines and culture

Dulbecco's Modified Eagles Medium-high glucose, Roche Cell Proliferation Kit I (MTT), dimethyl sulfoxide (DMSO), and trypsin–EDTA solution were obtained from Sigma Aldrich (Steinheim, Germany). Donor Equine Serum (DES) was purchased from Hyclone (UT, USA). Ethanol (99% absolute) was purchased from LabChem, Johannesburg, South Africa. Fetal Bovine Serum and Ham's F-12 Nutrient Mix (F12) were purchased from (PAN Biotech, Aidenbach, Germany). Rat (Rattus Norvegicus) adrenal gland pheochomocytoma (PC12) and human glioblastoma multiforme (A172) cells were purchased from Cellonex (Separations, South Africa). Penicillin/Streptomycin/Amphotericin B (P/S/AB) solution was purchased from Lonza (OR, USA).

5.3 Method

5.3.1 Aseptic technique

For the successful culture and accurate results to be obtained, aseptic technique was continuously employed during cell work. Decontamination of all surfaces within the laminar flow unit (Labotec, Midrand, South Africa) was performed using 70% v/v ethanol, and primary packaging of reagents were wiped down prior to addition to the laminar flow unit. All bottle caps and necks were flamed upon opening and closing. Masks and gloves were used during all stages of cell work and all discarded flasks, pipettes and culture equipment were incinerated. Other discarded reagents were treated with bleach before being discarded into the drainage system. Cell media was replaced every two days in an aseptic technique to remove dead cells and debris.

5.3.2 Seeding of PC12 and A172 cells in a 96-well plate

An XTT assay was performed to determine the cytotoxicity of the full IPN and semi-IPN formulations on rat pheochomocytoma cells isolated from rat adrenal medulla (PC12) and human glioblastoma cells (A172). The assay was only carried out on the full IPN and semi IPN conjugates and compared to proteosaccharide blends. The PC12 cells were cultured to 80% confluence in Ham's F12 growth medium, supplemented with 2.5% Fetal Bovine Serum (FBS), 15% Donor Equine Serum (DES) and 1%(v/v) Penicillin/Streptomycin. The medium was replaced after washing with phosphate-buffered saline (PBS) every second day to remove cellular debris.

A172 cells were cultured in Dulbecco's Modified Eagle's Medium (DMEM), supplemented with 10% fetal bovine serum (FBS) and 1% penicillin-streptomycin in a T-25 culture flask in an incubator set at 37 °C and 5% CO_2. For seeding, cells were detached using 0.25% Trypsin and neutralised by adding 1 mL of media. The cell suspension was then aspirated and centrifuged at 1500 rpm for five minutes and the cell pellet was resuspended in fresh, supplemented growth medium. The trypan blue dye exclusion method was used to quantify viable cells in a hemacytometer, visualized on an in-verted light microscope. Cells were seeded at a density of $3x10^4$ cells/mL, and a volume of 90 µl per well in a 96 well plate.

The cells were incubated overnight and 10 µL of IPN treatments was added to each well. Post-treatment, further cell incubation was done for 48 and 72 h at 37 °C. There-after, 50 µl of the XTT mixture (0.5 mL electron coupling reagent and 5 mL of XTT rea-gent) were added to each well and the plates were incubated for 4 h at 37°C. Absorbances were read on a Victor X3 microplate reader (Perkin Elmer, MA, USA) at 540 nm and 690 nm. The average absorbances were compared to that of the untreated and the positive control (10 µg/ml of 5-fluorouracil (5-FU)). The %cell viability was calculated using the following equation:

$$\%\ cell\ viability = \frac{Average\ absorbance\ of\ treated\ wells - blank}{Average\ absorbance\ of\ untreated\ wells}\ x\ 100$$

Equation 5.1.

5.3.3 Migration of A172 cells

A wound healing assay was used to determine the rate of migration and wound closure of A172 cells. Cells were cultured in DMEM, supplemented with 10% FBS and 1% penicillin-streptomycin. The cells were cultured to full confluence at 37 °C, 5% CO_2 in a humidified incubator. The cells were trypsinized and viable cells were quantified using the trypan blue dye exclusion method which made use of a trypan blue dye, a haemocytometer, and an inverted light microscope (Olympus CKX53, Olympus, Tokyo Japan), using the 4X objective lens. After quantifying viable cells, the cells were seeded at a density of $6x10^4$ cells/mL in a 12-well plate. The cells were incubated for 48 h at 37 °C until a monolayer was established. A scratch was made in the centre of each well using a 200 µl micropipette tip, after which the wells were gently washed with PBS to remove dislodged cells and to achieve a clear-cut wound. IPN Treatments were added at a 10% v/v concentration. The cells were observed over a period of 48 h, with images captured every 8 h using the phase-contrast feature and 4X objective lens of an inverted light microscope (Olympus CKX53, Olympus, Tokyo, Japan).

5.3.4 Image processing to determine percentage wound closure

All cell images were captured using an LC30 optical fluorescence microscopy (OFM) (Olympus DP 80) (Tokyo, Japan) equipped with the LCmicro software. Images were quantitatively analysed using the NIH ImageJ software. The percentage wound closure was calculated using the following equation:

$$\%\ wound\ closure = \frac{Area\ of\ wound\ at\ specific\ time\ point}{Initial\ Area\ of\ wound}\ x\ 100$$

Equation 5.2.

5.3.5 Statistical analysis

All experiments were carried out in triplicate and statistical significance was determined by a student p test with $p<0.05$ being statistically significant. Error bars were reported on all graphs.

5.4 Results and Discussion

5.4.1 Cytotoxicity analysis of proteosaccharide hydrogels on PC12 cells

Cell viability was calculated and expressed as a percentage and compared to the untreated wells. A cell viability of above 80% is considered non-cytotoxic, 60-80% is considered weak toxicity, 40-60% is considered moderate toxicity and <40% is considered severely toxic according to ISO 10993-5. Cell cytotoxicity (XTT) assays revealed that the blends of chitosan and gelatin, as well as the crosslinked hydrogels showed a cell viability of greater than 70%.

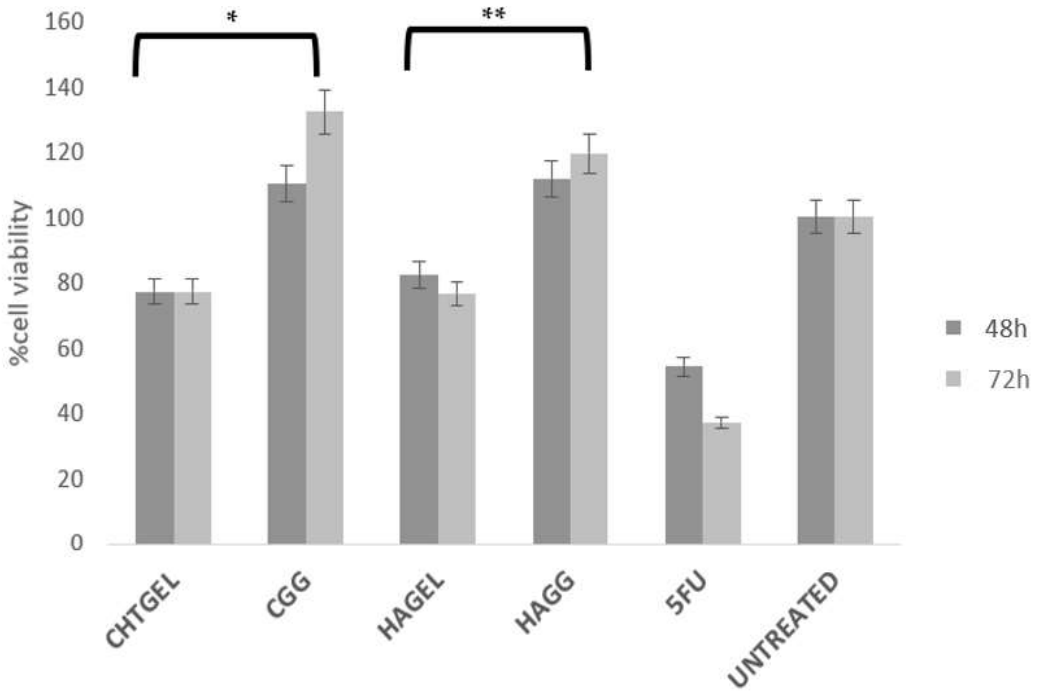


Figure 5.1. Bar graph showing cytotoxicity results from an XTT assay of each formulation over 72 hours on PC12 cells over 72 hours. 5FU (5-Fluorouracil, 10 µg/ml) was used as the positive control. (n=3) (*p<0.0001, **p=0.0011)

The CHTGEL and HAGEL blends showed average cell viabilities of 77.201% and 76.527% respectively at 72 h as shown in figure 5.1 which is considered weakly toxic, and proliferation was not observed. The crosslinked hydrogels showed a greater viability than the non-crosslinked hydrogels with the full IPN showing a viability of 132.24% and the semi-IPN showing a viability of 119.56%. P-values showed strong statistical significance between the uncrosslinked and crosslinked formulations as evident in the graph in figure 5.1. It can be deduced that crosslinking enhanced stiffness of the hydrogel and improved cellular activity. It must also be noted that a low concentration of genipin (0.01%w/v) was used in the crosslinking process, therefore the hydrogels did not exert any toxicity. Other researchers have reported that genipin concentrations of 5mM and greater were cytotoxic (Výborný *et al.*, 2019). PC12 cells have a doubling time of 48hs, therefore a 24h assay was not carried out. An increase in cell viability was observed on the crosslinked formulations over time thus indicating that the systems increase in bioactivity with time. Gelatin contains the RGD sequence which supports cell attachment and proliferation. Genipin has proven to have neuritogenic activity in PC12 cells and neuroprotective effects on β-amyloid peptide-treated primary hippocampal neurons of rats that express nNOS proteins. Furthermore, the crosslinked hydrogels showed a cell viability greater than that of the controlled. Genipin-crosslinked hydrogels can be applied in TBI'S due to its neuroprotective effect, and for prevention of secondary damage. This can be attributed to its architectural similarity to the ECM which permits cell attachment and proliferation. The XTT results therefore show that both the IPN and semi-IPN were neurocompatible and would be safe *in vivo.* A p-value of 0.0614 which denoted weak statistical significance was calculated between the IPN and semi-IPN. This shows that both formulations showed a similar performance *in vitro* performance.

From the bar graph (Figure 5.2), it can be seen that the PMCHT proteosaccharide system supported cellular proliferation to a greater extent than the untreated. Cell proliferation increased with time with the PM-CHT system having an average cell proliferation of 163.19% after 72 h. The PuraMatrix alone showed a cell viability of 149.16%, which is slightly lower than the proteosaccharide. Therefore, an increase in cell viability was observed with chitosan incorporated in the system after 72 h. The same can be seen at 48 h where the proteosaccharide showed an average cell viability of 122.44% which was higher than the PuraMatrix alone at 111.35%. The combination of chitosan and PuraMatrix was synergistic and brought about cell proliferation as compared to the chitosan alone, which was cytotoxic to the cells after 72 h. Therefore, the PMCHT hydrogel showed proliferative effects on PC12 cell

lines. Cytotoxic effects were seen with 5-fluourouracil with the cell viability dropping to 31.76% after 72 h. The proteosaccharide systems showed greater cell proliferation than the untreated cells. The cell viability of chitosan dropped to 72.152% from 91.02%, which shows that chitosan alone is weakly cytotoxic after 72 h as it is not intrinsically bioactive to support cell proliferation. Statistical analysis conducted between the Puramatrix and CHT-PM formulation shows extreme significance with p=0.006. Thus, *in vitro* cell viability analysis revealed that the proteosaccharide system was more bioactive than PuraMatrix alone.

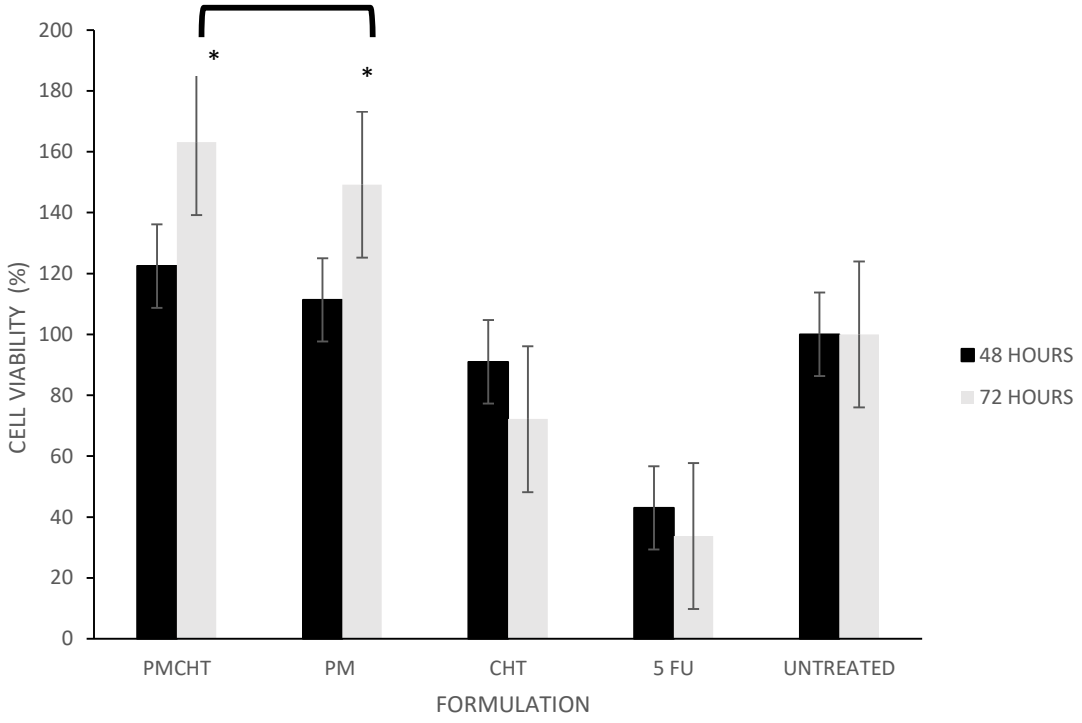


Figure 5.2. Bar graph showing cytotoxicity results from an XTT assay on the PMCHT formulation over 72 hours (n=3). 5FU (5-Fluorouracil, 10 µg/ml) was used as the positive control. *p=0.0006

5.4.2 Cytotoxicity analysis of the proteosaccharides on A172 cells

A172 cells proliferate more rapidly than PC12 cells. This is notably due to their nature as human glioblastoma cells with their doubling time ranging from 40 to 44 h. Therefore, for the purpose of this study, an XTT study was performed at 48 h. At 72 h, the rapid rate of proliferation and the limited growth media would result in apoptosis. The XTT assay of A172 cells showed results that are similar to the results obtained from the PC12 cell line (Figure 13). The uncrosslinked formulations showed a lower cell viability of 78.663% for CHTGEL and 72.136% for HAGEL. The IPN and semi-IPN showed cell viability of 97.52% and 89.72%, respectively. The apoptosis caused was due to the incorporation of genipin, which has

antiproliferative effects on glioblastoma cells. Ahani and co-workers (2018) demonstrated that genipin had an inhibitory effect on uncoupling protein 2(UCP2) which causes proton leaks though the inner mitochondrial membrane and uncouples oxidative phosphorylation from ATP synthesis and negatively regulates the production of reactive oxygen species (ROS) in the mitochondria. Genipin induces apoptosis though the UCP2 pathway and the induction of intracellular ROS (Ahani et al., 2018).

The PMCHT formulation showed cellular proliferation of 149.93% ECM mimetic peptides such as PuraMatrix have been used for culture of cancer cell lines due to their ability to support proliferation. In fact, cells grown within a 3D model are known to be more invasive and resistant to therapeutic interventions as compared to conventional hydrogels (Monteiro *et al.*, 2020). The PMCHT hydrogel showed a higher cell viability than the PuraMatrix hydrogel alone (133.29%). From this assay, the synergistic effect on proliferation by combining chitosan with PuraMatrix is highlighted again.

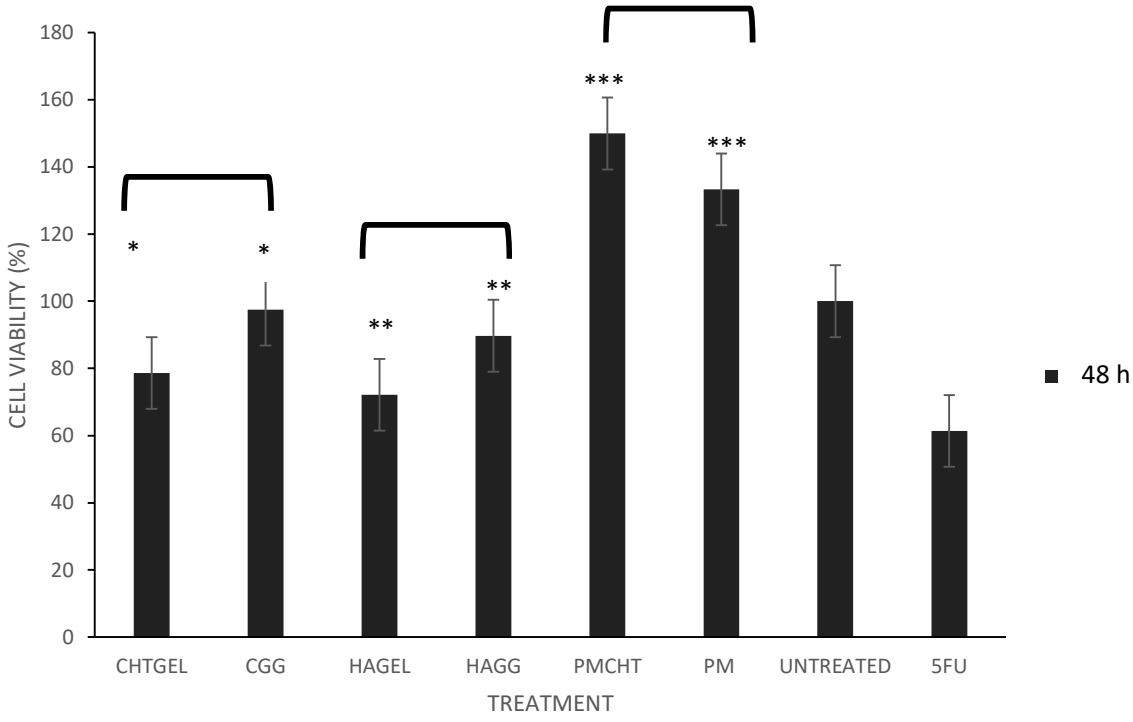


Figure 5.3. Bar graph showing cytotoxicity results from the XTT assay performed on A172 cells over 48 hours (n=3) 5FU (5-Fluorouracil, 10 µg/ml) was used as the positive control. *p=0.0009, **p=0.0005, ***p=0.0097.

5.4.3 Migration of A172 cells in response to the proteosaccharide systems

Migration studies were performed on A172 cells for a period of 48 h, due to their quick doubling time and easier attainability of a cell monolayer, though which a clear-cut incision could be made. Cells are known to migrate due to their response to their response to biophysical, topographical and chemical cues provided by the hydrogels. Sengupta and co-workers (2021) established four principles of directed migration. These are chemotaxis, which is migration towards chemical cues diffused in the media, hapotaxis ,where cells respond to chemical cues on the surface, durotaxis, where cells respond to the substrates mechanical stiffness and topotoxis which is the geometric features of the substrate (SenGupta *et al.*, 2021). Migration is an important factor in the renewal of damaged tissue and in tissue regeneration. It is vital for cells *in vivo,* to interact favourably with the hydrogel networks and establish a niche upon the hydrogel before the hydrogel degenerates. Therefore, a migration assay was used to determine if cells could not only proliferate but could direct the movement of resident cells *in vivo.* The migration of A172 cells in response to all thee formulations can be seen in the micrographs in figure 5.4-5.8 and the percentage wound closure was plotted in figure 5.9.

When the lesion was made (t=0), a clear gap can be seen between the two sides of each well. After 8 h, the untreated wound showed a 28.339% wound closure, which was higher than all of the treatments. This can be supported by the rapid proliferation of A172 cells and the untreated wells having the largest volume of media (1000µL) and the treated cells having 900µL of media available. The HAGLEGEN hydrogel showed the least wound closure. This was due to the presence of the uncrosslinked polymer i.e., hyaluronic acid which has anti-angiogenic and immunosuppressive activities. At 24 h, all of the treated wells showed a wound closure of greater than 60%. At 24 h, each treatment was given enough time to interact with the plated cells after being diluted in media. The CHTGELGEN hydrogel showed a wound closure of 74.785%, while the untreated showed a wound closure of 69.977%. The wound closure of the CGG hydrogel exceeded that of the CHT-PM hydrogel (70.96%). The PM hydrogel showed a wound closure of 60.21%. The full IPN hydrogel showed greater mechanical stability and thereby encouraged the migration of A172 cells to fill the lesion the most. The HAGELGEN hydrogen showed a wound closure of 66.141% at 24 h. In the gelatin containing hydrogels, the RGD motif found in gelatin served as a hapotactical cue to direct cell migration. At 48 h, all the lesions were closed, with the untreated slightly open (94.12%). The full IPN showed a 100% wound closure and was closely followed by the CHT-PM hydrogel. The PM hydrogel showed a wound closure of 90.24%. This showed that the thee hydrogels demonstrated better wound healing properties than the untreated formulation. A large amount of apoptosis can be seen in the images corresponding to the 48-hour time points. This was due to media not being replaced and the rapid doubling time which resulted in some

cell death. Also, a high seeding density was used to create a clear, linear lesion. The images of the 8 h and 24 h time point are turbid due to the presence of the hydrogel, which could not be washed, to monitor migration of the cells. The bar graph found in figure 5.9 shows the average wound closure of A172 cells at each time interval. In conclusion, the order of wound closure ranked as follows: CHTGELGEN>PMCHT>HAGELGEN>PM>untreated formulation.

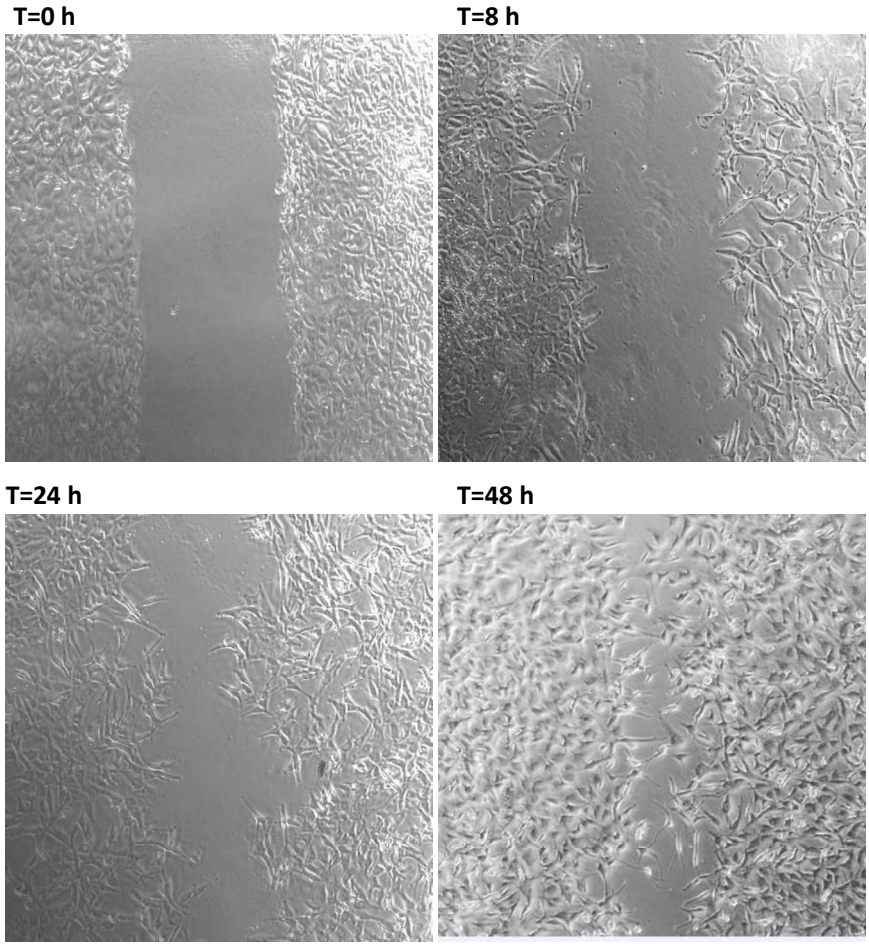


Figure 5.4. Micrographs of the migration of A172 cells from a wound healing assay of PM at A)0 h, B) 8 h C) 24 h D) 48 h. Images were captured using the 4X objective and the phase contrast feature of an inverted light microscope.

T=0 h **T=8 h**

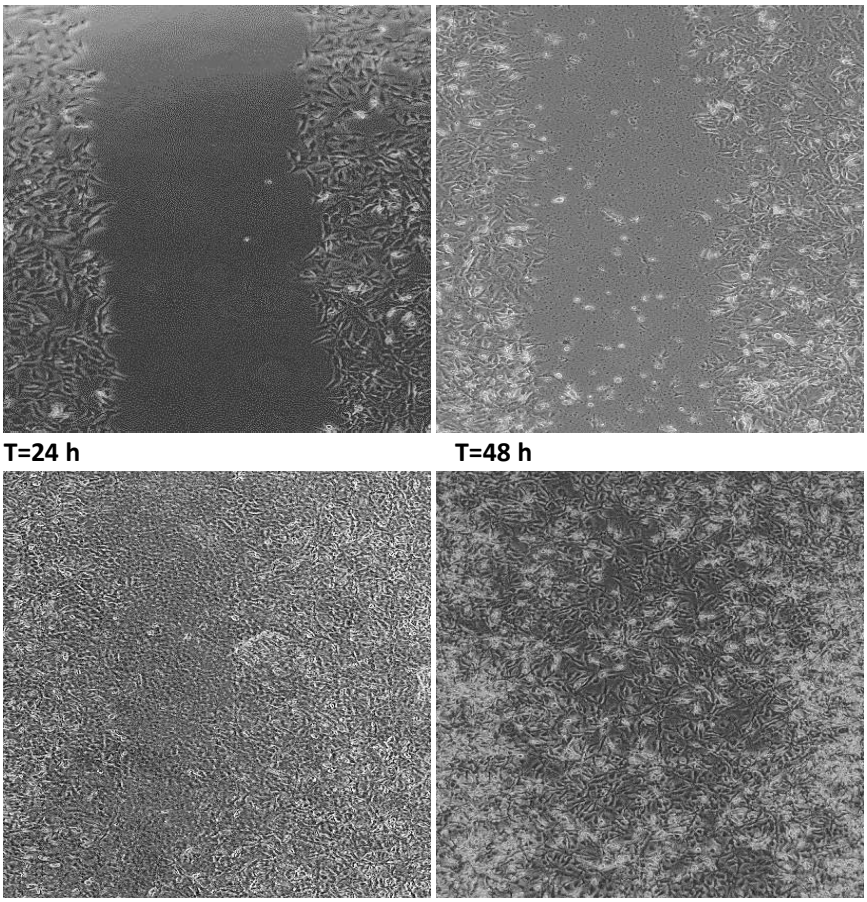
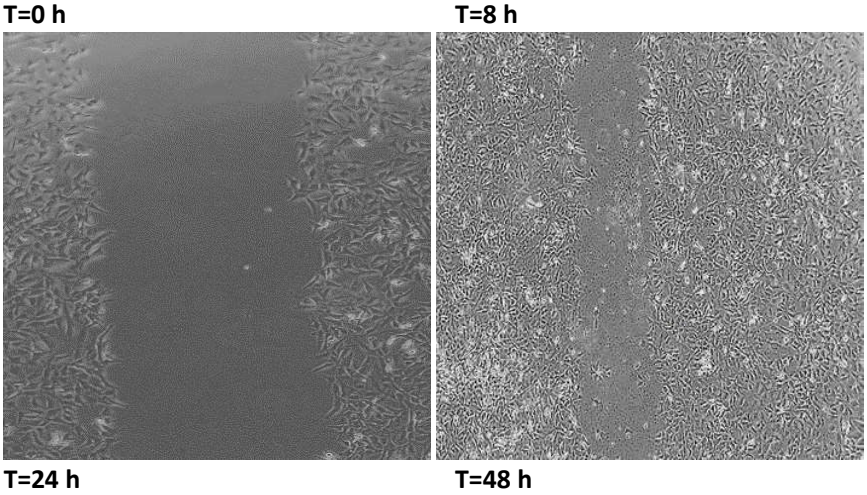


Figure 0.5. Micrographs of the migration of A172 cells from a wound healing assay of CHT-PM at A)0 h, B) 8 h C) 24 h D) 48 h. Images were captured using the 4X objective and the phase contrast feature of an inverted light microscope.



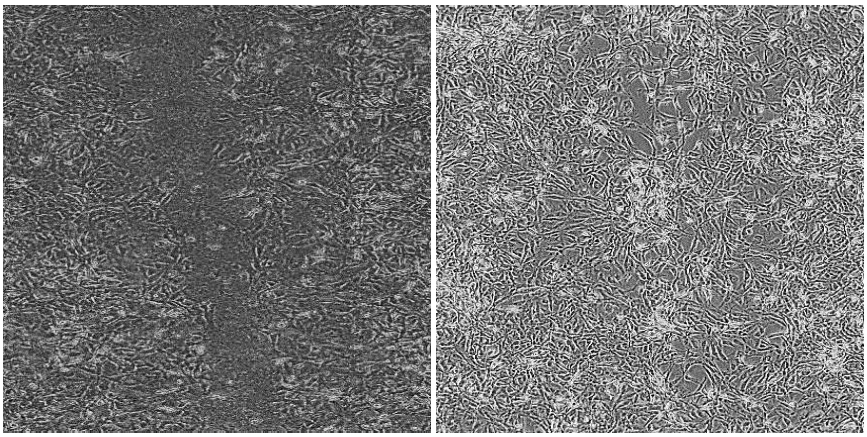


Figure 5.6. Micrographs of the migration of A172 cells from a wound healing assay of the full IPN at A)0 h, B) 8 h C) 24 h D) 48 h. Images were captured using the 4X objective and the phase contrast feature of an inverted light microscope.

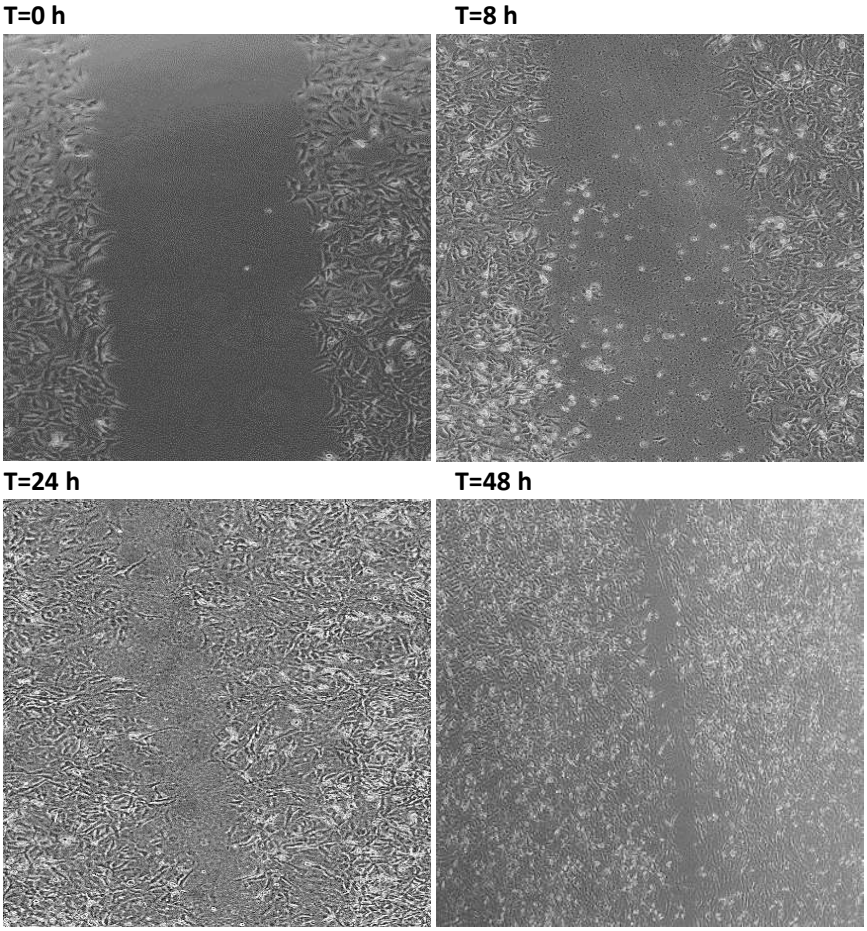


Figure 5.7. Micrographs of the migration of A172 cells from a wound healing assay of the semi-IPN at A)0 h, B) 8 h C) 24 h D) 48 h. Images were captured using the 4X objective and the phase contrast feature of an inverted light microscope.

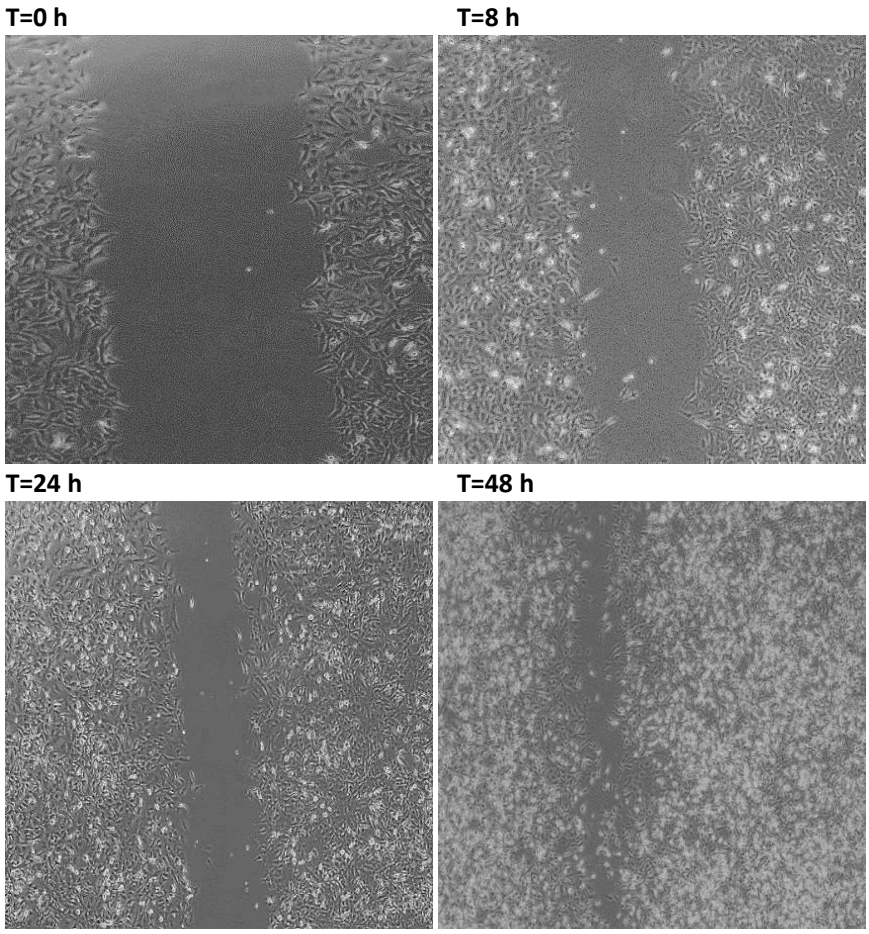


Figure 5.8. Micrographs of the migration of A172 cells from a wound healing assay of the untreated at A)0 h, B) 8 h C) 24 h D) 48 h. Images were captured using the 4X objective and the phase contrast feature of an inverted light microscope.

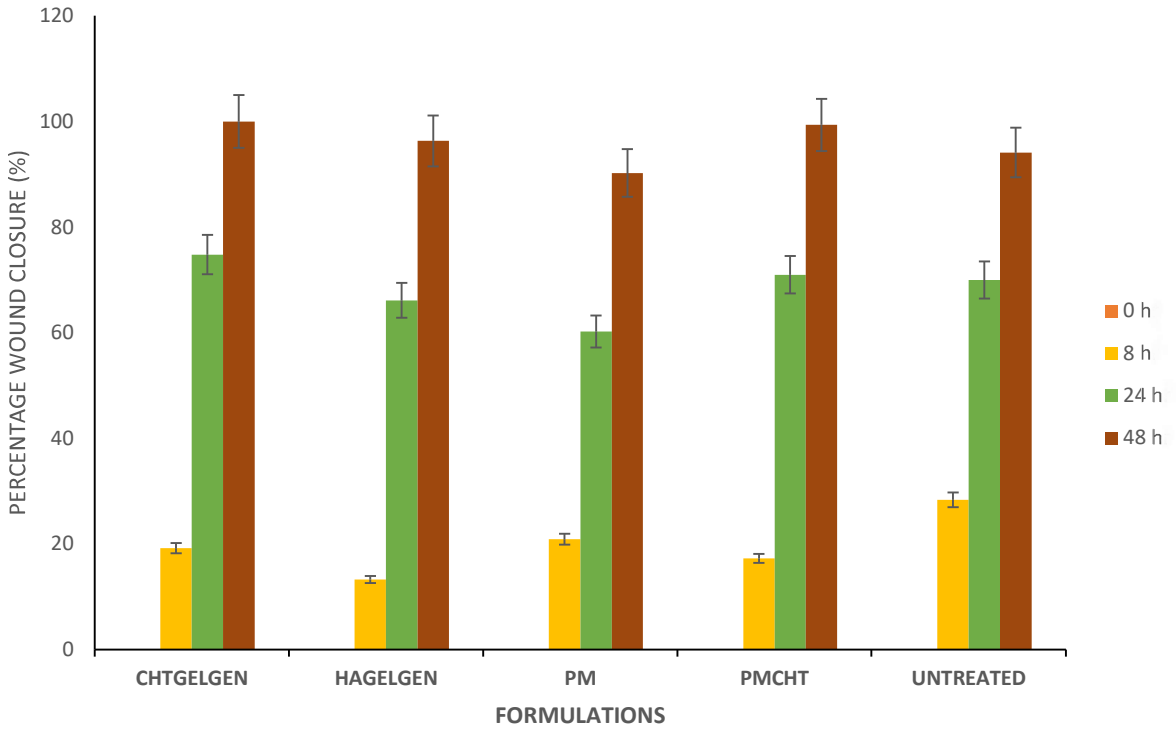


Figure 5.9. Bar graph showing the percentage wound closure at different time intervals calculated using ImageJ wound healing analysis n=3 (SD<2.52)

5.5 Concluding remarks

In vitro cytotoxicity and migration assays were conducted on each formulation, namely the semi-IPN, full-IPN and CHT-PM proteosaccharide. From the results stated in this chapter, it can be concluded that all formulations showed good *in vitro* performance and could be applied to traumatic brain injuries. The full-IPN closely followed the PM-CHT proteosaccharide formulation in terms of proliferation, however it showed a faster rate of migration, which could be attributed to the CHT-PM network not having any crosslinkers. The semi-IPN showed good performance but could be further developed to be applied more efficiently to TBI's.

REFERENCES

Arulmoli, J., Wright, H.J., Phan, D.T.T., Sheth, U., Que, R.A., … Flanagan, L.A. 2016. Combination scaffolds of salmon fibrin, hyaluronic acid, and laminin for human neural stem cell and vascular tissue engineering. Acta Biomaterialia. 43:122–138.

Bonnans, C., Chou, J. & Werb, Z. 2014. Remodelling the extracellular matrix in development and disease. Nature Reviews Molecular Cell Biology. 15(12):786–801.

Humphey, J.D., Dufresne, E.R. & Schwartz, M.A. 2014. Mechanotransduction and extracellular matrix homeostasis. Nature Reviews Molecular Cell Biology. 15(12):802–812.

Monteiro, M. V., Gaspar, V.M., Ferreira, L.P. & Mano, J.F. 2020. Hydrogel 3D in vitro tumor models for screening cell aggregation mediated drug response. Biomaterials Science. 8(7):1855–1864.

Munarin, F., Guerreiro, S.G., Grellier, M.A., Tanzi, || M C, Barbosa, M.A., … Granja, P.L. 2011. Pectin-Based Injectable Biomaterials for Bone Tissue Engineering. Biomacromolecules. 12:568–577.

SenGupta, S., Parent, C.A. & Bear, J.E. 2021. The principles of directed cell migration. Nature Reviews Molecular Cell Biology 2021 22:8. 22(8):529–547.

Výborný, K., Vallová, J., Kočí, Z., Kekulová, K., Jiráková, K., … Kubinová, Š. 2019. Genipin and EDC crosslinking of extracellular matrix hydrogel derived from human umbilical cord for neural tissue repair. Scientific Reports 2019 9:1. 9(1):1–15.

CHAPTER 6. CONCLUSIONS, LIMITATIONS AND FUTURE PROSPECTS

6.1 Conclusions

One of the main foci of neural regeneration is the re-establishment of continuity between neurons at the lesion site. To promote cell growth across the lesion, an artificial extracellular niche can be used upon which cells can grow and secrete growth factors. Various thee-dimensional scaffolds have been designed for this purpose, however there are still shortfalls associated with the performance of these scaffolds *in vivo.* It is therefore necessary to troubleshoot various properties of the scaffold so that these scaffolds can be correctly translated to clinical application. In this research, natural polymers such as chitosan, gelatin and hyaluronic acid were used, as a non-toxic cross-linker, genipin. These were chosen due to their non-toxic by-products as well as the ability to optimize their mechanical behaviour though structural modification.

Thee different formulations were designed, synthesised, and characterized for their use in neural tissue regeneration post a TBI. Each formulation possessed different properties. The CGG was a full IPN, crosslinked by genipin, while HAGG was a semi-IPN also crosslinked by genipin. Each polymer was of natural origin and by trouble-shooting various parameters, such as temperature and time, each network was non-toxic and possessed adequate mechanical strength and bioactivity to support neural cell survival and migration. The IPN and semi-IPN were loaded with Dexamethasone-21-Phosphate and the full IPN showed a sustained release of drug over a period of 10 days, while the semi-IPN showed a burst release due to no modification carried out on the HA component. Each system can be applied in neural regeneration as scaffolds which provide a surrogate matrix for neuronal cells. Cell studies were additionally undertaken on Chitosan-RGD and HA-RGD networks to evaluate any differences in cell viability as compared to CGG and HAGG networks (Appendix C). The CGG network was the most promising network in terms of mechanical strength, degradation, and drug release behaviour.

In chapter 4, a self-assembling peptide was combined with chitosan, devoid of any crosslinkers. Chitosan was included to add mechanical strength to the commercially available self-assembling peptide, PuraMatrix. Due to PuraMatrix only gelling at physiological pH and chitosan precipitating at a pH of greater than 6, an *in-situ* gelling scaffold was created though lyophilisation. The β-sheet structure of the peptide was maintained as shown by CD spectrometry and the young's modulus was improved by adding chitosan and using a lower percentage of PuraMatrix. Due to the incorporation of chitosan, the cost of production of the scaffold would be lowered, while the bioactivity was enhanced.

Cytotoxicity and migration studies showed that all thee proteosaccharides can be used as scaffolds for neural tissue engineering. The scaffolds supported cell growth and provided physicochemical cues which directed cell migration.

6.2 Limitations

Due to the lead times in obtaining the PuraMatrix hydrogel as well as the high cost of procurement, multiple ratios of protein: polysaccharide were not characterised extensively. The scaffolds formed were fibrous and lightweight, therefore resulting in DSC not being performed on the PuraMatrix scaffold alone. However, the addition of chitosan, increased the density of the scaffold which resulted in better handling and experimental characterization.

6.3 Prospects

Animal studies can be conducted on each scaffold to evaluate the *in vivo* regenerative potential of each scaffold. Due to the high viscosity of each hydrogel, 3D printing can be utilised to create scaffolds with more reproducible morphologies and controlled porosity. The hydrogels, specifically the full IPN and semi-IPN would be extrudable after crosslinking. The scaffolds may be seeded with neurotropic factors which can assist patients suffering from neurodegenerative diseases such as Parkinson's and Alzheimer's Disease and the challenge associated with crossing the blood brain barrier can be overcome. When the scaffold is loaded with bioactive, systemic side effects will be reduced due to more precise spatial distribution of the bioactive. Due to the biodegradable nature of the scaffold, there will be no need for surgery to remove the implanted scaffold and any degradation products yielded will be non-toxic in nature. Patient's quality of life will improve due to a restoration of lost function and financial strain associated with recurrent pharmacological treatments and increased hospital visits will be reduced. Using MRI/CT scan data, patient-specific scaffolds can be designed, and 3D printed to meet the requirements of the defective tissue.

Appendix A: Publications

PROTEOSACCHARIDE COMBINATIONS FOR TISSUE ENGINEERING APPLICATIONS

Henna Cassimjee [1], Pradeep Kumar [1], Yahya E Choonara [1], Viness Pillay [2]
DOI: 10.1016/j.carbpol.2020.115932
Wits Advanced Drug Delivery Platform Research Unit
Department of Pharmacy and Pharmacology
School of Therapeutic Sciences, Faculty of Health Sciences,
University of the Witwatersrand, Johannesburg, 7 York Road, Parktown, 2193,
South Africa
*Corresponding Author: viness.pillay@wits.ac.za

Abstract

Biomaterials that function as tissue surrogates ought to form thee dimensional structures which are conducive to cell proliferation and regeneration. Since the extracellular matrix (ECM) is composed of proteoglycans (long chain polysaccharides) and proteins, the combination of proteins and polysaccharides presents a logical strategy to mimic the ECM and guide cell growth and proliferation. Polysaccharides are distinctive scaffold materials for regeneration due to their biocompatibility, hydrophilicity, biodegradability and functional groups which may be modified to improve mechanical properties and cell signalling. However, modification of polysaccharides is often time consuming, and requires extensive chemical reactions. Therefore, to improve physiological signalling, tissue response and mechanical strength, polysaccharides are combined with proteins. This review will focus on naturally occurring proteins and polysaccharide combinations as well as draw attention to their specific use within the tissue engineering field.

Keywords: Alginate; Biomimicry; Chitosan; Crosslinking; Hyaluronic acid; Hydrogel; Proteosaccharide.

GENIPIN-CROSSLINKED, PROTEOSACCHARIDE SCAFFOLDS FOR POTENTIAL NEURAL TISSUE ENGINEERING APPLICATIONS

Henna Cassimjee, Pradeep Kumar, Philemon Ubanako and Yahya E. Choonara*

Wits Advanced Drug Delivery Platform Research Unit
Department of Pharmacy and Pharmacology
School of Therapeutic Sciences, Faculty of Health Sciences,
University of the Witwatersrand, Johannesburg, 7 York Road, Parktown, 2193, South Africa

* Correspondence: yahya.choonara@wits.ac.za

Abstract

Traumatic brain injuries (TBIs) are still a challenge for the field of modern medicine. Many treatment options such as autologous grafts and stem cells show limited promise for the treatment and the reversibility of damage caused by TBIs. Injury beyond the critical size necessitates the implementation of scaffolds that function as surrogate extracellular matrices. Two scaffolds were synthesised utilising polysaccharides, chitosan and hyaluronic acid in conjunction with gelatin. Bothscaffolds were chemically crosslinked using a naturally derived crosslinker, Genipin. The polysaccharides increased the mechanical strength of each scaffold, while gelatin provided the bioactive sequence, which promoted cellular interactions. The effect of crosslinking was investigated, and the crosslinked hydrogels showed higher thermal decomposition temperatures, increased resistance to degradation, and pore sizes ranging from 72.789 ± 16.85 µm for the full interpenetrating polymer networks (IPNs) and 84.289 ± 7.658 µm for the semi-IPN. The scaffolds were loaded with Dexamethasone- 21-phosphate to investigate their efficacy as a drug delivery vehicle, and the full IPN showed a 100% release in 10 days, while the semi-IPN showed a burst release in 6 h. Both scaffolds stimulated the proliferation of rat pheochomocytoma (PC12) and human glioblastoma multiforme (A172) cell cultures and also provided signals for A172 cell migration. Both scaffolds can be used as potential drug delivery vehicles and as artificial extracellular matrices for potential neural regeneration.

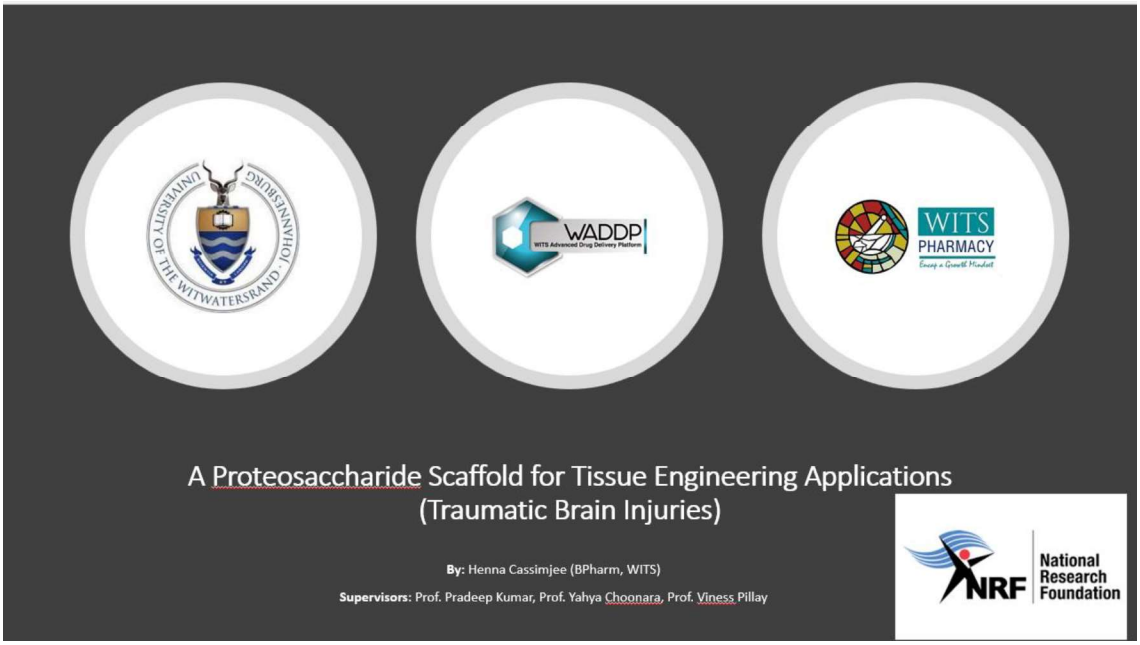
Keywords: chitosan; hyaluronic acid; neural; extracellular matrix; proteosaccharide; gelatin; crosslinking; genipin; dexamethasone; drug release; scaffold

Appendix B: Research outputs (oral and poster presentations)

1. **Abstract of presentation at the South Africa-Italy GYA-YSAP Mission: 17 November 2020. Oral presentation.**

A Proteosaccharide scaffold for tissue engineering applications (Traumatic Brain Injuries)

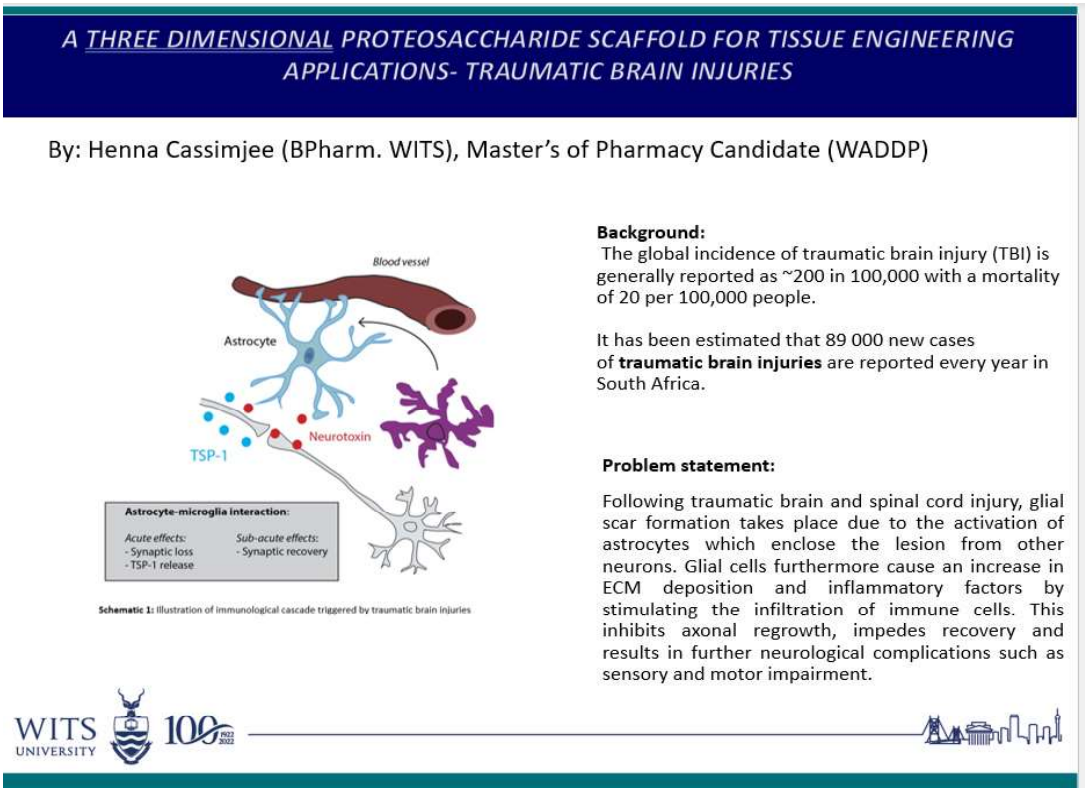
The utilisation of an extracellular matrix (ECM)-mimetic scaffold can greatly improve the therapeutic outcomes of patients suffering with traumatic brain injuries by providing regenerative cues for damaged neurons at the lesion site. For this, a proteosaccharide scaffold comprising of a self-assembling peptide (PuraMatrix i.e., RADA-16 I) and chitosan was synthesised. The scaffold will undergo in situ gelation and serve as a surrogate matrix upon which neurons can proliferate as the scaffold degrades. The scaffold showed increased thermal stability, preservation of the secondary structure of PuraMatrix, a microporous architecture and slower degradation. The scaffold also promoted the proliferation of rat adrenal medulla cells (PC12 cells) with a cell viability of 163.19% over 72 hours. This scaffold shows great potential for regenerating the central nervous system (CNS).



2. **Abstract of presentation at the BRICS Summit 2021: 04 November 2021. Oral presentation.**

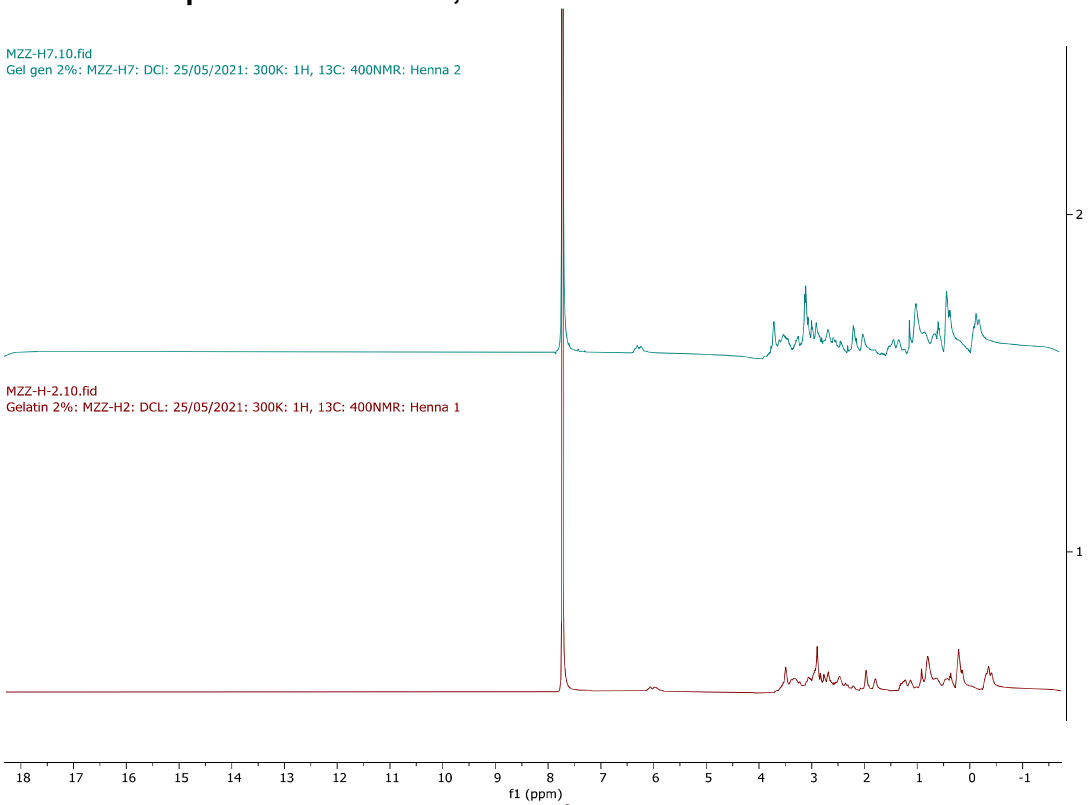
A 3D Proteosaccharide scaffold for tissue engineering applications (Traumatic Brain Injuries)

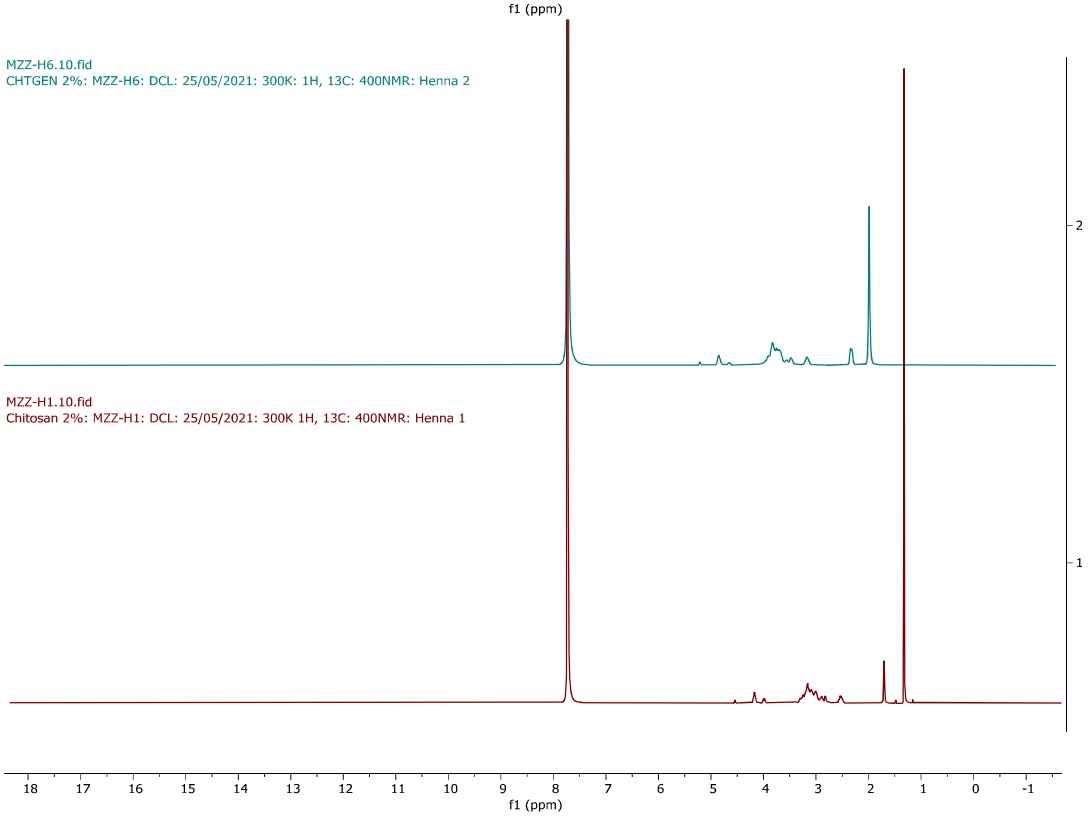
Traumatic brain injuries (TBI's) are still a challenge for the field of modern medicine. Many treatment options such as autologous grafts and stem cells show limited promise for the treatment and the reversibility of damage caused by TBIs. Injury beyond the critical size necessitates the implementation of scaffolds which function as surrogate extracellular matrices. Two scaffolds were synthesized utilizing polysaccharides, chitosan, and hyaluronic acid in conjunction with gelatin. The polysaccharides increased the mechanical strength of each scaffold while gelatin provided the bioactive sequence which promoted cellular interactions. The effect of crosslinking was investigated, and the crosslinked hydrogels showed higher thermal decomposition temperatures, increased resistance to degradation, and pore sizes ranging from 72.789 µm±16.85µm for the full IPN and 84.289 µm±7.658µm for the semi-IPN. The scaffolds were loaded with Dexame-thasone-21-phosphate to investigate their efficacy as a drug delivery vehicle, and the full IPN showed a 100% release in 10 days, while the semi-IPN showed a burst release in 6 hours. Both scaffolds encouraged the proliferation of rat pheochomocytoma (PC12) and human glioblastoma multiform (A172) and furthermore, provided cues for migration of A172 cells. Both scaffolds can be used as potential drug delivery vehicles and as artificial extracellular matrices for potential neural regeneration.

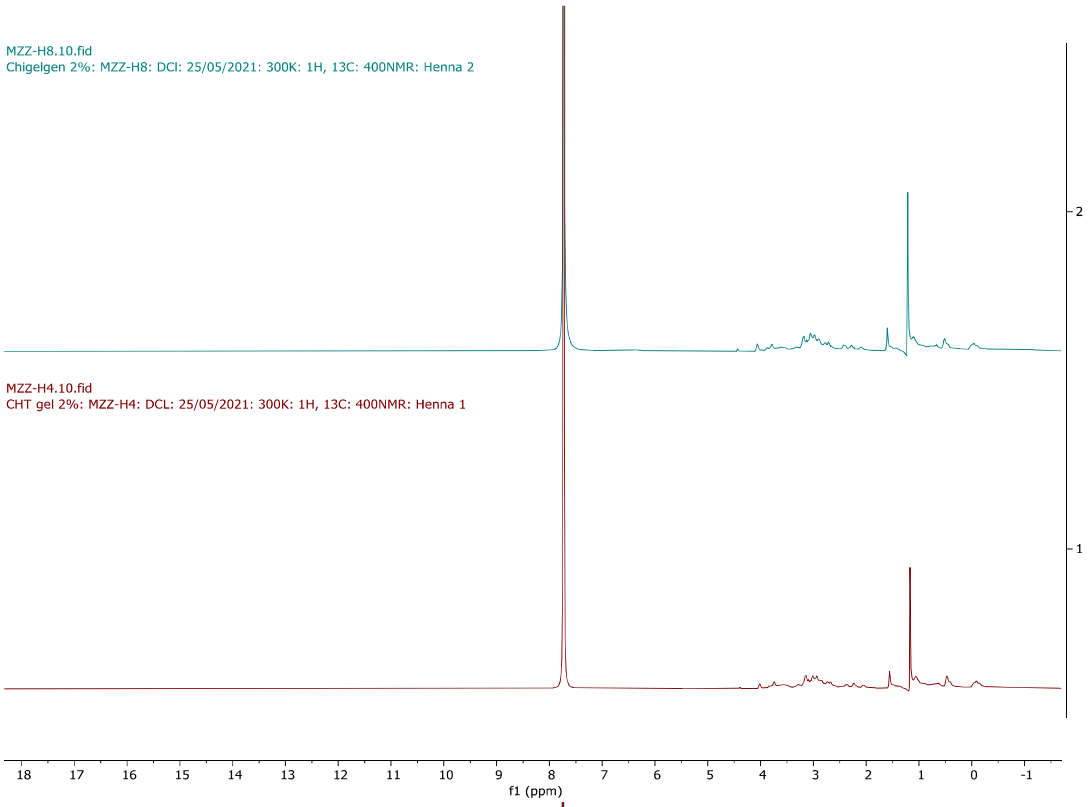


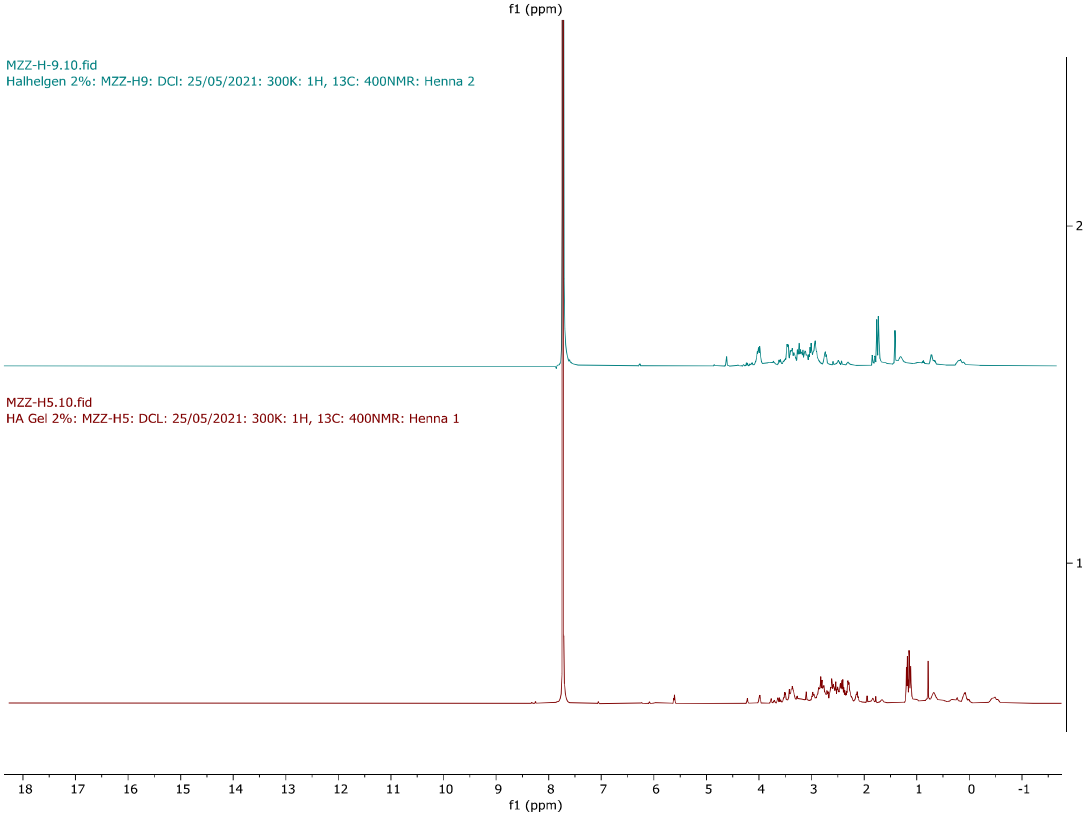
Appendix C: Supplementary data

1. NMR spectra of CHT-GEL, and HA-GEL and the crosslinked combinations

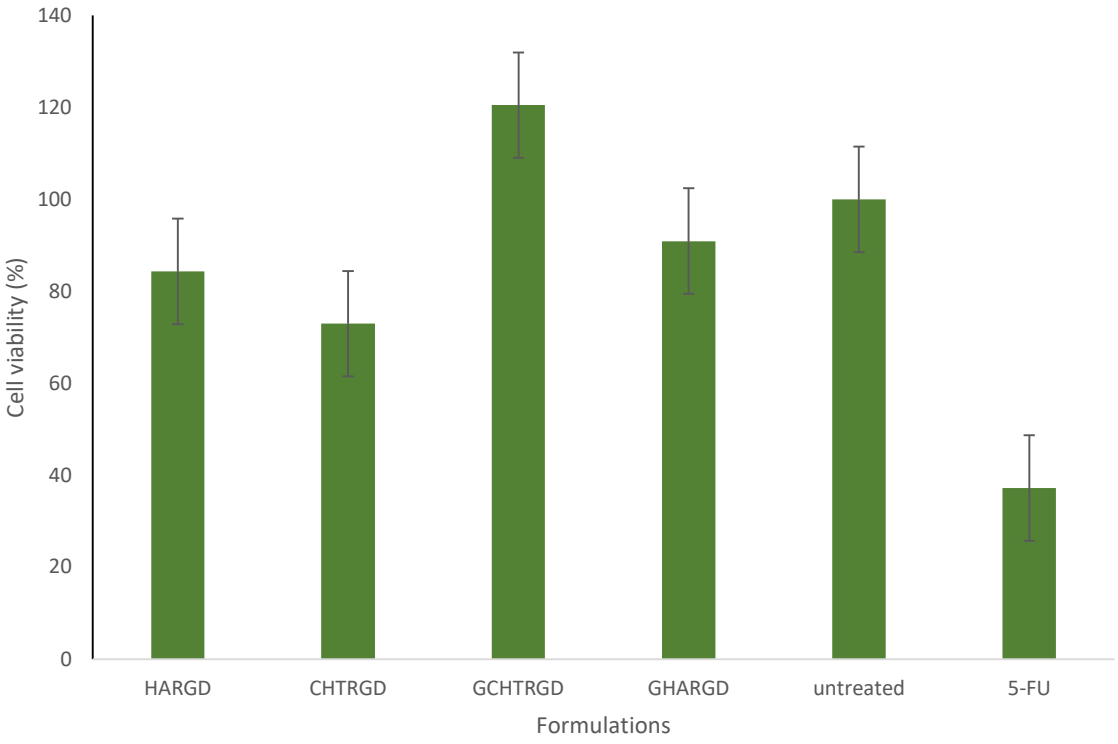





MZZ-H8.10.fid
Chigelgen 2%: MZZ-H8: DCl: 25/05/2021: 300K: 1H, 13C: 400NMR: Henna 2
MZZ-H4.10.fid
CHT gel 2%: MZZ-H4: DCL: 25/05/2021: 300K: 1H, 13C: 400NMR: Henna 1
2
1
18 17 16 15 14 13 12 11 10 9 8 7 6 5 4 3 2 1 0 -1
f1 (ppm)


MZZ-H-9.10.fid
Halhelgen 2%: MZZ-H9: DCl: 25/05/2021: 300K: 1H, 13C: 400NMR: Henna 2
MZZ-H5.10.fid
HA Gel 2%: MZZ-H5: DCL: 25/05/2021: 300K: 1H, 13C: 400NMR: Henna 1
2
1
18 17 16 15 14 13 12 11 10 9 8 7 6 5 4 3 2 1 0 -1
f1 (ppm)

2. XTT assay carried out on RGD-polysaccharide blends and genipin crosslinked RGD-polysaccharide combination



Bar graph showing the cytotoxicity of each genipin-crosslinked RGD hydrogel on A172 cell lines using an XTT assay (n=3) over 48 hours (n=3) 5-FU (5-Fluorouracil, 10 µg/ml) was used as the positive control.

3. **Permission obtained for the use of figure 3.1. (RightsLink®)**

Thank you for your order!

Dear Henna Cassimjee,

Thank you for placing your order through Copyright Clearance Center's RightsLink® service.

Order Summary

Licensee:	Henna Cassimjee
Order Date:	Jan 19, 2022
Order Number:	5232531060167
Publication:	Journal of Polymer Science Part A: Polymer Chemistry
Title:	Mechanism and kinetics of the crosslinking reaction between biopolymers containing primary amine groups and genipin
Type of Use:	Dissertation/Thesis
Order Total:	0.00 USD